

NOVEL IMMUNOGENS BASED ON THE GP41 PROTEIN OF HUMAN IMMUNODEFICIENCY VIRUS TYPE 1 AND DISPLAY SYSTEMS FOR THEIR AFFINITY MATURATION

Dissertation

submitted in partial Fulfillment of the Requirements for the

Degree of Doctor of Natural Sciences (rer. nat.)

of the Department of Biology, the Faculty of Mathematics, Informatics and Natural

Sciences,

of the University of Hamburg

submitted by

Thomas D. Benen

from Nürnberg, Germany

Hamburg 2011

Genehmigt vom Fachbereich Biologie
der Fakultät für Mathematik, Informatik und Naturwissenschaften
an der Universität Hamburg
auf Antrag von Herrn Prof. Dr. T. DOBNER
Weiterer Gutachter der Dissertation:
Prof. Dr. R. WAGNER
Tag der Disputation: 20. Mai 2011

Hamburg, den 05. Mai 2011

A handwritten signature in black ink, appearing to read 'A. Temming', with a stylized flourish at the end.

Professor Dr. Axel Temming
Leiter des Fachbereichs Biologie

1. Supervisor of dissertation: Prof. Dr. Thomas Dobner, Heinrich-Pette-Institute Institute for Experimental Virology, University of Hamburg

2. Supervisor of dissertation: Prof. Dr. Ralf Wagner, Institute of Medical Microbiology and Hygiene, University of Regensburg

1. Supervisor of disputation: Prof. Dr. Joachim Hauber, Heinrich-Pette-Institute for Experimental Virology, University of Hamburg

2. Supervisor of disputation: Prof. Dr. Günter Adam, Department of Phytomedicine, University of Hamburg

Chairman of disputation: Prof. Dr. Angelika Brandt, Department of Zoology, University of Hamburg

Outline

1	Abstract.....	1
2	Introduction	3
2.1	Human Immunodeficiency Virus type-1 (HIV-1) vaccines and neutralizing antibodies ..	3
2.1.1	HIV-1 epidemic and the need for a vaccine.....	3
2.1.2	State of the HIV-1 vaccine field	4
2.1.3	Role of envelope antibodies in HIV-1 prevention.....	6
2.1.4	Natural emergence of broadly neutralizing antibodies.....	7
2.1.5	Native envelope structure	7
2.1.6	Specificities of broadly neutralizing antibodies	9
2.2	gp41 – target for vaccine design.....	11
2.2.1	Structure and function of gp41.....	11
2.2.2	MPER – a conserved region of flexible structure.....	14
2.2.3	Ab response against gp41 and MPER in natural infection	15
2.2.4	Details on Broadly neutralizing antibodies binding the MPER.....	16
2.2.5	The importance of a membrane environment for 2F5 and 4E10	17
2.2.6	Associated vaccine adjuvants and delivery	18
2.3	Affinity enhancement of antigens.....	19
2.3.1	Display techniques.....	19
2.3.2	Retroviruses and retroviral vectors	21
2.3.3	Retroviral display	22
2.4	Objective of the present study	25
3	Methods	26
3.1	Nucleic acids molecular biology.....	26
3.1.1	Cloning of genes – general procedure.....	26
3.1.2	Cloning of DNA libraries (“IIS-ccdb” procedure)	26
3.1.3	DNA preparation	27
3.1.4	Oligonucleotides	27
3.1.5	Construction of genes and plasmids.....	28
3.1.5.1	Software-assisted design of gp41 derivatives.....	28
3.1.5.2	Trimer-stabilized constructs and molecular visualization.....	28
3.1.5.3	gp41ctm Mini-Libraries.....	29
3.1.5.4	gp41ctm degenerated library	29
3.1.5.5	Plasmids for gp41 immunogens.....	29
3.1.5.6	Plasmids for AIO system.....	29
3.1.5.7	Plasmids for lenti-cellular display.....	30

3.1.6	Reverse transcription (RT-PCR).....	31
3.2	Protein biochemistry	31
3.2.1	SDS-PAGE and Coomassie staining.....	31
3.2.2	Western and Slot Blots	31
3.2.3	ELISA.....	32
3.3	Cell biology	32
3.3.1	Cell lines and cultivation	32
3.3.2	Cell counting	32
3.3.3	Transient transfection	33
3.3.4	VLP production	33
3.3.5	Virus production.....	33
3.3.6	Cell and virus lysates.....	34
3.3.7	Sucrose gradients.....	34
3.3.8	Crosslinking	34
3.3.9	Electron microscopy	34
3.3.10	Cytometric analysis and fluorescence-activated cell sorting (FACS)	35
3.3.11	MACS sorting.....	35
3.3.12	Virus panning.....	35
3.3.13	Infectivity assay	36
3.4	Animal experiments	36
3.4.1	Rodent immunizations	36
3.4.2	Removal of anti-cell antibodies.....	36
3.4.3	Virus neutralization assays	37
4	Results	38
4.1	Novel gp41 immunogens	38
4.1.1	Design and characterization of trimer-stabilized and truncated gp41 derivatives..	38
4.1.1.1	Design of gp41 constructs with enhanced MPER exposure	38
4.1.1.2	Molecular modeling and prediction of correct protein topology.....	39
4.1.1.3	Membrane exposure and selective recognition by BNMAbs	40
4.1.1.4	Incorporation into VLPs.....	41
4.1.1.5	Functional preservation of BNAb epitopes on VLPs	42
4.1.1.6	Trimeric state of gp41 derivatives on the surface of VLPs.....	43
4.1.1.7	Quantification of gp41 molecules per VLP	44
4.1.1.8	Cytopathic effects of gp41 derivatives	45
4.1.1.9	Large scale production for immunization studies.....	46
4.1.2	Immunogenicity studies in rodents	47
4.1.2.1	Induction of anti-gp41 Abs	48

4.1.2.2	Removal of anti-cell antibodies	50
4.1.2.3	Induction of neutralizing antibodies.....	50
4.1.2.4	Removal of MPER-directed BNMAbs by incubation with cells	53
4.1.3	Summary	54
4.2	Selection of gp41 derivatives with high affinity for BNMAbs	55
4.2.1	Creation of a gp41 mini-library.....	55
4.2.1.1	Membrane localization of mini-library and selective binding to BNMAbs.....	56
4.2.1.2	Incorporation into VLPs and selective binding to BNMAbs.....	57
4.2.2	Development of the Lentiviral display system “All-in-One” (AIO).....	58
4.2.2.1	Design of AIO platform.....	58
4.2.2.2	Replacement of <i>nef</i> is reconcilable with particle production	59
4.2.2.3	Virus production after transfection	60
4.2.2.4	Virus production after infection	61
4.2.2.5	VSVG Pseudotyping	62
4.2.2.6	Optimization of further steps in panning procedure	63
4.2.2.7	Incorporation of inherently expressed gp41 _{ctm} into virions.....	64
4.2.2.8	Quantification of incorporated gp41 _{ctm}	65
4.2.2.9	Selective capture of virions and subsequent productive reinfection	66
4.2.2.10	Enrichment of high-affinity binders on clonal basis.....	66
4.2.2.11	Evidence for more efficient capture by anti-gp120 Abs than by gp41 Abs .	67
4.2.3	Lenti-cellular display systems	68
4.2.3.1	MACS-based Lenti-cellular display system.....	68
4.2.3.2	FACS-based Lenti-cellular display system	70
4.2.3.3	Gating strategy	70
4.2.3.4	Discrimination between high- and low-affinity binders	72
4.2.3.5	Proof-of-concept: Sorting and sequencing of mini-library	72
4.2.4	Creation of a complex library	73
4.2.4.1	Cloning of library into lentiviral vectors	75
4.2.4.2	Library screening	77
4.2.5	Summary	77
5	Discussion	79
5.1	Discussion of novel gp41 immunogens	79
5.1.1	gp41 MPER - challenges for targeted vaccine development.....	79
5.1.2	Tailor-made construct design for optimized MPER presentation.....	79
5.1.3	Experimental implementation of desired protein specifications	80
5.1.4	<i>In vivo</i> testing of novel gp41-derived immunogens.....	81
5.1.5	Beneficial effects of DNA prime and protein boost	82

5.1.6	Neutralization capacity and fine-mapping of MPER-directed vaccines	83
5.1.7	Adding a membrane in MPER vaccines	84
5.1.8	Effects of removing anti-cell activities in sera, and alternatives.....	85
5.1.9	CTB as carrier.....	85
5.1.10	Outlook for further MPER-based immunogen design	86
5.2	Discussion of affinity enhancement of antigens.....	87
5.2.1	Design of a novel lentiviral display platform.....	87
5.2.2	Creation of a 4E10-directed mini-library for validation of display systems	88
5.2.3	Performance of AIO system.....	89
5.2.4	Adaptation of currently developed “lenti-cellular” display systems	90
5.2.5	Comparison with a similar lenti-cellular display technology	91
5.2.6	Controlling the MOI in lenti-cellular display.....	92
5.2.7	Library screens	92
5.2.8	Outlook for lentiviral display systems.....	93
6	Appendix.....	94
6.1	Dependency of MOI and infection rates.....	94
6.2	Alignment of sequenced peer group of gp41ctm library	95
6.3	Synthetic oligonucleotides	102
6.4	Abbreviations	104
6.5	References.....	106
6.6	Acknowledgements.....	124

1 Abstract

As the Human Immunodeficiency Virus type 1 (HIV-1) pandemic progresses, a prophylactic vaccine is highly desirable. Neutralizing antibodies are thought to be crucial to mediate sterilizing immunity. A few broadly neutralizing monoclonal antibodies (BNMAbs) against HIV-1 have been described which target highly conserved regions of the envelope protein. The membrane-proximal external region (MPER) of gp41 is particularly conserved and target for the potent BNMAbs 2F5 and 4E10. Past immunization efforts were not able to induce a strong neutralizing immune response against this target so far. Besides epitope exposure and stabilization, affinity maturation of immunogens to BNMAbs might be a way to enhance the quality of immune responses. However, as gp41 is a membrane-bound mammalian protein, only limited display strategies like retroviral display are suitable for this purpose, and a display system based on HIV-1 might be an ideal platform.

The objective of this work was to design and evaluate novel immunogens based on the HIV-1 gp41 MPER with the potential to elicit cross-clade neutralizing antibodies. In a complementary approach, novel methods for the affinity maturation of gp41-based immunogens were to be established.

The following strategies were pursued to build an effective immunogen: gp41 was truncated N-terminally in order to dispose of immunodominant, non-neutralizing sites and enhance the exposure of conserved regions. Heterologous zipper domains were introduced to stabilize a trimeric conformation. Resulting constructs were modelled *in silico*, and checked *in vitro* for the desired specifications. Cell surface exposure and selective binding to BNMAbs 2F5 and 4E10 could be shown by cytometric analyses. Incorporation into VLPs and preservation of antigenic structures were verified by electron microscopy studies. Crosslinking experiments revealed an oligomeric state of all constructs and its stabilization by zipper domains. The immunogens were tested in two rodent immunization studies, as stand-alone constructs in a homologous DNA prime and VLP boost regimen, or in combination with two existing gp41-derived soluble proteins. Although sufficient titers of anti-MPER antibodies were measured by IgG ELISA in some groups, neutralizing activity was mostly limited. Best results were obtained by a DNA prime with a truncated gp41 construct and a boost with a soluble protein engrafting the MPER and stabilized by trimerization domains.

For affinity maturation of gp41 and its derivatives, a novel lentiviral display system based on HIV-1 was developed. Both packaging function and antigen library were integrated in a proviral genome. A mini-library, tailor-made for 4E10, was created and subjected to proof-of-concept studies. A second cell-based system using fluorescence-activated cell sorting (FACS) was adapted for use with gp41-derived antigens and further developed regarding the gating strategy. Both systems led to an enrichment of strong binders in only one round, with the cell-based

system being more effective as it enables normalization by antigen expression level. Finally, a complex gp41 library was created to be screened for affinity-enhanced variants.

Further refinements of the immunogens based on these results and successful affinity maturation might elicit functional immune responses towards the conserved MPER in future studies.

2 Introduction

This work is dedicated to the development of novel vaccines against HIV-1 and novel display strategies serving this goal. The following introduction aims at giving a review on the literature and clarifying the objective of the present study.

2.1 Human Immunodeficiency Virus type-1 (HIV-1) vaccines and neutralizing antibodies

2.1.1 HIV-1 epidemic and the need for a vaccine

Since the discovery of HIV in 1983 (1-3) more than 25 million people died of Acquired Immune Deficiency Syndrome (AIDS) (4). UNAIDS estimated that 33.3 million lived with human immunodeficiency virus type-1 (HIV-1) infection in 2010, 2.6 million become newly diagnosed with HIV-1 each year, and 1.8 million AIDS-related deaths occurred in 2009. Sub-Saharan Africa continues to bear the major burden with 22.5 million HIV-infected persons. With rare exceptions, an HIV-1 infection left untreated leads to depletion of CD4⁺ T cells, opportunistic infections and finally to death (5). Efforts for a cure concentrate on rendering patients resistant (6) or excise the proviral information out of the patients' genome (7), yet these studies are still in pre-clinical stages. Anti-retroviral therapy (ART) can suppress viral replication increasing life expectancy among those infected, but cannot cure infection. Sustaining affordable ART coverage in resource-poor, HIV-1 endemic regions is a massive global health problem.

Several modalities can reduce HIV-1 infection rates in persons at risk of exposure, including screening of donor blood products, risk reduction counseling, behavioral modifications, condom usage, and male circumcision. Preexposure or postexposure ART prophylaxis may reduce susceptibility, with two recent trials demonstrating 39% resp. 44% efficacy in lowering HIV-1 incidence rates using tenofovir as vaginal gel (8) or as oral drug (9). Treatment of infected persons can markedly reduce transmission risk from mother to child, in exposed persons living in high-seroprevalence communities, and between heterosexual discordant couples. Together, these interventions can slow the epidemic, but a safe, efficacious vaccine likely affords the best long-term solution (10).

Fundamental barriers to HIV-1 vaccine development lie within the unique properties of the virus: its entry is predominantly through mucosal surfaces, its preferred target is human CD4⁺ T cells, and its rapid establishment of a persistent reservoir of latently infected cells. Properties of transmitted (founder) viruses from mucosal transmission indicate that in 70%–80% of cases, a single virus or virus-infected cell establishes productive clinical infection (11). Such viruses typically exhibit C-C chemokine receptor type 5 (CCR5)-dependence, mask functional envelope trimers needed to trigger antibody neutralization, and undergo rapid mutation as productive infection ensues (12). Taken together, these viral properties have direct implications in defining

specific host innate and adaptive immune pathways that could efficiently defend against HIV-1 entry and productive infection, and in optimizing ways to elicit these responses at the site of exposure.

As a result of genetic sequence variability created by its error-prone reverse transcriptase as well as mutations selected by host immune pressure, HIV-1 has evolved into multiple subtypes or clades together with circulating recombinant forms (collected at Los Alamos National Library (13)). Because of this global diversity (up to 35% in envelope gp120), it might be impossible to design a universal vaccine candidate that can induce potent effector immunity to multiple key antigenic determinants among worldwide circulating HIV-1 strains. A solution to this problem may be a polyvalent vaccine covering multiple strains, as it is common in influenza vaccines (14). Centralized (consensus) or ancestral sequences may be another option to overcome viral diversity (15; 16).

2.1.2 State of the HIV-1 vaccine field

After the identification of HIV-1 as the etiologic agent of AIDS, nonhuman primate models were established to examine vaccine effects after experimental retroviral challenge; the utility and limitations of these models in predicting vaccine efficacy have been well described (17). Since 1987, more than 30 candidate HIV-1 vaccines whose prototypes have elicited varying degrees of protective responses in nonhuman primate models have advanced to human clinical trials, alone or in combinations (18; 19). (19) These include replication-competent or incompetent viral vectors (pox virus, adenovirus, alphavirus, adeno-associated virus) containing HIV-1 gene inserts, HIV-1-derived virus-like particles, DNA plasmids encoding HIV-1 genes, and soluble HIV-1 proteins and peptides, with or without adjuvant formulations. Heterologous prime-boost regimens have been employed to enhance the potency and breadth of antibody and T cell responses.

Those candidate regimens that have been extended to large-scale international phase IIb or III studies include the recombinant bivalent HIV-1 envelope gp120 vaccines, AIDSVAX B/E with alum (Vax003 trial, (20)) and AIDSVAX B/B with alum (Vax004 trial, (21)); the replication-incompetent adenovirus serotype 5 (Ad5) vectored HIV-1 trivalent vaccine (Step (22) and Phambili trials (23)); and the canarypox ALVAC-HIV vCP1521 plus AIDSVAX gp120 clades B and E (RV144 / “Thai” trial (24)). So far, only the RV144 trial, evaluating a recombinant canarypox-HIV vector prime and recombinant HIV-1 envelope gp120 subunit protein plus alum boost, showed statistically significant efficacy (31.2%) in reducing HIV-1 infection rates in low-incidence heterosexuals. All trials demonstrated the limitations of available laboratory and animal models to assess relevant vaccine-induced immune responses and predict clinical trial outcome (24; 25). No regimen has induced vaccine responses associated with set-point viral

load reduction after acute infection or elevated CD4⁺ T-cell count in subjects in whom HIV-1 infection was subsequently diagnosed.

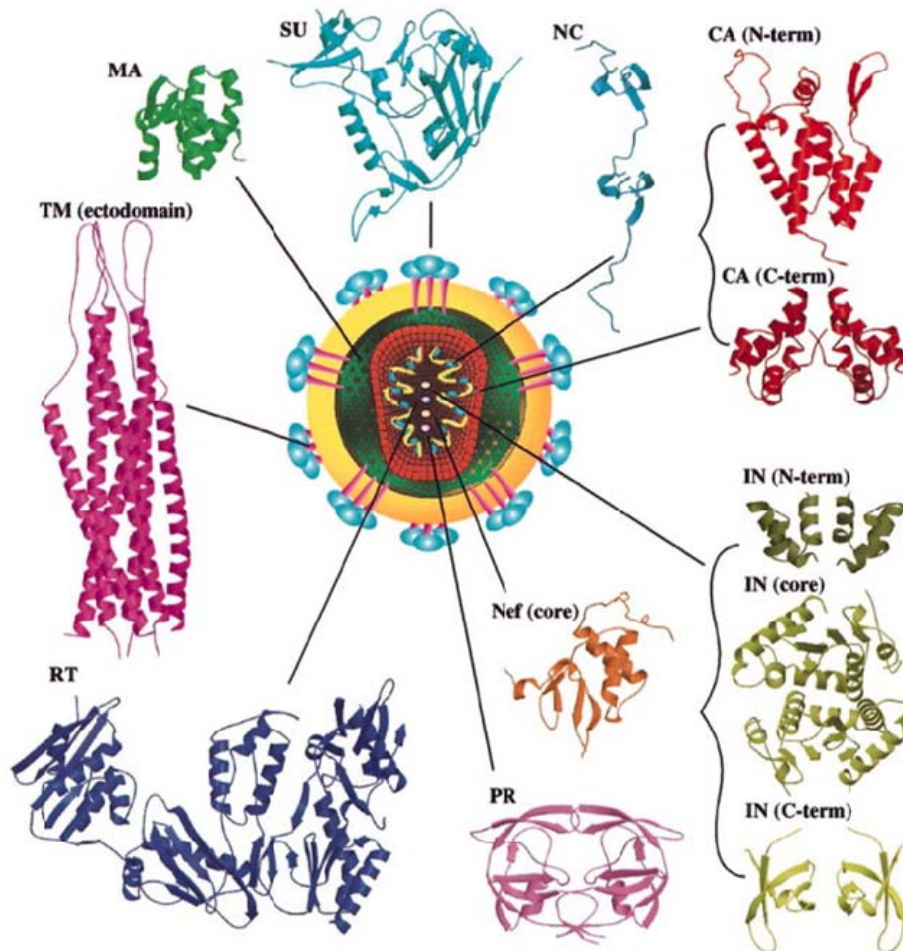


Figure 1. Schematic overview of the HIV-1 viral particle with protein structures. This figure shows the single components of the HIV-1 viral particle with a schematic protein structure. The capsid built of p24 (CA) contains two RNA genomes (yellow spirals) in complex with p7 (NC). Enzymes are derived from a Pol precursor protein and split into integrase (IN), protease (PR) and reverse transcriptase (RT). The interior of the viral membrane (yellow circle) is associated with the matrix protein p17 (MA). A trimeric complex of membrane-spanning gp41(TM) associated with gp120 (SU) is embedded in the membrane. Additional accessory proteins like Nef are also incorporated. Figure derived from (26).

Apart from safety issues, the overriding principle guiding HIV vaccine development has been the predicted ability of the immunogen to induce either HIV-1 neutralizing antibodies or HIV-1-specific CD8⁺ T cells, or both. Although there have been strong proponents of either antibodies or T cells alone as the most effective strategy, taking into account the correlates of immune protection against other viral pathogens as well as understanding the immune components that control HIV-1 *in vivo*, the consensus view now is that a highly effective vaccine will need to elicit coordinated B cell, CD4⁺ and CD8⁺ T cell responses (27). Moreover, it is anticipated that specific adjuvants and vectors can trigger innate immune signaling pathways that can improve the potency and quality of adaptive immunity.

Recent studies in acute infection have emphasized the rapidly destructive nature of HIV-1, and the need for protective immune responses to be present concurrently with, if not before, HIV-1 transmission (28; 29). While desired CD8⁺ T cell responses are primarily directed against Gag, Pol, Nef and Env, protective B cell responses are only targeted against Env. An overview of the structural components of an HIV-1 virion is shown in fig. 1.

2.1.3 Role of envelope antibodies in HIV-1 prevention

Neutralizing antibodies (NAbs) are common correlates of protective immunity of most vaccines against infectious agents. Although both infection and HIV-1 envelope immunization can induce NAbs, those antibodies that broadly neutralize a wide range of HIV-1 strains are not commonly induced. However, passive administration of rare human anti-Env broadly neutralizing monoclonal antibodies (BNMAbs) with titers that can be achieved by immunization can protect against simian-human immunodeficiency chimeric virus (SHIV, containing some HIV-1 genes, including *env*, *tat*, and *rev*, on a simian immunodeficiency virus [SIV] backbone) challenge in rhesus macaques (30-32). 90% neutralization at low serum dilutions (1/20) is a commonly referred benchmark to be attained by new vaccine candidates. If protective antibodies can be induced, the necessary plasma titers will be sufficiently low so as to be attainable by vaccination (33). This is probably also true for antibodies directed against the membrane-proximal external region (MPER) of gp41 like 2F5 and 4E10 (34). Thus, a major goal of HIV-1 vaccine development is to design immunogens capable of inducing antibodies that can broadly neutralize HIV-1 across various clades (18; 35).

In principal, only antibodies directed against the highly variable envelope protein are neutralizing (36). One major obstacle in HIV-1 vaccine development is constructing Env immunogens with immunogenic broadly neutralizing epitopes. First, conserved Env epitopes targeted by BNABs are poorly immunogenic because they either are masked by carbohydrates (37; 38), appear transiently (39), are sterically hindered (40), or must overcome entropy for antibody binding (41). Second, Env glycans are antigenically similar to host carbohydrates (42). Third, some Env protein epitopes have homologies with self proteins, and when immunogenic, induce polyreactive antibodies that may be subjected to tolerance mechanisms (43; 44). By contrast, easily induced HIV-1 Env antibodies typically recognize type-specific neutralizing epitopes located on variable loops or recognize dominant non-neutralizing, conserved epitopes in gp120 or gp41 (45; 46). Many of these non-neutralizing dominant epitopes are present only on structurally non-native Env. Finally, even when antibodies can neutralize the infecting strain, their effect is transient because rapidly evolving escape mutations are selected (47). Thus, immunization of non-human primates and humans with HIV-1 Env monomers or trimers has failed to induce antibodies recognizing broadly neutralizing envelope epitopes. Rather, induced antibodies neutralize the strain represented in the immunogen sequence or easily neutralizable

strains (termed Tier 1 strains); only sporadic and weak neutralization is observed for difficult to neutralize (Tier 2 and Tier 3 strains) primary HIV-1 isolates that are representative of clinically relevant field isolates (18).

2.1.4 Natural emergence of broadly neutralizing antibodies

Unlike the initial CD8⁺ T cell response in acute HIV-1 infection that rapidly selects for escape mutants (12), the initial antibody response to Env, although virion-binding, does not have neutralizing activity and does not drive escape mutation. The first autologous neutralizing antibody response does not develop until ~3 months after transmission (29). This autologous response occurs in virtually all infected subjects, is usually specific for the transmitted (founder) virus, and is frequently targeted to variable Env regions (46). Approximately 20% of chronically HIV-1 infected subjects have NABs that neutralize multiple HIV-1 strains, and ~2% – 4% of chronically infected subjects have serum antibodies that broadly neutralize most HIV-1 strains tested (48). Even though these subjects can make BNABs, they are not made until months to years after infection, and BNABs that develop in the context of chronic HIV-1 infection do not necessarily protect from disease progression (49). The magnitude of cross-neutralizing response can be attributed to antibodies directed towards gp120, however, effective anti-gp41-antibodies targeting the membrane-proximal region (MPER) can also be elicited (50).

2.1.5 Native envelope structure

Env is produced as a highly glycosylated gp160 precursor protein, which is processed by a host protease into the two subunits gp120 and gp41 (51). These two proteins remain associated by non-covalent interactions and form trimeric spikes on the viral surface (52). Env is the only viral protein exposed on the viral membrane as well as on the membranes of infected cells. The infection process is initiated when gp120 binds to the primary CD4 receptor on the target cell (53). This interaction induces conformational changes of gp120 that expose and/or form the coreceptor binding site that is specific for the chemokine receptors CCR5 and CXCR4. Coreceptor binding triggers several conformational changes in gp41, which leads to the fusion of viral and host membranes, pore formation, and, ultimately, the release of the viral nucleocapsid core into the cell.

Structural information on HIV envelope spikes is available through combination of cryo-electron tomography (cryo-ET) and X-ray diffraction analysis. In 2008, following up on earlier analyses (54; 55) of simian immunodeficiency virus (SIV) virion spikes, two groups (56; 57) published separate cryo-ET analyses of inactivated HIV-1 trimers from the BaL strain. Liu et al. (56) were able to fit existing high-resolution crystal structures of complexes consisting of gp120 and two BNMAbs (58; 59) into their corresponding cryo-ET maps.

One difference concerns the conformation of the gp41 region. The maps from Liu et al. show a compact stalk, consistent with a compact stalk in the Zanetti et al. (55) study of unliganded SIV trimers, whereas the maps from Zhu et al. (54; 57) reveal a somewhat disordered tripod in the unliganded state. A possible structural basis for a compact stalk in Liu et al. (56) was provided later by the same group (60) who demonstrated that the MPER could pack stably as a trimeric coiled coil. Determining the native spike gp41 conformation at higher resolution, and in various states including bound to BNMAbs 2F5 and 4E10, would inform vaccine design on the exposure and orientation of MPER epitopes relative to the virion membrane and the rest of the spike.

The second important difference between the mentioned studies concerns the packing density of the gp120 domains in the trimer. The maps from Liu et al. (56) show well separated gp120 core domains that interact only through the variable loops at the top and gp41 at the base, consistent with Zanetti et al. (55), whereas Zhu et al (54; 57) show a much more compact trimer with no clear separation between gp120 domains.

Additional structures were published recently by Wu et al., further supporting the tripod variant with separated core domains (61), and by White et al., who observed a single stalk for multiple HIV-1 and SIV strains (62). Thus, the question of the native conformation of the MPER remains open. For the transmembrane domain and the C-terminal tail of gp41, no structural information is available in the context of native envelope trimers. Concerning the structure of gp41 in intermediate and postfusion states, see section 2.1.7.

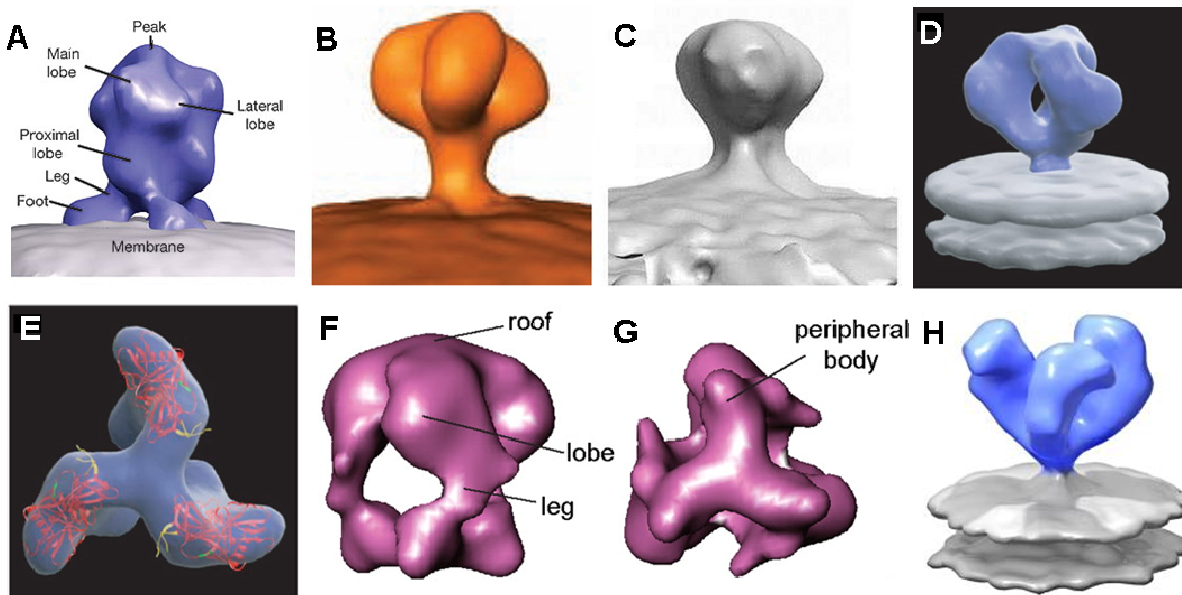


Figure 2. Alternative density maps of envelope spikes determined by cryo-ET. (A,B) Lateral views of SIV spikes from (54) and (55). (C,D) Lateral views of HIV-1 spikes from (57) and (56). Notably, in both SIV and HIV-1 spikes, either tripod-like legs or a single stem can be observed for the gp41 region, depending on image processing. (E) Top view from (56) with atomic coordinates from (59) fitted into the density map (PDB ID, 2NY7). (F,G) Lateral and bottom view from (61). (H) Lateral view of an open structure of a CD4-independent SIV isolate (62).

2.1.6 Specificities of broadly neutralizing antibodies

Broad serum reactivities can be explained either by many different antibodies that contribute to breadth (63), or by only one or a few antibody specificities that are responsible for breadth (64; 65). An important breakthrough of the past years has been the systematic generation and characterization of recombinant human monoclonal antibodies (MAbs) for HIV-1 vaccine development (65-68). Table 1 summarizes the specificities of representative types of BNMAbs and their targets, and figure 3 shows a structural model of an HIV-1 Env trimer and locations of conserved BNMAb epitopes. The specificities of most broadly neutralizing antibodies can be grouped into four categories: CD4 binding site; gp41 membrane proximal external region (MPER); quaternary V2, V3 loop; and carbohydrate. A potential fifth site, the coreceptor binding site, is sterically hindered and only accessible for small antibody fragments after CD4 binding (69).

Table 1. Characteristics of Human Antibodies Capable of Broadly Neutralizing HIV-1.

Antibody	Specificity	HCDR3 length
1b12	CD4 binding site	20
HJ16	CD4 binding site / DMR [#]	21
VRC01	CD4 binding site	14
2G12	Env glycans	16
PG9	Quaternary gp120 (V ₂ , V ₃)	30
PG16	Quaternary gp120 (V ₂ , V ₃)	30
2F5	gp41 MPER	24
4E10	gp41 MPER	20

[#] aa D474, M475, R476, see text for details.
References are to be withdrawn from text.

The prototype gp120 MAb, 1b12, binds to gp120 at its CD4 binding site, surrounded and protected by N-linked glycans (reviewed in (40)). An antibody specificity designated CD4bs/DMR is located near the CD4 binding site, depends on gp120 amino acids D474, M475, and R476 for reactivity, and can have considerable breadth (70). The epitope of antibody HJ16, identified by Corti et al (66), overlaps with DMR, the CD4 binding site and the 1b12 epitope. Wu and colleagues designed a resurfaced stabilized gp120 core to mimic the CD4 binding site to which BNMAbs but not weak or non-neutralizing antibodies bind. Using this resurfaced core as a fluorescently labeled probe to capture antigen-specific memory B cells, they isolated a CD4 binding site MAb, VRC01, which neutralized 91% of tested primary isolate Env pseudoviruses and exhibited the broadest neutralization activities of any antibody isolated to date (65).

Structural analyses of the CD4 binding site bound to MAbs 1b12 (neutralizing), F105 (non-neutralizing), and VRC01 (very broadly neutralizing) revealed the narrow site to which these antibodies must bind (59; 71). It was speculated that unusually long heavy chain

complementary determining region 3 loops (HCDR3) are required for neutralization ability; however, HCDR3 of broadest NMAb VRC01 has a mediocre length of only 14 aa.

Antibodies directed to a dominant linear epitope at the tip of the gp120 V3 loop are commonly made. Although potent against tier1 strains and T cell line-adapted (TCLA) strains, most V3 loop antibodies can neutralize neither tier 2 and 3 primary strains nor transmitted founder viruses (45). Zolla-Pazner isolated V3-specific human MAbs with a high degree of breadth from chronically infected HIV-1 subjects and recently identified an antibody, 2909, that recognizes a quaternary epitope involving gp120 V2 and V3 loops in the context of an Env trimer (reviewed in (72)). Two new BNMAbs, PG9 and PG16, also recognize quaternary gp120 V2 and V3 region epitopes, are dependent on V2 N-linked glycosylation sites, and neutralize ~80% of HIV-1 primary isolates (73; 74).

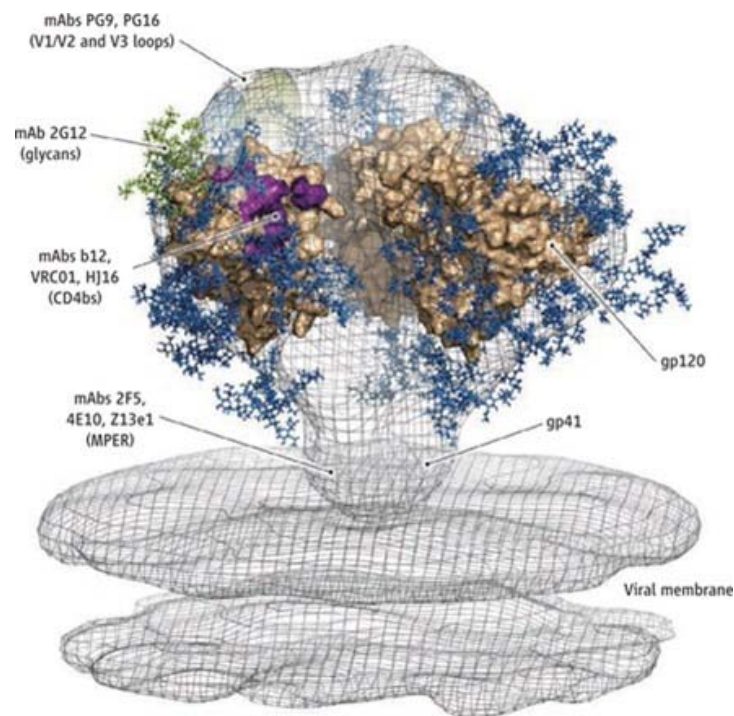


Figure 3. Broadly neutralizing monoclonal antibodies (BNMAbs) target epitopes on the viral envelope spike at the surface of HIV-1. The spike is a trimer containing the viral glycoproteins (gp120)₃ (gp41)₃. This model was generated by combining cryoelectron tomographic (56), crystallographic (59), and computational analyses. The gp120 core structure (tan) was fitted into the electron density map (gray). The membrane proximal external region (MPER) and viral membrane are shown. The V1/V2 and V3 protein loops are represented as ovals (light green and light blue) at the top of the spike. Glycans are represented in green and blue. The model was adopted from (75) and is produced on data from (40; 56; 76).

The 2G12 Env carbohydrate MAb is unusual in two aspects. First, it is the only purely glycan-targeted BNMAb isolated thus far. Second, it has a unique domain-swap structure such that its Fab region is composed of a heavy and light chain from two members of a 2G12 dimer (77). The glycans on gp120 are the result of host cell posttranslational glycosylation, and therefore resemble host carbohydrates, with oligomannose residues comprising most glycans on CD4+

T cell-derived virions (78). The glycans recognized by 2G12 comprise a unique conformational epitope of oligomannose glycans that is usually non-immunogenic (42).

Two prototype anti-gp41 membrane-proximal external region (MPER) NAbs have been identified. 2F5 binds to a core target in the heptad repeat-2 region of gp41, whereas 4E10 binds closer to the insertion site of the gp41 stalk into the virion membrane (79; 80). Z13e1 is an affinity-enhanced version and another, less potent BNMAb binding the MPER (81). Details on these anti-MPER antibodies including epitope conformation, membrane involvement and autoreactivity are elucidated below.

Thus, the HIV-1 envelope has at least four conserved regions that can be targets for broadly neutralizing antibodies. Many recombinant envelopes are antigenic and bind broadly neutralizing antibodies, but they are not immunogenic for these types of antibodies. However, BNMAbs can serve as templates to find immunogens which may induce neutralization. The design of a proper immunogen on the basis of BNMAb epitope information, as an approach to improve envelope vaccines, is termed “reverse vaccinology” (82).

2.2 gp41 – target for vaccine design

2.2.1 Structure and function of gp41

The lack of agreement between the cryo-ET studies described above (sec. 2.1.5) leaves the question of gp41 structure in native trimers open. gp41 anchors the infectious spike to the viral membrane and plays an important role in cell entry. It consists of ~345 amino acids (aa) with a molecular mass of 41 kDa, does not contain clearly defined variable regions, and is more conserved than gp120. As shown in fig. 4, it is divided into three major domains: the extracellular region, also called the ectodomain (aa 512 to 683; numbering is based on HIV-1 HXB2 (83)), the transmembrane (TM) domain (aa 684 to 705), and the cytoplasmic tail (CT) (aa 706 to 856). The ectodomain contains several distinct functional determinants involved in the fusion of viral and host cell membranes: (i) an N-terminal hydrophobic region that functions as a fusion peptide (FP) (aa 512 to 527); (ii) a fusion peptide-proximal region (FPPR) (aa 528 to 541); (iii) two α -helix repeat regions referred as the N-terminal heptad repeat (NHR) (aa 542 to 581) and the C-terminal heptad repeat (CHR) (aa 628 to 661); (iv) a disulfide-bridged hydrophilic loop that connects the two heptad repeats, also known as the connecting loop, the cluster I epitope, or the immunodominant (ID) loop (aa 598 to 604); (v) a Trp-rich region known as the MPER (aa 662 to 683). Numbering can vary depending on the study. Thus, gp41 is comprised of several distinct regions that each contribute unique functions.

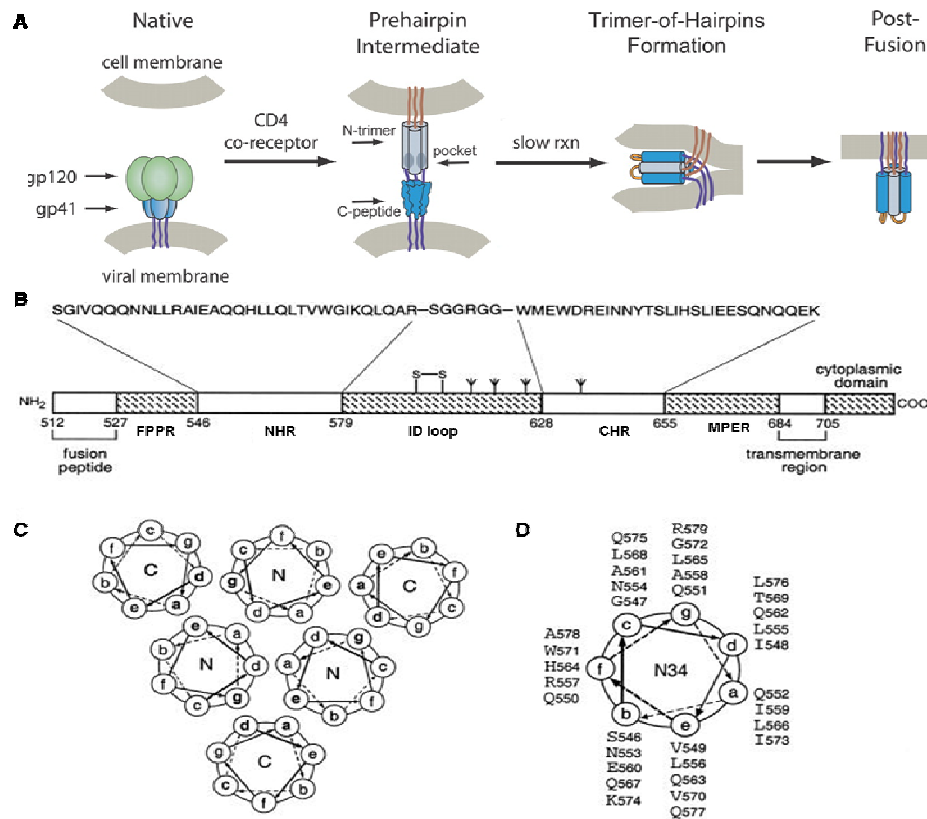


Figure 4. Structure and function of the HIV-1 gp41 envelope glycoprotein. (A) Upon cellular receptor recognition, gp120 and gp41 undergo conformational changes resulting in exposure of the N-trimer and its hydrophobic pocket in the prehairpin intermediate. Formation of the trimer-of-hairpins structure juxtaposes cellular and viral membranes and causes fusion. Figure A derived from (84). (B) Schematic representation of gp41. The important functional features of the gp41 ectodomain and the amino acid sequences of the N34 and C28 segments are shown. The disulfide bond and four potential N-glycosylation sites are depicted. (C) Cross-section of helix packing in the gp41 core. Residues at the a and d positions of the N helices form the hydrophobic interface of the trimeric coiled coil, and residues at the a and d positions of the C helices pack in an antiparallel orientation against residues at the e and g positions of adjacent N helices. (D) Helical wheel projection of the heptad repeat sequence of the N34 peptide. The view is from the N-terminus. Figures B-D adapted from (85).

The structure of whole gp41 is not clearly defined, since the available crystal structures of the HIV-1 gp41 ectodomain core do not contain the unstructured FP (86) and the ID loop (87-89). All studies revealed a six-helix bundle (6HB), which is considered to be the postfusion structure of the ectodomain and different from the native metastable structure of gp41 in the viral spike (90). The 6HB is a stable structure (a trimer of hairpins) in which three NHRs form a core bundle in parallel, with three CHRs associated in an antiparallel manner to the NHR bundle. The formation of 6HBs is accepted as being the process that brings the viral and the cellular membranes together and allows the aggregation of several activated Env complexes to form a pore, leading to the entry of the nucleocapsid into the cell (91). For a review of gp41 structure and fusion, see reference (92).

Two structures of gp41 including the MPER (93), one of them including also the FPPR (94), were published recently. Here, both regions form an alpha-helical extension of the rod, with the distal hydrophobic MPER residues bending and probably inserting into the membrane. In the pre-fusion and fusion intermediate states, the MPER is adopts different conformations. The

conformational differences among these three states are so great that each of them presents different distinct antigenic surfaces to the immune system. For example, non-neutralizing antibodies against cluster II recognize only the postfusion conformational state, which is different from the fusion-intermediate state targeted by MPER-directed BNMAbs (95).

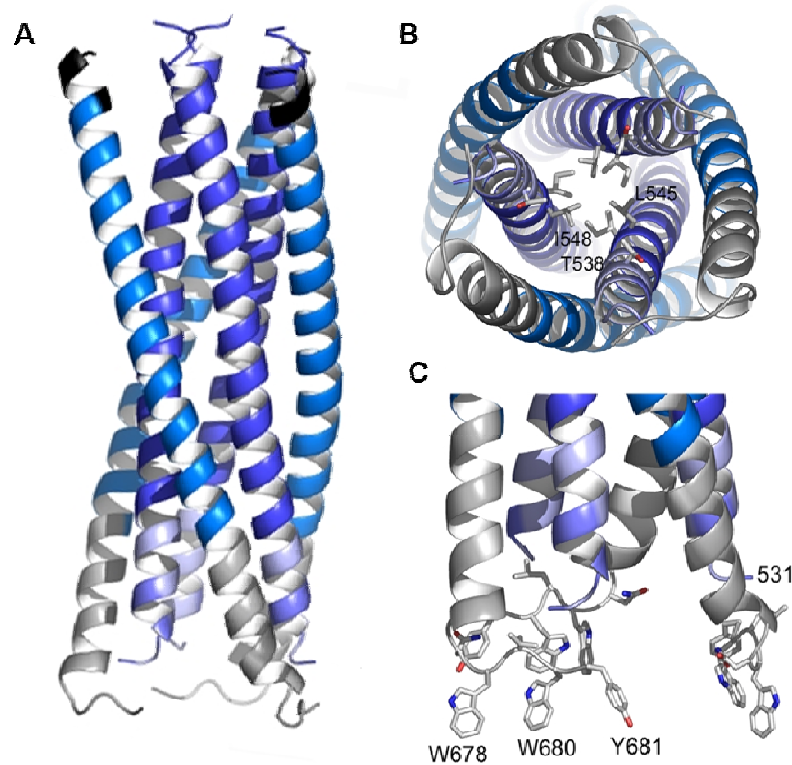


Figure 5. Ribbon representation of gp41 in a postfusion state. (A) The 6 helix bundle core (6HB) is colored dark blue (HR1) and marine blue (HR2). FPPR is colored in light blue and the MPER in grey. (B) View from the bottom showing residue Leu545 as the last coiled coil interacting residue of the HR1 core of gp41. The preceding heptad positions are Ala541 and Thr538. (C) Close up of the MPER and FPPR region shows the exposure of aromatic side chains Trp 678, Trp 680 and Tyr 681 towards the membrane. Figure adapted from (94).

For the TM region, structures are not available, but early computer modeling suggested that the TM region adopts an α -helix (96). The structure of the CT region is also not known, but a computer model predicts the presence of three aliphatic regions called lentivirus lytic peptides: LLP-3 (aa 789 to 815), LLP-2 (aa 768 to 788), and LLP-1 (aa 828 to 855) (97). The work of Cleveland et al., who used a MAb that targets intracellular CT, suggests that the protein could have other membrane-spanning domains (98). Thus, those authors proposed a model for a possible structure that shows CT doubling back through the membrane surface of the virus and back inside, possibly exposing a loop with the so-called Kennedy epitope on the surface of the virion (see fig. 6).

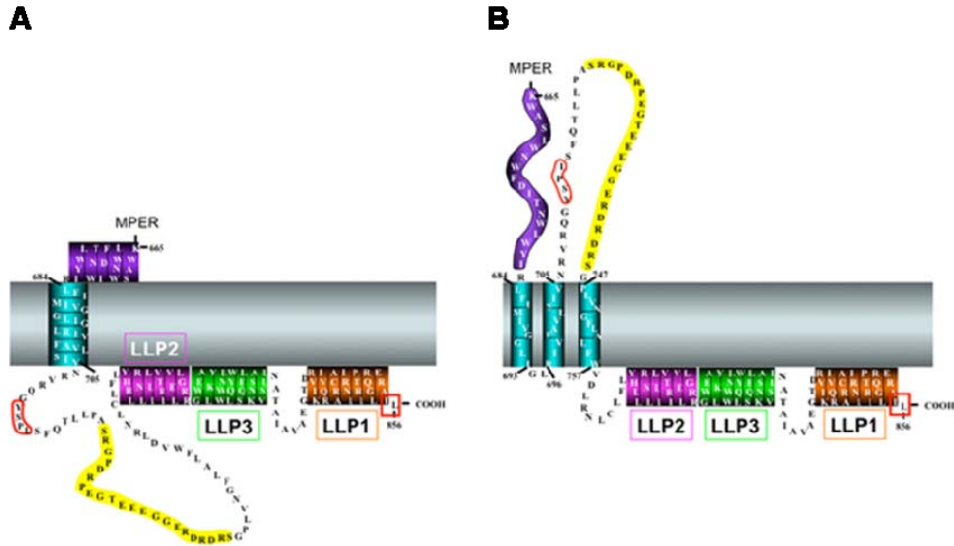


Figure 6. Alternative gp41 CT models. (A) Traditional CT model with one membrane-spanning α -helix and a completely cytoplasmic localization of the remaining CT sequence. LLP domains have been placed at their presumed membrane-localized position. (B) Alternative CT model with multiple TM segments as proposed by Hollier and Dimmock (99). This model proposes three membrane-spanning β -sheets and an extracellular localization of the Kennedy epitope. Independently of TM topology, two possible MPER confirmations are shown, one associated with the membrane (A) and one extending into the extracellular/viral space (B). Figure adapted from (100).

2.2.2 MPER – a conserved region of flexible structure

The MPER comprises the last 22 C-terminal amino acids of the gp41 ectodomain, ELDKWASLWNWFDITNWLWYIK (aa 662 to 683) (101), and contains at least two attributes that make it very attractive as a vaccine target: it is highly conserved, and the MPER contains epitopes that are recognized by three HIV-1 BNMAbs (102).

In order to fulfill its tasks during fusion, this region contains numerous hydrophobic residues and is unusually rich in Trp. The substitution of some of these residues dramatically inhibits viral entry into target cells (103). The MPER is a flexible region and adopts different conformations in different environments, or when bound to antibodies (induced fit conformations). In congruence with crystallographic studies of 6HB mentioned above, two NMR studies showed that the MPER adopts an α -helical conformation in DPC micelles in which the aromatic and polar residues are distributed around a helical axis (fig. 7) (104; 105).

Contrary to the studies that showed a helical MPER, structures of the 2F5 Fab bound to a peptide revealed (80) that this region forms an extended conformation with a distinct β -turn at the DKW in the core of the peptide epitope. The 4E10 epitope (aa 670 to 678) adopts an almost-helical structure (79) when bound to 4E10 Fab. Contrarily, Sun and colleagues observed that the MPER is kinked and L-shaped on the surface of micelles (104), with the 4E10 epitope embedded in the membrane. This supports the flexibility of the MPER, which undergoes large structural transition during fusion from an extended conformation to a helical structure. It is likely that hydrophobic residues interact with the membrane due to their proximity and the hydrophobic nature of the 4E10 paratope. Similarly, it was observed that 4E10 and Z13, which

neutralizing. The CHR bears the second-strongest immunodominant region, located near the N-terminal end of the 2F5 epitope and named epitope cluster II (aa 644 to 663) (111). Again, antibodies against this cluster are not neutralizing (112). Although it is thought that the CT of gp41 is contained by the viral membrane, there are several MAb that recognize a hydrophilic region in the Kennedy epitope at the N-terminus of the CT (aa 724 to 745) (113). Thus, regions within the CT could interact with the membrane, and perhaps cross it, to be exposed and form epitopes on the viral surface (section 2.1.7).

Against the MPER, only few reports showed an Ab response in natural infection. Unfortunately, most serum Ab responses to this region are not as broadly neutralizing as 2F5 or 4E10 in neutralization assays. Muhlbacher et al. found that serum reactivity against an MPER peptide (aa 642 to 673) corresponded directly to the recognition of infected T cells and to CD4 cell counts (114). More recently, Srisurapanon and coworkers studied the serum Ab reactivity against the peptide ELDKWA in HIV-1-infected subjects and showed that its frequency ranged from 15 to 35% (115). Opalka et al detected Ab responses to the MPER in HIV-1-positive serum, but there was no direct correlation between Ab binding and serum neutralization potency (116). This is not surprising, as the neutralizing activities in many sera are restricted to gp120 (117). Almost all long-term nonprogressors develop MPER binding Abs, albeit at very low levels, but it is unknown whether these reactivities are neutralizing (118).

2.2.4 Details on Broadly neutralizing antibodies binding the MPER

As mentioned above, three BNMAbs against the MPER, 2F5, 4E10, and Z13e1, have been discovered (102; 119; 120). Both 2F5 and 4E10 potentially neutralize a broad range of both laboratory-adapted and primary isolates of HIV-1 (120). Both MAbs were originally identified as IgG3s and were subsequently changed to IgG1; these are commonly used in the latter form. Of the two MAbs, 2F5 is a very potent neutralizing Ab, whereas 4E10 neutralizes a broader range of HIV-1 isolates, as shown by pseudovirus studies using an extensive panel of Envs derived from primary isolates (121). The 2F5 epitope was first mapped to a linear sequence (ELDKWA) (aa 662 to 667) on the MPER (122). This epitope has since been confirmed by others and has been expanded from the original 6-mer to a longer 17-mer linear epitope (aa 655 to 671) (123). The 4E10 epitope comprises the linear sequence NWFDIT (aa 671 to 676), which is just C-terminal to the 2F5 epitope in the MPER (102). As with 2F5, there is also conflicting information regarding the full 4E10 epitope, as a study suggested that 4E10 binds both the FP at the N-terminus of gp41 and the MPER epitope (124). Ala substitution studies of the MPER supported the crucial role of the conserved Trp672 in virus infectivity (103). Consistent with this, more sequence variation occurs on the opposite side of the helical epitope flanking the conserved WFXIT where there are fewer contacts with Ab. The critical MPER-contacting residues for Abs 4E10 and Z13e1 are located on opposing faces of the helix, placing the Z13e1 epitope on the

non-neutralizing face of the helix (125). The induced conformational change of Z13e1 upon binding is therefore negligible and could explain its lower neutralization potency compared to 4E10 and 2F5.

2.2.5 The importance of a membrane environment for 2F5 and 4E10

A study by Haynes and colleagues suggested that BNMAbs 2F5 and 4E10 are polyspecific, as they bind self-antigens (whole cells and cardiolipin (43)), and could be considered to be auto-Abs. However, the same group later observed differences in the kinetics of binding of 2F5 and 4E10 to membranes, to their protein epitopes, and to their protein epitopes conjugated to liposomes (126). Those authors concluded from this finding that 4E10 and 2F5 interact with the membrane and MPER protein epitope in a two-step model (127). Interestingly, when HIV-infected individuals were passively immunized with 2F5 and 4E10, no immunopathological side effects were reported (128). One can conclude that the autoreactivity of 2F5 / 4E10 is strong enough to support the recognition of their lipid-embedded epitopes, but weak enough not to lead to pathological effects (129). It is widely accepted now that cardiolipin autoreactivity is not the reason for difficulties in eliciting anti-MPER BNMAbs (130).

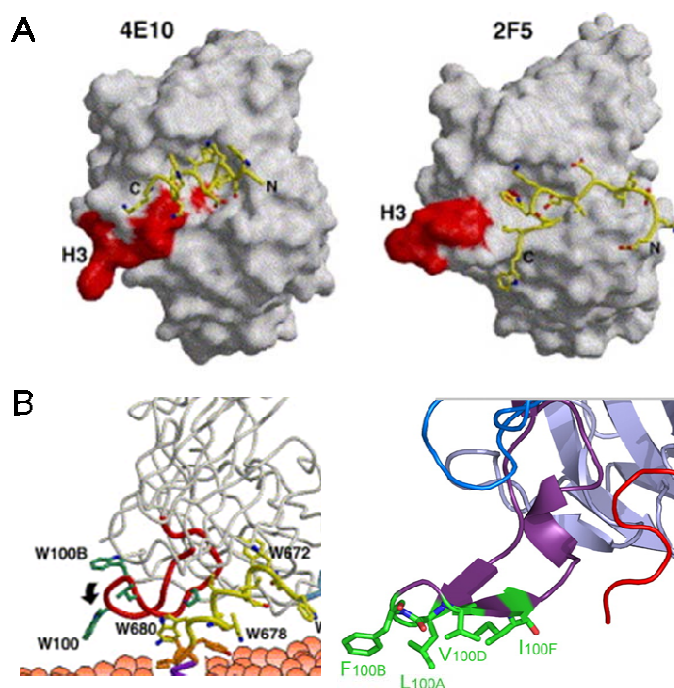


Figure 8. Hydrophobic residues on 4E10 and 2F5 interact with membranes. (A) View from bottom with hydrophobic residues (in red) in the CDR H3 loops forming a membrane interaction site next to the peptide interaction site (79). (B) View from side, with hydrophobic residues in green (79; 80).

It was suggested by crystal studies that the membrane-binding residues are located in the extended CDR H3 loops (79; 80), and recently they have been mapped down to aromatic residues at the edge of the antibodies (131). The notion that the lipid membrane is important for

the formation of the 2F5 and 4E10 epitopes in the MPER is further supported by functional data. Grundner et al. used proteoliposomes and flow cytometry to characterize the interaction of 2F5 and 4E10 Abs with their epitopes (in the context of gp145) presented in a lipid environment and observed enhanced binding in this context (132). In addition, several studies showed that MAbs 2F5 and 4E10 bound better to MPER in the context of liposomes than to the MPER without lipid (133; 134).

For 2F5 there was conflicting data about the absolute necessity of membrane binding for neutralization (133). However, recent studies comparing 2F5 and non-neutralizing antibodies targeting the same peptide epitope presume a critical role of its membrane-binding component for neutralization (112; 135). Efforts to understand the neutralization mechanism of BNMAbs 2F5 and 4E10 indicate that Ab-mediated fusion inhibition occurs at the same time as inhibition by the peptide C34 (corresponding to a region of the CHR like T-20), although by different mechanisms (136). This finding is consistent with other studies, which suggest that the 2F5 / 4E10 epitopes are mostly exposed in a fusion intermediate step after receptor binding (137; 138). Structurally, BNABs disrupt HIV-1 MPER fusogenic functions critical for virus entry either by preventing hinge motion or by perturbing MPER orientation (108). The comparison of the Z13e1 and 4E10 epitope structures revealed a conformational switch such that neutralization can occur by the recognition of the different conformations and faces of the largely amphipathic MPER (106). Taken together, it is likely going to be beneficial for vaccines to expose these epitopes in a membrane-bound, fusion intermediate conformation. Virus-like particles (VLPs) could be a suitable vehicle for an MPER-based vaccine, as they resemble mature virions and embed envelope proteins in their membrane.

2.2.6 Associated vaccine adjuvants and delivery

Appropriate adjuvants and delivery routes can account for success or failure of any vaccination effort. A variety of classical and molecular adjuvants were evaluated for serving in an HIV vaccine (139), with Alum and MF59 adjuvants being widely used with soluble envelope immunogens in phase II or III studies. The preservation of the antigenic structure of HIV-1 envelope immunogens, particularly conformational neutralizing epitopes, is an important requirement. Recently, polyanionic carbomers have been shown to be an effective alternative as adjuvant (140). For vaccines containing VLPs, carbomers might be the adjuvant of choice as the integrity of membrane-surrounded particles might be retained herein. Besides offering an environment for membrane proteins, VLPs harbour further advantages. A study compared the efficacy of humoral and cellular immune responses elicited by HIV-1 Env displaying VLPs, soluble monomeric gp120, and soluble trimerized gp140. Env-displaying VLPs not only elicited a broader antibody response, recognizing more linear Env epitopes and resulting in overall higher titers of neutralizing antibodies as compared to soluble Env variants, but were also the

only formulation which induced a robust Env-directed cellular immunity after intranasal immunization of BALB/c mice (141). Moreover, it should be noted that VLPs *per se* are potent activators of innate immune responses and induce maturation of DCs as judged by the upregulation of surface expressed CD80, CD86 and the enhanced secretion of inflammatory cytokines (142; 143). However, this intrinsic adjuvant property of retroviral VLPs has been mainly investigated using VLPs expressed by baculovirus in insect cells and could be in part attributed to the impurities carried over from this heterologous expression system.

2.3 Affinity enhancement of antigens

It is common to enhance an antibody's affinity to its antigen. Affinity-maturated antibodies can be used for diagnostic, research or therapeutic purposes. Contrarily, affinity-maturation of antigens is a novel idea. Antigens that have been matured against BNMAbs are supposed to be superior immunogens when it comes to induction of broadly neutralizing immune responses. The underlying intention is to identify a perfectly matching counterpart for the BNMAb with aid of display techniques. When presented to the immune system, the enhanced antigen might more likely induce a perfectly fitting counterpart, a BNMAb similar to the one used during the display procedure. However, the validity of this hypothesis – which is not a topic of this thesis - has yet to be proven.

2.3.1 Display techniques

Affinity enhancement of antigens can be achieved by maturation in display systems. Here, peptides or proteins ("phenotype") are coupled to their genetic information ("genotype"), good binders are selected by their phenotypic properties and the genetic information is retrieved. DNA libraries encoding a protein to be matured are transformed into screenable vehicles and screened for desired features. A variety of cell-based, viral and cell-free display systems has been developed (for a comprehensive review, see (144)). A schematic representation is shown in fig. 9. Cell-free, *in vitro* systems include ribosome display (145; 146), mRNA display (147; 148) and DNA display (149; 150). These systems are optimized for evolution of intracellular peptide ligands or proteins, like enzymes. Cell-based and viral display systems are able to present surface-exposed and transmembrane proteins, or any polypeptide coupled to a carrier protein. In prokaryotic phage display, polypeptides are fused to phage coat proteins for exposure on phage surface (151). BNMAbs b12 and Z13e1, as well as therapeutic antibodies against a variety of diseases, were discovered by using this technology (152).

If eukaryotic features like glycosylation are desired, baculoviruses and insect cells can be exploited (153; 154). Retroviral (155; 156) and adeno-associated viral (157) display systems on the basis of mammalian cells have become available, too. Instead of viral surfaces, polypeptides can also be screened directly on the surface of cells. Both Gram-positive and Gram-negative bacteria

have been exploited for bacterial cell display (158; 159). For eukaryotic proteins, yeast surface display has been established (160; 161). This cell-based technique has the advantage that flow cytometry and sorting technologies can be used for finer affinity discrimination of selected proteins.

In the last five years, also mammalian-cell-based systems have been developed. HEK293T cells (human embryonic kidney cell line) (162; 163), supt-1 and Jurkat-e cells (human T cell line) (164), DT-40 cells (chicken B cell line) (165), BHK cells (Syrian hamster kidney cell line)(166), HeLa (human epithelial cervical cancer cell line) and HT1080 (human sarcoma cell line)(167) served as display cells. Genetic information can be introduced into mammalian cells by transfection or infection. The method of choice usually is infection by retroviral vectors, because genetic material is stably integrated into the host cell genome, which leads to an unambiguous coupling of genetic information and phenotype displayed. For the display of membrane-embedded glycosylated proteins derived from mammals or pathogens thereof, retroviral vectors and mammalian cells offer the closest fit to nature.

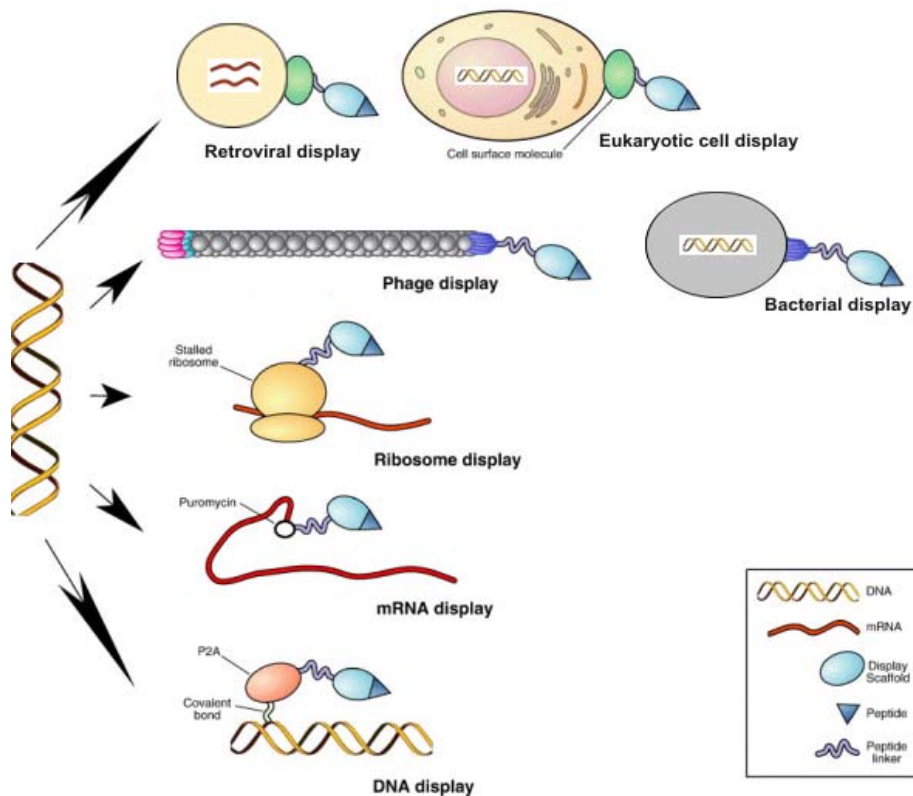


Figure 9. Scheme of available display technologies. All display platforms are based on the ability to physically link the polypeptide produced by a library clone to its corresponding genotype. This allows one to recover the DNA encoding the clone selected by the desired polypeptide phenotype, such as binding to a target molecule (figure modified from (144)).

2.3.2 Retroviruses and retroviral vectors

Retroviruses are enveloped viruses with two copies of a positive-sense, single-stranded RNA genome. The viral genome contains the genes *gag*, *pol*, and *env* encoding the core proteins (*gag*), the viral protease, integrase, reverse transcriptase (*pol*), and the envelope protein (*env*). Two identical long terminal repeats (LTR) harboring regulatory sequences such as promoters, enhancers, and polyadenylation signals flank the genome, and a single Ψ -site ensures selective packaging of the RNA genome into viral particles (fig. 10A).

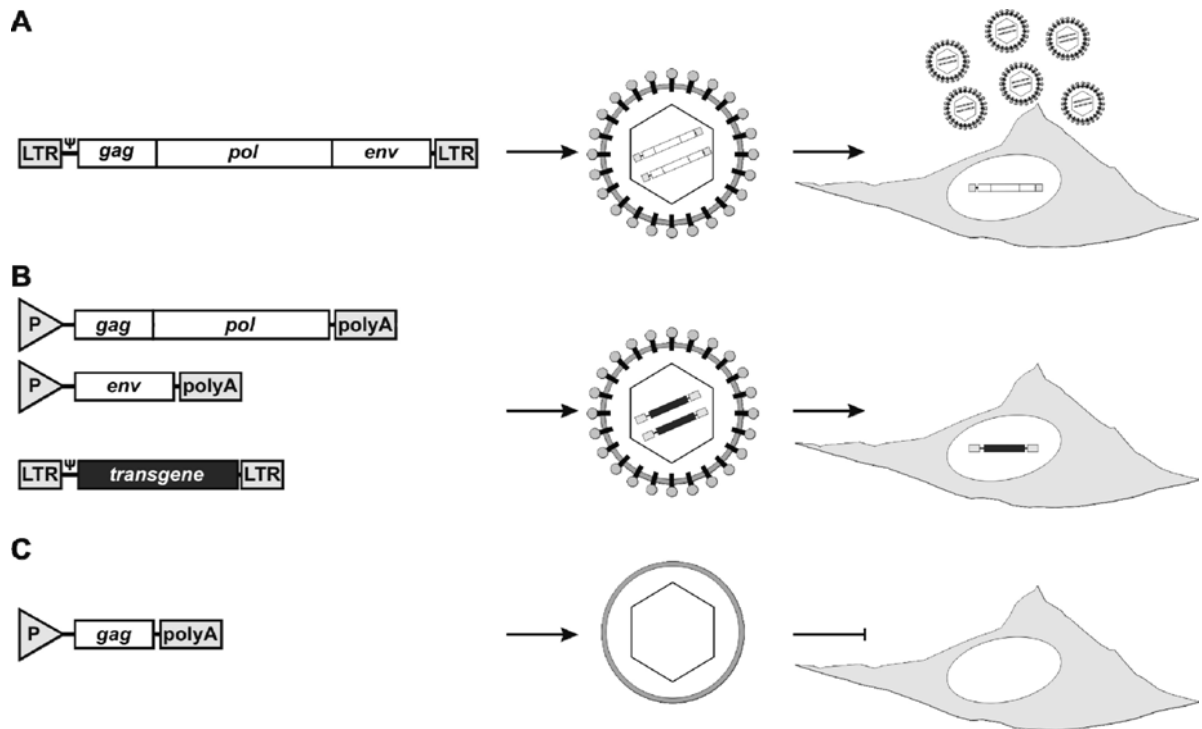


Figure 10. Retrovirus, retroviral vector and retrovirus-derived virus-like particle. (A) Transfection of DNA plasmids encoding full-length viral genomes (left) into producer cells results in the release of infectious replication-competent viruses carrying two copies of the viral RNA genome (middle). Following infection of target cells the viral genome is reverse transcribed into DNA and integrated into the host genome, and progeny virus is produced (right). (B) Retroviral vectors are produced by cotransfection of DNA plasmids providing *in trans* the *gag/pol* and *env* genes under the control of constitutive promoters (P) and harboring polyadenylation (polyA) signals along with a transfer plasmid encoding an LTR-flanked transgene of interest (left). Only the transfer vector RNA but no viral genes are packaged into particles by means of the Ψ -site (middle). Infection of target cells results in stable integration and expression of the transgene, which can be enhanced by a constitutive promoter between LTR and transgene, but no viral progeny are produced (right). (C) Transfection of plasmids expressing the *gag* precursor (left) into producer cells results in the release of plasma membrane-derived VLPs lacking genomic information (middle) and being noninfectious (right), and being thus suitable for vaccinations. Figure adapted from (156).

The retroviral life cycle is initiated by binding of the viral envelope protein Env to the cognate receptor on the target cell. For all retroviruses, Env is a trimeric transmembrane protein composed of heterodimers that are formed by the surface unit (SU) and the transmembrane protein (TM). Receptor binding induces conformational changes in SU and TM and ultimately leads to fusion of the viral and the host cell membranes and the release of the viral core into the

cytoplasm. Here, the genomic RNA is reverse transcribed into double-stranded DNA, which gets integrated into the host genome upon transport into the nucleus. A maximum of two copies (168), but mostly only one copy (169) is integrated, even after superinfection, because more integration events lead to cell death (168). Full-length genomic viral RNA, transcribed by the cellular machinery, is packaged into viral particles during the assembly process, and progeny virions bud from the host cell plasma membrane containing incorporated Env proteins.

Retroviral vectors are used to stably transfer genomic information of choice to target cells but encode an incomplete genome and are therefore replication-incompetent. To establish retroviral vectors, the genetic information of interest is flanked by retroviral LTRs, equipped with a Ψ -site and cloned into a transfer plasmid. All retroviral genes required for particle formation (*gag*, *pol*, and *env*) are provided in *trans* either on separate plasmids or chromosomally encoded in a packaging cell line (fig. 10B). Transfection of the transfer plasmid into a packaging cell line or cotransfection along with plasmids providing *gag/pol/env* leads to formation of infectious particles that have packaged the transgene encoding RNA but lack the genomic information for viral replication.

Virus-like particles (VLPs) resemble mature virions in terms of structure and membrane composition but do not contain any viral RNA and are noninfectious (170). VLPs have been shown to efficiently bud from cells that express only the retroviral precursor protein encoded by the *gag* gene (171), even in the absence of a functional *env* gene (fig. 10C). Co-expression of *pol*, which encodes the retroviral protease, along with *gag* leads to proteolytic processing of the Gag precursor into the matrix (MA), capsid (CA), and nucleocapsid (NC) proteins and also supports the self-assembly and budding of VLPs (172).

2.3.3 Retroviral display

Since retroviruses and retroviral vectors have plasma membrane-derived envelopes, the display of foreign polypeptides on their surface is guided by the same principles. Although the rules for efficient membrane incorporation are not fully understood, the overexpression of proteins equipped with a signal sequence directing the polypeptide to the secretory pathway and a transmembrane domain is likely to result in particle display but needs to be tested and confirmed empirically. The basic steps of retroviral display comprise library construction and selection (see fig. 11). Construction: DNA library construction by PCR or any other method creating gene mutants, cloning into provirus genome at appropriate site, amplification of proviral DNA in *E. coli*, transfection of permissive cells to produce an unlinked library (explained below), (5) low MOI infection of cells to produce a linked library. Selection: binding of virions to an antibody-coated solid phase, panning in form of stringent washing conditions, addition of cells for reinfection and amplification of bound virions. The selective steps can be repeated in an iterative way to enrich high affinity binders.

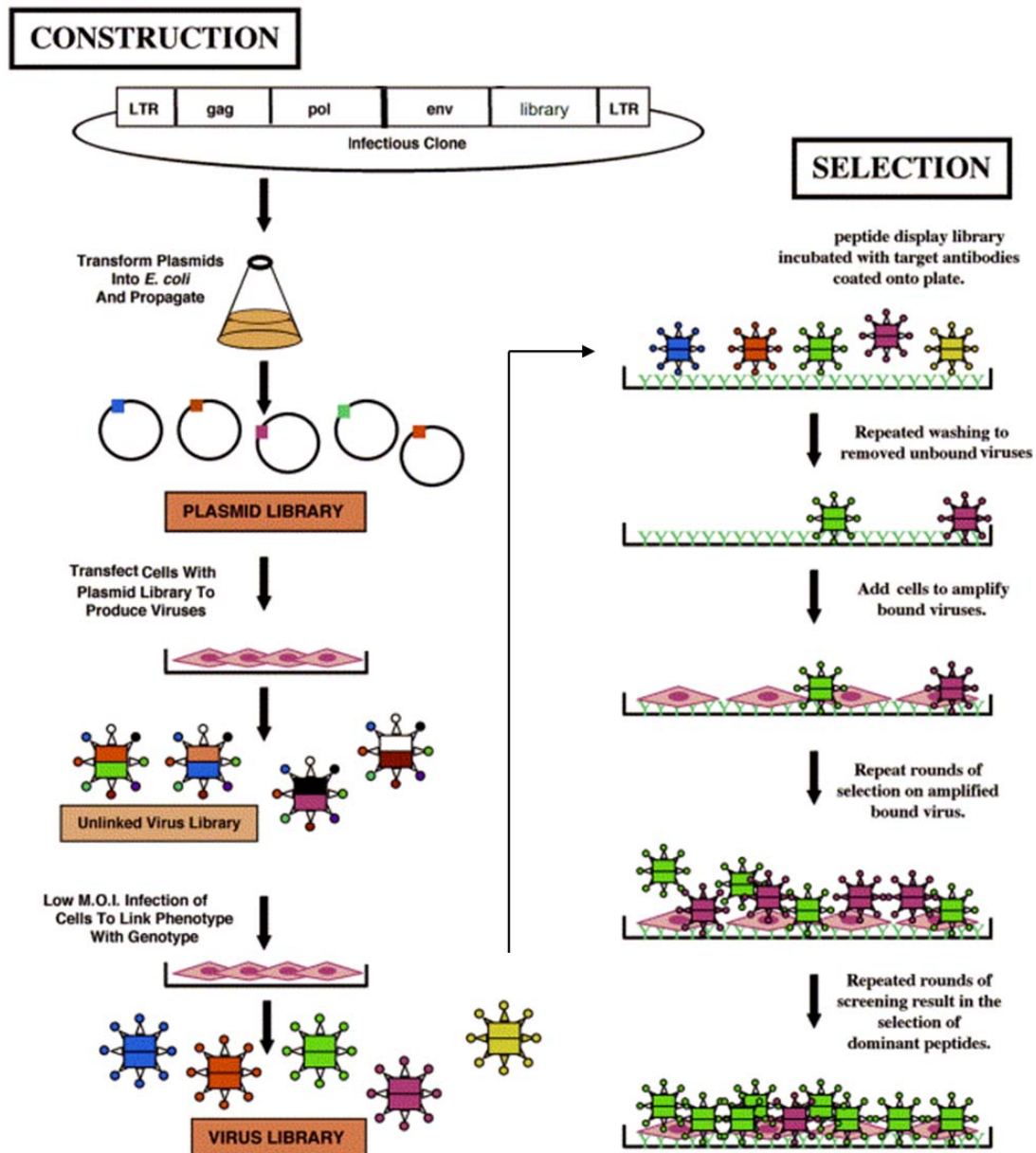


Figure 11. Schematic representation of a retroviral display system. Construction: A plasmid library encoding the provirus is constructed by inserting fragments generated by PCR or recombination. The virus is derived from an infectious molecular clone containing the gag and pol viral genes and a gene library, flanked by viral long-terminal repeats (LTRs). The resulting plasmids are transformed into *E. coli* to amplify the cloned plasmid library (each different gene variant is represented by a differently colored square). Virions displaying the heterologous envelope glycoproteins are produced by transfecting plasmid library DNA containing the infectious molecular clones into permissive cells (the different protein variants are represented as colored circles; the two strands of viral genomic RNA are represented by colored rectangles). Fresh cells are infected with the unlinked virus library at a low MOI to link the displayed glycoprotein phenotype with the packaged genotype in each virus of the virus library. Selection: A target antibody (Y) is coated onto a solid support, treated to reduce nonspecific virus binding, and incubated with the retroviral library. After washing to remove unbound viruses, cells are added to amplify the bound viruses. The selection strategy can be repeated in iterative rounds to select dominant peptides that bind a protein target. Figure adapted from (173).

Since the DNA transfection procedure results in the entry of multiple plasmids into a cell, and each plasmid encodes a different peptide, each transfected cell will express many different chimeric glycoproteins that can be incorporated into viral particles which will not carry the corresponding genes in the viral genomic RNA. Therefore, the initial production of recombinant

virus results in an unlinked virus library, i.e. the proteins expressed on the virion surface are not encoded by the viral RNA. Fresh cells are infected with the unlinked virus library at a low multiplicity of infection (MOI) to link the displayed glycoprotein phenotype with the packaged genotype in each virus of the Virus Library.

Retroviral display systems have been established on several retrovirus genera and for several purposes. Most retroviral display strategies aimed at changing infectivity and cell type tropism to direct gene therapy particles to designated tissues. Screening for catalytic activity is also possible, as was shown recently by MLV display in combination with a microfluidic technology to find highly active tissue plasminogen activator (TPA) genes (174).

Finally, retroviral display is applied in screening for binding affinity. Federspiel and co-workers randomized an octapeptide library and fused it to the envelope protein of avian leukosis virus (ALV) (173). Using two different immobilized antibodies as targets, octapeptides with specific binding affinities were successfully selected. Sequence analysis of the displayed octapeptide variants revealed no obvious bias, thus demonstrating potential advantages compared to the phage system, in which preferred codon usage and misfolding of eukaryotic polypeptides frequently results in sequence censorship (175).

In a similar approach, single-chain variable antibody fragments (scFvs) were selected from a library after fusion to the N-terminus of SU of MLV (176). In direct comparison to the phage system, the scFvs recovered from the MLV library showed strongly improved expression levels in human HEK293T cells. Lentiviruses have not been used as display vehicles until recently (163), and display systems based on lentiviruses were not available at the start of the present study.

It should be mentioned that in comparison to the phage system, the actual diversity of eukaryotic libraries is drastically decreased (typically $\sim 10^6$ for retroviruses and up to 10^{12} in the phage system). This is mainly due to limitations in the volume of eukaryotic cultures (significantly lower cell numbers compared to bacterial cultures) and the fact that the applied plasmids are usually large (>6 kb), for which reason the cloning of highly diverse libraries becomes more difficult. Hence, retroviral display seems advantageous solely for applications in which a eukaryotic expression system is really required.

2.4 Objective of the present study

A few broadly neutralizing monoclonal antibodies against HIV-1 have been described. These antibodies target highly conserved regions of the envelope protein. The exposure of these regions is thought to be an essential feature of a protective vaccine. In particular, the MPER of gp41 is highly conserved and target for potent BNMAbs 2F5 and 4E10.

The objective of this work was to design and evaluate novel immunogens based on HIV-1 gp41 with the potential to elicit BNMAbs. For this purpose, variants of truncated gp41 proteins were to be designed *in silico* with heterologous peptides for trafficking and heterologous zipper domains for trimerization. All immunogens should strongly expose the MPER with binding sites to known BNMAbs. After immunization of rodents, the presence of anti-MPER Abs with neutralizing activity in immune sera should be analyzed.

In a complementary approach, methods for the affinity maturation of gp41-derived proteins were to be established. For this purpose, a lentiviral display system based on HIV-1 was to be created which concurrently incorporates genetic information for both packaging function and antigenic phenotype within one genome. This procedure should be compared to a mammalian cell display system for its use with gp41-directed BNMAbs. Finally, a complex gp41-based library was to be created for screening of strong binders in the newly developed systems.

3 Methods

3.1 Nucleic acids molecular biology

3.1.1 Cloning of genes – general procedure

Cloning of genes, except for DNA libraries, was executed using standard cloning techniques (177). Vector plasmids were digested with restriction enzymes (NEB New England Biolabs, Ipswich, USA), dephosphorylated with Calf Intestine Phosphatase (CIP, Roche, Basel, Switzerland) and purified from a 1% agarose gel using QIAquick Gel Extraction Kit (Qiagen, Düren, Germany). Inserts were attained by (i) restriction of plasmids or (ii) PCR amplification (178) using a proof-reading polymerase (DeepVent, NEB) and subsequent restriction and gel purification. Tags and restriction sites were attached by primer extension PCR. Intervening sequences like zipper domains were introduced by fusion PCR. For a list of corresponding primers, see section 6.3. The constructs based on molecular clone HIV-1 96ZM651 were more efficiently amplified by adding 10% v/v DMSO. Ligation was carried out using a 3-fold molar ratio of insert to vector with Quick Ligase (NEB). The complete ligation assay was used to transform chemically competent *E. coli* K12 DH5 α (179) (supE44 Δ lacU169 (ϕ 80 lacZ Δ M15) hsdR17 recA1 endA1 gyrA96 thi-1 relA1) or DH10B (180) (F^- mcrA Δ (mrr-hsdRMS-mcrBC) Φ 80dlacZ Δ M15 Δ lacX74 endA1 recA1 deoR Δ (ara,leu)7697 araD139 galU galK nupG rpsL λ^-), prepared with RbCl₂ method (179) and plated on selection plates containing 100 μ g/ml ampicillin or 50 μ g/ml kanamycin. Colonies were screened for inserts with 2x PCR Mastermix (Promega, Madison, USA).

3.1.2 Cloning of DNA libraries (“IIS-ccdb” procedure)

To clone DNA libraries before or after sorting, the library was amplified with Phusion Polymerase (Finnzymes, Keilaranta, Finland) using primers extending for Esp3I (Fermentas) recognition and restriction sites (primers 8C8 & 6F8, see sec. 6.3). PCR products were gel-purified and eluted in buffer EB (10 mM Tris pH 8.5). In a IIS-ccdb reaction, inserts and pQL vectors (section 3.1.5.7) were mixed in a molar ratio of 3:1 up to 200 ng of total DNA, buffered in buffer Tango (Fermentas), complemented with 1 mM DTT and 10 units of enzyme Esp3I, filled up to a volume of 20 μ l and incubated at 37°C for 45 min. A reaction mix of 10 μ l consisting of Tango buffer, 1 mM DTT, 3 mM ATP, 10 U T4 ligase, and 10 μ l dH₂O, was subsequently added to a total volume of 30 μ l and incubated at 25°C, 37°C, 25°C for 45 min each. Ligase was heat-inactivated at 65°C for 10 min. For precipitation of DNA, 1 μ l of tRNA (10 μ g/ μ l, Roche) and 500 μ l of cold 100% ethanol were added, incubated at -20°C for 15 min and centrifuged at 20,000 g and 4°C for 15 min. The pellet was washed with 200 μ l of cold 70% ethanol, centrifuged at 20,000 g for 10 min, and resuspended in 10 μ l of 10 mM Tris pH 8.0. 2.5 μ l of concentrated DNA was added to 100 μ l of electrocompetent DH10B bacteria, incubated 1

min on ice, pulsed with 1.8 kV (GenePulser, BioRad), diluted with 500 µl of pre-warmed TB Terrific Broth medium (12 g Bacto tryptone, 24 g Bacto yeast extract, 4 ml Glycerol, 100 ml 0.17 M KH_2PO_4 and 0.72 M K_2HPO_4 , ad 1L), shaken at 37°C with 800 rpm for 30 min and plated on selection plates. Electrocompetent DH10B were generated by first growing a starter culture over night in LB medium Medium ((181), 0,5% (w/v) yeast extract, 1% (w/v) tryptone, 1% (w/v) NaCl, pH 7.4) without supplements, then inoculating a preparative culture (e.g. 200 ml) with an $\text{OD}(600)=0.02$, and finally incubating over night at 18°C until an $\text{OD}(600)=0.5$. Bacteria were centrifuged at 3,000 g for 10 min, resuspended carefully in ice-cold dH_2O (e.g. with 20 ml), washed two additional times with ice-cold dH_2O (e.g. with 10 ml), resuspended in a small volume of cold dH_2O (e.g. 1 ml), divided in 100 µl aliquots and used directly for electroporation. For long-term storage, bacteria were washed and resuspended in dH_2O containing 7% DMSO, shock-frozen in liquid nitrogen and stored at -80°C.

3.1.3 DNA preparation

After growing in LB medium with corresponding antibiotics (ampicillin or kanamycin), plasmids were prepared (“mini” format) with an alkaline lysis method and subsequent isopropanol precipitation (182). Plasmids were digested with appropriate restriction enzymes and analyzed by agarose gel electrophoresis and ethidium bromide staining. Sequencing was performed at Geneart AG Regensburg, Germany, using custom primers.

Transfection grade DNA was purified using Plasmid Midi or Maxi Kits (Qiagen), eluted with 10 mM Tris pH 8.0 and stored at -20°C. Immunization grade DNA was prepared with EndoFree Plasmid Mega or Giga Kits (Qiagen), eluted in endotoxin-free buffer QN (1.6 M NaCl, 50 mM MOPS pH 7.0, 15% (v/v) isopropanol) and stored at -80°C. All prepared DNA was controlled by restriction analysis, UV spectra and absorption ratio of wavelengths 260/280 (NanoDrop-1000 Spectrophotometer, Peqlab) resulting in ratios of 1.8 to 2.0. Immunization grade DNA was additionally checked for low endotoxin levels with aid of Limulus Amebocyte Lysate QCL-1000 assay (Lonza Group Ltd, Basel, Switzerland), with an outcome of <20 EU/ml.

High-throughput preparation of plasmids was done in 96well plates (sterile PP plate U-shape, Greiner Bio-One GmbH, Frickenhausen, Germany) by inoculating 200 µl of TB(Amp) medium in each well with a colony and growing over night at 37°C and 800 rpm. For sequencing purposes, bacteria were pelleted for 2 min at 3,000 g and treated like conventional mini-preparations. For transfection-grade DNA, plasmids were purified with QIAwell 96 Ultra Plasmid Kit (Qiagen).

3.1.4 Oligonucleotides

Synthetic oligonucleotides, used as primers in PCR and sequencing reactions, were purchased from Metabion International AG (Martinsried, Germany) or Invitrogen GmbH (Karlsruhe, Germany). A complete list of used oligonucleotides can be found in appendix 6.3.

3.1.5 Construction of genes and plasmids

3.1.5.1 Software-assisted design of gp41 derivatives

An N- and C-terminally truncated gp41 (“gp41ctm” or shortly “CTM”) was designed according to Lenz et al. 2006 (183). Wild-type sequences for synthesis of viral gene fragments were obtained from GenBank (184) and codon-optimized by use of GeneOptimizer program (185) at Geneart AG. Molecular clones of viral isolates HIV-1 89.6 (subtype B, accession number U39362), HIV-1 96ZM651 (subtype C, AF286224) and SIVmac239 (M33262) served as templates with aa 629-724 of 89.6 and 96ZM651 (HXB2 reference numbering) and aa 639-740 of SIVmac239 (SIVmac239 numbering). Membrane incorporation and orientation of all constructs was checked with aid of the transmembrane prediction TMHMM Server v. 2.0 (186), resulting in a C-terminal 9 aa extension for the SIV-derived sequence to ensure proper membrane incorporation. A human tissue plasminogen activator (TPA) leader sequence (187; 188) was fused N-terminally. Correct cleavage of the leader sequence was predicted by SignalP 3.0 software (189). A Kozak consensus sequence (GCCGCCACC, (190)) was inserted 5’ of the start codon for enhanced transcription. The corresponding sequences were optimized for human codon usage and synthesized by Geneart AG, and delivered in vector pGA4. The sequence for an HA-tag from *Influenza* virus Hemagglutinin HA1 protein (YPYDVPDYA, (191)) was codon-optimized using JCat (192) and inserted C-terminally by primer extension PCR (primers 3E8 & 2H4/2H5/2H6) for recognition of recombinant proteins. The resulting genes are called TPA-gp41ctm(89.6/96ZM/SIVmac239)-HA. A further N-terminally truncated gp41 version, called gp41ctm2, was constructed by PCR (primers 4H3/4H5/4H7 & 4H9/4I2/4I4), comprising aa 655-724 for 89.6 and 96ZM or aa 664-740 for SIVmac239. The topology of all gene variants was checked with Phobius Prediction Server (193).

3.1.5.2 Trimer-stabilized constructs and molecular visualization

Two zipper domains were inserted between TPA leader and gp41ctm sequences by fusion PCR. One motif was derived from the HA2 protein (amino acids 372–417, primers 3H4 & 3H5/3H6/3H7) of human *Influenza* virus strain H3 followed by a linker composed of amino acids Gly-Ser-Thr (194), resulting in the genes TPA-H3-gp41ctm(89.6/96ZM/SIVmac239)-HA. A second domain was derived from the GCN4 protein of *Saccharomyces cerevisiae* (195), resulting in the constructs TPA-GCN4-gp41ctm(89.6/96ZM/SIVmac239)-HA (primers 3B6 & 3B7/3B8/3B9). Sequences for GCN4 and H3 zippers were derived from Genbank (CY002064, BK006939) and codon-optimized with aid of JCat. To confirm the correct gene fusion position of zippers to gp41 fragments, molecular models were built using Modeller (196) and evaluated by calculating the DOPE score (Discrete Optimized Protein Energy, (197)). Resulting atomic models were visualized using PyMOL Molecular Graphics System (198).

3.1.5.3 gp41ctm Mini-Libraries

Eight point mutants of TPA-gp41ctm(96ZM) were designed for differential recognition by human monoclonal antibodies 2F5 and 4E10. Four constructs each were obtained from Geneart AG and cloned into pcDNA3.1(+) with NheI and KpnI. The panel of four constructs called 4E10-MiniLibrary comprises gp41ctm4E10++++, 4E10+++ , 4E10++ and 4E10+. The 2F5-MiniLibrary consists of gp41ctm2F5+, 2F5++ , 2F5+++ and 2F5++++.

3.1.5.4 gp41ctm degenerated library

A degenerated gp41ctm library was synthesized by Geneart AG using degenerate oligonucleotides. A total of 10^{10} different molecules were created ("raw non-amplified library"). This library was amplified by primers 8C8 and 8C9, and cloned into pWPXLd (see 3.1.5.7) via BamHI and EcoRI. Electrotransformation of *E. coli DH10B* resulted in 1×10^6 independent transformants ("cloned library") and delivered as plasmid preparation and bacterial glycerol stock. The raw library was amplified by PCR with primers extending for the HA-tag (8C8, 6F8) and cloned into pQL1 and pQL9 (see 3.1.5.7), resulting in 1.7×10^6 and 1.2×10^6 independent transformants, respectively.

3.1.5.5 Plasmids for gp41 immunogens

The plasmid pcDNA3.1(+) (Invitrogen Corp., Carlsbad, USA) served as expression vector humanized GFP, HIV-1 Gag(IIIB) and envelope genes (for humanized GFP and Gag sequences, see Graf et al. 2006 (199) and Graf et al. 2000 (200), resp.). In pcDNA3.1(+), gene expression is driven by a *human cytomegalovirus* (CMV) immediate early promotor/enhancer (201) and a bovine growth hormone (BGH) polyadenylation site (202). Envelope genes encoding for gp145(89.6P), gp120(89.6P), gp41(89.6P), gp41ctm and gp41ctm2, with or without HA tag, were adapted to human codon usage by Geneart AG and introduced via NheI and KpnI. Sequences were verified by primers T7-fw and BGH-rev.

3.1.5.6 Plasmids for AIO system

pTN-AIO is based on pTN7-Stop (203) and was kindly provided by M. T. Dittmar. pTN7-Stop is based on pNL4-3 (204), but has a gene for *Renilla reniformis* (Sea pansy) Luciferase (RLuc, (205)) inserted into the nef frame and a frameshift mutation in env leading to an early stopped Env protein. A G7069C mutation was introduced using site-directed mutagenesis (primer 1D1) by K. Schilling to remove a KpnI site and create a unique KpnI site 5' of RLuc at position 10448 (pTN7-Stop numbering). A unique FseI site and a Kozak sequence was inserted (primer 1H2) directly 5' of RLuc by T.-H. Bruun, resulting in pTN-AIO. RLuc was replaced by GFP via NcoI and KpnI for pTN-AIO-GFP. This reading frame was also replaced by a number of variants of TPA-gp41ctm-HA genes resulting in pTN-AIO_TPA-gp41ctm(89.6/96ZM/SIVmac239)-HA.

Inserts were checked by sequencing both strands (primers 1E6 & 1D5). Inserts were also amplified by primer extension PCR (primers 5G8 & 5D2) and inserted into the *vpr* reading frame according to Ali et al. (206).

Particles were pseudotyped by cotransfection with the plasmid pcDNA3.1-VSV-G (207) expressing a codon-optimized envelope glycoprotein of *Vesicular stomatitis virus* (VSV-G protein). For tetracycline-inducible expression, VSV-G was cloned into pcDNA5/FRT/TO (Invitrogen) via BamHI and EcoRI by A. Kliche (208) resulting in pcDNA5/FRT/TO_VSV-G. This plasmid was also used for generation of a stable cell line with Flp-In T-REx 293 cells following the manufacturer's protocol (Invitrogen).

3.1.5.7 Plasmids for lenti-cellular display

Packaging vector pTN7*/KpnI-mut/deltaSL1/3/BGH/CMV-LNGFR (or shortly pTN-Pack-Tat) is based on pTN7* and was created by K. Schilling (209). Essentially, the KpnI site at bp 7069 was mutated, a stop mutation was introduced into Tat reading frame, stem loops SL1 and SL3 were deleted to impair the Ψ packaging site, the 3'LTR was exchanged for a BGH polyadenylation site and RLuc was replaced by a low affinity nerve growth factor receptor (LNGFR) gene preceded by a CMV promotor.

MACS-based display (sec. 3.3.11) was performed using plasmids based on lentiviral vector pWPXLd (plasmid #12258, Addgene Inc., Cambridge, USA) for expression of envelopes. This plasmid carries a lentiviral expression cassette, consisting of 5'LTR, splice donor, Ψ site, splice acceptor, EF1 α promotor, GFP, WPRE (210), and 3'LTR. A master gene of gp41ctm was inserted after digestion with XhoI and EcoRI replacing the GFP reading frame, resulting in plasmid pWPXLd_TPA-gp41ctm. In a similar manner the degenerated gp41 library was inserted into this vector for panning in MACS-based display. A modified vector pPCR-WPXLd-QL (or shortly pQL1) was created by T.-H. Bruun (211) for use in the IIS-ccdb protocol. In pQL1, the lentiviral expression cassette from pWPXLd was fused with pPCR-Script (Agilent Technologies, Santa Clara, USA) backbone, and a gene coding the killer protein ccdb (212) flanked by restriction sites for Esp3I was introduced instead of GFP. pQL1 was used in both MACS- and FACS-based sorting. For FACS-based sorting only, a vector expressing both huGFP and the gene of interest was created by THB, called pcDNA-WPXLd-GFP-IVS-IRES-QL (or shortly pQL9). This plasmid was constructed by cloning the lentiviral cassette from pQL1 into the backbone of pcDNA3.1(+) (Invitrogen) and inserting a mammalian expression cassette between the EF1 α promotor (213) and the ccdb frame. The mammalian expression cassette consists of GFP, a synthetic intron called IVS (intervening sequence, (214)), and an internal ribosomal entry site (IRES) derived from encephalomyocarditis virus (215). TPA-gp41ctm-HA library and master gene were introduced into pQL1 and pQL9 by quick ligation using Esp3I. Inserts were sequence-verified by double-stranded sequencing (primers 3D2/3D5 & 5H7)

3.1.6 Reverse transcription (RT-PCR)

Immobilized virus was lysed in SideStep Lysis and Stabilization Buffer (Agilent Technologies), and 1 µl of lysate was applied to a reverse transcription reaction of 25 µl with *Moloney Murine Leukemia Virus* Reverse Transcriptase (MoMLV RT, Promega, Madison, USA), following the manufacturer's protocol, supplemented with a dNTP mix (Roche) following manufacturer's instructions.

3.2 Protein biochemistry

3.2.1 SDS-PAGE and Coomassie staining

SDS-PAGE was done as described before (216) with acrylamide concentrations of 12.5% or 15% in Hoefer systems (Hoefer, Holliston, USA). Protein content of cell lysates was determined prior to loading with the aid of Bradford staining (Biorad, München, Germany). All samples were heated to 95°C for 5 min in 2x sample buffer (125 mM Tris, 2% (w/v) SDS, 10% (v/v) β-mercaptoethanol, 1 mM EDTA, 10% (w/v) glycerol, 0.01% (w/v) bromophenol blue, pH 6.8). For quantification of VLP preparations, gels were incubated in Coomassie staining solution (0.125 % (w/v) Coomassie Brilliant Blue R-250, 50% (v/v) ethanol, 7% (v/v) acetic acid) for 30 min, washed for 10 min in dH₂O and destained over night in 7% (v/v) acetic acid.

3.2.2 Western and Slot Blots

Western Blot transfers of proteins from SDS gels were done in a semi-dry system (Serva, Heidelberg, Germany) according to manufacturer's instructions. For slot blots, protein solutions were loaded onto a Bio-Dot SF (Biorad) apparatus including 5 layers of pre-wetted Whatman Chromatography paper (Whatman International Ltd, Maidstone, UK) instead of pre-scribed Biorad filter paper and absorbed with a vacuum of 800 mbar. For both methods, nitrocellulose membranes with a pore size of 0.2 µm were applied (Millipore, Bedford, USA) and blocked in TBS (150 mM NaCl, 50 mM Tris/HCl, pH 7.4) containing 5% skim milk powder over night at 4°C. For antibody staining, blots were incubated for 1 h in TTBS (TBS + 0.3 % (v/v) Tween-20) with primary antibody, washed four times for 15 min in TTBS, incubated for 1 h in TTBS with secondary antibody, washed again four times for 15 min in TTBS, and subjected to either ECL (2.5 mM luminol, 0.4 mM coumaric acid, 0.1 M TrisHCl pH 8.5 plus equal volume of 0.018% H₂O₂, 0.1 M TrisHCl pH 8.5) or alkaline phosphatase (AP) staining solution 5 mM TrisHCl pH 9.5, 5 mM NaCl, 2.5 mM MgCl₂ plus 1/50 volume of NBT/BCIP stock (Roche)). AP reactions were stopped with excess of dH₂O and ECL reactions were measured in a ChemiluxPro device (Intas, Göttingen, Germany). Intensity of bands was quantified with the aid of Gel-Pro Analyzer software (Media Cybernetics, Bethesda, USA). Human monoclonal antibodies (MAbs) 2F5 and 4E10 (diluted to 5 µg/ml each) served for detection of gp41 derivatives, the HA-tag was recognized by rat MAb 3F10 ("anti-HA High Affinity", 0.1 µg/ml, Roche). p24 or Pr55 were

detected with mouse MAb M13/5 (cell culture supernatant, 1:500, (217)). As secondary antibodies served polyclonal HRP- or AP-coupled anti-human-IgG, anti-rat-IgG, and anti-mouse-IgG antibodies (all 1:2,000, all from Dako, Glostrup, Denmark).

3.2.3 ELISA

The amount of Pr55 or p24 protein in cell or virus lysates was quantified with the aid of an Enzyme-linked Immunosorbent Assay (ELISA) using MAb M01 (1:1000, Polymun, Vienna, Austria) as coating antibody. The method was previously described in detail (218).

An ELISA with gp41-derived peptides was used to quantify anti-gp41 immunoglobulins in animal sera, performed according to Deml et al. (219) by the end-point dilution method. Peptides spanning the MPER (96ZM-derived, EQNEKDLLALDSWNNLWNWFDITKWLWYIK, and 89.6-derived, EKNEKELLELDKWASLWNWFDITNWLWYIR) and CHR regions (96ZM-derived only, MQWDREISNYTNTIYRLLEDSQSQQEQNEK, all from Pepscan Presto BV, Lelystad, Netherlands) were used for coating at 100 ng/ml on Nunc Maxisorp plates (Thermo Fisher Scientific, Waltham, USA). HRP-coupled polyclonal anti-human-IgG antibody served as secondary antibody (1:4,000, Dako). Washing was done with the aid of a high-throughput microplate washing device (MAP-C2 workstation, Titertek Instruments Inc., Huntsville, USA).

3.3 Cell biology

3.3.1 Cell lines and cultivation

All eukaryotic cell lines were maintained in an atmosphere of 37°C and 5% CO₂ for adherent cells or 8% CO₂ for suspension cells. Human embryonic kidney (HEK) 293T epithelial cells (ATCC Microbiology Collections, (220)), FlpIn-T-Rex-293-derived tetracycline-inducible VSVG-expressing cells (293-TO-VSVG, by A. Kliche) and TZM-bl HeLa-derived indicator cells (NIH AIDS Research & Reference Reagent Program, (221)) were grown in Gibco Dulbecco's Modified Eagle Medium (DMEM) supplemented with 10% fetal calf serum, 100 U/ml penicillin and 0.1 mg/ml streptomycin (Invitrogen). Cells were sub-cultured twice a week at a ratio of approximately 1:15 using 0.05% trypsin and 0.02 M EDTA, as required. FreeStyle 293F cells (Invitrogen, suspension-adapted 293 cells (222)) were grown in Gibco FreeStyle 293 expression medium (Invitrogen) supplemented with 50 U/ml penicillin and 0.05 mg/ml streptomycin at 125 rpm and handled according to the manufacturer's instructions.

3.3.2 Cell counting

For manual cell counting, cell suspensions were stained 1:1 with 0.4% trypan blue in phosphate buffered saline (PBS, 137 mM NaCl, 2.7 mM KCl, 4.3 mM Na₂HPO₄, 1.47 mM KH₂PO₄, pH 7.4). The number of viable cells was determined with the use of a Neubauer Improved counting chamber (Roth, Karlsruhe, Germany). For automated counting, cells were loaded into a cell

viability analyzer (Vi-cell XR, Beckman Coulter GmbH, Krefeld, Germany) and counted with the aid of associated software.

3.3.3 Transient transfection

HEK293T cells were seeded in 6-well plates (4×10^5 cells in 2 ml medium). 24 h after seeding, medium was replaced by 1 ml of DMEM without supplements. Cells were transfected with the respective expression vector(s) according to the poly-ethylenimine (PEI) transfection method (223) using a total of 2 μ g DNA and 8 μ l of a 1 mg/ml PEI in H₂O solution and 50 μ l DMEM without supplements. Components were mixed on a vortex device, left standing for 10 min at room temperature and added drop-wise to the cell suspension. 4 h later, transfection medium was replaced with 2 ml of supplemented growth medium. For smaller (24- / 48- / 96-well) or larger (10 cm / 15 cm Petri dishes) assays, the number of cells, the amount of DNA and PEI, and the volume of medium was down- or up-scaled, based on the vessel surface area.

293F cells were adjusted to 1 million cells/ml in fresh FreeStyle medium and 30 ml of cell suspension were transferred to 125 ml flasks. 37.5 μ g of DNA and 150 μ l of PEI and 1.8 ml DMEM without supplements were mixed for transfection of one flask. 4 h later, transfection medium was replaced with 30 ml of supplemented FreeStyle medium.

3.3.4 VLP production

VLPs for immunization purposes were produced in 293F (gp41ctm, GCN4-gp41ctm, H3-gp41ctm, non-pseudotyped) or 293T cells (gp41ctm2) with the use of a codon-optimized, Rev-independent gene for Gag(IIIB) (200). For pseudotyped VLPs, plasmids encoding for Gag and Env were mixed in a ratio of 2:1 in a co-transfection assay. VLPs were harvested 72h p.tr., cleared by centrifugation at 3,000 *g* for 15 min, loaded onto a 30% sucrose in PBS cushion (5 ml for 30 ml of supernatant) and ultra-centrifuged at 100,000 *g* for 2h. The pellet was resuspended over night in PBS and stored at -80°C, with an aliquot analyzed by SDS gel electrophoresis and Coomassie staining for quality control.

3.3.5 Virus production

Virus for the AIO system was produced by co-transfection of 293T cells (3.3.3) with a plasmid bearing the respective molecular clone and an expression plasmid encoding the VSV-G gene in a molar ratio of 1:4. Alternatively, 293-TO-VSVG cells were transfected with provirus and induced with 1 μ g/ml doxycycline. Virus for lenti-cellular display was generated by triple-transfection of 293T cells with pTN-Pack Tat (for packaging), pQL1 or pQL9 (for Env expression) and pcDNA3.1-VSV-G (for infection) using a ratio of 4:3:1.

For both systems, virions were harvested 96 h p.tr. and cleared by centrifugation at 3,000 *g* for 15 min. An aliquot was lysed for p24 quantification. Remaining virus was stored at 4°C until low

MOI infection of fresh cells. MOI was determined once by an infectivity assay and later deduced from p24 content with a parallel simultaneous AIO-GFP or pQL1-GFP control.

3.3.6 Cell and virus lysates

Virus and VLP supernatants were lysed for subsequent analysis with a final concentration of 0.5% Triton-X100 for 1 h at room temperature. Cells were harvested in ice-cold PBS and lysed in triple detergent lysis buffer (TDLB, 50 mM Tris pH 8.0, 150 mM NaCl, 0.1 % (w/v) SDS, 1 % (v/v) Nonidet P-40, 0.5 % (w/v) sodium desoxycholate) supplemented with a protease inhibitor cocktail (Complete Mini, Roche).

3.3.7 Sucrose gradients

After purification through a sucrose cushion, VLPs or virions were loaded onto a 10 ml 10-50% sucrose gradient and ultra-centrifuged at 100,000 *g* for 2.5 h. 20 fractions of 0.5 ml each were collected. For Western Blot analysis, particles were pelleted by trichloroacetic acid (TCA) precipitation. ¼ volume of 100% (w/v) TCA was added to the samples, incubated for 10 min at 4°C and spun at 14,000 *g* and 4°C for 5 min. The pellet was washed two times with cold acetone, dried at 95°C for 5 min and resuspended in SDS sample buffer. For crosslinking and EM experiments, fractions 13-17 were pooled, diluted in PBS to 12 ml, ultra-centrifuged at 100,000 *g* for 1.5 h and resuspended in PBS.

3.3.8 Crosslinking

Gradient-purified VLPs were incubated with indicated concentrations of BS³ (“no-weigh format”, Pierce, Thermo Fisher Scientific) for 30 min at room temperature. The reaction was quenched by adding 1 µl of 1 M Tris pH 8.0 and 1/5 volume of 5x SDS sample buffer was added for SDS gel electrophoresis.

3.3.9 Electron microscopy

Sucrose-cushion purified VLPs were incubated with primary antibodies 4E10 (anti-gp41) or 3F10 (anti-HA) for 1 h at 37°C and further purified on a sucrose gradient. Pooled and resuspended VLPs were adsorbed to grids after fixation with 2% glutaraldehyde. Grids were washed in TBS (Leica EM IGL), blocked with 3% gelatine in TBS for 1 h at RT, and incubated with an anti-human IgG immuno-gold conjugate (particle size: 10 nm; Aurion, Wageningen, Netherlands) for 1 h at room temperature. After three washes in TBS, grids were contrasted with phosphoric tungstic acid and examined in an electron microscope (Zeiss EM 10C/CR).

3.3.10 Cytometric analysis and fluorescence-activated cell sorting (FACS)

Cells were detached 48 h p.tr from wells in PBE buffer (PBS + 1% FCS, 1 g/l NaN₃, 2 mM EDTA), pelleted at 300 g for 3 min, washed in PBE, incubated with the indicated fluorochrome-labeled antibodies (3 µg/ml 2F5 or 4E10, anti-HA-antibodies 1:10) for 1 h at room temperature and washed 2 times with cold PBE. 2F5 and 4E10 antibodies were labeled with AlexaFluor-647 (Protein Labeling Kit, Invitrogen) according to the manufacturer's instructions. A mean of 6 fluorochromes was attached to each IgG molecule, as measured by photometric analysis (NanoDrop software v3.7.1). anti-HA-antibodies were purchased as conjugates with Fluorescein (clone 3F10, Roche), PerCP and AlexaFluor-405 (both polyclonal rabbit sc805, Santa Cruz Biotechnology Inc, USA). Apoptosis staining was done by the use of 7-AAD and Annexin-V-APC antibody (both 1:100, both BD). Finally, cells were subjected to cytometric analysis in FACS Canto II or sorted in FACS Aria (both BD, both with FACS Diva software v6.0).

3.3.11 MACS sorting

Cells were incubated with 20 µg/ml of 2F5 or 4E10 for 1 h at room temperature, washed two times with cold PBE buffer, incubated with a mixture of anti-human-IgG antibodies coupled to APC (1:500, goat F(ab')₂ fragment, Jackson ImmunoResearch Ltd, Suffolk, UK) or magnetic beads (1:5, microbeads, Miltenyi Biotec), washed another two times, filtered through 30 µm pre-separation filters and applied to MS MACS columns in an OctoMACS magnetic stand (both Miltenyi Biotec). Cells were rinsed two times with 0.5 ml degassed PBE, pressure-eluted with 1 ml PBE and cytometrically analyzed. Genomic DNA was isolated by use of QIAamp DNA Blood Mini Kit (Qiagen) following the manufacturer's instructions and inserted envelope genes were amplified by PCR using primers 6F8 and 8C8.

3.3.12 Virus panning

96-well Nunc Maxisorp plates (Thermo Fisher Scientific) were coated with 20 µg/ml of anti-human-IgG in 100 mM carbonate buffer pH 9.5 over night at 4°C, washed 3 times with PBS-T (PBS + 0.2% Tween 20 using Hydroflex washer, Tecan AG, Männedorf, Switzerland), incubated with 10 µg/ml of indicated BNMAb, washed 3 times with PBS-T, blocked with 10% FCS in DMEM, washed another 3 times in PBS-T and flicked on paper towels. Virus produced for lentiviral display was titrated by use of p24 sandwich ELISA (3.2.3) and applied with a maximum p24 concentration of 100 ng in a total of 100 µl. Plates were incubated at 37°C for 1 h and washed 3 times with PBS by the use of a multi-channel pipet. Immobilized virus was lysed in 0.5% Triton-X for ELISA or in SideStep Lysis and Stabilization buffer (Stratagene) for RT-PCR (sec. 3.1.6). Alternatively to lysis, wells were covered with 5x10⁴ TO-VSVG cells in DMEM growth medium supplemented with 8 µg/µl Polybrene for reinfection and cells were transferred to cell culture-treated 48-well plates next day in growth media containing 1 µg/ml doxycycline.

For infectivity assays, wells were covered with 2.5×10^4 TZM-bl cells and stained 48 h p.inf. (sec. 3.3.13).

3.3.13 Infectivity assay

The adherent TZM-bl cell line expresses the β -galactosidase and *Photinus pyralis* (firefly) luciferase reporter genes under the control of the HIV-1 long terminal repeat promoter. To determine virus infectivity on this cell line, supernatants of transfected 293T cells were filtered through a 0.45 μ m pore size filter and analyzed for total amounts of particle-associated CA antigen by ELISA. A total of 1.5×10^4 TZM-bl cells were seeded in cell culture-treated 96-well plates and infected 24 h later with different dilutions of the virus-containing supernatants. At 48 hours after infection, number of infected cells was determined as described previously (224). Basically, cells were fixed, washed with PBS, stained with the β -galactosidase substrate X-Gal (5-bromo-4-chloro-3-indolyl- β -d-galactopyranoside) for 1 h, washed again and blue cell nuclei were counted using a robotic Elispot system (EIRob05i, Advanced Imaging Devices GmbH, Straßberg, Germany, with AID Elispot software v6.0).

3.4 Animal experiments

3.4.1 Rodent immunizations

Female BALB/c mice (Charles River, Sulzfeld, Germany) and New Zealand rabbits (Harlan UK Ltd, Belton, Leicestershire, UK) were pre-bled at the age of 12 weeks. Rodents were immunized 2 times with 100 μ g (mice) resp. 500 μ g (rabbits) of plasmid by i.m. saline injection with 50 μ l / 250 μ l of plasmid DNA in both *tibialis anterior* resp. *quadriceps* muscles, followed by i.m. booster immunizations with either 40 μ g / 200 μ g of VLP or 10 μ g / 50 μ g of recombinant protein, adjuvanted with 1% Carbopol (140). The integrity of pseudotyped VLPs in Carbopol was checked by sucrose gradient ultracentrifugation and following Western Blot analysis.

Blood was recovered from mice by tail vein bleeding and from rabbits by ear vein lancing at the indicated time points. Serum was obtained by incubation for 1 h at 37°C, 1 h on ice, centrifugation at 20,000 *g* for 15 min, and complement inactivation by incubation of supernatant at 56°C for 30 min. Anti-gp41 antibodies were quantified by an end-point dilution ELISA assay (in duplicate) on samples from individual animals (see 3.2.2).

3.4.2 Removal of anti-cell antibodies

HEK293T or 293F cells were stacked by centrifugation at 300 *g* for 3 min, supernatant was aspirated and cells were stored at 4°C for up to one week until usage. Stacked cells were dissolved in an equal volume of animal serum and shaken 3, 6 or 9 times for 4 h at 800 rpm at room temperature, until the signal of anti-cell antibodies was below two times the background signal in cytometric analysis.

3.4.3 Virus neutralization assays

Virus neutralization assays were performed in the laboratories of groups of Prof. Mike Seaman (TZM-bl assay, Harvard Medical School, Boston, USA) and Prof. David Montefiori (A3R5 assay, Duke University School of Medicine, Durham, USA), according to the published protocol (225).

4 Results

4.1 Novel gp41 immunogens

Four novel gp41-derived immunogens were created and characterized in this work. These immunogens were functionally tested in two animal immunization studies, as stand-alone constructs in homologous DNA prime / VLP boost regimens or in combination with two gp41-derived soluble proteins.

4.1.1 Design and characterization of trimer-stabilized and truncated gp41 derivatives

4.1.1.1 Design of gp41 constructs with enhanced MPER exposure

As the most potent broadly neutralizing antibodies directed against gp41 target the MPER of gp41, the present study aimed at focussing the immune response against this part of the protein, by using a truncated gp41 variant. The second factor influencing the design was the observation that membrane proximity seems to be important for proper folding of the MPER epitopes. Due to this reason, we chose to present the protein in its natural environment, incorporated into a membrane of virus-like particles. A previously described gp41-derived protein ("gp41ctm", (183)) is a recombinant N-terminally truncated gp41 protein, consisting of CHR, MPER, TM, and a shortened CT, which can be incorporated into liposomes. This protein was likely to fulfill our requirements of epitope focusing and membrane incorporation, and served as basis for the development of novel gp41-derived immunogens. The molecular clones 96ZM651 (HIV-1 clade C), 89.6 (HIV-1 clade B) and SIVmac239 served as sequence templates. A signal peptide from the human tissue plasminogen activator gene (TPA) was N-terminally fused to ensure that the protein is efficiently directed towards the cell membrane in mammalian cells (226). An HA-tag of nine amino acids was added C-terminally for uniform detection of the corresponding proteins (fig. 12). The C-terminal tail is thought to loop back to the extracellular / extraviral space, enabling access to antibodies (98; 113; 227). As proper trimerization is thought to be beneficial for proper display of immunologically relevant sites, two heterologous trimerization domains were introduced between the signal peptide and the gp41-derived part. Both GCN4 and H3 zipper domains have been successfully before to stabilize a gp41 post-fusion (195) or intermediate structure (194). To further focus the immune system on the relevant MPER region, another construct called gp41ctm2 was created, with a further shortened CHR domain. As previous immunization experiments showed success not only with VLPs but also with soluble proteins as booster reagents, two existing recombinant gp41-derived proteins were included in the study. GCN4-gp41ctm-FD is a trimer-stabilized recombinant protein with a gp41 CHR part, surrounded N- and C-terminally by zipper domains (194). CTB-

MPER, on the other hand, is a fusion protein of only a 30 aa MPER peptide and the non-toxic subunit of cholera toxin B as a molecular adjuvant (228).

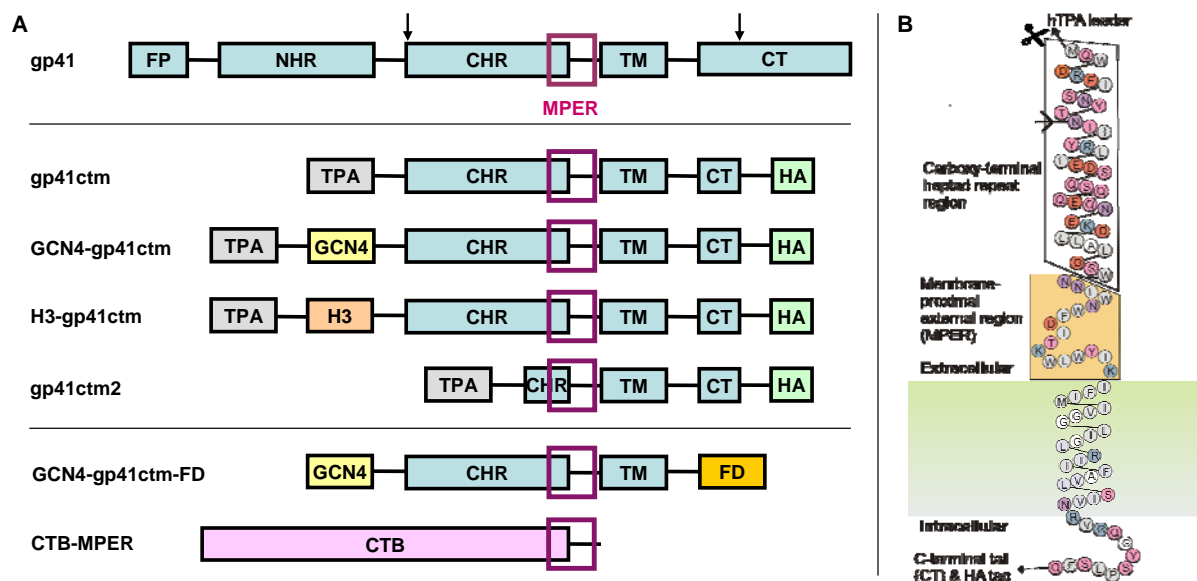


Figure 12. Design of novel gp41-derived immunogens. (A) Four proteins based on gp41 were designed in this work. Two of them are stabilized in a trimeric conformation by heterologous zipper motifs (GCN4, H3). All of them are directed by a TPA signal peptide towards the cell membrane and can be detected by a C-terminal HA tag. Two previously described soluble gp41-derived proteins (GCN4-gp41ctm-FD and CTB-MPER) were used in booster combinations. (B) Scheme of truncated gp41 proteins on the surface of cellular membranes. The amino acid sequence in this figure is derived from isolate 96ZM651 (clade C).

4.1.1.2 Molecular modeling and prediction of correct protein topology

Two crucial steps, the cleavage of the signal peptide and the membrane orientation, were controlled with appropriate prediction software. SignalP server was used for analysis of signal peptide cleavage, TMHMM Server 2.0 for prediction of membrane incorporation and orientation, and Phobius server for a combination of both. Proper signal peptide cleavage was predicted for all constructs. In contrast, a wrong membrane orientation was predicted for the SIVmac239-based gp41ctm construct. For this reason, the cytoplasmic tail was elongated for 9 aa compared to 96ZM651- and 89.6-based templates, resulting in a 1 kDa heavier protein. Correct membrane topology was predicted for all constructs after this modification (fig. 13A exemplarily for basic construct TPA-gp41ctm(96ZM)-HA).

The correct insertion position of the GCN4 trimerization domain was predicted by homology modeling. A molecular model of a GCN4-gp41ctm fusion protein was built based on a solved structure of a GCN4-NHR fusion protein (1ENV, (195)). Another three models were built with insertion of one, two, or three flexible aa (G, S, T) in the GCN4 fusion site as linkers, changing the orientation of hydrophobic and hydrophilic residues in the helices. The structures of all models were optimized using the Modeller server, and the minimized energy was calculated by the aid of DOPE score (fig. 13B). As expected, the original model without insertions showed the minimal energy and was chosen for cloning as it represents the structure with the highest

stability, followed by the structure with insertion of a 3 amino acid linker. The calculated energy of the models was close to those calculated for the template GCN4-NHR with -30.8 kJ/mol. For the H3 zipper domain, the orientation was adopted from existing fusion proteins by Hinz et al. (194), including a three amino acid spacer.

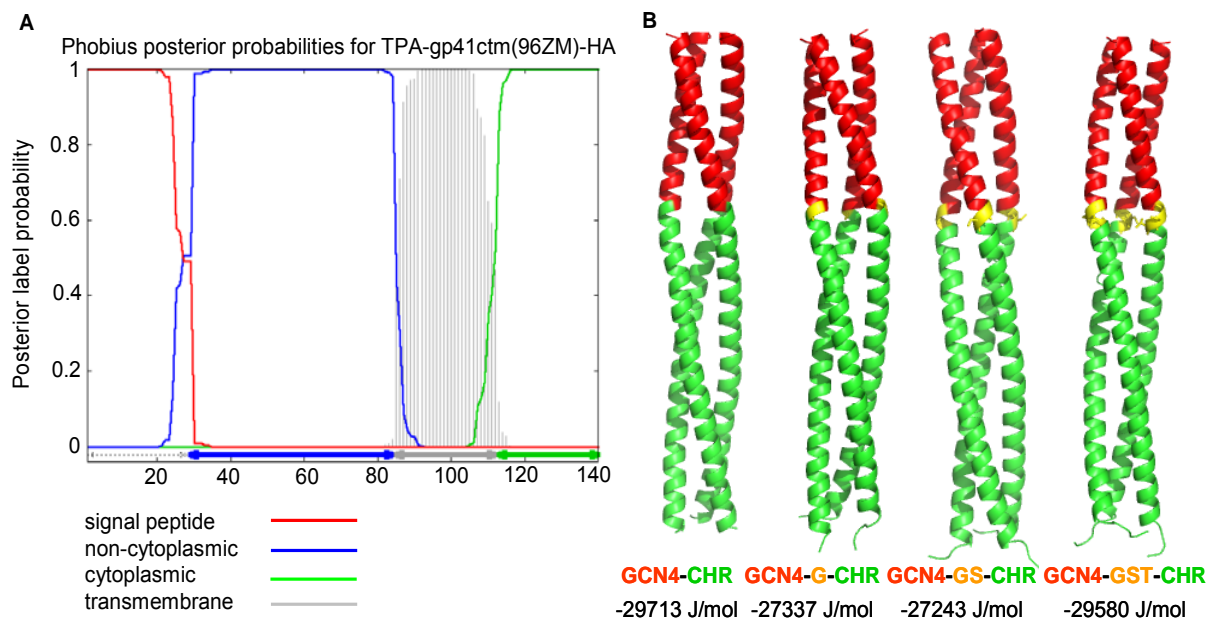


Figure 13. Topology prediction and molecular modeling of gp41ctm variants. (A) Correct cleavage of heterologous signal peptide, protein topology and membrane incorporation were predicted for the basic TPA-gp41ctm(96ZM)-HA protein and all derivatives. (B) The optimal fusion site of the GCN4 zipper domain and the gp41 CHR part was modeled by comparative modeling with the existing structure GCN4-NHR, and free energy was calculated with aid of DOPE score.

4.1.1.3 Membrane exposure and selective recognition by BNMAbs

Expression and membrane location of gp41 variants is a prerequisite for incorporation into VLPs, display of relevant epitopes and usability in immunization studies. In a first experiment, *in vivo* properties of the basic construct gp41ctm were evaluated in comparison of full-length gp41 and gp160. Clade B molecular clone 89.6 was chosen for this purpose, as it bears both the epitopes for 2F5 and 4E10. After transfection and staining of HEK293T cells with these BNMAbs, gp41ctm exhibited a similar mean fluorescence intensity (MFI) in cytometric analysis (fig. 14A) compared to full-length gp41 and a slightly enhanced MFI compared to gp160. Subsequently, all further designed variants were analyzed in cytometric analysis. Following staining of the HA-tag with an anti-HA-antibody, all variants showed proper membrane localization and similar expression levels (fig. 14B). The staining with 2F5 and 4E10 showed a selective binding of 2F5 to 89.6-based constructs only, whereas 4E10 bound to both 89.6 and 96ZM651-based constructs (fig. 14C,D), as expected. For normalization of BNMAb binding to expression level, MFIs of 2F5 and 4E10 were normalized to the anti-HA intensity. The SIVmac239-based variants bound to none of the tested BNMAbs and were only detectable by the HA-tag. Accessibility of BNMAb epitopes was similar for the basic and trimer-stabilized constructs, and slightly enhanced for the further truncated variant gp41ctm2.

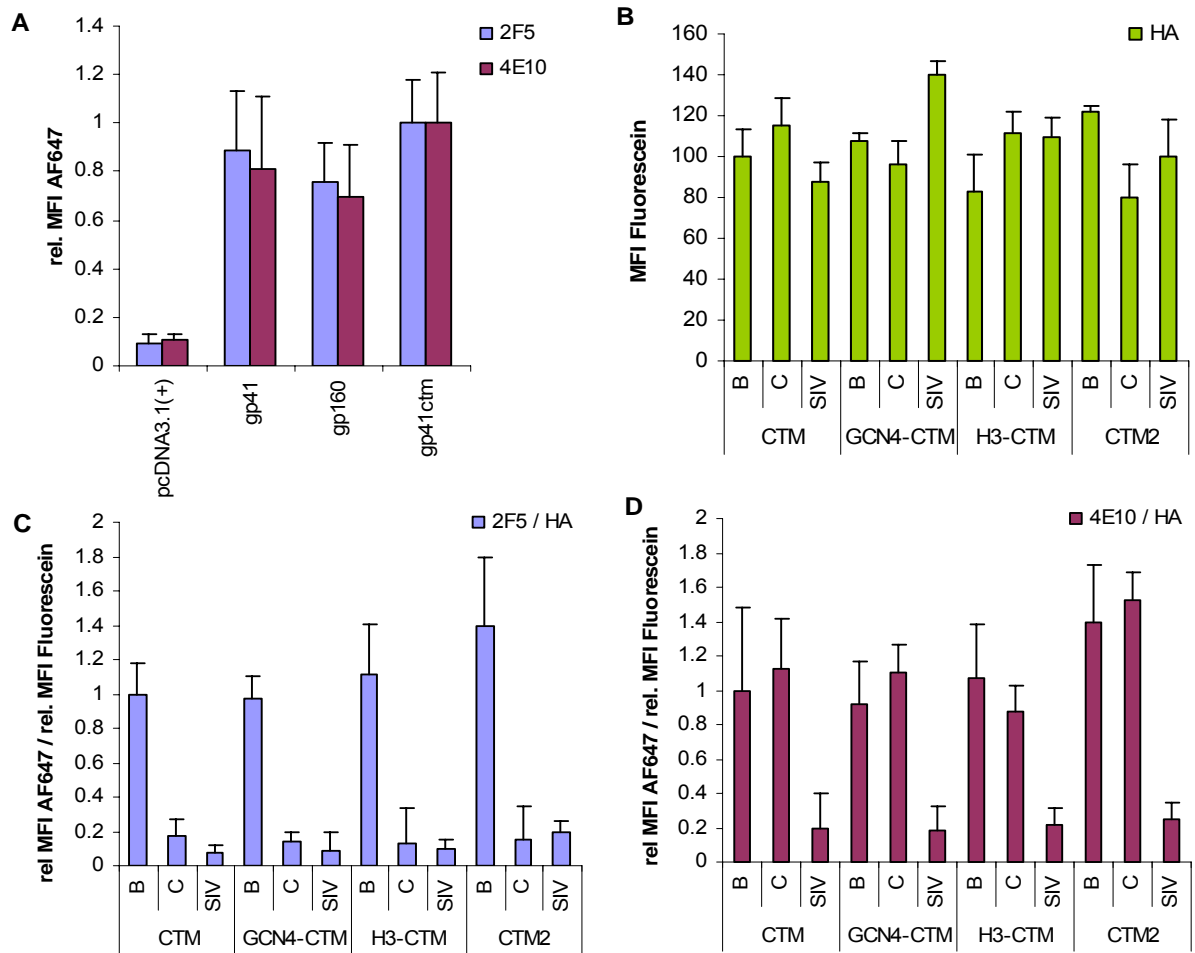


Figure 14. Membrane exposure of novel constructs and recognition by BNMAbs. 293T cells were transfected with equal masses of pcDNA3.1(+) expression plasmids containing envelope genes and stained 48h p.tr. with AlexaFluor647-labelled 2F5 or 4E10 BNMAbs and Fluorescein-labeled anti-HA antibody. (A) Comparison of gp41ctm to gp41 and gp160. MFI for all constructs was normalized to those of gp41ctm. (B) Detection of gp41 variants by extracellular staining with anti-HA antibody. (C, D) 2F5 and 4E10 binding to gp41 variants, normalized to fluorescence intensity of simultaneous anti-HA staining.

4.1.1.4 Incorporation into VLPs

Further analysis of gp41 variants was restricted to the construct based on molecular clone 96ZM651, because this was the clone chosen for following immunization studies. As it is known that HIV-1-derived VLPs band at a density of 1.14-1.18 g/cm³ corresponding to ~35% glucose in PBS (229), the incorporation of novel gp41 immunogens into VLPs was addressed by sucrose gradients and Western Blot analysis. VLPs were produced by co-transfection of HEK293T cells with plasmids encoding for codon-optimized gag and gp41ctm genes. Supernatants were harvested 72 h later and purified by ultracentrifugation through a 30% sucrose cushion. Resuspended pellets were loaded on a 10-50% sucrose gradient and 20 fractions were obtained after ultracentrifugation. After extraction of proteins and SDS-PAGE, Gag and gp41 derivatives were detected in Western Blot analysis by specific antibodies. All variants showed a co-banding of both Gag and gp41 in fractions 12-14, suggesting successful incorporation

(fig. 15). Higher molecular weight bands for GCN4-gp41ctm and H3-gp41ctm might indicate formation of stable dimers and trimers, even in presence of the denaturing agent SDS.

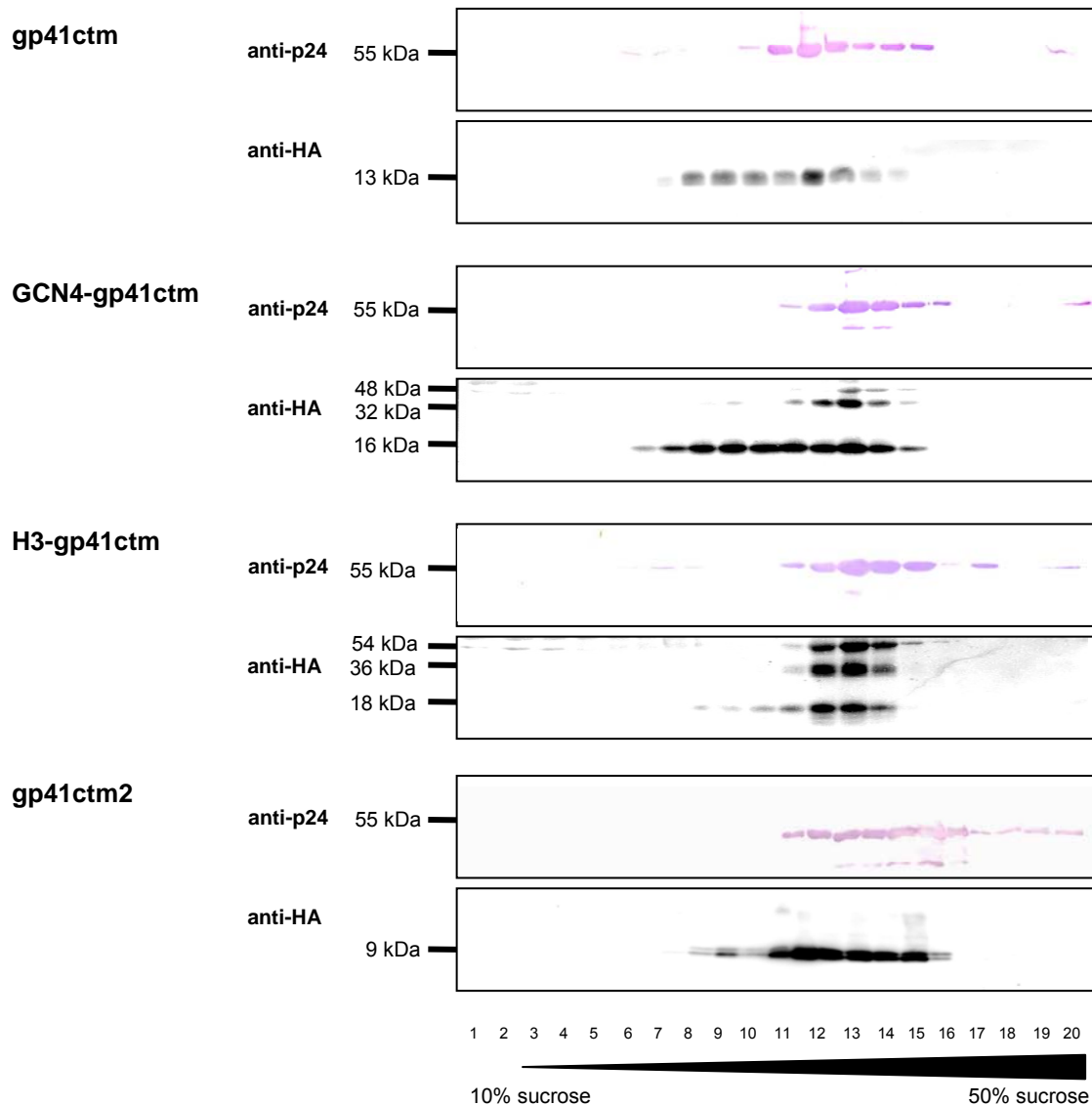


Figure 15. Incorporation of gp41 variants into VLPs. VLPs were produced as described in the methods section and loaded onto a 10 to 50% sucrose gradient. 20 fractions were collected and subjected to SDS PAGE. gp41 variants were detected by anti-HA antibody and Pr55Gag by anti-p24 MAb 13/5. Co-banding of Gag and gp41 variants in fractions 11-15 indicates incorporation into particles. VLPs produced by single transfection of Gag without gp41 were negative for anti-HA-antibody staining (data not shown).

4.1.1.5 Functional preservation of BNAbs epitopes on VLPs

The morphology of VLPs pseudotyped with gp41 derivatives and the antigenic properties of incorporated proteins were evaluated by electron microscopy. Briefly, pseudotyped VLPs were produced and purified as described above, with an incubation of 1 h in the presence of primary antibodies 4E10 or anti-HA-Ab before loading onto sucrose gradients. Primary labeled VLPs were subjected to immuno-gold staining with a secondary gold-labeled anti-IgG antibody and negatively stained with tungstic acid. gp41 derivatives had no apparent impact on particle

morphology and size of 150 - 200 nm in diameter (fig. 16A,F). Staining with 4E10 showed specific staining for VLPs pseudotyped with all four types of gp41 derivatives (fig. 16A,C-F). The HA-tag was also accessible on the surface (fig. 16B), as was expected according to cytometric analysis.

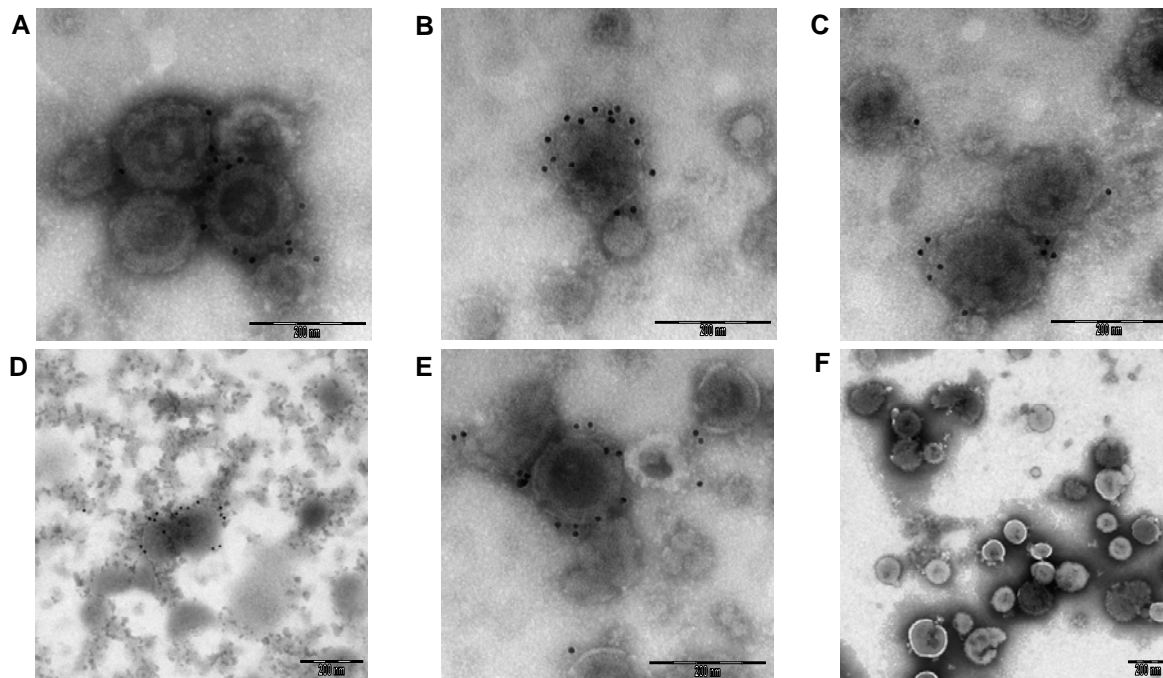


Figure 16. Functional preservation of BNMAb epitopes on VLPs. VLP morphology and epitope preservation was verified by immuno-gold labeling and electron microscopy. VLPs were purified by sucrose cushion and gradient centrifugation, and incubated with human BNMAb 4E10 (A, C-E) or rat anti-HA-antibody (B) and anti-human (A, C-F) or anti-rat (B) antibodies conjugated with gold particles of 10 nm size. VLPs pseudotyped with gp41ctm (A, B), H3-gp41ctm (C), GCN4-gp41ctm (D) and gp41ctm2 (E) showed specific staining with 4E10 (A, C-E) and gp41ctm with anti-HA (B). VLPs without pseudotyping showed no specific staining (F).

4.1.1.6 Trimeric state of gp41 derivatives on the surface of VLPs

An oligomeric conformation of envelope molecules is thought to be advantageous over monomeric immunogens due to preservation of the natural conformation. Thus, the oligomeric state of all created gp41-derived proteins was analyzed in crosslinking experiments. Briefly, VLPs pseudotyped with different gp41ctm variants were produced and purified as described above, and incubated with the crosslinking reagent BS³. This chemical covalently links free amino groups with a spacer arm of 11.4 Å length, thus irreversibly building a bond between molecules in close spatial proximity. Following denaturing SDS PAGE and Western Blot with anti-HA-Ab, higher molecular weight bands corresponding to dimers and trimers could be observed for all gp41 variants. Regarding the trimer-stabilized constructs with GCN4 and H3 zipper domains, the intensity of bands corresponding to dimers and trimers seemed to be slightly enhanced compared to the non-stabilized constructs gp41ctm and gp41ctm2. Also, an increased fraction of oligomers was observed for constructs including GCN4 and H3. Additional bands for monomers might indicate degradation products.

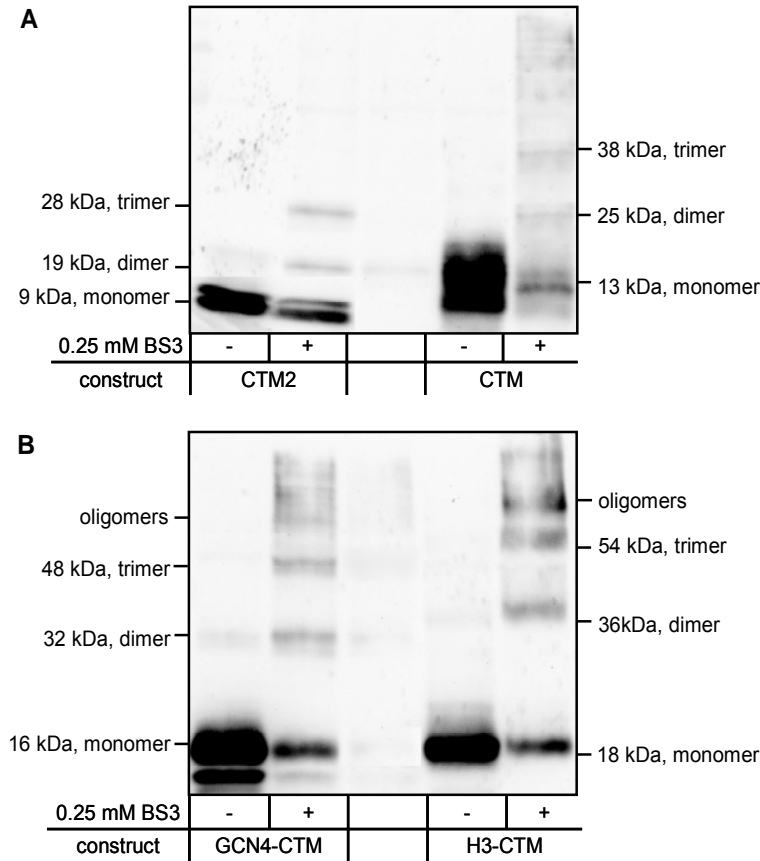


Figure 17. Trimeric state of gp41 derivatives on the surface of VLPs. Pseudotyped VLPs were purified by sucrose cushion and gradient, and incubated with 0.25 mM of crosslinking reagent BS³. Reaction was quenched with excess of Tris-HCl. VLPs were lysed and loaded on a denaturing SDS gel. Higher molecular weight bands are visible only for cross-linked VLPs.

4.1.1.7 Quantification of gp41 molecules per VLP

For the induction of neutralizing antibodies, a high amount of incorporated gp41 molecules on the surface of VLPs is supposed to be beneficial. A suitable recombinant protein as standard reference and an antibody recognizing both the reference and the gp41_{ctm}-derived proteins are needed for absolute quantification. The recombinant GCN4-gp41-FD protein (95) with a size of 20 kDa was chosen as reference protein, as it includes the relevant part of gp41 which is also present in our immunogens. 4E10 served as detection antibody, as its epitope is present in all tested immunogens and the standard protein. VLPs were purified, quantified and 1 µg of Gag and dilutions of the standard protein were incubated in the presence of 1% TritonX100 for 1h for lysis and loaded onto a slot blot, followed by detection with 4E10. The obtained standard curve shows the dose-dependent intensity and hereby recognition by 4E10. All gp41 variants exhibited similar signal intensities, with a slightly increased value for the construct gp41_{ctm2}. Masses of gp41 variants were calculated by use of the standard curve. The calculation of gp41 to Gag molecules indicates that only a relative but no absolute quantification is possible with this pair of antibody and standard protein, because a nearly equal mass distribution of these proteins in VLPs is unlikely. It has been observed by others that the 4E10 epitope can be

presented differently in different proteins or peptides, although the linear epitope was preserved (102). As a conclusion, it is feasible to use this pair of standard protein and antibody to compare between constructs and not as absolute numbers.

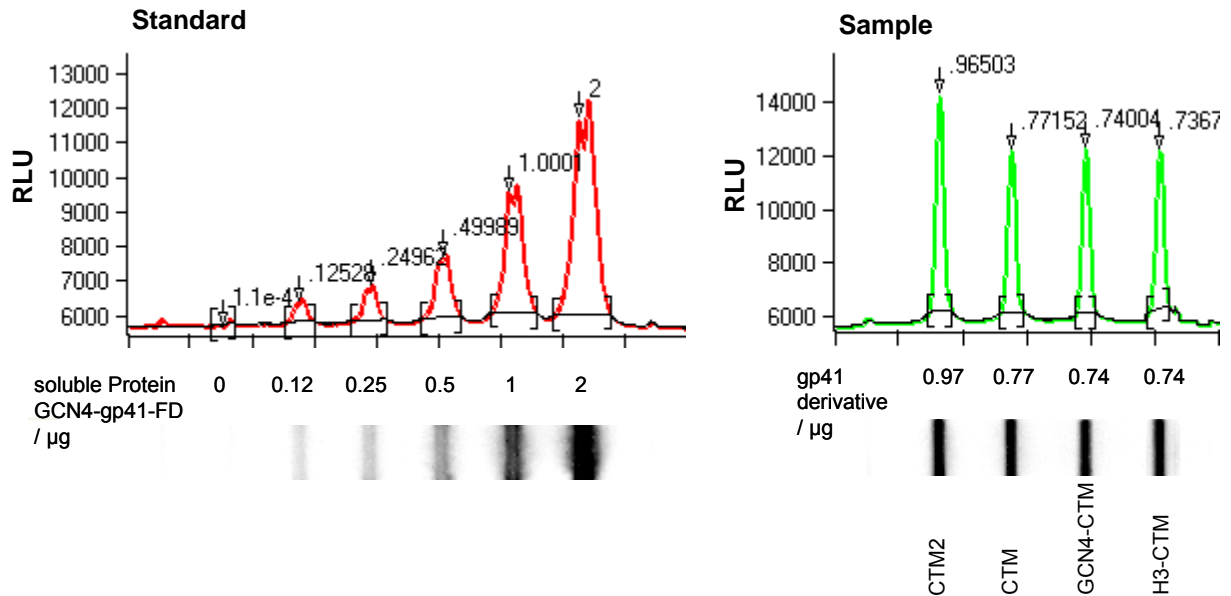


Figure 18. Quantification of gp41 variants incorporated into VLPs. Indicated amounts of soluble protein GCN4-gp41-FD (left) and 0.25 µg of indicated lysed pseudotyped VLPs (right) were loaded onto a slot blot, and stained with 4E10 and anti-human-HRP antibody. Calculated masses of gp41 derivatives were comparable to each other, though only suitable for a relative quantification.

4.1.1.8 Cytopathic effects of gp41 derivatives

It is known from the literature that envelope proteins from HIV-1 have cytopathic effects, depending on cell type and viral isolate (230). Regarding gp41_{ctm}, it quickly became apparent in this work that cell proliferation and particle production were affected in co-transfection experiments with Gag. Additionally, cell populations were shifted towards typical apoptotic cell populations with diminished forward scatter in cytometric analysis. In order to quantify cytopathic effects of gp41 variants, cells were stained with 7AAD and AnnexinV 48h after transfection. 7AAD is a marker for necrosis (231), whereas AnnexinV is an indicator of apoptosis (232). Transfection with gp145, gp41, gp41_{ctm} and gp41_{ctm2} led to increased necrosis and apoptosis compared to cells receiving huGFP or gag (fig. 19A, upper diagram). Cell proliferation was biased in a similar manner (fig. 19B, lower diagram) with a factor of ~2. Effects on particle release were more drastic with a factor of ~3 while co-transfecting gp41_{ctm} versus non-cytopathic proteins like GFP (fig. 19B). Trimer-stabilized constructs showed similar influences on cytopathicity and particle production as the basic construct gp41_{ctm} (data not shown).

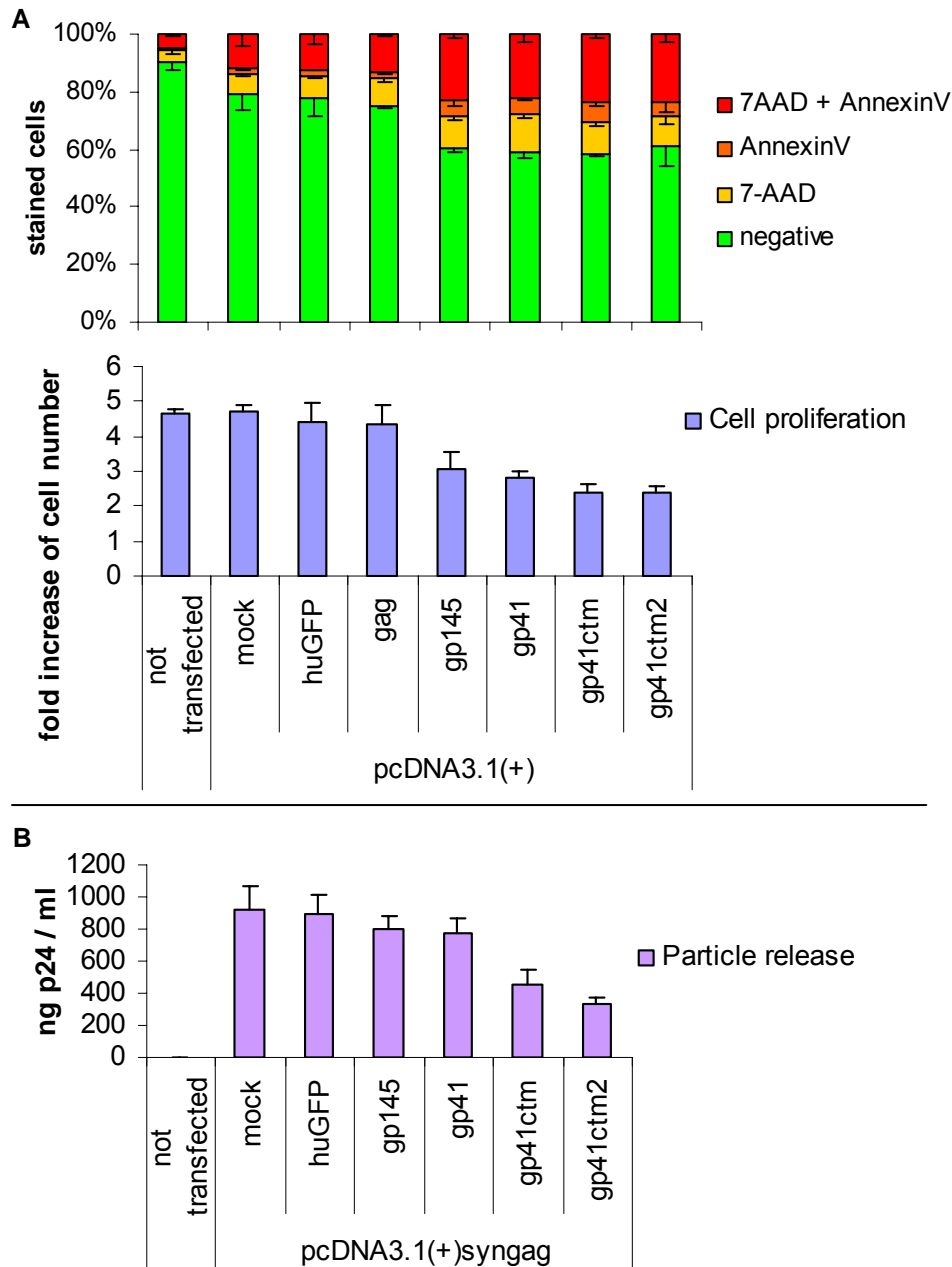


Figure 19. Effects of gp41 variants on cytopathicity and VLP production. (A) 293T cells were transfected with indicated expression plasmids and stained with apoptosis marker AnnexinV and necrosis marker 7AAD (upper panel). Cell proliferation after transfection was determined by counting cells 48 h p.tr. (lower panel). (B) Effects on particle production were determined by co-transfection of pcDNA3.1(+)-syngag and the indicated plasmids. VLPs were quantified 72 h p.tr. by p24 ELISA.

4.1.1.9 Large scale production for immunization studies

All tested gp41 variants showed correct membrane topology, incorporation into VLPs, preservation of BNMAb epitopes and (at least partly) trimeric structure, and were therefore eligible to be used as immunogens in rodent immunization studies. A HEK293-derived suspension cell line, 293F ("FreeStyle"), was used to produce VLPs presenting gp41ctm, H3-gp41ctm and GCN-gp41ctm. Cytometric analysis and Western blots following sucrose gradients indicated a similar biochemical behavior of 293F- compared to 293T-derived VLPs. 293F cells

allowed for a production of VLPs pseudotyped with the three mentioned constructs, which were used in a rabbit immunization study. Only gp41ctm2 was less properly expressed in the suspension cells, and therefore this construct was produced in adherent 293T cells in smaller amounts and tested later in a mouse immunization study. As a quality control and for quantification, VLPs were analyzed on a Coomassie gel following SDS PAGE. The same expression vectors used for VLP production were also prepared in large quantities as DNA immunogens. DNA was analyzed on agarose gels after endonuclease restriction for quality control purposes (data not shown). All immunogens were tested in *Limulus* ameobocyte lysate assay for presence of endotoxins prior to immunization, and exhibited EU levels of < 20 EU/ml.

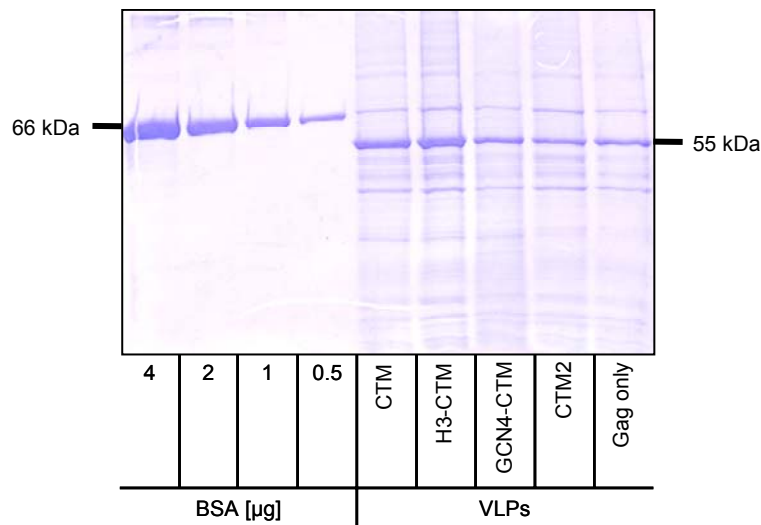


Figure 20. Quality control and quantification of VLPs produced for immunization purposes. Pseudotyped VLPs were purified by ultracentrifugation through a sucrose cushion and suspended in PBS. 5 µl of resuspended VLP preparations were lysed, loaded on a 12.5% SDS gel and stained with Coomassie. As Gag (Pr55) accounts for the main protein mass of VLPs, the band at 55 kDa was quantified by comparison to defined amounts of BSA, which served as standard protein.

4.1.2 Immunogenicity studies in rodents

The immunogens were functionally tested in a rabbit and a mouse immunization study. A DNA prime and VLP / protein boost regimen was chosen, as this kind of heterologous immunization schedule had shown greater effectiveness in the past, compared to DNA or VLP / protein alone (233; 234). Two gp41-derived soluble proteins, HA2-gp41-GCN4 (W. Weissenhorn, unpublished) and CTB-MPER (R. Kapzan, (228)) were included in this study to compare them with VLP-anchored proteins. Soluble proteins as well as VLPs were formulated with 1% carbopol as adjuvant. Carbopol was chosen because of its non-denaturing properties towards lipid membranes, compared to Freund's adjuvant or similar formulations. The integrity of VLPs and incorporated proteins after mixing with Carbopol was verified by sucrose gradient and Western Blot analysis (data not shown). Rabbits received two times 500 µg of DNA at weeks 0 and 4 and two times 100 µg of VLPs or protein at weeks 12 and 16 (fig. 21A). Mice were immunized with 100 µg of DNA at weeks 0 and 4 and with 35 µg of VLPs or protein at days 8

and 12 (fig. 21B). Bleeds were taken 2 weeks before the first immunizations, between DNA primes and VLP boosts, and 2 weeks after the last immunizations. Sera were prepared from all bleeds and heated to 56°C for 30 min in order to inactivate the complement system. All animals were sacrificed after the terminal bleed.

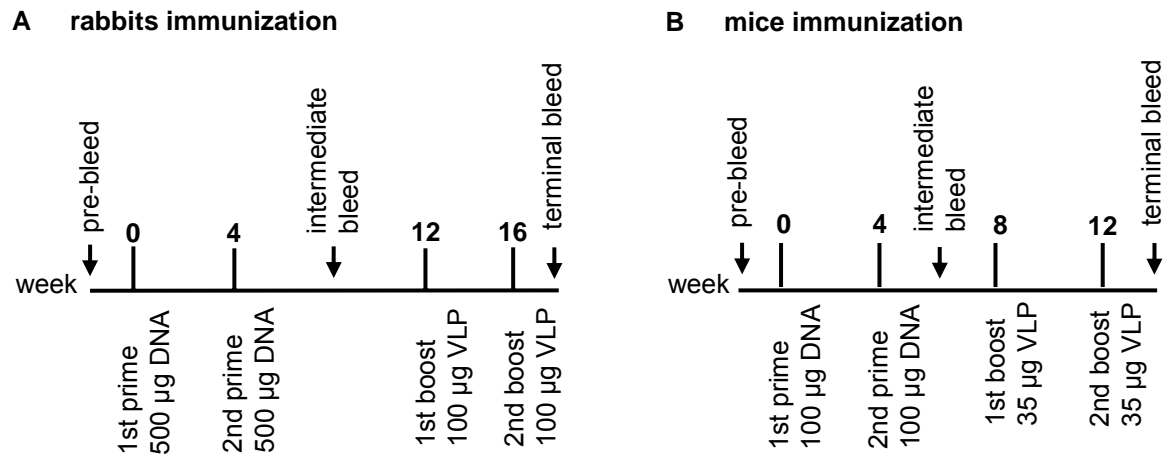


Figure 21. Schemes for rodent immunization studies. (A) Rabbits were immunized twice with DNA encoding for trimer-stabilized constructs and twice with homologous VLPs or recombinant protein at indicated time points. (B) Mice were immunized twice with DNA encoding for further truncated gp41 and twice with homologous VLPs or recombinant protein at the indicated time points.

4.1.2.1 Induction of anti-gp41 Abs

The induction of anti-gp41 Abs is a prerequisite for effective neutralization, and was analyzed with the aid of an IgG ELISA. Two soluble peptides spanning the MPER and CHR regions of gp41 were coated on plates and tested with BNMAbs 2F5 and 4E10, resulting in signals up to high dilutions (data not shown). Reactivity of rabbit sera (terminal bleed) is shown in fig. 22.

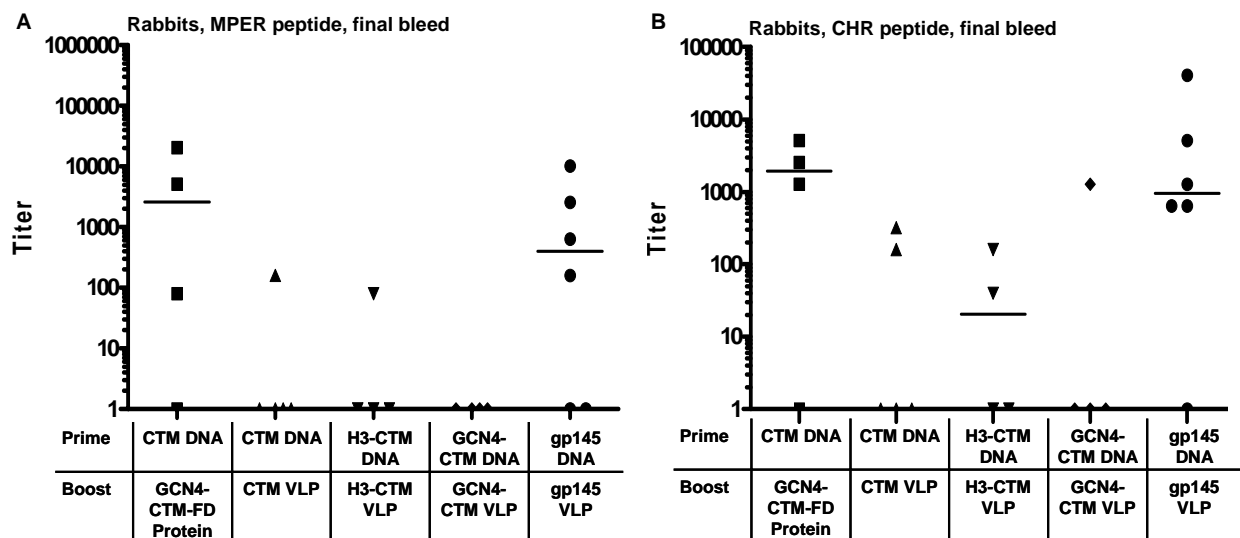


Figure 22. Anti-gp41 antibodies induced by rabbit immunization. Terminal bleeds of rabbits were analyzed by IgG ELISA. Peptides spanning the CHR (A) and MPER (B) served as coating peptides. Anti-rabbit-HRP coupled antibody was used as secondary antibody. Titers are calculated as reciprocal dilutions of specific signals at least two-fold above pre-bleed signals.

The group receiving gp145 serves as a positive control group. Mediocre titers against both peptides were observed for the group receiving gp41ctm DNA / GCN4-gp41ctm-FD protein, and for the gp145 control group. Low titers were obtained for the groups receiving gp41ctm DNA and boost, and trimer-stabilized constructs, with some animals not reacting at all.

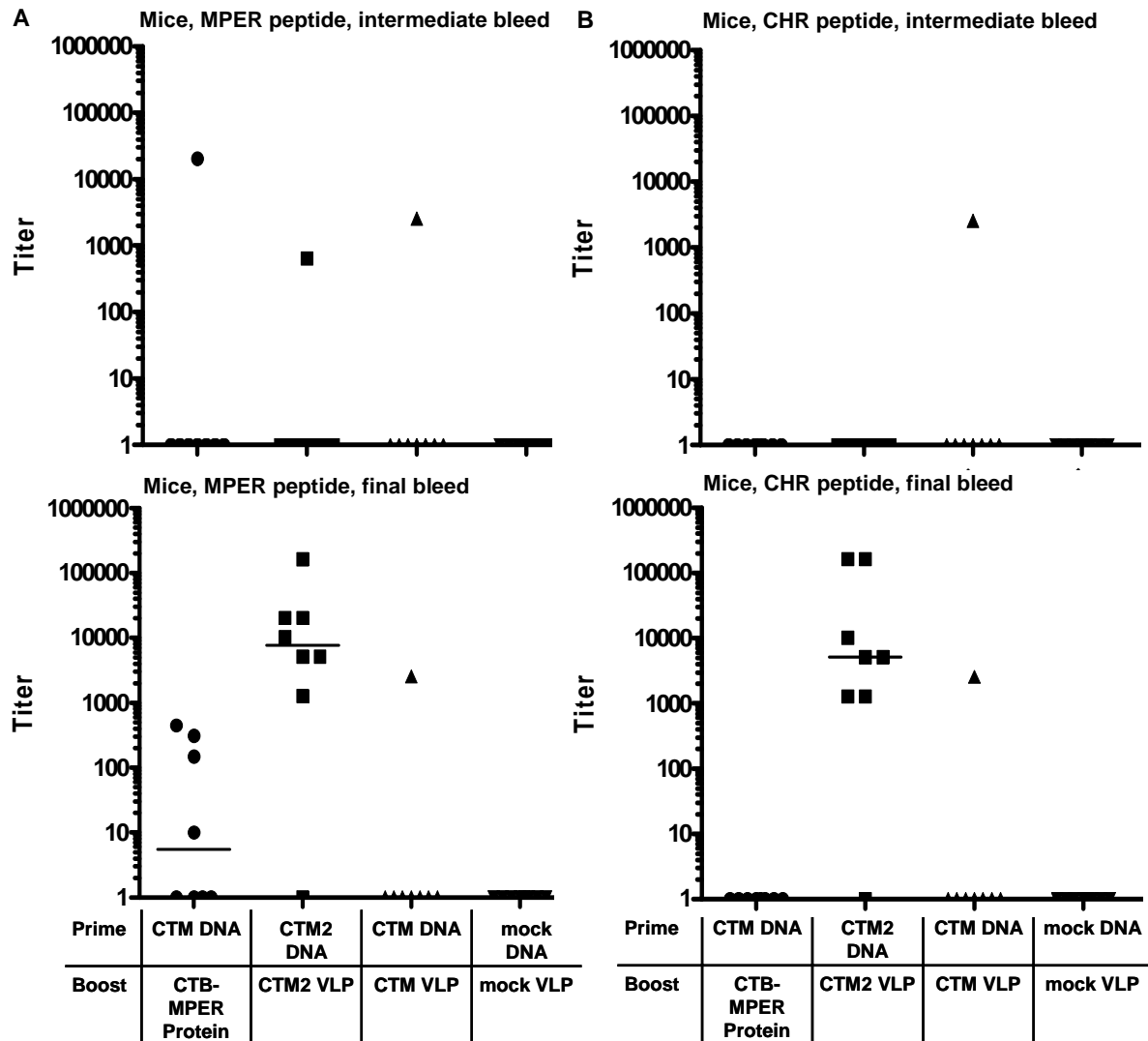


Figure 23. Anti-gp41 antibodies induced by mouse immunization. Intermediate (upper panels) and terminal bleeds (lower panels) of mice were analyzed by IgG ELISA. Peptides spanning the CHR (A) and MPER (B) served as coating peptides. Anti-mouse-HRP coupled antibody was used as secondary antibody. Titers are calculated as reciprocal dilutions of signals at least two-fold above pre-bleed signals.

Both intermediate and final bleeds of mice were examined in analogous ELISA (fig. 23). After two DNA primes, only few animals reacted, regardless of immunogen or readout peptide. After boosting, the group receiving gp41ctm DNA and CTB-MPER fusion protein had mediocre IgG titers against the MPER peptide. The group receiving gp41ctm2 DNA and homologous VLPs exhibited high titers after boosting and showed the most promising titers of all groups tested.

4.1.2.2 Removal of anti-cell antibodies

VLPs are surrounded by a membrane derived from the host cell, which was a human embryonic kidney cell line in the present study. Membrane proteins from this cell line are embedded in VLPs and can induce a significant immune response in immunization studies. The induced so-called anti-cell antibodies can falsify results in neutralization experiments, both positively and negatively (235-239) and should therefore be removed before performing neutralization tests. All sera were tested for the presence of anti-cell Abs in cytometric analysis and incubated with HEK293F cells until anti-cell activity was below two times the background signal. The titer of anti-cell Abs varied widely between animals and required an incubation of up to nine times for efficient absorption (fig. 24). This procedure had no impact on the titer of anti-gp41 antibodies, as measured in ELISA (data not shown).

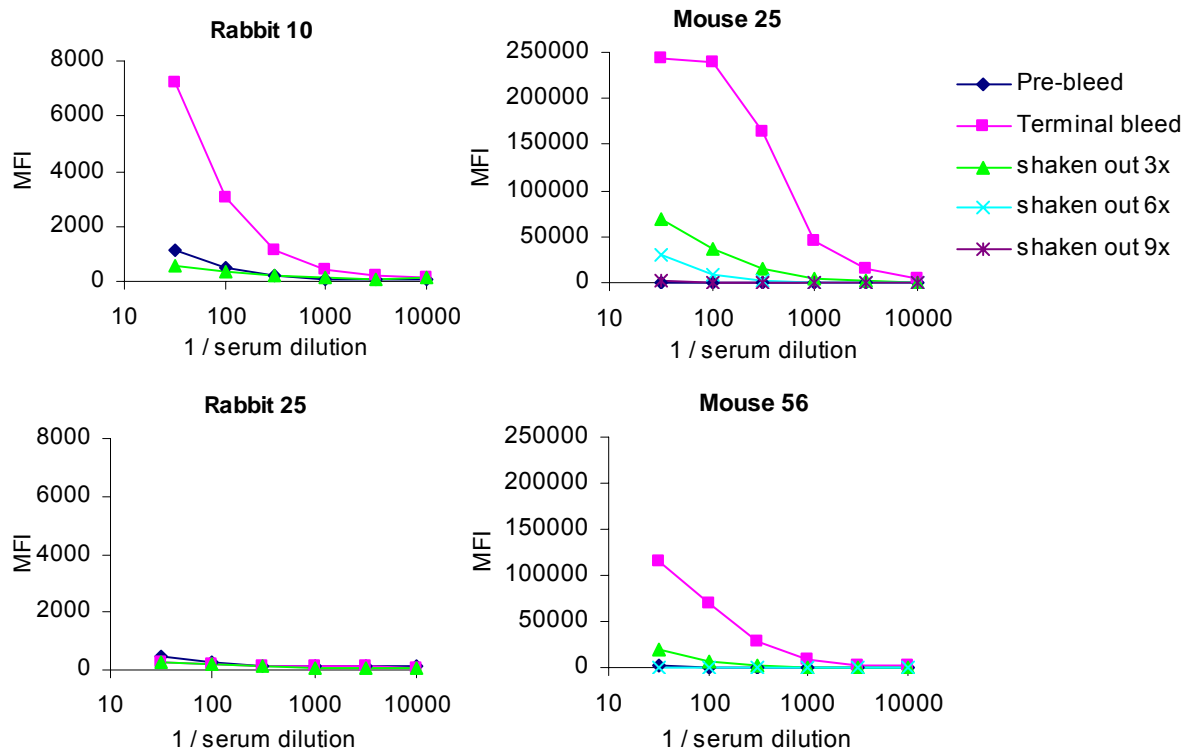


Figure 24. Effective removal of anti-cell antibodies. Sera of rabbits and mice were incubated with human 293 cells for 4 h at room temperature with moderate shaking. Incubation up to nine times was necessary to remove all significant anti-cell activity, measured by staining of human 293T cells with dilutions of sera and anti-rabbit / anti-mouse antibodies. Mean fluorescence intensities (MFI) of two representative sera of each rabbits (left) and mice (right) are shown.

4.1.2.3 Induction of neutralizing antibodies

As sera showed specific binding to gp41 peptides in a dilution of up to 32,768 (rabbits) and 131,072 (mice), all sera were tested in standardized assays for neutralizing activity. Two different test systems were chosen, TZM-bl and A3R5 assays. The TZM-bl assay is based on a HeLa-derived reporter cell line and uses an env-deleted virus, pseudotyped with different

4 Results

Table 2. Induction of low neutralizing antibody titers in rabbit sera. After removal of anti-cell antibodies, sera were tested in TZM-bl (HeLa cell-based) and A3R5 (CEM cell-based) neutralization assays. Dilutions mediating inhibition of 50% infection (ID50) two-fold over background (respective pre-bleed serum) are considered as neutralizing.

Rabbit sera			ID50 in TZM-bl/ Tier 1		ID50 in A3R5/ Tier 1	ID50 in A3R5/ Tier 2	
2x prime + 2x boost	No. - week	Bleed #	SHIV 89.6P.18 Clade B	MW965.26 Clade C	SF162.LucRN. T2A.ecto Clade B	CH40.LucT .T2A.ecto Clade B	THRO.LucR. T2A.ecto Clade B
CTM DNA + GCN4-gp41ctm-FD protein	2-0	pre	<20	<20	178	29	35
	2-22	terminal	<20	<20	167	49	65
	3-0	pre	<20	<20	59	28	31
	3-22	terminal	<20	<20	46	28	63
	4-0	pre	<20	<20	77	25	28
	4-22	terminal	<20	<20	62	103	99
	5-0	pre	<20	<20	100	<20	24
	5-22	terminal	<20	<20	129	219	132
CTM DNA + CTM VLP	7-0	pre	nt	<20	85	nt	nt
	7-22	terminal	nt	26	56	nt	nt
	8-0	pre	nt	<20	98	nt	nt
	8-22	terminal	nt	23	113	nt	nt
	10-0	pre	nt	<20	173	nt	nt
	10-22	terminal	nt	37	114	nt	nt
	11-0	pre	nt	<20	86	nt	nt
	11-22	terminal	nt	25	113	nt	nt
H3-CTM DNA + H3-CTM VLP	12-0	pre	nt	<20	115	nt	nt
	12-22	terminal	nt	21	99	nt	nt
	13-0	pre	nt	<20	<20	nt	nt
	13-22	terminal	nt	28	104	nt	nt
	14-0	pre	nt	<20	<20	nt	nt
	14-22	terminal	nt	<20	138	nt	nt
	15-0	pre	nt	<20	71	nt	nt
	15-22	terminal	nt	21	119	nt	nt
GCN4-CTM DNA + GCN4-CTM VLP	17-0	pre	nt	<20	45	nt	nt
	17-22	terminal	nt	<20	120	nt	nt
	19-0	pre	nt	<20	88	nt	nt
	19-22	terminal	nt	44	140	nt	nt
	20-0	pre	nt	<20	48	nt	nt
	20-22	terminal	nt	54	117	nt	nt
	21-0	pre	nt	<20	36	nt	nt
	21-22	terminal	nt	<20	59	nt	nt
gp145 DNA + gp145 VLP	22-0	pre	nt	876	109	nt	nt
	22-22	terminal	nt	<20	103	nt	nt
	25-0	pre	nt	20	47	nt	nt
	25-22	terminal	nt	763	357	nt	nt
	26-0	pre	nt	<20	71	nt	nt
	26-22	terminal	nt	1175	56	nt	nt
	27-0	pre	nt	<20	99	nt	nt
	27-22	terminal	nt	794	54	nt	nt
	28-0	pre	nt	<20	35	nt	nt
	28-22	terminal	nt	415	184	nt	nt
	29-0	pre	nt	32	163	nt	nt
	29-22	terminal	nt	6450	105	nt	nt
	30-0	pre	nt	<20	26	nt	nt
	30-22	terminal	nt	683	126	nt	nt

ID50 of terminal bleed compared to pre-bleed

	not tested
	< 2x
	> 2x
	> 10x
	> 50x

4 Results

Table 3. Induction of low neutralizing antibody titers in mice sera. After removal of anti-cell antibodies, sera were tested in TZM-bl (HeLa cell-based) and A3R5 (CEM cell-based) neutralization assays. Dilutions mediating inhibition of 50% infection (ID50) two-fold over background (respective pre-bleed serum) are considered as neutralizing.

Mice sera			ID50 in TZM-bl/ Tier 1		ID50 in A3R5/ Tier 1	ID50 in A3R5/ Tier 2	
2x prime + 2x boost	No. - week	Bleed #	SHIV 89.6P.18 Clade B	MW965.26 Clade C	SF162.LucR. T2A.ecto Clade B	CH40.LucT. T2A.ecto Clade B	THRO.LucR. T2A.ecto Clade B
CTM DNA + CTB-MPER protein	17-0	pre	<20	<20	nt	nt	nt
	17-18	terminal	33	23	nt	nt	nt
	18-0	pre	<20	<20	11383	<20	<20
	18-18	terminal	<20	<20	13092	<20	30
	19-0	pre	<20	<20	8756	<20	57
	19-18	terminal	<20	<20	9163	<20	39
	20-0	pre	<20	<20	2166	<20	31
	20-18	terminal	<20	<20	10531	<20	39
	23-0	pre	<20	<20	5563	<20	32
	23-18	terminal	<20	<20	9969	21	44
CTM2 DNA + CTM2 VLP	24-0	pre	<20	<20	nt	nt	nt
	24-18	terminal	243	nt	nt	nt	nt
	25-0	pre	nt	<20	2750	nt	nt
	25-18	terminal	nt	26	39	nt	nt
	26-0	pre	nt	<20	7467	nt	nt
	26-18	terminal	nt	30	42	nt	nt
	27-0	pre	nt	<20	7192	nt	nt
	27-18	terminal	nt	42	46	nt	nt
	28-0	pre	nt	22	5159	nt	nt
	28-18	terminal	nt	29	55	nt	nt
CTM DNA + CTM VLP	30-0	pre	nt	32	12130	nt	nt
	30-18	terminal	nt	64	64	nt	nt
	31-0	pre	nt	<20	9919	nt	nt
	31-18	terminal	nt	23	30	nt	nt
	32-0	pre	nt	<20	5591	nt	nt
	32-18	terminal	nt	38	58	nt	nt
	33-0	pre	nt	25	6918	nt	nt
	33-18	terminal	nt	31	43	nt	nt
	34-0	pre	nt	<20	5800	nt	nt
	34-18	terminal	nt	60	84	nt	nt
	35-0	pre	nt	23	7514	nt	nt
	35-18	terminal	nt	68	55	nt	nt
	36-0	pre	nt	21	7171	nt	nt
	36-18	terminal	nt	73	41	nt	nt
	37-0	pre	nt	<20	4903	nt	nt
	37-18	terminal	nt	26	32	nt	nt
	38-0	pre	nt	23	3111	nt	nt
	38-18	terminal	nt	37	40	nt	nt
	39-0	pre	nt	33	4209	nt	nt
	39-18	terminal	nt	23	44	nt	nt
	40-0	pre	nt	<20	4875	nt	nt
	40-18	terminal	nt	38	40	nt	nt

ID50 of terminal bleed compared to pre-bleed

	not tested
	< 2x
	> 2x
	> 10x
	> 50x

envelopes encoded on expression plasmids. For the A3R5 assay, every isolate is cloned individually as a provirus and tested for propagation on CEM (human T cell lymphoblast-like) cells, in the presence of immune sera (see methods for details). A small panel of tier 1 (laboratory-adapted strains, easy to neutralize) and tier 2 (primary isolates, moderately hard to

neutralize) viruses were tested for neutralization. Specifically, all samples were tested against molecular clones SF162 (clade B) and MW965.26 (clade C), independently of immunization strain. Sera obtained from animals immunized with clade B immunogens were furthermore tested against homologous SHIV89.6P and heterologous CH40 and THRO isolates. Due to restricted sample volumes and experimental constraints, not all sera could be tested against all viral isolates.

Effective neutralization was observed only for the rabbit group receiving gp145 DNA and homologous VLPs, with two rabbits showing titers >1,000 and >50x above background for at least one tested isolate (table 2). Env from this isolate was known to induce modest neutralizing titers against the homologous isolate and the tier-1 strain MW965.26 when administered mucosally as soluble gp140 protein (240). Rabbit group 1 receiving a gp41ctm DNA prime and GCN4-gp41ctm-FD protein boost showed weak to moderate neutralization in the A3R5 assay, but no neutralization was detected in TZM-bl assay. For all three rabbit groups receiving gp41-derived DNA prime / VLP boost, only some weak neutralizing activity was detected in single animals. Taken together, results from rabbit neutralization tests tended to reflect titers of anti-gp41 antibodies as measured in ELISA. However, rabbit group 1 showed fair antibody titers against the vaccination strain but neutralizing activity only against other strains.

The basic construct gp41ctm was also tested as DNA prime / VLP boost immunization in mice and induced only weak neutralizing activity here as well (table 3). This is also the case for the further truncated version gp41ctm2, although it induced high titers of anti-gp41 antibodies as measured in ELISA. The mice group 1 receiving gp41ctm DNA as prime and CTB-MPER fusion protein as boost contained also only two animals reacting significantly above background. Taken together, neutralization data of mice also tend to reflect the ELISA data, with exception of group number 2 with high antibody and low neutralizing titers.

4.1.2.4 Removal of MPER-directed BNMAbs by incubation with cells

After completion of the studies described above, other groups published evidence for the paramouncy of membrane-binding components in MPER-directed BNABs like 2F5 and 4E10 (81; 241). To assess the effect of cell absorption on membrane-binding antibodies, dilutions of 2F5 and 4E10 were incubated with HEK293F cells for 4h up to nine times. Antibody concentrations were reduced significantly in each round of incubation, as can be seen in fig. 25. It can be concluded that membrane-binding antibodies in immune sera are removed by this procedure as well, which renders the procedure detrimental for sera obtained after vaccination with immunogens including a membrane-embedded MPER.

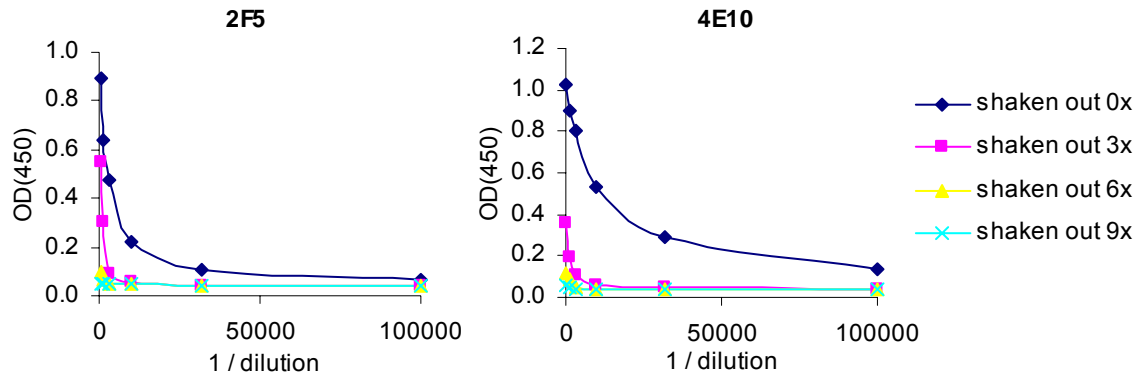


Figure 25. Anti-MPER antibodies 2F5 and 4E10 are removed by incubation with cells. Serial dilutions of 2F5 and 4E10 in PBS were incubated up to nine times with an equal volume of HEK293F cells. Supernatants were read out in a gp41 ELISA with MPER peptide as coating reagent, and anti-human-HRP coupled antibody as secondary antibody.

4.1.3 Summary

Requirements for state-of-the-art immunogens based on gp41 were defined with the aid of pre-existing BNMAbs 2F5 and 4E10, directing the attention to the MPER region. Four novel gp41-derived immunogens were designed and endowed with features for membrane localization, trimerization and antibody recognition. The resulting proteins were analyzed *in silico* with aid of appropriate prediction and modeling software. After cloning, the expression and antigenicity of these membrane-bound proteins were tested in cytometric analyses. The correct incorporation of the gp41 antigens into virus-like particles was verified by analysis of sucrose gradients and by electron microscopy. Crosslinking experiments revealed a partially trimeric state of all novel immunogens. Despite cytopathic effects, pseudotyped VLPs and homologous endotoxin-free DNA were produced for immunization of rabbits and mice. The immunogens were functionally tested in two animal immunization studies, as stand-alone constructs in homologous DNA prime / VLP boost regimens or in combination with two gp41-derived soluble proteins. Although sufficient titers of anti-gp41 antibodies were measured by ELISA for some groups, neutralizing activity was limited. Boosts with soluble protein tended to be more effective than boosts using VLPs. Best results were obtained by priming with gp41ctm DNA and boosting with trimeric GCN4-gp41ctm-FD protein. If membrane-binding antibodies have been present in immune sera, these were likely depleted by the procedure of removing anti-cell antibodies.

4.2 Selection of gp41 derivatives with high affinity for BNMAbs

The second part of this work deals with the affinity maturation of membrane-bound gp41 immunogens towards BNMAbs 2F5 and 4E10, following the hypothesis, that antigens with enhanced affinity might more likely induce antibodies similar to known BNMAbs. Initially, a virus-based display system was developed for this purpose. In this system, proteins responsible for both packaging and antigenicity (i.e. an envelope library) are encoded in a single lentiviral genome. The system was therefore called “All-in-One (AIO)”. A 4E10-directed mini-library was created to evaluate the performance of this system. After defining limitations of this system, a cell-based display system (“lenti-cellular display”) was adapted to the gp41 context and validated in proof-of-concept studies. Finally, a complex library was constructed and screened for affinity-enhanced variants.

4.2.1 Creation of a gp41 mini-library

The performance of antigen display systems can be evaluated by use of defined small libraries, in which every member has a known binding affinity for the selecting antibody. During a successful panning procedure, the best binder(s) should be selected in one or more rounds of selection. In the case of gp41, precise information on specific isolates and their affinity to 4E10 was not available. However, the influences of some alanine substitutions on viral fitness and 4E10 neutralization (101; 125) as well as an overview on 4E10 epitopes and corresponding neutralization data (121) have been described. Furthermore, it was clear from cytometric analysis that 4E10 does not bind to gp41 derived from molecular clone SIVmac239 (section 4.1.1.3).

Table 4. Design of a gp41 mini-library for the 4E10 antibody. The 4E10 epitope was gradually mutated, with the expected corresponding binding pattern indicated in the right column.

subtype	2F5 epitope	4E10 epitope	2F5 binding	4E10 binding
HIV-1 B (89.6)	ELDKWAS	WNWFDITNWLW	+++++	+++++
HIV-C (96ZM)	ALDSWNN	WNWFDITKWLW	-	+++++
4E10-directed	ALDSWNN	GNWFDITNWLW	-	++++
mini-library, based	ALDSWNN	GNWFDITNWLW	-	+++
on HIV-1 C	ALDSWNN	GNWFDLANWLW	-	++
(96ZM)	ALDSWNN	GNWFDALANWLW	-	+
SIV(mac239)	KLNSWDV	GNWFDLASWIK	-	-

Based on the information on binding (96ZM651) and non-binding sequences (SIVmac239), and relevant positions for alanine substitutions, a 4E10-directed gp41ctm mini-library with four

additional members was created based on clone 96ZM651 (table 4). The constructs were named 4E10++++ / 4E10+++ / 4E10++ / 4E10+, respective of their expected binding behavior towards 4E10. Residues crucially important for antibody binding were left untouched. A similar mini-library was designed for antibody 2F5, but omitted later, as there was no gradual binding observable in this case (data not shown).

4.2.1.1 Membrane localization of mini-library and selective binding to BNMAbs

All mutants were tested in flow cytometric analysis for efficient expression, membrane localization and antigenicity. HEK293T cells were transfected transiently with expression plasmids encoding for the mutants, and stained simultaneously for anti-HA and 4E10 or 2F5. Signals for the HA-tag were similarly intense, suggesting similar expression levels and proper membrane incorporation of all mutants (fig. 26). BNMAb 2F5 exclusively stained the 89.6-derived protein. 4E10 bound to both 89.6- and 96ZM651-derived constructs and to the 4E10-directed mini-library in a gradual manner. This finding indicates that the members of the mini-library bind each with different affinity to BNMAb 4E10 while being equally expressed.

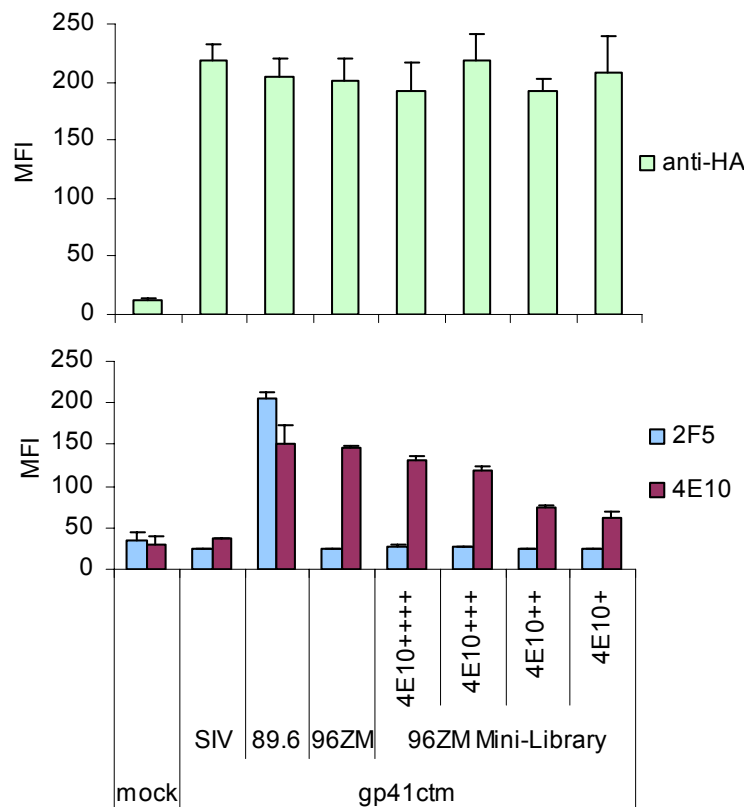


Figure 26. Membrane localization of mini-library and selective binding to BNMAbs on cells. 293T cells were transiently transfected with expression plasmids carrying the indicated gp41 variants, stained with anti-HA (upper panel) and BNMAbs 2F5 / 4E10 (lower panel) and subjected to flow cytometric analysis.

4.2.1.2 Incorporation into VLPs and selective binding to BNMAbs

This gradual binding pattern was also to be verified for gp41 variants incorporated in viral or virus-like particles for the desired panning based on virions and not only on cells. Thus, VLPs pseudotyped with members of the gp41ctm mini-library were produced, incubated with 4E10, purified by sucrose gradient centrifugation, lysed and stained in a Western Blot (fig. 27). p24 served as an input control. gp41 variants were quantified by anti-HA-Ab, whereas bound 4E10 was visualized by anti-hlgG. The intensities of 4E10 to anti-HA-Ab were quantified (fig. 27, lower panel) and corresponded to a decreasing binding pattern for 4E10 also on the surface of virus-like particles, while the amount of gp41 derivatives incorporated into VLPs was similar (anti-HA staining). This finding is consistent with cytometric analyses, where cell membrane exposure was similar but binding to 4E10 was specific for each member (fig. 26). The *in silico*-designed 4E10 mini-library therefore is a functional tool for the evaluation of 4E10-directed display systems both on cells and HIV-derived viral particles.

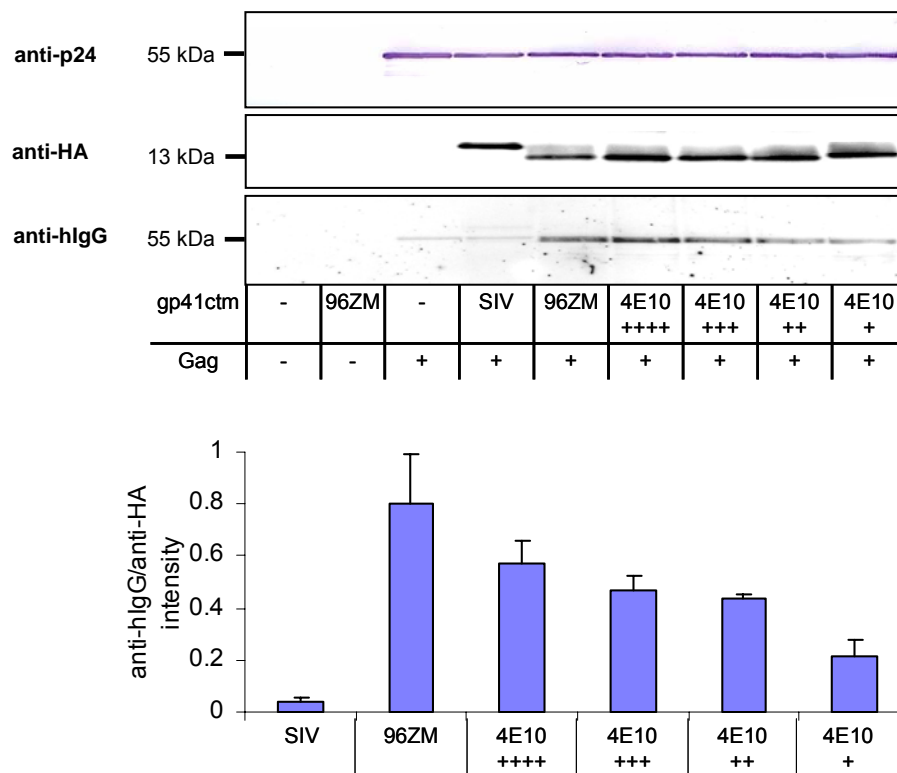


Figure 27. Incorporation of gp41ctm into virus-like particles and selective binding to 4E10. Pseudotyped VLPs were produced by co-transfection with the indicated constructs, purified by sucrose cushion, incubated with MAb 4E10 and further purified by gradient centrifugation. Fractions containing VLPs were pooled, lysed and subjected to SDS-PAGE and Western Blot (upper panel). Signals of 4E10 and anti-HA-antibody were detected by ECL staining and quantified, and their ratio was calculated (lower panel).

4.2.2 Development of the Lentiviral display system “All-in-One” (AIO)

4.2.2.1 Design of AIO platform

Pre-existing display systems suffer from disadvantages, as described earlier (sec. 2.3.1). Requirements for a novel display system included that the antigens should be (i) derived from human cells with natural post-translational modifications including glycosylation, (ii) trimeric or otherwise naturally oligomeric, and (iii) membrane-embedded. An HIV-1-derived provirus was chosen as vector platform, as it offers the mentioned qualities to display a huge diversity of antigens in a natural setting.

The display system should furthermore separate the function of infectivity from affinity maturation, making it possible for non-infectious envelopes like gp41ctm or other surface antigens to be selected by the system. This was achieved by deleting the natural env frame by a frameshift mutation, and pseudotyping of virions with glycoprotein G of vesicular stomatitis virus (VSV-G), which mediates infection into a wide array of mammalian cell types (242). The antigen to be displayed was inserted in the nef reading frame, as this frame is known to be negligible for infectivity and supportive for expression of heterologous short proteins. The viability of an env-deleted virus based on NL4-3 with luciferase in the nef reading frame was already shown by Dittmar et al. (203). The virus called pTN7* was extended for a Kozak consensus sequence 5' of the nef frame and both the NcoI and KpnI sites for insertion of foreign genes were rendered unique.

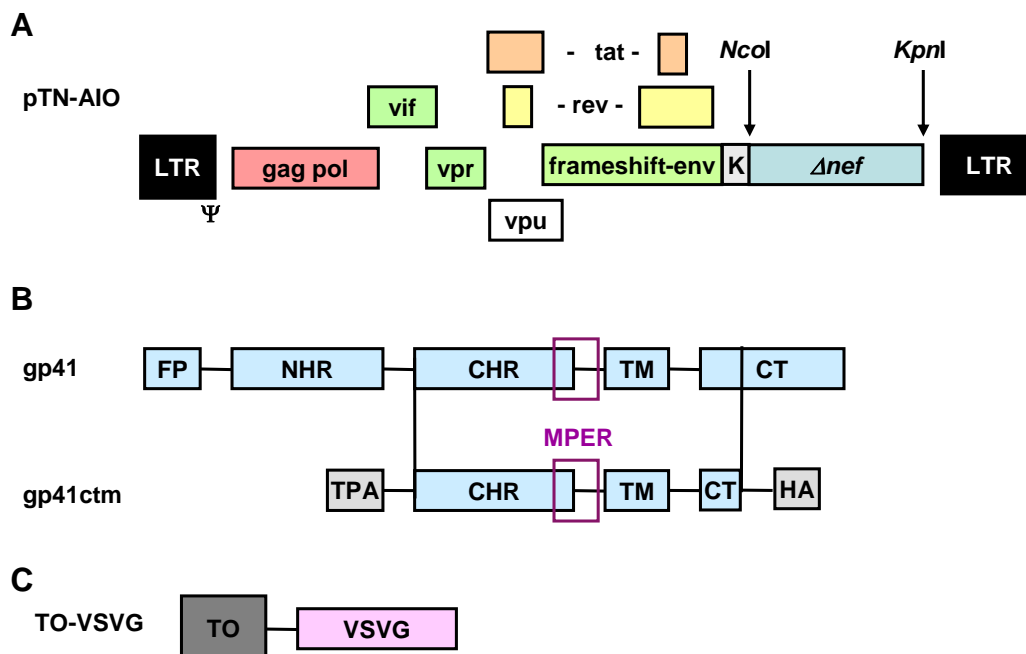


Figure 28. DNA constructs for the lentiviral display platform “All-in-One (AIO)”. (A) Design of AIO vector, based on the HIV-1 provirus pNL4-3. The original envelope reading frame contains a frameshift mutation for a stopped Env protein. Instead of nef, the antigen is inserted with a preceding Kozak consensus sequence. (B) The antigen used in this system called gp41ctm is derived from gp41 and described above. (C) Infectivity is mediated by cell line expressing VSV-G under a tetracycline-inducible promotor.

A round of panning begins with the transfection of HEK293T cells with proviral AIO plasmids (fig. 29) containing the gene of interest within the *nef* reading frame. Cells express VSV-G simultaneously, which can be achieved by (i) tetracycline-dependent induction of stably transfected HEK293-TO-VSVG cells or (ii) co-transfection of a VSVG-encoding expression plasmid. Virus is harvested 72 to 96 h p.tr. and pseudotyped with both VSV-G and the library of interest. The respective BNMAb is coated on a plate and virions are allowed to bind for 1 h at 37°C. Stringent washing removes unspecific and low-affinity binders, with only high-affinity binders being left immobilized on the plate. Genetic information can either be retrieved by reverse transcription and PCR for analysis and backup, or alternatively virions can directly infect fresh cells for another round of panning. Retrieved gene variants can later be cloned into expression vectors for cytometric analysis and sequencing of selected clones.

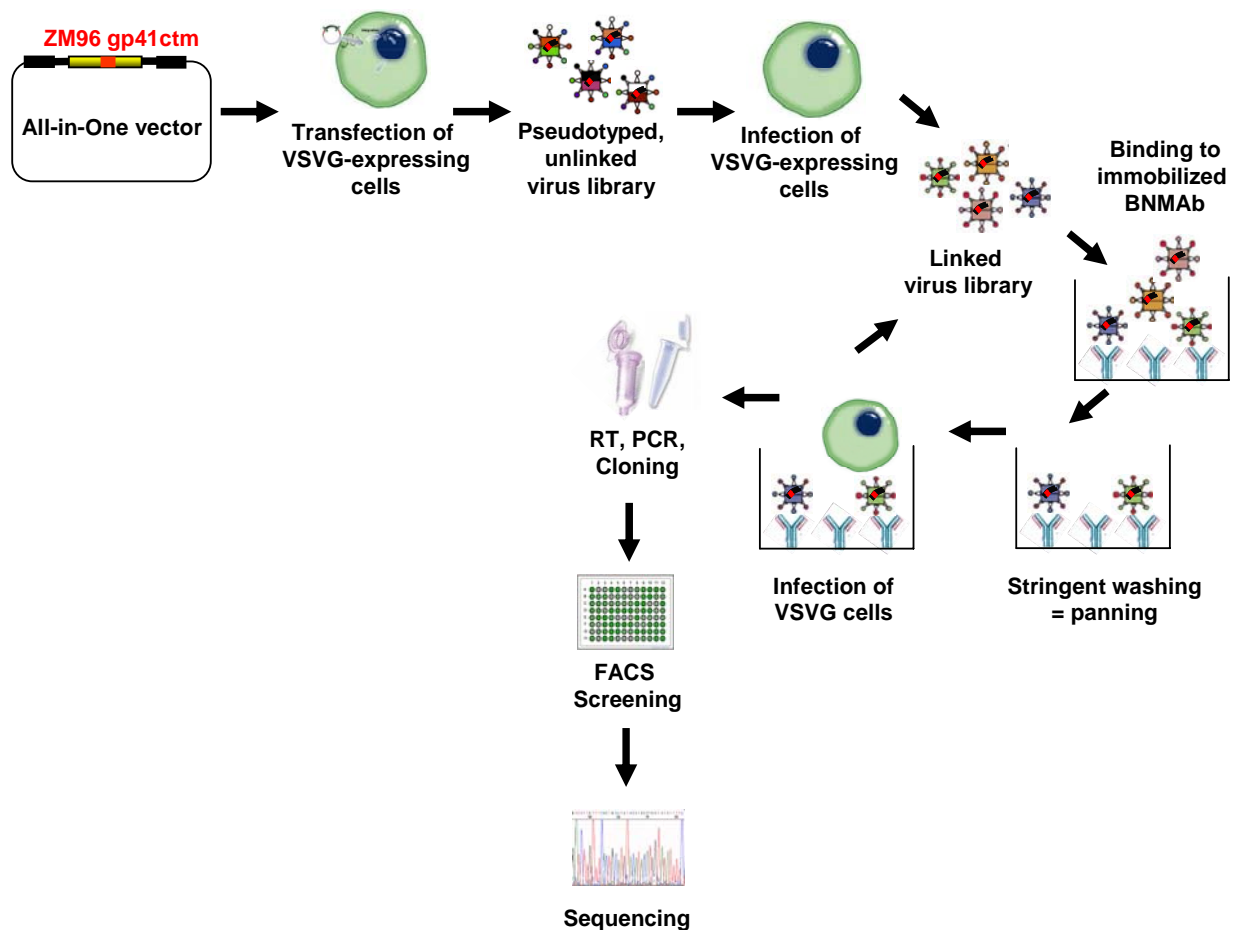


Figure 29. Overview of AIO panning procedure. HEK293 cells expressing VSVG are transfected with AIO provirus (including library) for production of pseudotyped, antigen-presenting virions. Virions are panned against immobilized BNMAbs and stringently washed. Bound virus is either lysed and genomic information is retrieved, or used for direct infection of fresh cells for another round of panning. Finally, single clones are evaluated in flow cytometric analysis and sequencing.

4.2.2.2 Replacement of *nef* is reconcilable with particle production

After cloning, the impact of the replacement of *nef* by heterologous genes on particle production was assayed. As described earlier, *Renilla* luciferase (RLuc) is tolerated in the *nef* reading

frame without significant impact on particle production or infectivity in cell culture. This could also be shown for AIO virus bearing GFP (fig. 30). Insertion of gp41ctm in the *nef* frame diminished particle production by 20-25%. While GFP expression was measurable in cytometric analysis, staining of gp41ctm expressed from the *nef* frame by 4E10 or 2F5 was barely detectable and not significant above background (data not shown), which indicated a very low expression level. In the following experiments, the single required steps of the AIO system were tested and optimized.

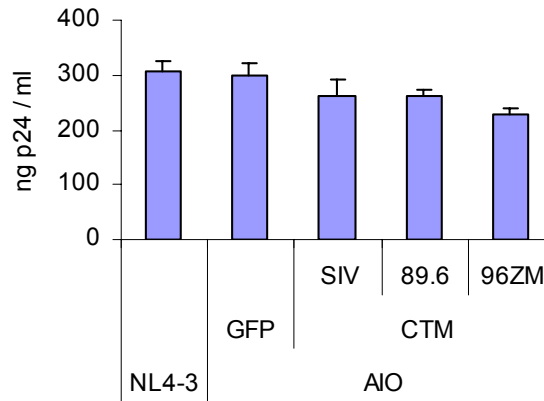


Figure 30. Production of pseudotyped virus. HEK293 cells were transfected with proviral plasmids, supernatants were pre-cleared by centrifugation 72 h later and virions were lysed and quantified by p24 ELISA. Proteins expressed from the *nef* reading frame are indicated for AIO constructs.

4.2.2.3 Virus production after transfection

Viral particles employed in a display system should be (i) infective in order to enter a second round of panning, and (ii) high in absolute number in order to present a large gene library abundantly. The AIO system was optimized in these regards by determining viral titers in form of capsid amounts and infectious units at different time points after transfection or infection of cells. Transfection of provirus is carried out in the beginning of the first round of panning for the initial virus production, whereas infection takes place in the first and every optional following round.

Virus production after transfection was monitored for a time-course of 96 hours and revealed a peak for NL4-3 after 84 h and for AIO after 96 h. After 96 h, the experiments were terminated as cells began to detach from wells. Particle release from HEK293T cells was generally higher than from doxycycline-induced HEK293-TO-VSVG cells, likely due to VSVG-mediated cytotoxicity. Infectious units reached a peak after 72 h for NL4-3 and after 96 h for AIO. The number of infectious units (IU) per ng p24 ranged from ~1,000 to ~50,000, with particle infectivity dropping with longer production times. In conclusion, the optimal time point for harvesting virus was set to 96 h p.tr. to gain the highest number of infectious particles. The nature of the heterologous gene within the *nef* frame, RLuc or gp41ctm, had no significant impact on the determined time points.

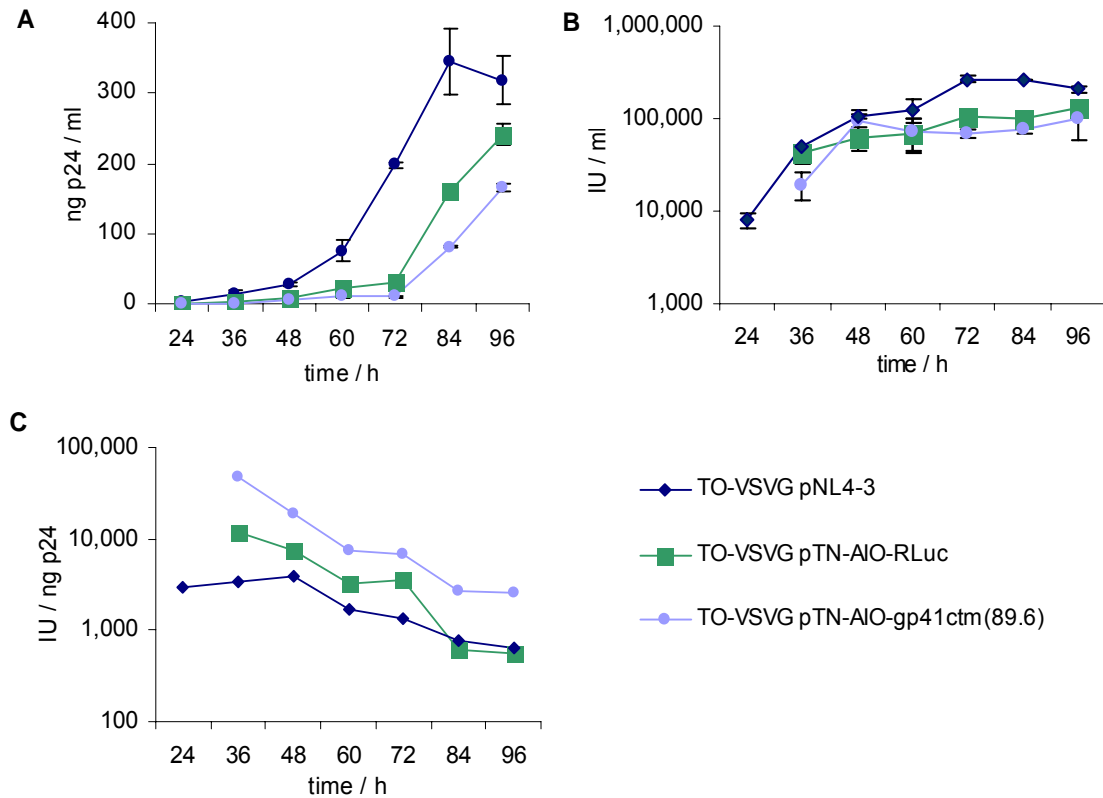


Figure 31. AIO virus production after transfection. HEK293T and inducible HEK293-TO-VSVG cells were transfected with the indicated proviral plasmids. (A) Supernatants were harvested at indicated timepoints and quantified by p24 ELISA. (B) VSVG-pseudotyped virus was used in MAGI assays to determine amount of infectious particles. (C) The infectivity was calculated as infectious units (IU) per ng p24.

4.2.2.4 Virus production after infection

In order to determine optimal panning time points after infection, virus was produced by harvesting 96 h p.t.r., HEK293-TO-VSVG cells were infected, and supernatans were analyzed as described above. Additionally, different multiplicities of infection (MOIs) of 1, 0.1 and 0.01 were tested in this controlled situation. After infection with an MOI of 1, p24 was detectable 24 h p.inf. and raised constantly until 96 h p.inf. (fig. 32A). For an MOI of 0.1 and 0.01, virion release started later at 48 h or 72 h p.inf., respectively. Generally, overall particle production increased with the applied MOI. The number of infectious units was dependent on the number of input capsid copies, as was expected, with a peak at 48 to 72 h for MOI of 1, and peak at 96 h for an MOIs of 0.1 and 0.01 (fig. 32B). In the actual panning setting, an MOI of 0.1 or 0.01 is more likely and desirable than an MOI of 1. Virus infectivity, determined as infectious units per ng p24, decreased during production time (fig. 32C), but was over-compensated with increasing virus release between 48 and 96 h after infection with low MOIs of 0.1 or 0.01 (fig 32B). The optimal time point for virus panning after infection was therefore determined as being 96 h p.inf. to obtain the highest number of infectious particles.

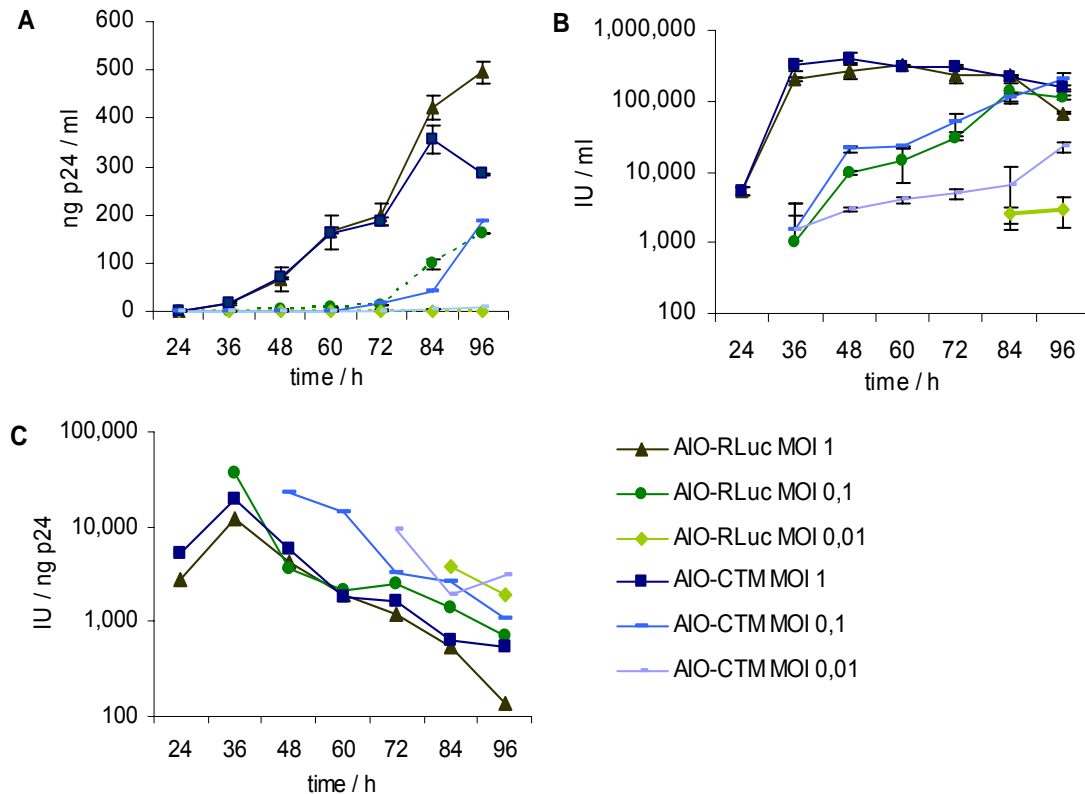


Figure 32. Virus production after infection. Indicated viruses were harvested 96h p.tr. and cells were infected at MOIs of 1, 0.1 or 0.01. (A) Supernatants were harvested at indicated time points and quantified by p24 ELISA. (B) VSVG-pseudotyped virus was used in MAGI assays to determine amount of infectious particles. (C) The infectivity was calculated as infectious units (IU) per ng p24.

4.2.2.5 VSVG Pseudotyping

The amount of VSVG pseudotyping has to be balanced. High copy numbers of VSVG on viral particles are desirable as they promote infectivity, but excessively high expression level induce cell toxicity and therefore impair proper particle production. Thus, the amount of VSVG pseudotyping was optimized empirically.

First, doxycycline (DOX) induction during particle production was titrated from 1 $\mu\text{g/ml}$, as recommended by the manufacturer, to 0.001 $\mu\text{g/ml}$. It could be shown that DOX concentrations from 1 to 0.01 $\mu\text{g/ml}$ are effective for VSVG pseudotyping, with only a slight decrease in fluorescence intensity (fig. 33A). Secondly, emanating virus was normalized for particle number by ELISA, with no apparent differences in p24 levels (data not shown). Virions were panned against BNMAbs 4E10 or 2G12 and immobilized infectious units were visualized by TZM-bl reporter cells (fig. 33B). For AIO-CTM virus, pseudotyping with 1 or 0.1 $\mu\text{g/ml}$ resulted in effective capture and reinfection by 4E10, whereas for NL4-3 a concentration of 0.01 $\mu\text{g/ml}$ was still effective. AIO-huGFP did not show significant capture or reinfection, as was expected due to the lack of any BNMAb binding site. As a conclusion, a concentration of 1 $\mu\text{g/ml}$ was used further on for effective pseudotyping.

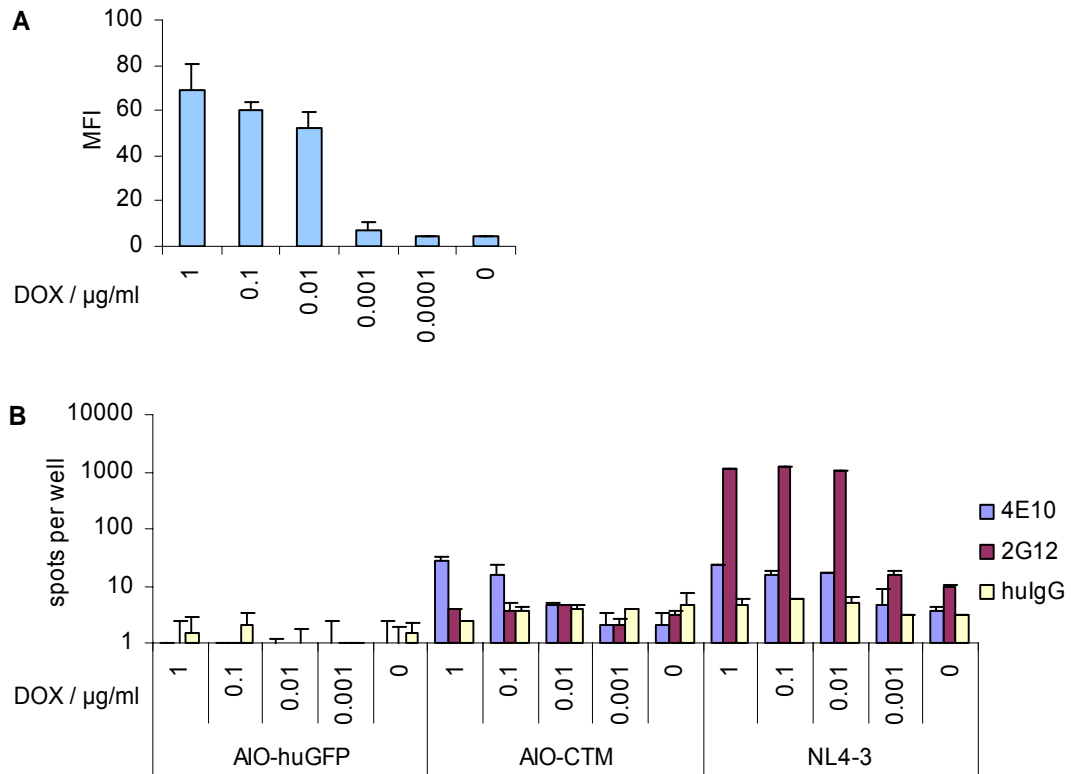


Figure 33. Effective VSVG pseudotyping of AIO-CTM virions. (A) VSVG-expressing cells were induced by the indicated concentrations of doxycycline (DOX) for 5 h and incubated for further 24 h in fresh medium. VSVG expression was measured with the aid of an anti-VSVG-antibody in cytometric analysis. (B) Indicated viruses were produced with simultaneous induction of several concentrations of DOX and panned against indicated BNMAbs. TZM-bl reporter cells were added to immobilized virus and infected cells were read out by beta-galactosidase staining.

4.2.2.6 Optimization of further steps in panning procedure

During the establishment of the AIO panning procedure, a multitude of further parameters were optimized for efficient antigen expression, virion binding, washing and reinfection (table 5). Besides the *nef* reading frame, also the *vpr* reading frame was tested as antigen expression frame. Cloning was performed according to Ali et al 2003 (206). Unfortunately, insertion of codon-optimized gp41ctm genes completely abolished virus production (data not shown), so this approach was not pursued any further. Optimization of virus production was described above. VSVG pseudotyping by co-transfection of HEK293T cells with a VSVG-encoding expression plasmid was also tested, and led to similar viral infectivity as the production in stable doxycycline-inducible HEK293-TO-VSVG cells, but was more time-consuming when applied after panning. Both magnetic beads and plates were evaluated as solid phases for antibody linkage and virion capture, with plates showing a higher signal to background ratio. Besides Nunc Maxisorp microtiter plates for the immobilization of the panning antibody, also plates with other binding profiles and plates of other manufacturers were tested, including plates pre-coated with anti-hIgG antibodies. For coating, the composition of buffers and blocking reagents were varied. The binding of virions was optimized regarding incubation temperature and time. For the panning itself, the composition of washing buffer (addition of Tween 20), and the number of

washing steps was evaluated. Finally, the reinfection of cells was examined with and without use of additives like polybrene or saponin. The final optimized protocol can be found in the methods section (3.3.12).

Table 5. Parameters tested for AIO panning.

Parameter tested	Values tested	Optimal value
Antigen reading frame	<i>nef</i> , <i>vpr</i>	<i>nef</i>
Virus production time, after transfection	24, 36, 48, 60, 72, 96 h	96 h
Virus production time, after infection	24, 36, 48, 60, 72, 96 h	96 h
VSVG pseudotyping	transfection of 293T cells, induction of 293-TO-VSVG cells	induction of DOX-inducible 293-TO-VSVG cells
DOX concentration	1, 0.1, 0.01, 0.001 µg/ml	1 µg/ml
Solid phase	plates, magnetic beads	plates
Plate type	Nunc: Maxisorp, Medisorp, Polysorp, untreated; Greiner: Microlon 600 high, Microlon 200 low	Nunc Maxisorp
Direct vs indirect coating	coating of BNMAb directly, pre-coating with anti-hIgG, use Protein-G-precoated plates	pre-coating with anti-hIgG
Coating buffer	100 mM or 20 mM carbonate pH 9.5, PBS pH 7.0	100 mM carbonate pH 9.5
Capture antibody concentration	2.5, 10, 40 µg/ml	10 µg/ml
Blocking reagent	5% BSA in PBS, 5% milk powder in PBS, DMEM with 10% FCS	DMEM with 10% FCS
Virus concentration	10, 25, 50, 100, 250, 500 ng/ml	50 ng/ml
Virus incubation temperature	4, 20, 37°C	37°C
Washing buffer	PBS, TBS, PBS + 2% Tween 20, TBS + 2% Tween 20	PBS + 2% Tween 20 after coating and blocking, PBS after virus binding
No. of washing steps	3, 6, 9	3
Additives during infection	1% saponin, 8 µg/ml polybrene	8 µg/ml polybrene

4.2.2.7 Incorporation of inherently expressed gp41ctm into virions

The expression of gp41ctm from the *nef* reading frame and incorporation into viral particles was examined by Western Blot analysis. Following optimized virus production, the supernatant was loaded onto a sucrose gradient, and 20 fractions were collected after ultracentrifugation. p24 and gp41ctm could be detected in the same fractions corresponding to viral particles, thus proving proper particle incorporation (fig. 34). However, signals were close to the detection limit. In contrast, gp120 or gp145 cloned into the *nef* frame could not be detected by this method (data not shown). It can therefore be assumed that expression and incorporation of short codon-optimized gp41 derivatives are supported from this reading frame at low level.

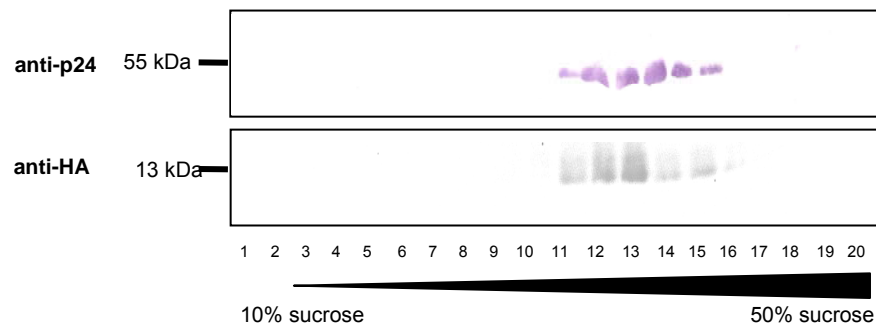


Figure 34. Incorporation of inherently expressed gp41ctm into virions. AIO-CTM virions were purified by ultracentrifugation through a sucrose cushion and loaded onto a 10-50% sucrose gradient. 20 fractions were collected, and protein was extracted and analyzed by SDS-PAGE. Gag was stained with an anti-p24 antibody (upper blot) and gp41ctm was detected with aid of an anti-HA-antibody (lower blot).

4.2.2.8 Quantification of incorporated gp41ctm

The amount of gp41ctm molecules incorporated into viral particles was assessed in the same way as for VLPs (sec. 4.1.1.7). AIO virions were normalized for p24 by ELISA, lysed and loaded onto a slot blot. Soluble GCN4-gp41-FD served as standard protein and 4E10 as detection antibody.

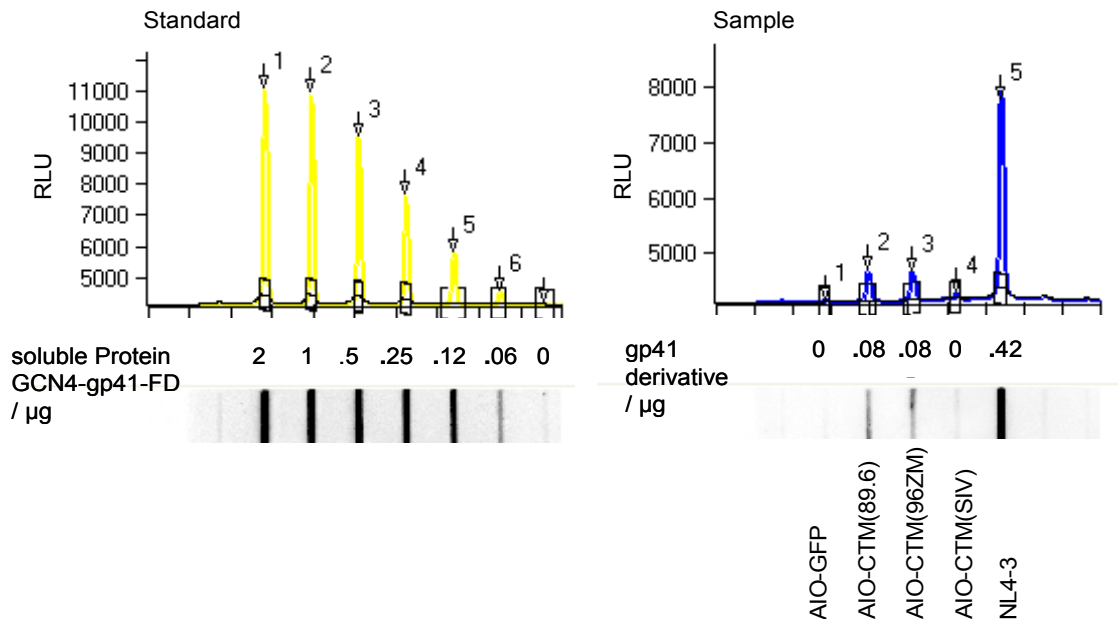


Figure 35. Quantification of incorporated gp41ctm. Indicated virions (right) were produced in HEK293T cells, harvested 72h p. tr. and purified through a sucrose cushion. Lysates were loaded onto a slot blot and stained by BNMAb 4E10. Soluble protein GCN4-gp41-FD served as standard protein (left).

Again, an absolute quantification was not possible, but standard curves were suitable for relative quantification. A comparative analysis showed that gp41ctm derived from molecular clones 89.6 and 96ZM651 was incorporated at similar amounts, and about 5 times less than wild-type gp160 in NL4-3 (fig. 35). Current estimations suggest a number of 7-15 envelope trimers per HIV-1 virion (54; 243), which would lead to 1-3 gp41ctm trimers or 3-9 single molecules per AIO virion. A copy number in this range is comparable to the 5 copies of p3

protein on the surfaces of phages as used in page display (151), and may therefore be sufficient for successful antigen presentation during the panning procedure.

4.2.2.9 Selective capture of virions and subsequent productive reinfection

A round of panning involves selective capturing of virions, efficient washing and successful reinfection. These crucial steps were checked by use of the 4E10 mini-library. AIO virions of each library member were produced separately, normalized for p24 in ELISA and individually subjected to the lentiviral panning procedure. After washing, captured particles were lysed and quantified again by p24 ELISA. As shown in fig. 36 (upper panel), capturing was dependent on binding affinity and led to a step-wise binding pattern, similar to flow cytometric data (section 4.2.1.1). Immobilized virions were covered with fresh HEK293T cells, and infected cells were read out 48 h later. The distribution of infected cells corresponded to the amounts of captured particles. These results suggest that immobilized virions can be selectively captured by BNMAbs and productively infect cells for another round of panning.

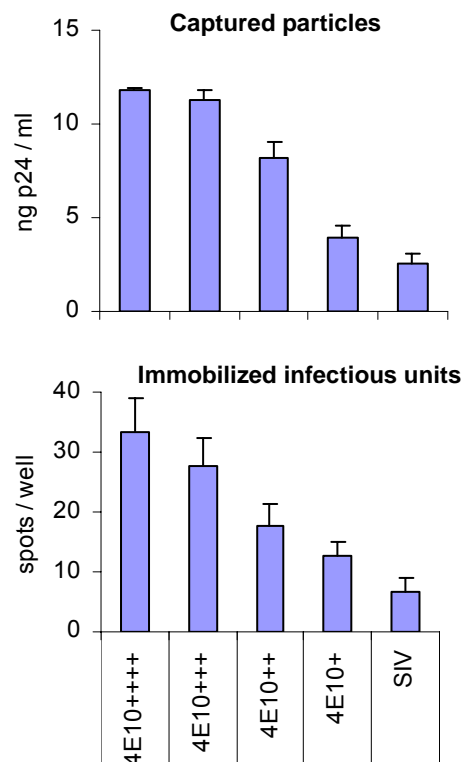


Figure 36. Selective capture of virions by immobilized BNMAb and subsequent productive reinfection. The 4E10 mini-library of AIO-CTM variants was panned against immobilized 4E10 antibody. Half of the wells was lysed and captured particles were quantified by p24 ELISA (upper figure). The other half of the wells was covered with TZM-bl reporter cells and stained for beta-galactosidase expression 48 h later, as marker of infection.

4.2.2.10 Enrichment of high-affinity binders on clonal basis

The effectiveness of the AIO display system was assessed by sequencing a peer group of clones after panning. Briefly, virions bearing the gp41ctm mini-library were produced in separate

wells as described above. Equal amounts of virions, normalized by p24, were mixed and panned against 4E10. Captured virus was lysed, genetic information was reverse transcribed, gp41ctm genes were amplified by PCR with specific primers and cloned back into the proviral vector pTN-AIO. 94 clones were picked and sequenced. The distribution of gp41ctm variants in this peer group resembled that found in ELISA (sec. 4.2.2.5) or cytometric analysis (sec. 4.2.1.1). It can be concluded that the AIO display system leads to an enrichment of binders with higher affinity for the panning antibody, already after a single round panning. Notably, there was only one clone of the SIV-based construct present in the sequencing peer group, which indicates an enrichment factor of ~25, for separately produced virions. This procedure has to be extended with a low MOI infection step when using virions from a mixed transfection (see fig. 29), to link genotype and phenotype (as described in sec. 2.1.16 and fig. 11).

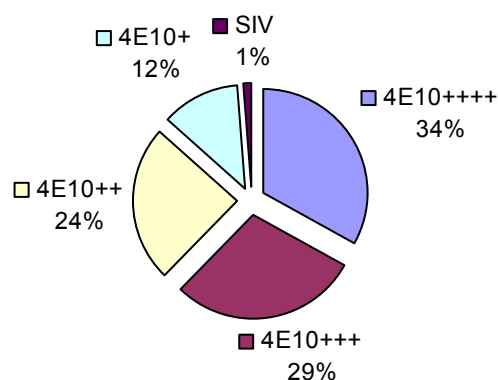


Figure 37. Enrichment of high-affinity binders in AIO lentiviral display on clonal basis. Virions of the AIO-CTM mini-library were produced following the optimized protocol, and panned against 4E10 with stringent washing. Immobilized virions were lysed and RNA was reverse transcribed. Following PCR, gp41ctm genes were cloned back into the proviral plasmid and 94 samples of the resulting clones were analyzed by sequencing.

4.2.2.11 Evidence for more efficient capture by anti-gp120 Abs than by gp41 Abs

During the development of the AIO system, it became obvious that the accessibility of the antigen and a high number of presented molecules are important parameters for effective panning. Besides 4E10, also 2F5 and Z13e1 were evaluated as capture antibodies for gp41ctm. 2F5 also led to significant enrichment, whereas capture by Z13e1 was not above background (data not shown). Similar results were obtained for capturing wild-type NL4-3 with its native envelope. Also, anti-gp120 antibodies like b12, 2G12 and HJ16 were tested with this isolate. Capturing was significantly more effective with these antibodies compared to anti-gp41 antibodies (fig. 38). Consequently, reinfection also led to higher p24 titers in a second or third round of panning. It seems that well-exposed antigens like gp120 and anti-gp120 antibodies are superior components in the AIO system compared to gp41-derived antigens and corresponding antibodies. Besides restricted sterical access, the immobilization of 4E10 might also influence its binding capacity and therefore effectiveness in the panning procedure.

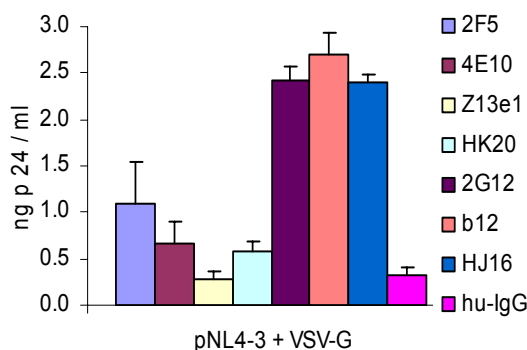


Figure 38. Evidence for more efficient capture by anti-gp120 Abs. NL4-3 virus was produced with VSVG pseudotyping and panned against indicated immobilized BNMAbs. Immobilized virus was lysed and quantified by p24 ELISA. Anti-gp41 antibodies include 2F5, 4E10, Z13e1 and HK20; anti-gp120 antibodies comprise 2G12, b12 and HJ16.

4.2.3 Lenti-cellular display systems

Members of the gp41ctm mini-library showed a reproducible binding pattern in flow cytometric analysis (sec 4.2.1.1). In this analysis format, the BNMAb binds to its target without being immobilized like in the AIO lentiviral display system. This has the advantage that also targets which are not compatible with the capture antibody's orientation after immobilization are more accessible. This seems to be the case for the 4E10 antibody, which captures only very low amounts of viral particles after immobilization (fig. 36). It is possible that the antigen needs to bend three-dimensionally for immobilized 4E10 to be able to bind and be captured. A display system, in which antigens can retain their natural conformation, would therefore be advantageous and desirable.

4.2.3.1 MACS-based Lenti-cellular display system

This goal was realized by the development of a cellular display system, which uses magnetic beads and a magnetic separation column for separation of antigen-expressing cells which are stained by a BNMAb. The system was expanded by a genetic delivery system consisting of lentiviral vectors, thus called "lenti-cellular" display. Briefly, HEK293T cells are triple-transfected by an integration-competent lentiviral vector encoding for the DNA library (pPCR-WPXLd, (211)), a lentiviral packaging construct (pTN-Pack-Tat, (208)) and a VSVG expression plasmid (fig 39). Emanating virus is pseudotyped with VSVG and carries two incorporated copies of library information. Fresh cells are infected at low MOI to ensure that most cells take up only one virion and a maximum of two RNA molecules. This step can be monitored in parallel by using a lentiviral vector expressing GFP instead of the antigen library. Generally, an MOI of <0.2 was used, as this ensures that most cells are only singly infected. 48 h later, infected cells are stained with BNMAbs for expression of antigens, and labeled with a secondary antibody coupled to magnetic beads. Labeled cells are loaded onto a magnetic cell separation column (MACS) and washed stringently, which constitutes the panning step. Bound cells are eluted,

gDNA is isolated, and envelope genes are retrieved by PCR and cloned back into the lentiviral vector for a second round of panning. Single clones are evaluated in flow cytometric analysis and sequencing.

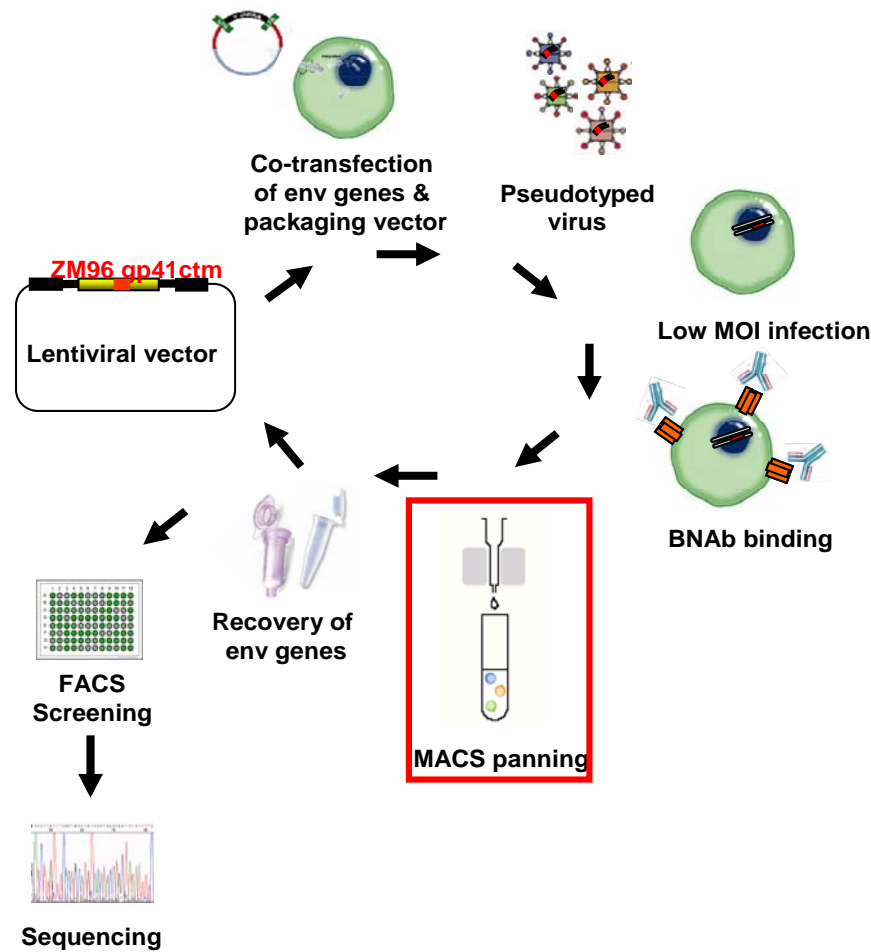


Figure 39. Overview on MACS-based Lenti-cellular display system. A lentiviral vector expressing the gp41ctm library is co-transfected with vectors responsible for packaging and VSVG pseudotyping. Cells are infected at low MOI by emanating virus, bind to BNMAbs and are panned in a MACS column. Envelope genes are recovered for another round of panning and / or screening in flow cytometric analysis and sequencing.

The gp41ctm DNA library was screened in the MACS-based system over five rounds. After each round, 94 library members panned against each 2F5 and 4E10 were analyzed by flow cytometry. After five rounds of panning, the input library and the enriched libraries were also compared by cytometry. However, no effective enrichment could be observed in the analysis of either single clones or the enriched library (data not shown). A variation in the number of washing steps in order to increase stringency did not significantly change the number of output cells or their binding stringency. It is possible that MACS columns sort primarily for expression level and not for binding strength. Expression of the members of the gp41ctm mini-library was similar between cell populations (fig. 26), but was varying largely between single cells within a population (fig. 41). Thus, a second parameter besides BNMAb binding level was introduced into the screening system, which is the expression level of the antigen on basis of single cells.

4.2.3.2 FACS-based Lenti-cellular display system

The expression level of antigens can be monitored and normalized by an antibody that binds independently of the BNMAb target site. A fluorescein-coupled anti-HA-antibody was used for this purpose. Virions are produced in the same way as in MACS-based lenti-cellular display. After infection, cells are doubly stained with both normalization antibody and BNMAb. Separation is performed in a FACS device, which allows for discrimination of binding strength on single-cell basis and sorting of cells highly positive for the BNMAb. Again, *env* genes are recovered by preparation of gDNA and PCR, and cloned back for another round of panning. Single clones can subsequently be analyzed in flow cytometric analysis and sequencing.

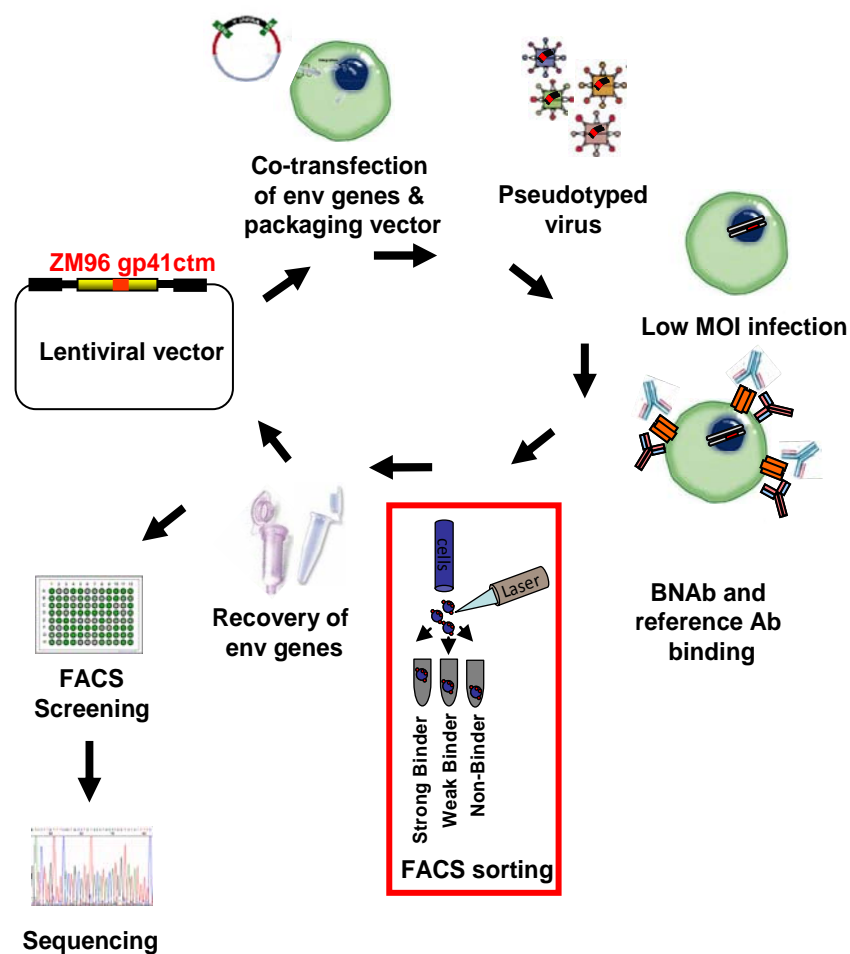


Figure 40. Overview on FACS-based Lenti-cellular display system. A lentiviral vector expressing the gp41ctm library including a tag for normalization is co-transfected with vectors responsible for packaging and VSVG pseudotyping. Cells are infected at low MOI by emanating virus, bind to BNMAbs and are sorted in a FACS device, according to their binding strength. Envelope genes are recovered for another round of panning and / or screening in cytometric analysis and sequencing.

4.2.3.3 Gating strategy

The proper adjustment of gates is critically important for successful FACS sorting. Only living single cells are gated in a first step, and thus separated from apoptotic cells, cell debris and cell clumps (fig. 41A). Cells expressing the wild-type (or “master”) gene form a population doubly

positive for the normalization antibody (anti-HA-Fluorescein) and BNMAb (4E10-AlexaFluor647). The sorting gate is adjusted so that cells with a high ratio of BNMAb to normalization Ab are sorted. In consequence, the sorted gate forms a triangular shape above a hypothetical line in which the master population appears. This gating strategy was further called “triangle gating”.

Vector pQL9 allows for quantification of an additional parameter, the multiplicity of infection. The MOI can be deduced from the number of infected cells, by gating cells positive for GFP and calculating the MOI by assuming a Poisson distribution (fig. 46B in sec. 6.1). For subsequent sorting, cells expressing GFP very strongly were not included in the sorting gate, as these may represent multiply infected cells.

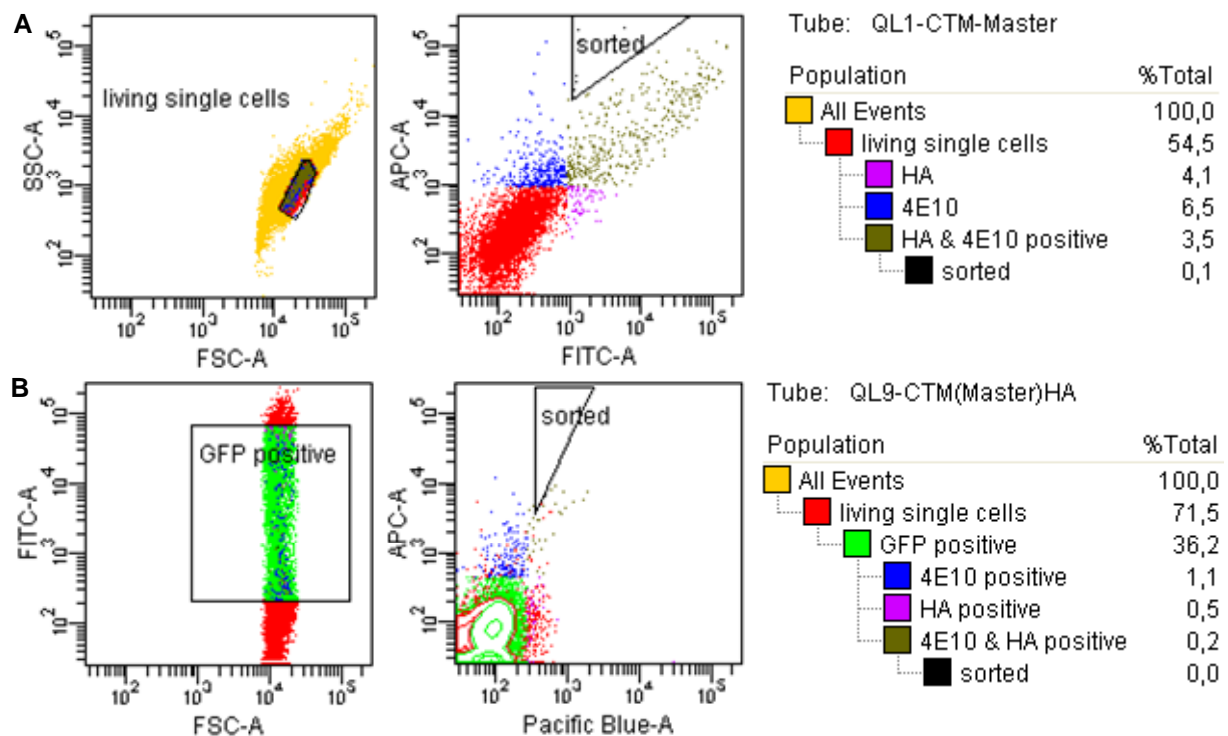


Figure 41. Gating strategy in FACS-based panning. (A) Generally, only living single cells were gated. For the library in vector pQL1, two parameters defined sorting: intensity of BNMAb (4E10) and anti-HA-Ab for normalization of envelope expression. (B) For the library in vector pQL9, cells were gated additionally for GFP positive cells. As the fluorescein channel is blocked by GFP, normalization was done with an AlexaFluor405-conjugate (Pacific Blue channel).

AlexaFluor405- or PerCP-conjugated antibodies were chosen for normalization, as Fluorescein cannot be used together with GFP. In principle, this triple-staining is functional. However, staining with Alexa405 or PerCP resulted only in weak fluorescence intensities, and should therefore be used only with highly expressing antigens. Here, the sorting gate for gp41ctm was forced to be very narrow. For this reason, subsequent experiments were performed using pQL1 and not pQL9. Infection rates were determined separately with a pQL1 vector with GFP as surrogate of the antigen.

4.2.3.4 Discrimination between high- and low-affinity binders

The performance of the FACS-based lenti-cellular display system was evaluated by screening of the 4E10-directed mini-library. Each member was transfected individually after cloning into pQL1. The ratio of 4E10 to anti-HA antibody decreased in a stepwise manner from 0.86 to 0.08, as indicated in the upper right corner of dot plots in fig 42.

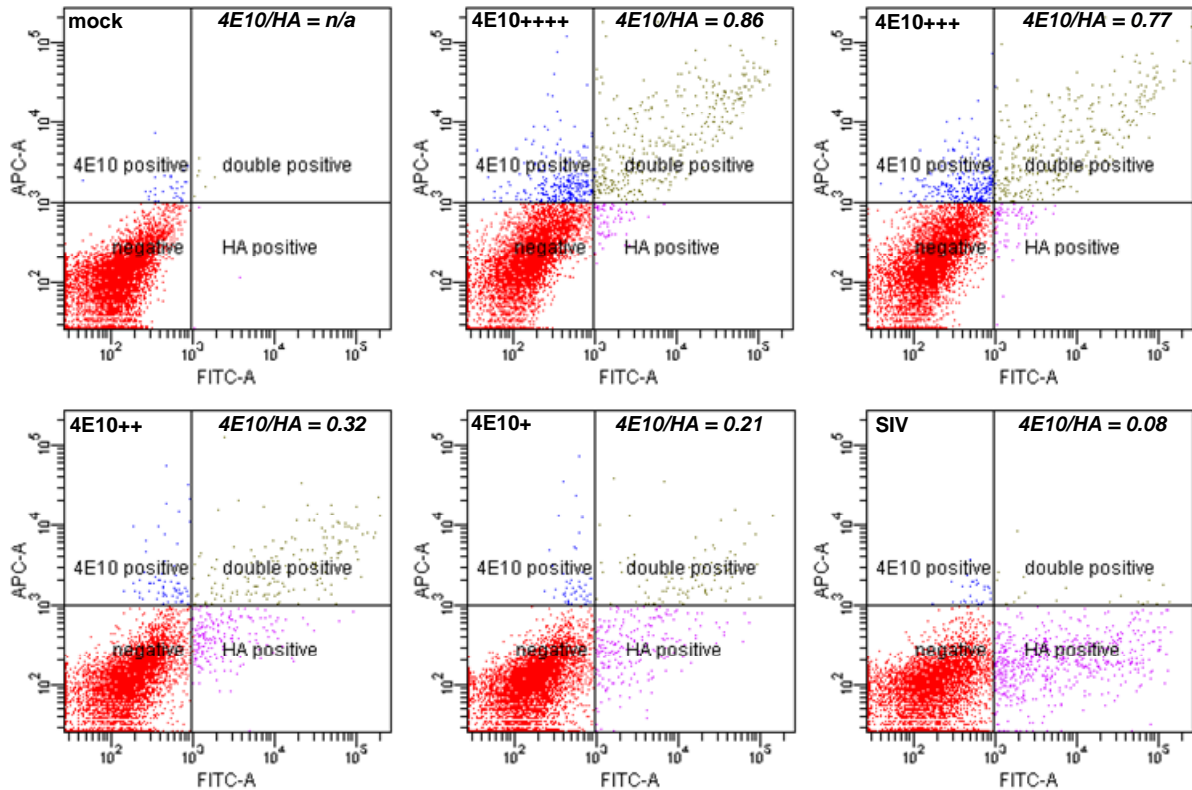


Figure 42. Discrimination between high- and low-affinity binders in the 4E10-directed mini-library. HEK293T cells were separately transfected with gp41ctm variants of the 4E10 mini-library in pQL1 and stained with 4E10 as target and anti-HA as normalization antibody. The ratio of 4E10 to anti-HA intensity is indicative for the 4E10 binding strength.

4.2.3.5 Proof-of-concept: Sorting and sequencing of mini-library

Next, virus representing the 4E10 mini-library was produced by either transfecting cells with separate constructs and mixing supernatants later, or by mixing constructs before transfection. While the first case of separate transfection allows for the evaluation of the sorting procedure itself, the second experiment of a mixed transfection more closely reflects the real situation in which a complex library containing too many variants for separate handling is used. Cells were infected with a low MOI between 0.1 and 0.2 for both assays and sorted by the triangle gating strategy like in fig. 41. Genetic information was cloned back and 94 clones each were analyzed by sequencing. Likewise, infected cells before sorting were treated analogously for comparison of input and output. Members of the 4E10 mini-library were roughly distributed equally before sorting (fig. 43A). For separately produced virions, enrichment of high-affinity binders was highly efficient with 59% of clones representing the best binder 4E10++++, and no SIVmac239-based

sequence within the peer group. Thus enrichment of binders compared to the non-binder was above the detection limit (>25-fold). This indicates that the system yields an enrichment superior to the lentiviral AIO system. Concerning virions resulting from mixed transfection, 4% sequences based on SIV were present in the peer group, and enrichment of good binders after one round of panning was not as stringent as by using separately produced virions. This is due to double infections or to infections by virions bearing a second RNA coding for a non-binder. Still, enrichment of binders compared to the non-binder is significant (~5-fold) after one round and suitable for screening of a larger library. Strong binders may be further enriched by additional rounds of panning (211).

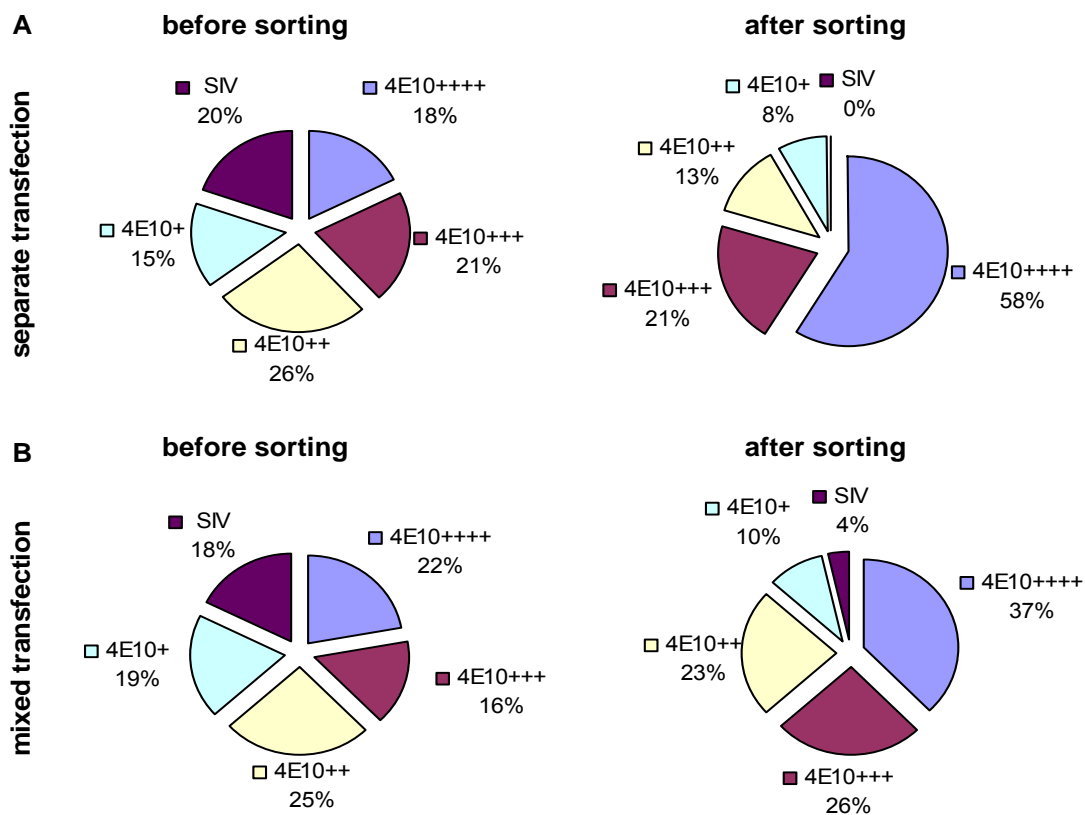


Figure 43. Enrichment of high-affinity binders in FACS-based lenticellular display on clonal basis. Cells were infected with virions presenting the 4E10 mini-library after production by (A) separate or (B) mixed transfection, and sorted for a high 4E10 to anti-HA ratio. Cells were lysed and genomic DNA was isolated. Following PCR, gp41ctm genes were cloned back into the retroviral expression vector and 94 samples of resulting clones were analysed by sequencing.

4.2.4 Creation of a complex library

A large randomized library was to be created in order to select an antigen with enhanced binding affinity to MPER-directed BNMAbs. As scaffold for this library, the codon-optimized gp41ctm gene based on molecular clone 96ZM651 was chosen. The 2F5 epitope was restored by mutation of amino acids ALDSWNN to ELDKWAS. Residues in and around these epitopes were mutated, except central core residues whose mutation would result in total loss of binding, i.e. KW for 2F5, and NF and I for 4E10. Additionally, the transmembrane domain, conserved

shown). The library was cloned into the lentiviral vector pPCR-WPXLd and both library integrity and diversity were verified by sequencing of a peer group of 94 clones (data not shown). All clones were unique and the average mutation rate was 3 aa substitutions per clone. Sequences of 25% of clones were aberrant due to unwanted substitutions like stop mutations or frameshift mutations.

4.2.4.1 Cloning of library into lentiviral vectors

As no internal independent normalization antibody was available, the gp41ctm library had to be extended with an HA-tag for use in FACS-based lenti-cellular display. The tag was fused by PCR, analogously to the constructs described in section 4.1.1.1. The raw, uncloned library served as template. As target vectors, further developed variants of vector pPCR-WPXLd were used, which contain restriction sites for the highly efficient IIS-ccdb cloning procedure (pQL1 and pQL9, (211)). Vector pQL9 also expresses constitutively GFP from the same transcript as the antigen library, which allows for simultaneous determination of multiplicity of infection. For detailed information on vectors and cloning strategies, see methods section 3.1 and (211). The simultaneous usage of type IIS restriction enzymes and a vector with killer gene ccdb ensure an efficient restriction / ligation and zero background. With aid of the IIS-ccdb procedure, $>10^6$ independent transformants for both vectors pQL1 and pQL9 were obtained (table 6).

Table 6. Cloning of gp41ctm library into lentiviral vectors pQL1 and pQL9.

	vector	insert	Transformation rate / μg DNA	Number of independent transformants
Ligations	pQL1	TPA-Library-HA	8.0×10^6	1.7×10^6
	pQL9	TPA-Library-HA	5.8×10^6	1.2×10^6
	pQL1	-	0	n/a
	pQL9	-	0	n/a
Plasmids	pUC18	-	1.2×10^{10}	n/a
	pWPXLd	-	8.0×10^9	n/a
No DNA	-	-	0	n/a

The number of amino acid mutations resembled a Gaussian distribution with a peak at three mutated residues per molecule (fig 45). 27 clones resp. 29% encoded premature stop codons or exhibited frameshift mutations and were considered as erroneous sequences, which is in agreement with the documentation of the same library cloned into pPCR-WPXLd. The conservation of amino acids within mutated regions ranged from 70 to 97%, and randomly introduced residues were present ranging from 1 to 12% (table 7). The same peer group was also transfected in 293T cells and stained by 2F5 and 4E10. Protein expression for in-frame clones could be verified, with some clones exhibiting a reduced MFI compared to the master

4 Results

gene, as was expected. In conclusion, the library is highly diverse with a majority of functional clones, and thus suitable for being subjected to a panning procedure.

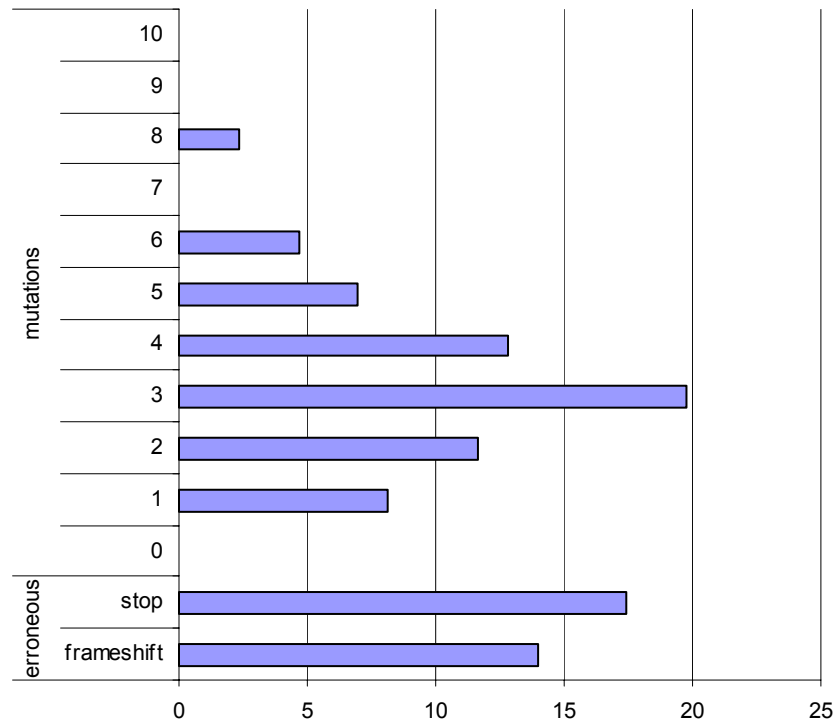


Figure 45. Analysis of gp41ctm library in pQL1 on clonal level. Sequences of 94 clones were analyzed, with all of them being unique. The number of amino acid substitutions and number of erroneous clones in this peer group are shown.

Table 7. Detailed analysis of amino acid substitutions within peer group.

	Position																			
	196	199	202	208	211	217	220	223	229	232	235	238	247	250	253	259	268	274	277	295
	Q	S	Q	E	Q	E	K	D	L	E	L	D	A	S	L	N	D	T	K	K
A		2		3		1	1			2		2	86	2			3	2		
C																				
D				5		5		76		5		73	2			3	92			
E			5	71	1	78		6		77		9					2		2	
F																2				
G				3		4		3		3		5	6							
H	1		5		8			3								3				
I							1									5		2		
K	4	1	4	3	1	3	72									2			98	97
L	12	1	5		8		4		84		91			6	87					
M							1				2				3					
N	1						5	1				2				80		2		2
P	5	4	3		7			1	6					5						
Q	73		72	3	70	1				6	3				5					2
R			4		4		3		4		2									
S	1	83											3	82				2		
T	1	2					1	1					3					93		
V	1			12		5	1	4	4	8	2	9			5		3			
W																				
Y				1				3								3				
*		5	3		1		7							5						
fs	1	1				3	3		1		2					2				

The percentage of each amino acid occurring at the randomized positions is given. Residues of the master gene are indicated in bold font.

4.2.4.2 Library screening

Preliminary lenti-cellular display screens were performed with this library, without identification of a member binding substantially (>1.5 -fold) stronger than the master-gene so far. Infection of a plate with 3×10^7 adherent cells with an MOI of 0.2 resulted in a calculated 5×10^6 singly infected cells, which covered the transformed library of 1.7×10^6 clones with a mean of 3 cells expressing each single gene. The calculated completeness of coverage is 99.99%, according to the Poisson distribution (244). However, a limiting step was the weak expression level of gp41ctm. Only few cells met the criteria of over-proportional BNMAb binding and were sorted, leading to little genomic material to be screened afterwards. Depending on gate positioning, only about 1 cell out of 10^5 showed a clearly enhanced BNMAb to anti-tag ratio and was eligible for being sorted. It is strongly advised to use large amounts of cells in further screens for efficient subsequent PCR amplification.

4.2.5 Summary

A novel lentiviral display platform called All-in-One was created, which combines the genetic information for both the packaging functions and the antigen library in one lentiviral genome. In this system, the gene of interest is inserted into the viral *nef* reading frame. A protocol for particle production, binding, washing and retrieval of genetic information was established. A second round of panning can be executed after infection of fresh cells by immobilized, VSVG-pseudotyped virions. The performance of the system was monitored with aid of a tailor-made, 4E10-directed mini-library on the basis of gp41 from isolate 96ZM651. Here, the 4E10 binding site was successively mutated, resulting in a gradual binding pattern of 4E10 towards the mini-library on the surface of both cells and VLPs. Strong binding members of the mini-library were enriched after a single round of panning, as was evident in virion capture assays and reinfection experiments. Sequencing of 96 panned clones also revealed a clonal enrichment of strong binders. However, the system may be more useful for screening of antigenic sites with higher accessibility, as suggested by proof-of-concept experiments using full-length gp160 and anti-gp160 antibodies. Thus, a second technique, called lenti-cellular display system, was adapted for the screening with anti-MPER Abs. In this system, cells are infected with particles created by lentiviral vectors, and screening is performed directly on the surface of cells. Cells are sorted for both well-expressing and strongly binding antigens, thus taking the expression level as important parameter into account and outcompeting the MACS-based system. The FACS-based system was also evaluated by use of the 4E10 mini-library and showed a clear enrichment of strong binders after one round of panning, as verified by clonal sequencing. Finally, a complex degenerate library consisting of $>10^{10}$ molecules was produced and cloned into appropriate vectors with transformation efficiencies of $>10^6$. The mean number of mutations in the MPER was three amino acids, with $\sim 75\%$ of clones expressing functional proteins. No

improved binders could be identified so far. Yet, the library is ready for further screening in the lenti-cellular display system.

5 Discussion

5.1 Discussion of novel gp41 immunogens

5.1.1 gp41 MPER - challenges for targeted vaccine development

An MPER-based vaccine is expected to direct Ab responses against this region, avoiding the problem of non-neutralizing Abs against other sites on Env. This "targeted vaccine design" is a new challenge for vaccinologists. Initial attempts to elicit BNABs against the 2F5 epitope (245-247) and the 4E10 epitope (248; 249) have failed, emphasizing the challenges associated with producing a targeted vaccine against the MPER. First, the current approach to vaccine design favors the presentation of the MPER in the context of the membrane, which is more complicated than using soluble antigens. A second challenge is identifying methods that produce high titers of Abs to the MPER. An approach that combines the exposure of neutralizing sites on the immunogen in the correct structure, masking (250) or silencing (251) of ID epitopes, membrane embedment, new adjuvants, and the use of novel immunization strategies (e.g., prime-boost) may be effective. Thus, the first part of this work focused on the creation and immunological evaluation of novel gp41-derived immunogens, which meet all mentioned requirements of an up-to-date MPER-based vaccine.

5.1.2 Tailor-made construct design for optimized MPER presentation

As induction of BNABs directed against the MPER rarely results after exposure to native envelope proteins, different steps were undertaken to improve exposure of conserved regions, stabilization of relevant conformations and immunofocusing. First, gp41 was truncated N-terminally to eliminate dispensable sites like FP, FPPR, NHR, and the immunodominant loop. The CHR was partially included to promote proper trimerization and folding of the nearby MPER. However, as it was unknown to which extent the CHR is needed for this purpose, two variants with full-length CHR ("gp41ctm") and a truncated CHR ("gp41ctm2") were created. The C-terminus was also shortened to enhance incorporation into VLPs. A protein with the desired features was described by Lenz et al. (183), so both name and dimensions were adopted for the basic construct gp41ctm. Fusion of an N-terminal signal peptide was supposed to promote membrane localization, and attachment of a C-terminal HA-tag served as detection marker. Resulting patchwork proteins were analyzed by *in silico* protein topology programs, and signal peptide cleavage, membrane incorporation and orientation were predicted as desired. Next, the stabilization of a desired trimeric structure was implemented by introduction of two alternative heterologous zipper domains. The correct fusion sites were deduced by combining existing crystal structures of both zipper domains and gp41 in post-fusion states. But, instead of fusing the zipper domains to the NHR building the inner core of 6HB (89), these domains were fused N-terminally to the CHR, anticipating the stabilization of an intermediate conformation (95). In

absence of NHRs, CHRs are supposed to form trimers by contacts of the same residues which form contacts with the NHRs in 6HB. The correct (energetically optimal) fusion sites could be approved by molecular modeling. Thus, a total of four constructs focusing on MPER, some with additional conformational stabilizations, all membrane-embedded, were designed and approved in their desired specifications by appropriate state-of-the-art model software.

5.1.3 Experimental implementation of desired protein specifications

Each required property of gp41 variants was tested empirically in experiments. First, protein expression and molecular weight was verified by Western Blot analysis (data not shown) for constructs based on molecular clones 89.6, 96ZM651 and SIVmac239. Next, membrane topology and binding to BNMAbs 2F5 and 4E10 could be validated by cytometric analysis. Signals for both BNMAbs and normalization antibody were low, but significant and specific, indicating a low level of presentation, yet a proper membrane incorporation and protein folding. The about 30% higher BNMAb signals for heavily truncated gp41ctm2 compared to other constructs might be due to an enhanced accessibility exposure of the MPER region. The normalization by the HA-tag located in the putatively exposed CT was possible, supporting the hypothesis of three membrane-spanning domains of Cleveland et al. (98).

Incorporation into VLPs was successful, as verified by sucrose gradient analysis. Higher molecular weight bands of trimer-stabilized constructs likely indicated an unusual high stability of dimeric and trimeric assemblies. Trimeric conformation was desired as it was shown that trimeric gp140 immunogens are superior to monomeric gp140 variants when it comes to inducing neutralizing responses (252; 253). The oligomeric state was further affirmed by crosslinking experiments. Here, all constructs formed dimers and trimers, independently of heterologous trimerization domains. It is possible that only the stability and not the fraction of trimerization is largely affected by the introduction of zipper domains for gp41ctm. This finding is consistent with data from Lenz et al. (183), who detected proper trimerization of gp41ctm in liposomes without additional zipper domains, and an improved stability in detergent SDS after introduction of trimerization domains (D. Hulsik, personal communication). However, signals in Western Blots after crosslinking with higher concentrations of crosslinking reagent were weak in the present study, so this method had limitations in giving a terminal answer to what extent the trimeric state was the predominant one.

Also, it was not possible to determine the absolute number of gp41ctm molecules on the surface of VLPs, as the recognition by 4E10 of the closest to find soluble standard protein (GCN4-gp41-FD) was substantially lower than that of gp41ctm and variants. However, a comparative quantification was possible, which indicated that all variants are incorporated to similar levels, with shortened gp41ctm2 displaying a ~30% stronger signal. This stronger signal is either due to an enhanced recognition by 4E10, which was already observable in cytometric

analysis, or an enhanced incorporation. As all variants were planned to be used as immunogens in VLPs, corresponding pseudotyped VLPs were prepared and stained by immunogold-labeling. VLPs retained an intact morphology and binding of 4E10 on the surface of VLPs was possible, indicating a proper exposure of all antigens in this environment. The successful staining also with anti-HA-antibody suggests an exposure also of the CT, in accordance with Cleveland et al. (98), but contrarily to recent findings of Steckbeck et al. (100), who suggest an exposure only on cells but not on viral particles. Another recent publication by Liu et al. (254) draws a different picture, where the CT is only exposed during membrane fusion, but this paper also highlights the possibility of artifacts depending on sample preparation, so further investigations are needed to determine the precise circumstances of the formation of one or three membrane spanning domains. Unambiguously, all gp41 derivatives showed cytopathic effects, which has been reported earlier for HIV envelope proteins (255) and might be attributed to an increased flexibility of the membrane-perturbing MPER in the presented gp41 derivatives (256).

In summary, the models of designed gp41 variants could be implemented into proteins with the desired specifications to a large extent. Although protein expression was below optimal levels and cytopathic effects delayed VLP production, endotoxin-free batches of pseudotyped VLPs as well as corresponding DNA were prepared for immunization purposes.

5.1.4 *In vivo* testing of novel gp41-derived immunogens

After appropriate quality control of prepared immunogens (257), a DNA prime and VLP / protein boost regimen was set up for immunization of rodents in order to test their immunostimulatory properties and capacities of inducing neutralizing antibodies. Two existing soluble proteins from different sources were included as booster reagents (see methods section), to test their potential in combination with gp41ctm DNA prime. Generally, induction of anti-MPER Abs is thought to be a prerequisite for neutralizing capacity of gp41-based immunogens, and was therefore monitored in a first step by a sandwich ELISA. Inter-individual deviations in IgG responses within groups were high (sec. 4.1.2.1), which has also been observed by others (252; 258). Reactivities for any gp41 DNA / VLP boost combination were weak, except for the gp41ctm2 construct, for which anti-MPER titers were very promising (fig. 23). However, antibody pre-bleed titers were also very high in mice receiving this construct, so artifacts for the group gp41ctm2 cannot be ruled out totally. A paper by Alam et al. suggested that the presence of the ID epitope in the region corresponding to the CHR (previously defined as the cluster II epitope), which is included in the gp41ctm but not gp41ctm2 construct, can mask the Ab response elicited against the MPER (259), supporting the approach of a heavy truncation like in gp41ctm2. Kim et al. (248) also used truncated constructs, and after immunization, Abs were directed to the CHR but not to peptides that bear the MPER linear sequence, hence no

neutralization was observed. However, in the present study, reactivities against MPER and CHR were similar, independently of the immunization construct. A potential reason for this finding could be that the MPER is better exposed by the constructs of the present study, compared to earlier studies using larger constructs. Still, the low reactivity against both the CHR and MPER in groups receiving gp41ctm and trimer-stabilized constructs remains unclear.

Significant antibody titers were induced by gp145 DNA / VLP and gp41ctm DNA / soluble protein boost. In all sera obtained with VLP boosting, anti-cell antibodies were removed. Neutralization followed the principle, that only sera reactive in ELISA were able to mediate neutralization, however, antibody titers in ELISA were not a guarantee for neutralization. In particular, high anti-MPER titers induced by gp41ctm2 DNA / VLP did not promote better neutralization than sporadically occurring antibodies in sera obtained after gp41ctm DNA / VLP immunization (fig. 23). Trimer-stabilized constructs induced similar weak antibody and neutralization titers like the native construct gp41ctm, which means the relevant epitopes are neither better nor worse exposed (fig. 22).

5.1.5 Beneficial effects of DNA prime and protein boost

The group receiving gp41ctm DNA prime and GCN4-gp41ctm-FD protein boost showed the best neutralization capacity of all tested gp41-based vaccines, neutralizing tier-2 strains in the A3R5 assay in dilutions up to 1:219 (table 2). This is remarkable, as immunizations with protein alone, without DNA prime, did not lead to neutralization in PBMC or TZM-bl assays (Weissenhorn, personal communication). Neutralization is likely to be attributed to anti-gp41 Abs in this group, as only Abs of this type could be raised after gp41ctm DNA prime. A strong positive effect of DNA priming has already been observed by Law et al., where the MPER was engrafted into variable regions of gp120 (249). Devito et al. tried several immunization conditions, which included priming mice intranasally with DNA plasmids encoding gp160 and boosting intranasally with a mixture of peptides, including 2F5 epitope peptides from clades A through D and a gp41 coiled-coil peptide (260). This approach showed that the DNA immunization followed by a peptide boost was more effective than immunization with peptide alone, as demonstrated by the improved IgA response and neutralizing activity. In addition, those authors showed that the immunity lasted for 12 months corresponding to 50% of the life span of a mouse. DNA alone, however, also results in lower titers compared to prime-boost regimens. This was tracked by the antibody responses in mice with an intermediate bleed after two DNA vaccinations. No significant titers were detected at that time point, contrarily to the final bleed after two more protein / VLP immunizations (fig. 23). Thus, the strengthening effect of prime-boost regimens could be affirmed in the presented study.

Still, the overall highest neutralization capacity in the presented study was achieved in the control group receiving gp145 DNA / VLP with titers up to 1:6450 against a tier-1 strain (table 2).

However, it is likely that neutralization in this control group was mediated by anti-gp120 instead of anti-gp41 Abs. The reason, why antibodies raised in groups immunized with gp41ctm DNA / HA2-gp41ctm-GCN4 protein were able to mediate neutralization, whereas those of the group receiving gp41ctm2 DNA / VLP were not, remains elusive. Aside from a different MPER conformation presented in these constructs, the removal of anti-cell antibodies in this group could play an important role here (see below).

5.1.6 Neutralization capacity and fine-mapping of MPER-directed vaccines

Some approaches that display MPER in the context of a chimeric virus have elicited strong peptide reactivities like in the presented study, yet they have not been very successful in eliciting HIV-1 neutralizing Abs (245; 261-264). The same holds true for fusion proteins, engrafting MPER epitopes in Env variable loops (249; 265) or unrelated proteins (247; 266; 267), MPER peptides conjugated to a carrier such as tetanus toxin (268), bovine serum albumin (68), a CD4 helper T-cell epitope (269), multivalent peptides on a carbohydrate scaffold, combined peptides bearing 2F5 epitope sequences and gp41 fusion peptide to make a complex that could resemble the prefusion structure of gp41 (270), and peptide mimotopes (271). These studies show the trend that immunization with MPER peptides elicits anti-peptide antibodies but does not produce neutralizing Abs.

In the mentioned study by Law et al. (249), neutralizing Abs were induced, but these were mapped to bind to gp120 areas surrounding the engrafted MPER. Importantly, those authors dissected the Ab response and showed to which epitopes the neutralization activity was directed. A similar approach was followed in the presented study, where CHR and MPER peptides were used as readout reagents, and MPER reactivity could be monitored (fig. 22 and 23). As new data for epitopes of overlapping, very broadly 4E10 and less broadly neutralizing Z13e1 antibodies are available (108), fine-mapping of immune responses becomes even more important and is strongly recommended for future immunization studies.

Qi et al. immunized mice with a fusion protein built of NHR, FD and human IgG Fc fragment, which was used as enhancer of immunogenicity (272). Antibody titers directed against the gp41-derived part were comparable to those in the present study. However, significant neutralizing capacity of sera (up to a titer of 663) was only achieved after fusion of the Fc fragment to the FD domain. The authors suggested that enhancing the immunogenicity of gp41-derived immunogens by this means could improve neutralizing responses, which might also hold true for MPER-based vaccines.

The highest reported neutralizing activity after immunization with a gp41-derived construct was recently reported by Bianchi et al., who also used a trimer-stabilized NHR peptide as fusion intermediate-resembling construct (273). Neutralizing titers were as high as ~1000 for the homologous strain, but <100 for all other tested strains. No neutralization of tier-2 strains could

be detected. Notably, neutralizing capacity was induced in guinea pigs only, and not in rabbits, without reasoning.

5.1.7 Adding a membrane in MPER vaccines

Recent papers by Alam et al. and others (126; 127; 241) elaborated the importance of the membrane component and autoantigens in MPER vaccines. The epitope of neutralizing antibodies contains both membrane/autoantigen and protein components, whereas epitopes of non-neutralizing antibodies either bind to only the protein component or to the membrane in combination with non-neutralizing protein parts, like cluster II epitopes. Consequently, current vaccine design favors the presentation of the MPER in the context of the membrane so as to present the putative 2F5 and 4E10 epitopes in a state that resembles that of the natural Env epitope.

Recombinant enveloped viruses are one approach to achieve this. For example, Luo et al. generated recombinant VSV particles displaying the HIV-1 MPER as a fusion to the C-terminal end of the p15E protein from porcine endogenous retrovirus (PERV); p15E has structural similarities to gp41 (274). 2F5 was shown to bind to cells expressing these constructs by flow cytometry; 4E10 binding was not analyzed. Sera from rabbits that were immunized with recombinant VSV and soluble protein produced anti-gp41 MPER Abs, but the neutralizing activity of correspondent sera was below 50% neutralization of HXB2 and JRFL HIV-1 strains at 1/20 serum dilutions. DNA vaccines are another way to present the MPER in the context of a membrane, provided that the protein to be expressed is fused to a TM domain. Ye et al. made a DNA vaccine in which the HA2 domain of the influenza virus HA was replaced with gp41, reasoning that HA1, a slightly smaller protein than gp120, would conserve the prefusogenic structure of gp41 while exposing epitopes that are normally obscured by gp120 (275). Sera from mice immunized with plasmid DNA encoding the HA/gp41 fusion bound to whole gp41 and neutralized SF162 at a 1/40 dilution compared to empty-vector-immunized control sera. A recent study by Matyes et al. immunized mice with MPER peptides in liposomes (276). Although resulting sera were entitled to be neutralizing, purified murine MAbs from immune sera were not able to neutralize 50% of tier-1 SF162 strain at 500 µg MAb/ml.

These three examples show that the presentation of gp41 in the context of a membrane can produce low-titer neutralizing Abs, yet highlight the difficulty of achieving high titers. In the presented study, best results were obtained by priming with DNA encoding a membrane-bound truncated gp41_{ctm}, and boosting with soluble MPER-containing trimeric protein GCN4-gp41_{ctm}-FD. 3 of 4 rabbits showed neutralization titers higher than 40, with one animal with an IC₅₀ of 219, at least for one viral isolate. Thus, the gp41 constructs presented here (membrane-bound gp41_{ctm} DNA prime and soluble GCN4-gp41_{ctm}-FD protein boost) delivered results which are about as effective as the other few neutralization-inducing gp41 immunogens that

have been published so far (272; 273; 277). Notably, neutralization of tier-2 but not tier-1 strains was detectable in this group. This puzzling finding highlights the importance of testing immune sera against multiple strains, not only in TZM-bl, but also in PBMC or A3R5 assay, which all can deliver different results.

5.1.8 Effects of removing anti-cell activities in sera, and alternatives

The importance of membrane-/autoantigen-binding components in MPER-directed antibodies also has important consequences for the production of MPER-incorporating immunogens. VLPs produced in heterologous cell systems, i.e. different species of production cells (human) and vaccinated organisms (rodents), are known to induce undesired side reactivities (278). Therefore, sera were incubated several times with production cells to remove anti-cell activities in the presented study. The mean fluorescence intensities (MFI) of anti-cell antibodies reached the upper detection limit (~250,000) in the presented study, whereas MFI of gp41ctm-expressing cells stained by 4E10 or 2F5 was in the range of ~100. Similar results were reported by Kim et al., who observed significant anti-VLP Ab titers, with endpoint titers ranging from 10,000 to 15,000, however, anti-MPER/TM Ab responses were substantially lower, with endpoint titers to 1,000. These results indicate that while there were significant Ab responses to cell membrane proteins, this was not the case for the expressed fusion protein, highlighting the importance of anti-cell removal to avoid false positive or false negative results in neutralization assays. But importantly, by this procedure also membrane-binding/polyreactive antibodies like 2F5 and 4E10 are removed, as could be shown in this work (sec. 4.1.2.2). Similar antibodies – if present, yet highly necessary for neutralization – were removed in immune sera obtained after VLP immunization. In consequence, further immunization studies engrafting the MPER in VLPs or other cell-derived membrane environments should emphasize on producing in homologous cell systems, to avoid the problem of anti-cell Abs *a priori*.

An alternative to cell-derived membranes are synthetic liposomes like those developed by Lenz et al., who produced proteoliposomes with trimeric truncated gp41 comprising the C-terminal heptad repeat, the MPER, and the TM region of gp41 (183). Mice were immunized with truncated gp41, truncated gp41 in liposomes, or empty control liposomes. Ab titers reached 2,500 in the mouse group immunized with truncated gp41 in liposomes but not when the immunogen was presented without liposome. Serum Abs did not neutralize HIV-1, although the immunogens were shown to inhibit viral entry. It may be important to optimize lipid content, as bilayer thickness can alter the tilt of a TM helix, potentially affecting antigen display (279).

5.1.9 CTB as carrier

Matoba et al. designed a vaccine to target the MPER by fusing it (aa 649 to 684) to the cholera toxin B (CTB) subunit (280). They immunized mice seven times using immunization protocols

that included intraperitoneal (i.p.) and intranasal (i.n.) immunizations, or a combination thereof, resulting in anti-MPER Ab endpoint titers as high as 100,000. Fecal and vaginal mucosal Abs were shown to decrease HIV-1 transcytosis in a human tight epithelial model compared to control Ab, but neutralization data was not reported. In the present study, a MPER-CTB fusion protein was used as booster reagent after gp41_{ctm} DNA prime. In two out of four animals, significant neutralization was achieved, however, only against one viral isolate each. This indicates again, that DNA priming may be beneficial, also when using immunostimulatory carriers like CTB. The lower neutralization capacity compared to the booster reagent HA2-gp41_{ctm}-GCN4 in the present study might be attributed to conformational differences of the MPER in the two fusion proteins.

5.1.10 Outlook for further MPER-based immunogen design

Core of the present immunization study were truncated gp41 variants, administered as plasmid DNA and presented on VLPs. Measurable antibody titers against the MPER are a prerequisite of neutralizing activity, and might be elevated by raising the number of displayed molecules. The cytoplasmic tail of gp41 was truncated for this purpose. However, a putative envelope incorporation motif 3' of the TM region was retained (281). Incorporation might be further enhanced by a systematic approach, in which display and incorporation are analyzed after step-wise truncation of the CT. Alternatively, fusion proteins of gp41 and heterologous transmembrane domains from e.g. CD28 (163) or EBV gp220/350 (282) have been shown to mediate enhanced incorporation.

The use of a less immunogenic cell type was mentioned earlier and would make depletion of anti-cell Abs redundant. This would preserve antibodies with reactivity against membranes or autoantigens like known anti-MPER BNMAbs.

One of the most challenging questions is the conformation in which the MPER is best to be displayed. Future structural studies of intermediate conformations might lead to a better understanding of the structures relevant to be presented. So far, further empirical studies, also with trimer-stabilized constructs, will give an idea if vaccinologists are on the right track. Other zipper domains are a possibility. However, introduction of immunodominant sites should clearly be avoided. In this light, use of tagged proteins like the 9 aa HA tag in the present study is also not optimal, as these tags are often immunodominant sites in their native proteins (191). A systematic readout with overlapping peptides spanning the whole immunization proteins is recommended to map antibody reactivity and detect unwanted immunodominant epitopes.

Two soluble proteins were used in the present study with success in inducing anti-MPER antibodies and limited neutralization. The priming immunization with gp41 derivatives was intended to activate and expand a variety of B-cell clones that include clones producing the targeted anti-MPER Abs, with a boosting immunogen comprising an MPER-specific peptide.

The reverse approach may also be effective, as priming with a peptide was successful for an antigen different to HIV Env (283). Ab production could be further enhanced by incorporating helper T-cell epitopes into the priming and boosting immunogens.

The delivery of DNA by electroporation may improve immunogenicity. This has been shown in animal models (284) and recently also in humans (285). Finally, regarding adjuvants, understanding the key properties of innate immunity that lead to durable, protective B and T cell responses will guide a further way to better adjuvant formulations (286).

A recent study by Bomsel et al. showed that not only neutralization, but also transcytosis-blocking properties and antibody-dependent cellular-cytotoxicity can protect from SHIV infection after animals had been immunized with virosomes containing an MPER peptide (287). Thus, assessment of IgG neutralizing activity of sera *in vitro* does not reflect protection at mucosal sites *in situ*, and further readout parameters beyond IC50 might be of value in future studies.

5.2 Discussion of affinity enhancement of antigens

In the second part of the present study, suitable systems for the affinity enhancement of the novel immunogens were explored. Antigens that have been improved in their affinity to BNMAbs might be superior to conventional immunogens, when it comes to induction of similar neutralizing antibodies. Common *in vitro* display techniques like phage display neither support a membrane environment nor posttranslational modifications. However, gp41 is a membrane-embedded and glycosylated antigen. Novel techniques including retroviral display have become available recently. A similar system based on HIV, tailor-made for HIV-derived envelope proteins, yet universally applicable, was developed here and tested in proof-of-concept studies. Notably, a display system based on lentiviruses was not available at the starting point of this project.

5.2.1 Design of a novel lentiviral display platform

A novel lentiviral display platform was created in this study. The system integrates common display system features like production of presenting particles, panning based on antibody-antigen binding affinity, evaluation of resulting clones by sequencing, and re-aplication to enter a new round of panning. Contrarily to other lentiviral systems working with multiple vectors (209), functions for both packaging and coding of the antigen library were implemented in one viral genome. The system was therefore called All-in-One (AIO).

An existing engineered molecular HIV-1 clone with deleted Env was chosen as basis. An early stop mutation in Env in this clone preserves all genetic regulatory elements and overlapping reading frames, while no functional protein is expressed. As substitution of the *nef* frame by heterologous proteins without compromising viral replication *in vitro* had been described earlier, this was a suitable locus for insertion of antigens to be matured. Slightly reduced amounts of

viral particles were measured following Nef substitution, likely attributed to cytopathic effects of gp41ctm. Protein expression was detectable only in Western Blot but not in cytometric analysis after fixation of cells by glutaraldehyde, indicating a very weak expression. Low expression levels had already been observed in the context of pcDNA3.1(+) expression plasmids (4.1.13) and seemed to be an inherent property of gp41ctm, and expression was further reduced in the proviral context. Numbers of infectious units were quantified for production after transfection and infection, and were similar to those previously reported for HIV particles, in the range of 10^3 to 10^5 IU / ng p24 (288). Usually Nef-deleted viruses reach only less infectious doses (289), but this effect was likely over-compensated by the enhanced infectivity mediated by VSVG (290). Similar titers were attained by a trans-complementing lentiviral vector platform which also uses both Nef-deleted virions and VSVG pseudotyping (208). A relative quantification of gp41ctm molecules on the surface of virions indicated that only 1-3 trimers of gp41ctm in AIO were incorporated, independently of clade underlying. However, a low copy number of molecules on virion surface can theoretically be advantageous for display purposes theoretically, as avidity effects are minimized in this way. So, development of the system was driven forward with optimization of virus production time after transfection or infection. Infectious viral titers peaked at 96 h p.tr., where media began to acidify. After infection, optimal production time was dependent on the MOI, with 96 h p.inf., being optimal for the desired low MOI infections. Regulation of inducible VSVG pseudotyping was found to be tight in the absence of doxycycline, and to form a plateau at 0.1 μ g/ml. This supports an On/Off mechanism of the TO operator, in which a critical concentration of inductor (DOX) leads to a quick saturation of operator sequences and thus plateauing expression.

5.2.2 Creation of a 4E10-directed mini-library for validation of display systems

For proof-of-principle, a set of defined gp41ctm variants with different binding affinities to 4E10 was created. Precise information on specific isolates and their affinity to 4E10 was not available at that time point. By now, surface plasmon resonance data is available for some mutants (104). However, the influences of some alanine substitutions on viral fitness and 4E10 neutralization were described by other groups (101; 125). One study gave an overview on 4E10 epitopes and corresponding neutralization (121). Additionally, it was obvious from cytometric analysis that 4E10 did not bind to gp41 derived from molecular clone SIVmac239 (section 4.1.1.3). So, the 4E10 binding site was successfully depleted in a gradual manner, which resulted in a striking step-wise reduction of binding on the surface of both cells and virus-like particles. Importantly, antigen expression was normalized by the epitope-independent HA tag. Thus, a functional mini-library tailor-made for 4E10 was generated, which may also be useful for other investigators in the context of a gp41, gp145 or gp160 protein.

Creation of a mini-library for 2F5 was also attempted, but binding here was only significantly dependent on residues DKW (data not shown). This finding is consistent with a study screening phage-displayed peptides by 2F5, selecting peptides which contained the core sequence DKW with large sequence variability in surrounding regions (291), and a structural study which observed a vast epitope promiscuity of 2F5 beyond the DKW core (292).

5.2.3 Performance of AIO system

The performance of the AIO system was evaluated by use of the 4E10-directed mini-library. Important parameters are selective virion capture, subsequent amplification of genomic material or alternatively reinfection to start a new round of panning. Both capture and re-amplification of separate constructs mirrored the antigen:antibody affinity as measured before on the cellular and viral surfaces. This indicates that capture and reinfection could be promoted by immobilized antibody, a procedure which had been successful before for MLV (176) and ALV (173). Thus, there is no need for elution procedures so that high-affinity antigens cannot get lost during selection. The data showed that as few as ~10 antibody-bound infectious particles were sufficient to start a following round (fig. 36B). Following reinfection by fresh cells for virus propagation, specific gene amplification was possible by RT-PCR. Enrichment of good binders could be verified by clonal sequencing, with better binders being more often captured and re-amplified than worse binders. Thus, the fundamental feature of high binding affinity resulted in better capture in the first step, and could be translated to a higher fraction of sequenced clones in the last step. Regarding the non-binding (SIVmac239-based) construct, depletion was beyond detection level (>25-fold) in one round (It has to be emphasized that this data is based on separately produced virions.) As reinfection by fresh pseudotyping cells resulted in proliferative production, multiple rounds can be performed to further enrich good binders out of a large library in an exponential way.

The AIO system was further tested for its suitability for other antigens and antibodies. A panel of both anti-gp41 and gp120 revealed that generally, full-length gp160 captured by anti-gp120 antibodies delivered results with both increased specificity and sensitivity. Selective capture and reinfection by the factor of ~100 of gp160-bearing virions with anti-gp120 MAbs 2G12 and b12 was observed (fig. 33B). Thus, it seems that well-exposed antigens like gp120 with corresponding antibodies are superior components in the AIO system compared to gp41-derived antigens and corresponding antibodies. The low number of captured particles by 4E10 (30-40 IU per well, fig. 36) likely is a barrier to the screening of large libraries. Thus a different, cell-based display system was adapted for the affinity maturation of gp41 variants.

The only lentiviral display system published so far performs its screening not on the viral but the cell surface (163). Other retroviral systems based on ALV (173) and MLV (176) follow a similar selection strategy like the lentiviral system presented here and perform a panning on the viral

surface. An important point is the task of coupling genotype to phenotype after initial proviral plasmid transfection. Usually, a multitude of plasmids is taken up in form of transfection reagent complexes, which leads to multiple gene variants in single cells. Emanating virions bear multiple variants of library proteins and carry two RNA genomes encoding for different library variants. Buchholz and colleagues forgo an explicit linkage and seem to achieve an enrichment only by panning over multiple rounds (176). Federspiel and colleagues preferred to include a step of low MOI infection after initial transfection, which leads to an efficient coupling (173). Analogously, the AIO system based on HIV was extended by a low MOI (~ 0.1) infection after transfection and subsequent production for 96 h. Four days are equivalent to ~ 3 viral replication cycles before entering the first round of panning, if a replication cycle of ~ 1.3 days is assumed (293; 294), limiting reinfection by pseudotyped virions during this production time. Occasionally occurring multiple infections are not supposed to be detrimental, as it was shown that only one or two integration events take place per cell, because Rev inhibits multiple integrations (168; 295). Of course, coupling is only necessary when using virions produced by mixed and not by separate production.

Concerning the efficiency of the AIO system compared to others, Khare et al. were able to obtain a ~ 100 - to ~ 400 -fold enrichment in one cycle using ALV. Buchholz and colleagues report a 10^3 -fold enrichment in one cycle using separately produced virions of MLV. These enrichment factors are higher than in the AIO system, where enrichment by factor of ~ 20 (using 4E10) resp. ~ 100 (using 2G12) was observed (for separately produced virions). However, as the combination of antigen and antibody was shown to be crucial for the performance of the AIO system, there is still potential for improvement.

5.2.4 Adaptation of currently developed “lenti-cellular” display systems

A mammalian cell-based system, which is currently still under development (211), was evaluated for its usability in the affinity enhancement of gp41-derived antigens. This display system is based on the results of the gp41_{ctm} 4E10-directed mini-library in cytometric analyses of 293T cells (section 4.2.1.1). Here, gradual binding to 4E10 by its members was shown, and normalization was possible with a tag-directed antibody. As a vehicle to introduce genetic material into cells, a lentiviral vector created by T.-H. Bruun was used (211), and a suitable packaging construct was provided by the trans-complementing system developed by K. Schilling (208). First, enrichment was headed for solely by magnetic separation, but efficient enrichment was not observed by magnetic beads.

In order to include parameter for normalization of expression into the system, separation was performed in a FACS device instead of a magnetic column, which allows for multi-parameter staining. The 4E10-directed mini-library showed a clear step-wise pattern of decreasing MFI ratios of BNMAb 4E10 to normalization antibody (fig. 26). It should be noted that expression

levels of gp41ctm variants from the lentiviral vector backbone were low, and further diminished after infection instead of transfection. However, cells were infected and stained sufficiently to be sorted, and genetic material was amplified by PCR. Clonal sequencing revealed enrichment of strong 4E10-binding members of the mini-library (fig. 43). Enrichment was even more pronounced when cells were infected separately by individual members of the mini-library, which indicates that some virions bear RNA genomes encoding for different members. Remarkably, no "negative" SIVmac239-based clones were detected, which means that enrichment is >25-fold. Sequencing of larger peer groups or mixing non-binder and good binder in different ratios prior to sorting may be necessary to substantiate the real enrichment factor and compare it with other retroviral systems. Without doubt, the parameter of normalizing antigen expression level makes the lenti-cellular system superior to the lentiviral AIO system. Taken together, lenti-cellular display provides a suitable platform for the affinity maturation of gp41-derived antigens.

5.2.5 Comparison with a similar lenti-cellular display technology

Recently, Taube and co-workers expressed bivalent scFvs on a gp41 scaffold and used the resulting retrovirus library for the stable transduction of 293T cells, similarly to our system, in the sole published lentiviral display system so far (163). This work also showed a similar binding behavior of both lentiviral particles and subsequently infected cells, enabling a selection on both virions and cells. Notably, MACS-based separation was also applied; however, the authors used it only in a pre-separation step, before subjecting the cells to a FACS-based separation. With both separation methods combined, the authors claim to have achieved an enrichment of 10^3 -fold each, resulting in a final enrichment of 10^6 -fold between a binder and a non-binder. While enrichment in the magnitude of $\sim 10^3$ by FACS is consistent with the present study, MACS-based enrichment was not observed. Notably, cells were gated in the mentioned study for those expressing high levels of both normalization and target protein. This favors selection of highly expressing cells instead of improved binders. It was sufficient to discriminate between a very weak and a very strong binder in the study of Taube and colleagues, but may be not enough when handling a library with slightly diverse binding members. Contrarily, by the "triangle gating" strategy applied in the present study (sec. 4.2.3.3), binders with higher affinity than the main population are sorted. This is important as avidity effects likely overrun desired affinity separation if normalization is not considered. Fluorescence intensities from cell to cell can vary in log grade, reflecting differences in antigen expression level. In our hands, the triangle gating strategy was superior to simply gating a population with high MFI. In this light, magnetic separation can serve as a pre-selection feature when screening large libraries, however, normalization which is only possible in FACS seems to be a mandatory step. Furthermore, virions were produced separately and cells were infected separately by a binder and non-binder

before panning in the experiments of Taube et al. Enrichment out of a mixedly produced library was not shown. Therefore, the reported enrichment factor of 10^6 can only be applied to the artificial situation of separately infected cells.

5.2.6 Controlling the MOI in lenti-cellular display

A low MOI in lenti-cellular display is desired to ensure a proper linkage of genotype and phenotype. Although cells undergo apoptosis and are thereby eliminated if multiple integration events (>2) occur, it is not known how long this process exactly takes, and superinfections should therefore be avoided (168). The percentage of infected cells can be controlled in a separate batch of cells, where a fluorescent protein like GFP is expressed instead of the antigen. This control was included in the experiments described above. A balanced MOI is important to not produce too many multiply infected cells on the one hand, and still providing enough infected expressing cells for separation on the other hand. In our experiments, MOIs of ~ 0.2 were headed for, which equivalents to $\sim 18\%$ total GFP-positive cells, $\sim 16\%$ singly infected cells, $\sim 2\%$ multiply infected cells, and $\sim 82\%$ non-infected cells, as can be deduced from the Poisson distribution. A chart displaying the impact of various MOIs on infection level can be found in the appendix (fig. 46A). Diagram 46B can be used to estimate the MOI at various GFP counts, and the fraction of singly or multiply infected cells can be withdrawn from 46A and 46C. When GFP is encoded on the same vector like the antigen, an even more accurate estimation of the MOI would be possible. For this purpose, a new vector was designed by T.-H. Bruun, which separates the GFP frame from the antigen frame by an IRES. The vector was shown to express both GFP and an antigen to similar levels (211). As triple-staining is required when using this vector, a bright fluorochrome not interfering with GFP or AlexaFluor-647 was needed, but those tested so far (AlexaFluor-647 and PerCP) were too weak for efficient sorting. An infrared fluorochrome like PE-Cy7 might be worth testing. Also in lenti-cellular display, antigen expression could be enhanced by use of heterologous transmembrane domains like those mentioned above (5.1.10) including those of Taube et al. (163).

5.2.7 Library screens

A gp41ctm gene library was created by the spiked oligonucleotide method (296) to mutate residues in and around binding sites for BNMAbs 4E10 and 2F5. The design was influenced by conserving residues absolutely required for BNMAb binding and those mediating trimerization. The library was cloned into lentiviral vectors for lenti-cellular display with high transformation rates of $>10^6$ independent clones. Library diversity and mutation rate were analyzed by sequencing of a peer group, revealing that the targeted mean of three mutations on amino-acid level was realized, with $\sim 75\%$ of clones expressing functional proteins. Thus, a functional library with high diversity has been made available in appropriate vectors. However, PCR amplification

of genomic DNA after sorting was inefficient, and no significantly improved binders could be identified in preliminary screens. Screening of a larger number of cells, giving each binder a multiple chance of being sorted, might be a possibility to increase genomic material for subsequent single clone analysis.

5.2.8 Outlook for lentiviral display systems

Concerning affinity maturation and neutralization capacity, the question whether an affinity-enhanced antigen is a better immunogen still remains open. For 2F5, it is known that factors other than binding affinity have a critical role in inducing neutralization (267). On the other hand, antibodies with both increased binding affinity and neutralization capacity like Z13e1 have been identified (81). A drawback might be the inherent ability of BNMAbs to recognize antigens in different conformational states. E.g., all 4E10, 2F5, b12, and VRC01 bind to Env in an induced-fit mechanism, that means recognizing Env in one conformation and locking it in a different one. This ability might be limited for Abs induced by perfect matching antigens, as these likely present an already locked-in conformation. The answer will have to be determined empirically. The two novel display techniques described in this study complement existing display systems by virtue of providing properties unique to antigen expression in human cells. The All-in-One lentiviral platform may be of use for screening of large libraries, or as a pre-selection tool before applying a cell-based technique. The lenti-cellular display system, by using the “triangle gate” strategy, offers adjustment of sorting by the critical parameter of normalization for expression level and has potential to select even only slightly improved binders out of large libraries. Both technologies may be also applicable for affinity maturation of other proteins like antibodies. As tool for vaccinologists, they may be of use to generate improved immunogens not only against HIV but also other pathogens.

6 Appendix

6.1 Dependency of MOI and infection rates

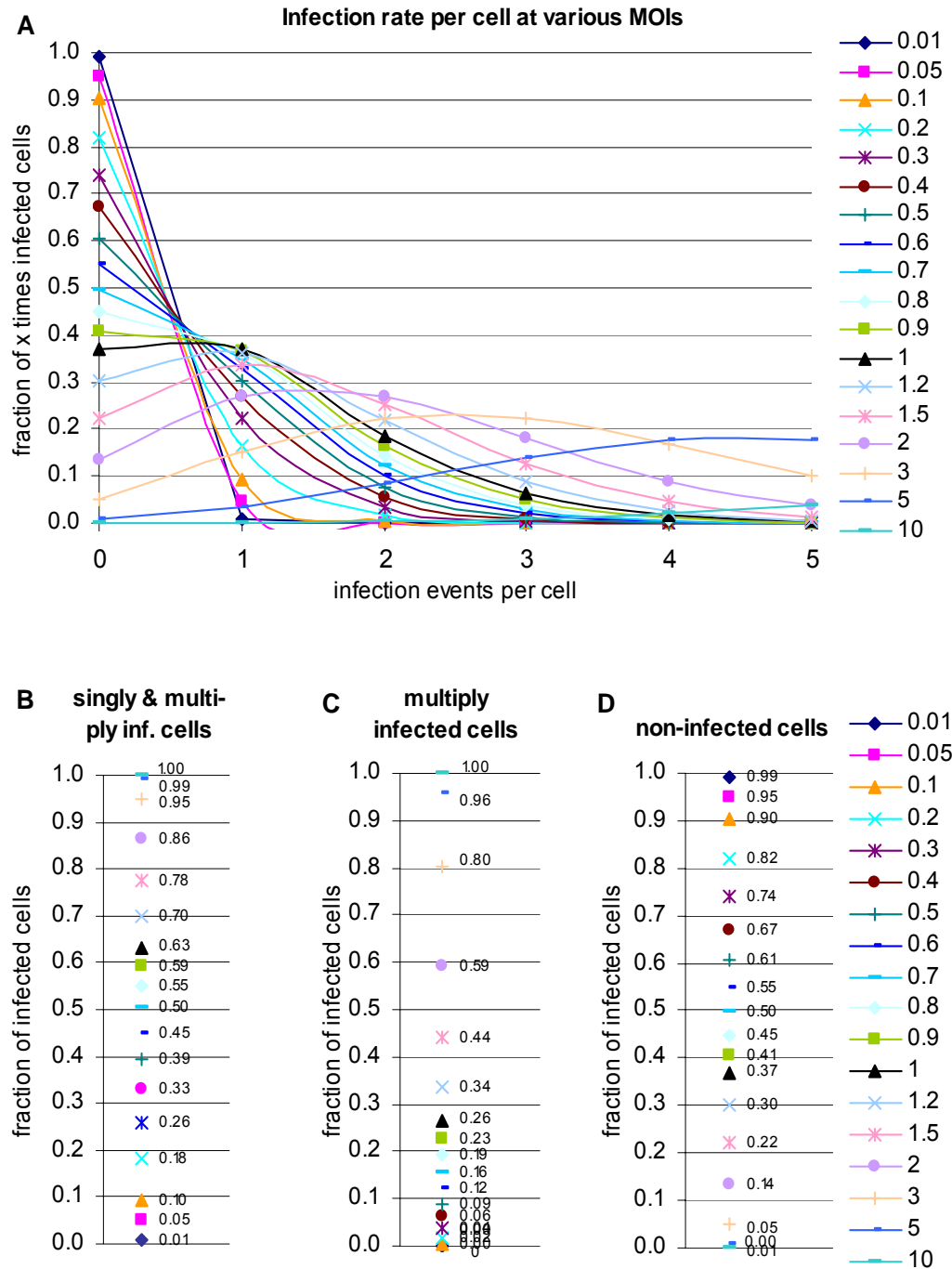


Figure 46. Calculation of MOI at given apparent infection rates. With rising MOI, the fraction of infected cells does not rise in a linear manner because of multiply infected cells in the population. (A) Number of infection events per cell at various MOIs is shown, as calculated by Poisson distribution. (B) The fraction of infected cells (left), multiply infected cells (middle) and non-infected cells (right) at various MOIs according to Poisson is depicted. In order to estimate an MOI, the fraction of infected cells is determined by e.g. flow cytometry, compared to the numbers shown at lower left (B), and the MOI can be deduced from the legend.

[illegible]

Table 8, continued

	110	120	130	140	150	160	170	180	190	200
Protein	-Q--E--I--H--A--R--F--R--R--G--A--R--M--Q--W--D--R--E--I--S--N--Y--T--N--T--I--Y--R--L--L--E--D--S--									
GP41CTM-HA	CCAGGAAATCCACGCCCGGTTCGCGAGAGGCCGAGATGCAGTGGGACCGGGAGATCAGCAACTACACCAACACCATCTACCGGCTGCTCGAGGATAGC									
CTMLIB_A4										
CTMLIB_A5										
CTMLIB_A6										
CTMLIB_A7										
CTMLIB_A8										
CTMLIB_A9										
CTMLIB_A10										
CTMLIB_A11										
CTMLIB_A12										
CTMLIB_B2										
CTMLIB_B3										
CTMLIB_B4										
CTMLIB_B5										
CTMLIB_B6										
CTMLIB_B7										
CTMLIB_B8										
CTMLIB_B9										
CTMLIB_B10										
CTMLIB_B11										
CTMLIB_B12										
CTMLIB_C1										
CTMLIB_C2										
CTMLIB_C3										
CTMLIB_C4										
CTMLIB_C5										
CTMLIB_C6										
CTMLIB_C8										
CTMLIB_C9										
CTMLIB_C10										
CTMLIB_C11										
CTMLIB_C12										
CTMLIB_D1										
CTMLIB_D2										
CTMLIB_D3										
CTMLIB_D5										
CTMLIB_D6										
CTMLIB_D7										
CTMLIB_D8										
CTMLIB_D9										
CTMLIB_D10										
CTMLIB_D11										
CTMLIB_D12										
CTMLIB_E1										
CTMLIB_E2										
CTMLIB_E3										
CTMLIB_E5										
CTMLIB_E6										
CTMLIB_E7										
CTMLIB_E8										
CTMLIB_E9										
CTMLIB_E10										
CTMLIB_E11										
CTMLIB_E12										
CTMLIB_F1										
CTMLIB_F3										
CTMLIB_F4										
CTMLIB_F5										
CTMLIB_F6										
CTMLIB_F7										
CTMLIB_F8										
CTMLIB_F10										
CTMLIB_F11										
CTMLIB_F12										
CTMLIB_G1										
CTMLIB_G2										
CTMLIB_G3										
CTMLIB_G4										
CTMLIB_G5										
CTMLIB_G6										
CTMLIB_G7										
CTMLIB_G8										
CTMLIB_G10										
CTMLIB_G11										
CTMLIB_G12										
CTMLIB_H1										
CTMLIB_H2										
CTMLIB_H3										
CTMLIB_H4										
CTMLIB_H5										
CTMLIB_H6										
CTMLIB_H7										
CTMLIB_H8										
CTMLIB_H9										
CTMLIB_H10										
CTMLIB_H11										
CTMLIB_H12										

Table 8, continued

	210	220	230	240	250	260	270	280	290	300
Protein	Q--S--Q--Q--E--Q--N--E--K--D--L--L--E--L--D--K--W--A--S--L--W--N--W--F--D--I--T--K--W--L--W--Y--I--									
GP41CTM-HA	CAG-TCACAGCAGGAGCAGAACGAGAAGGACCTGCTGGAGCTGGACAAGTGGGCCTCACTGTGGAACGGTTCGACATCACCAAGTGGCTGTGGTACATC									
CTMLIB_A4	..G.		T.			C.				
CTMLIB_A5	..-A.	..T.T.	..CC.	..T.	..G.	..A.	..G.			
CTMLIB_A6	..-.	..T.	..A.	..CC.	..C.	..C.				
CTMLIB_A7	..-.	..T.		..T.						
CTMLIB_A8	..-.	..T.	..C.	..T.	..G.	..G.				
CTMLIB_A9	..-.	..T.								
CTMLIB_A10	..-.		..CA.	..A.			..G.			
CTMLIB_A11	..-.	..T.	..G.	..T.		..C.	..TT.			
CTMLIB_A12	..-.	..G.C.	..T.	..C.		..A.	..T.			
CTMLIB_B2	..-.	..GC.			..T.	..G.				
CTMLIB_B3	..-.	..C.	..GC.		..A.	..TT.				
CTMLIB_B4	..A-	..G.		..A.	..G.	..ATC.				
CTMLIB_B5	..-.	..C.T.		..A.	..G.					
CTMLIB_B6	A.	..T.		..C.						
CTMLIB_B7	..-.	..AG.	..T.C.	..T.	..G.T.	..T.				
CTMLIB_B8	..-.	..A.		..G.						
CTMLIB_B9	..T-		..G.			..G.				
CTMLIB_B10	..-.	..C.	..C.	..C.		..A.		..T.		
CTMLIB_B11	..-.	..GG.	..C.	..TT.	..T.			..T.		
CTMLIB_B12	..C-	..T.		..T.A.	..T.	..A.				
CTMLIB_C1	..-.		..A.GA.	..T.		..AG.	..A.			
CTMLIB_C2	..TC-	..T.	..T.	..C.				..G.		
CTMLIB_C3	GT-	..A.	..G.	..G.	..T.	..A.		..C.		
CTMLIB_C4	..C-	..T.	..G.			..TT.	..G.			
CTMLIB_C5	..-.	..G.	..C.	..C.	..G.	..A.				
CTMLIB_C6	..T-	..A.C.								
CTMLIB_C8	..-.	..T.	..T.							
CTMLIB_C9	..-AA	..A.	..C.	..G.						
CTMLIB_C10	..-.	..T.	..C.	..G.	..T.C.	..A.G.				
CTMLIB_C11	AC-	..C.			..G.					
CTMLIB_C12	..T-	..A.	..T.	..C.	..A.			..C.		
CTMLIB_D1	..-.	..GG.	..C.	..TT.	..T.			..T.		
CTMLIB_D2	..-.	..A.	..T.		..C.					
CTMLIB_D3	..-.	..G.T.	..A.	..G.						
CTMLIB_D5	..-.		..C.		..G.T.A.	..C.	..A.			
CTMLIB_D6	..-.	..G.T.	..A.	..G.						
CTMLIB_D7	..-.	..T.	..T.T.	..TG.	..C.					
CTMLIB_D8	..-.		..CG.	..T.	..G.	..T.				
CTMLIB_D9	..TA-	..T.C.T.	..T.	..G.	..T.					
CTMLIB_D10	..T-	..T.	..C.	..C.	..G.					
CTMLIB_D11	..-.	..T.	..C.	..C.		..T.	..C.			
CTMLIB_D12	..T-	..C.	..G.	..T.	..G.G.					
CTMLIB_E1	..-.	..C.	..T.	..T.C.	..C.	..T.				
CTMLIB_E2	..A-	..T.	..T.T.		..A.G.	..G.				
CTMLIB_E3	..-.		..C.T.		..T.					
CTMLIB_E5	..-A	..A.	..A.	..A.						
CTMLIB_E6	A.	..A.								
CTMLIB_E7	..-.	..A.	..T.				..G.T.			
CTMLIB_E8	..-.			..G.	..T.TG.					
CTMLIB_E9	..TC-	..G.	..T.	..C.	..T.					
CTMLIB_E10	..-.	..G.	..C.	..G.	..A.	..T.	..A.			
CTMLIB_E11	..-.			..A.						
CTMLIB_E12	..-.	..GT.	..C.	..T.	..TT.					
CTMLIB_F1	..-.	..T.	..C.	..T.T.	..T.	..T.				
CTMLIB_F3	..-.	..C.	..ATC.	..T.G.	..TT.	..T.	..C.			
CTMLIB_F4	..-.	..A.	..C.	..CAC.		..A.	..A.			
CTMLIB_F5	A.	..A.	..C.	..T.	..T.	..G.	..AT.			
CTMLIB_F6	..-.			..G.		..GC.	..G.			
CTMLIB_F7	..-.	..C.	..A.	..TT.	..C.	..T.				
CTMLIB_F8	..-.	..G.	..T.		..C.					
CTMLIB_F10	..T-	..G.	..G.	..G.	..G.					
CTMLIB_F11	..-.	..G.			..G.	..A.				
CTMLIB_F12	..-.	..A.		..C.	..C.	..T.				
CTMLIB_G1	..C-	..T.	..G.	..C.	..G.			..A.		
CTMLIB_G2	..-.	..G.		..A.		..T.				
CTMLIB_G3	..-.	..T.	..T.	..TA.	..T.					
CTMLIB_G4	..-.		..C.	..G.						
CTMLIB_G5	..T-	..T.	..G.		..T.					
CTMLIB_G6	A.	..T.	..T.	..C.	..A.		..C.			
CTMLIB_G7	..-.	..A.	..T.		..T.T.					
CTMLIB_G8	..-.	..T.		..A.	..T.	..T.				
CTMLIB_G10	..-.	..T.	..T.	..G.	..G.					
CTMLIB_G11	..-.			..G.	..T.	..T.				
CTMLIB_G12	..-.	..G.	..C.	..T.	..A.					
CTMLIB_H1	A-	..T.	..G.	..A.	..T.	..A.	..GA.	..T.	..C.	
CTMLIB_H2	..C-	..T.	..T.	..G.	..C.	..T.	..T.	..T.		
CTMLIB_H3	..-.		..C.	..T.	..T.	..G.T.	..G.			
CTMLIB_H4	..-.		..C.	..T.						
CTMLIB_H5	..-.	..C.	..T.	..A.						
CTMLIB_H6	TC-	..TT.	..TA.		..A.		..G.A.			
CTMLIB_H7	..-.		..GC.	..T.	..G.					
CTMLIB_H8	..-.		..G.	..C.			..T.			
CTMLIB_H9	..-.	..C.	..T.	..T.T.	..C.	..G.				
CTMLIB_H10	..C-	..T.	..T.							
CTMLIB_H11	..-.	..G.	..T.	..A.						
CTMLIB_H12	..-.	..G.								

Table 8, continued

	310	320	330	340	350	360	370	380	390	400
Protein	K--I--F--I--M--I--V--G--G--L--I--G--L--R--I--I--F--A--V--L--S--I--V--N--R--V--R--Q--G--Y--S--P--L--S									
GP41CTM-HA	AAGATCTTCATCATGATCGTGGGCGGCCTGATCGGCCTGCGGATCATCTTCGCCGTGCTGTCCATCGTGAACAGAGTGC									
CTMLIB_A4										
CTMLIB_A5										
CTMLIB_A6										
CTMLIB_A7										
CTMLIB_A8										
CTMLIB_A9										
CTMLIB_A10										
CTMLIB_A11										
CTMLIB_A12										
CTMLIB_B2										
CTMLIB_B3	C									
CTMLIB_B4										
CTMLIB_B5										
CTMLIB_B6										
CTMLIB_B7										
CTMLIB_B8										
CTMLIB_B9										
CTMLIB_B10										
CTMLIB_B11										
CTMLIB_B12										
CTMLIB_C1										
CTMLIB_C2										
CTMLIB_C3										
CTMLIB_C4										
CTMLIB_C5										
CTMLIB_C6										
CTMLIB_C8										
CTMLIB_C9										
CTMLIB_C10										
CTMLIB_C11										
CTMLIB_C12										
CTMLIB_D1										
CTMLIB_D2										
CTMLIB_D3										
CTMLIB_D5										
CTMLIB_D6										
CTMLIB_D7										
CTMLIB_D8										
CTMLIB_D9										
CTMLIB_D10										
CTMLIB_D11										
CTMLIB_D12										
CTMLIB_E1										
CTMLIB_E2										
CTMLIB_E3										
CTMLIB_E5										
CTMLIB_E6										
CTMLIB_E7										
CTMLIB_E8										
CTMLIB_E9										
CTMLIB_E10										
CTMLIB_E11										
CTMLIB_E12										
CTMLIB_F1										
CTMLIB_F3										
CTMLIB_F4										
CTMLIB_F5										
CTMLIB_F6										
CTMLIB_F7										
CTMLIB_F8										
CTMLIB_F10										
CTMLIB_F11										
CTMLIB_F12										
CTMLIB_G1										
CTMLIB_G2										
CTMLIB_G3										
CTMLIB_G4										
CTMLIB_G5										
CTMLIB_G6										
CTMLIB_G7										
CTMLIB_G8										
CTMLIB_G10										
CTMLIB_G11										
CTMLIB_G12	C									
CTMLIB_H1										
CTMLIB_H2										
CTMLIB_H3										
CTMLIB_H4										
CTMLIB_H5										
CTMLIB_H6										
CTMLIB_H7										
CTMLIB_H8										
CTMLIB_H9										
CTMLIB_H10										
CTMLIB_H11										
CTMLIB_H12										

Table 8, continued

	410	420	430	440	450	460	470	480	490	500
Protein	--F--Q--T--L--I--P--N--P--Y--P--Y--D--V--P--D--Y--A--*--*--									
GP41CTM-HA	GCTTCCAGACCCCTGATCCCCAACCCCTACCCCTACGACGTGCCCGACTACGCCTGATGACTCGAGCATATGATAATCAACCTCTGGATTACAAAATTTGT									
CTMLIB_A4										
CTMLIB_A5										
CTMLIB_A6										
CTMLIB_A7										
CTMLIB_A8										
CTMLIB_A9										
CTMLIB_A10										
CTMLIB_A11										
CTMLIB_A12										
CTMLIB_B2										
CTMLIB_B3										
CTMLIB_B4										
CTMLIB_B5										
CTMLIB_B6										
CTMLIB_B7										
CTMLIB_B8										
CTMLIB_B9										
CTMLIB_B10										
CTMLIB_B11										
CTMLIB_B12										
CTMLIB_C1										
CTMLIB_C2										
CTMLIB_C3										
CTMLIB_C4										
CTMLIB_C5				A						
CTMLIB_C6										
CTMLIB_C8										
CTMLIB_C9				T						
CTMLIB_C10										
CTMLIB_C11										
CTMLIB_C12										
CTMLIB_D1										
CTMLIB_D2										
CTMLIB_D3										
CTMLIB_D5										
CTMLIB_D6										
CTMLIB_D7				A						
CTMLIB_D8										
CTMLIB_D9										
CTMLIB_D10										
CTMLIB_D11										
CTMLIB_D12										
CTMLIB_E1										
CTMLIB_E2										
CTMLIB_E3										
CTMLIB_E5										
CTMLIB_E6										
CTMLIB_E7										
CTMLIB_E8										
CTMLIB_E9				A						
CTMLIB_E10										
CTMLIB_E11										
CTMLIB_E12										
CTMLIB_F1										
CTMLIB_F3										
CTMLIB_F4										
CTMLIB_F5										
CTMLIB_F6										
CTMLIB_F7										
CTMLIB_F8										
CTMLIB_F10										
CTMLIB_F11										
CTMLIB_F12										
CTMLIB_G1										
CTMLIB_G2										
CTMLIB_G3										
CTMLIB_G4										
CTMLIB_G5										
CTMLIB_G6										
CTMLIB_G7										
CTMLIB_G8										
CTMLIB_G10										
CTMLIB_G11										
CTMLIB_G12										
CTMLIB_H1										
CTMLIB_H2										
CTMLIB_H3										
CTMLIB_H4										
CTMLIB_H5										
CTMLIB_H6										
CTMLIB_H7										
CTMLIB_H8										
CTMLIB_H9										
CTMLIB_H10										
CTMLIB_H11				A						
CTMLIB_H12										

sequence of master gene in blue, randomized part shaded in grey, translation into protein in green, frameshift mutations in the coding region in yellow

Table 9. Protein sequence analysis of gp41ctm library including HA tag, cloned into pQL1.

100

Table 9, continued

	105	115	125	135	
GP41CTM-HA	GLRIIFAVLS	IVNRVRQGYG	PLSFQTLIPN	PYPYDVPDYA	**
CTMLIB_A04	RPADHLRRRAV	HREQSAAGLQ	PELPPDPDPQ	PLPLRRRARLR	LM
CTMLIB_A05	GLRIIFAVLS	IVNRVRQGYG	PLSFQTLIPN	PYPYDVPDYA	**
CTMLIB_A06	GLRIIFAVLS	IVNRVRQGYG	PLSFQTLIPN	PYPYDVPDYA	**
CTMLIB_A07
CTMLIB_A08	GLRIIFAVLS	IVNRVRQGYG	PLSFQTLIPN	PYPYDVPDYA	**
CTMLIB_A09	GLRIIFAVLS	IVNRVRQGYG	PLSFQTLIPN	PYPYDVPDYA	**
CTMLIB_A10
CTMLIB_A11	GLRIIFAVLS	IVNRVRQGYG	PLSFQTLIPN	PYPYDVPDYA	**
CTMLIB_A12
CTMLIB_B02	GLRIIFAVLS	IVNRVRQGYG	PLSFQTLIPN	PYPYDVPDYA	**
CTMLIB_B03	GLRIIFAVLS	IVNRVRQGYG	PLSFQTLIPN	PYPYDVPDYA	**
CTMLIB_B04
CTMLIB_B05	GLRIIFAVLS	IVNRVRQGYG	PLSFQTLIPN	PYPYDVPDYA	**
CTMLIB_B06	GLRIIFAVLS	IVNRVRQGYG	PLSFQTLIPN	PYPYDVPDYA	**
CTMLIB_B07	GLRIIFAVLS	IVNRVRQGYG	PLSFQTLIPN	PYPYDVPDYA	**
CTMLIB_B08	GLRIIFAVLS	IVNRVRQGYG	PLSFQTLIPN	PYPYDVPDYA	**
CTMLIB_B09	GLRIIFAVLS	IVNRVRQGYG	PLSFQTLIPN	PYPYDVPDYA	**
CTMLIB_B10	GLRIIFAVLS	IVNRVRQGYG	PLSFQTLIPN	PYPYDVPDYA	**
CTMLIB_B11	GLRIIFAVLS	IVNRVRQGYG	PLSFQTLIPN	PYPYDVPDYA	**
CTMLIB_B12	GLRIIFAVLS	IVNRVRQGYG	PLSFQTLIPN	PYPYDVPDYA	**
CTMLIB_C01
CTMLIB_C02
CTMLIB_C03	GLRIIFAVLS	IVNRV ^L QGYG	PLSFQTLIPN	PYPYDVPDYA	**
CTMLIB_C04
CTMLIB_C05
CTMLIB_C06	GLRIIFAVLS	IVNRVRQGYG	PLSFQTLIPN	PYPYDVPDYA	**
CTMLIB_C08
CTMLIB_C09	GLRIIFAVLS	IVNRVRQGYG	PLSFQTLIPN	PY ^L YDVPDYA	**
CTMLIB_C10
CTMLIB_C11	GLRIIFAVLS	IVNRVRQGYG	PLSFQTLIPN	PYPYDVPDYA	**
CTMLIB_C12
CTMLIB_D01	GLRIIFAVLS	IVNRVRQGYG	PLSFQTLIPN	PYPYDVPDYA	**
CTMLIB_D02
CTMLIB_D03
CTMLIB_D05	GLRIIFAVLS	IVNRVRQGYG	PLSFQTLIPN	PYPYDVPDYA	**
CTMLIB_D06
CTMLIB_D07
CTMLIB_D08	GLRIIFAVLS	IVNRVRQGYG	PLSFQTLIPN	PYPYDVPDYA	**
CTMLIB_D09	GLRIIFAVLS	IVNRVRQGYG	PLSFQTLIPN	PYPYDVPDYA	**
CTMLIB_D10	GLRIIFAVLS	IVNRVRQGYG	PLSFQTLIPN	PYPYDVPDYA	**
CTMLIB_D11	GLRIIFAVLS	IVNRVRQGYG	PLSFQTLIPN	PYPYDVPDYA	**
CTMLIB_D12	GLRIIFAVLS	IVNRVRQGYG	PLSFQTLIPN	PYPYDVPDYA	**
CTMLIB_E01
CTMLIB_E02
CTMLIB_E03	GLRIIFAVLS	IVNRVRQGYG	PLSFQTLIPN	PYPYDVPDYA	**
CTMLIB_E05	GLRIIFAVLS	IVNRVRQGYG	PLSFQTLIPN	PYPYDVPDYA	**
CTMLIB_E06	GLRIIFAVLS	IVNRVRQGYG	PLSFQTLIPN	PYPYDVPDYA	**
CTMLIB_E07	GLRIIFAVLS	IVNRVRQGYG	PLSFQTLIPN	PYPYDVPDYA	**
CTMLIB_E08	GLRIIFAVLS	IVNRVRQGYG	PLSFQTLIPN	PYPYDVPDYA	**
CTMLIB_E09
CTMLIB_E10	GLRIIFAVLS	IVNRVRQGYG	PLSFQTLIPN	PYPYDVPDYA	**
CTMLIB_E11	GLRIIFAVLS	IVNRVRQGYG	PLSFQTLIPN	PYPYDVPDYA	**
CTMLIB_E12	GLRIIFAVLS	IVNRVRQGYG	PLSFQTLIPN	PYPYDVPDYA	**
CTMLIB_F01	GLRIIFAVLS	IVNRVRQGYG	PLSFQTLIPN	PYPYDVPDYA	**
CTMLIB_F03
CTMLIB_F04	GLRIIFAVLS	IVNRVRQGYG	PLSFQTLIPN	PYPYDVPDYA	**
CTMLIB_F05
CTMLIB_F06	GLRIIFAVLS	IVNRVRQGYG	PLSFQTLIPN	PYPYDVPDYA	**
CTMLIB_F07	GLRIIFAVLS	IVNRVRQGYG	PLSFQTLIPN	PYPYDVPDYA	**
CTMLIB_F08	GLRIIFAVLS	IVNRVRQGYG	PLSFQTLIPN	PYPYDVPDYA	**
CTMLIB_F10	GLRIIFAVLS	IVNRVRQGYG	PLSFQTLIPN	PYPYDVPDYA	**
CTMLIB_F11	GLRIIFAVLS	IVNRVRQGYG	PLSFQTLIPN	PYPYDVPDYA	**
CTMLIB_F12	GLRIIFAVLS	IVNRVRQGYG	PLSFQTLIPN	PYPYDVPDYA	**
CTMLIB_G01	GLRIIFAVLS	IVNRVRQGYG	PLSFQTLIPN	PYPYDVPDYA	**
CTMLIB_G02
CTMLIB_G03	GLRIIFAVLS	IVNRVRQGYG	PLSFQTLIPN	PYPYDVPDYA	**
CTMLIB_G04	GLRIIFAVLS	IVNRVRQGYG	PLSFQTLIPN	PYPYDVPDYA	**
CTMLIB_G05	GLRIIFAVLS	IVNRVRQGYG	PLSFQTLIPN	PYPYDVPDYA	**
CTMLIB_G06	GLRIIFAVLS	IVNRVRQGYG	PLSFQTLIPN	PYPYDVPDYA	**
CTMLIB_G07	GLRIIFAVLS	IVNRVRQGYG	PLSFQTLIPN	PYPYDVPDYA	**
CTMLIB_G08	GLRIIFAVLS	IVNRVRQGYG	PLSFQTLIPN	PYPYDVPDYA	**
CTMLIB_G10	GLRIIFAVLS	IVNRVRQGYG	PLSFQTLIPN	PYPYDVPDYA	**
CTMLIB_G11	GLRIIFAVLS	IVNRVRQGYG	PLSFQTLIPN	PYPYDVPDYA	**
CTMLIB_G12
CTMLIB_H01
CTMLIB_H02	GLRIIFAVLS	IVNRVRQGYG	PLSFQTLIPN	PYPYDVPDYA	**
CTMLIB_H03
CTMLIB_H04	GLRIIFAVLS	IVNRVRQGYG	PLSFQTLIPN	PYPYDVPDYA	**
CTMLIB_H05	GLRIIFAVLS	IVNRVRQGYG	PLSFQTLIPN	PYPYDVPDYA	**
CTMLIB_H06	GLRIIFAVLS	IVNRVRQGYG	PLSFQTLIPN	PYPYDVPDYA	**
CTMLIB_H07	GLRIIFAVLS	IVNRVRQGYG	PLSFQTLIPN	PYPYDVPDYA	**
CTMLIB_H08	GLRIIFAVLS	IVN ^I VRQGYG	PLSFQTLIPN	PYPYDVPDYA	**
CTMLIB_H09	GLRIIFAVLS	IVNRVRQGYG	PLSFQTLIPN	PYPYDVPDYA	**
CTMLIB_H10
CTMLIB_H11
CTMLIB_H12	GLRIIFAVLS	IVNRVRQGYG	PLSFQTLIPN	PYPYDVPDYA	**

sequence of master gene in blue, randomized part shaded in grey, mutated residues in red, frameshift mutations in orange

6.3 Synthetic oligonucleotides

Table 10. Overview on synthetic oligodesoxyribonucleotides used for cloning and sequencing.

ID	Sequence	Name
<u>Cloning of gp41ctm variants</u>		
3E8	CTGGCTAGCGCCGCCACCATGGATGCCATGAAGCGGGG	NheI-Kozak-TPA fw
2H4	GGTACCTTACTAGGCGTAGTCGGGCACGTCGTAGGGGTAGCTGGCGGGCAG CAGGGTCTGGAAGC	KpnI-gp41ctm(89.6)-HA rev
2H5	GGTACCTTATTAGGCGTAGTCGGGCACGTCGTAGGGGTATGGGTTCGGGATA AGGGTCTGAAACGTGAGTATCC	KpnI-gp41ctm(96ZM)-HA rev
2H6	GGTACCCTATCAGGCGTAGTCGGGCACGTCGTAGGGGTAGTCCTGTTGGATA TGGGTCTGCTGGAATAAGAGG	KpnI-gp41ctm(SIVmac239)-HA rev
3B6	TCGTTCTCGATGTGGTAGATCTTGCTCAGGATCTCCTCGATCTTGTCTCGAT CTGCCTGGCGCCCTTCTGAACCGGGCGT	TPA-GCN4-Fusion rev
3B7	CCTGAGCAAGATCTACCACATCGAGAACGAGATCGCCCGCATCAAGAAGCTG ATCATGGAATGGGAGCGGGAGATCGACAAC	GCN4-gp41ctm(89.6)-Fusion fw
3B8	CCTGAGCAAGATCTACCACATCGAGAACGAGATCGCCCGCATCAAGAAGCTG ATCATGCAGTGGGACCGGGAGATCAGCAAC	GCN4-gp41ctm(96ZM)- Fusion fw
3B9	CCTGAGCAAGATCTACCACATCGAGAACGAGATCGCCCGCATCAAGAAGCTG ATCCAGGAATGGGAGCGGAAGGTCGACTTCC	GCN4-gp41ctm (SIVmac239)- Fusion fw
3H4	CTCGCTGAACCTCTTCTCGATCTGGTGGAACCTTCTCGTTGGTCTTCTCGATCA CGCGGTTTCAGCTTGCCGTTGATCTGGTCGATCCGGGCTCCCCGTCTGAACCG GGCGT	TPA-H3-Fusion rev
3H5	TTCCACCAGATCGAGAAGGAGTTCAGCGAGGTGGAGGGCCGCATCCAGGAC CTGGAGAAGTACGTGGAGGACACCGGCAGCACCATGGAATGGGAGCGGGAG ATCGACAAC	H3-gp41ctm(89.6)-Fusion fw
3H6	TTCCACCAGATCGAGAAGGAGTTCAGCGAGGTGGAGGGCCGCATCCAGGAC CTGGAGAAGTACGTGGAGGACACCGGCAGCACCATGCAGTGGGACCGGGAG ATCAGCAAC	H3-gp41ctm(96ZM)-Fusion fw
3H7	TTCCACCAGATCGAGAAGGAGTTCAGCGAGGTGGAGGGCCGCATCCAGGAC CTGGAGAAGTACGTGGAGGACACCGGCAGCACCCAGGAATGGGAGCGGAAG GTCGACTTC	H3-gp41ctm(SIVmac239)- Fusion fw
4H3	GGGCCAGCAGGTCTTCTCGTTCTGCCGGGCTCCCCGTCTGAACCGGGCG	TPA-gp41ctm2(96ZM)-Fusion rev
4H5	GTTCCAGCAGCTCTTCTCGTTCTCCGGGCTCCCCGTCTGAACCGGGCG	TPA-gp41ctm2(89.6)-Fusion rev
4H7	GCTTCTGCAGCTCGTACATGTTCTTCCGGGCTCCCCGTCTGAACCGGGCG	TPA-gp41ctm2 (SIVmac239)- Fusion rev
4H9	CGCCCGGTTTCAGACGGGGAGCCCGGCAGAACGAGAAGGACCTGCTGGCCC	gp41ctm2(96ZM)-Fusion-TPA fw
4I2	CGCCCGGTTTCAGACGGGGAGCCCGGAAGAACGAGAAAGAGCTGCTGGAAC	gp41ctm2(89.6)-Fusion-TPA fw
4I4	CGCCCGGTTTCAGACGGGGAGCCCGGAAGAACATGTACGAGCTGCAGAAGC	gp41ctm2(SIVmac239)-Fusion- TPA fw
	TAATACGACTCACTATAGGG	T7 fw (sequencing)
	TAGAAGGCACAGTCGAGG	BGH rev (sequencing)

<u>Cloning for All-in-One lentiviral display</u>		
1D1	CCGTCTATTATGGGCTACCTGTGTG	KpnI-mut fwd
1H2	CTTATCCATGGTGGCGGCGGCCGCTTATAGCAAAATCCTTTCCAAGCCC TGTCTTATTCTTC	Env-FseI-Kozak-NcoI rev
5G8	AATGTCGACACCCAATTCTGAAATGGATAAACAGCAGTTGTTGCAGAATTCTTT ATCAGGCGTAGTCGGGCACGTCGTA	HA-Sall (in vpr) rev
5D2	TCTTCTAGAGAGTCGCGCCGCGCGCCGACGGAGCGGACATGGATGCCATGA AGCGGGGCCTGTGCT	XbaI-Prom-TPA (in vpr) fw
1E6	GATCCATTCGATTAGTGAACGG	Tat10 fwd (sequencing)
1D5	CCCTTCCAGTCCCCCCTTTTC	RLuc rev (sequencing)
<u>Cloning for Lenti-cellular Display</u>		
6F8	CTTAAGCAGAGCTCGAGGGCGTAGTCGGGCACGTCGTAGGGGTAGGGGTTG GGGATCAGGGTCTGGAA	gp41ctm(96ZM)-HA-XhoI- BsmBI rev
8C8	GCAACTCGGATCCCGTCTCGCTAGCGCCGCCACCATG	0922890.A.fwd
8C9	CCTGACGAATTCGTCTCCTCGAGGGTACCTCATCAGGGGTTGG	0922890.C.rev
3D2	TCTTCCATTTCAAGGTGTCGTG	Seq-pLIB-1 fw (sequencing)
3D5	CTTGCCACAACCCAATTCG	Seq-pLIB-4 fw (sequencing)
5H7	CGTATCCACATAGCGTAAAAGGAG	5H7 rev (sequencing)

6.4 Abbreviations

If not stated otherwise, common abbreviations follow recommendations from the Chicago Manual of Style (297), and biochemical abbreviations follow the Gold Book of IUPAC (298) and the list of common abbreviations by the Journal of Biological Chemistry (299).

A3R5	a T cell lymphoblastoid cell line	<i>g</i>	relative centrifugal force
Ab	antibody	Gag	group-specific antigen
AIO	All-in-One	GCN4	General Control Nondepressible Protein 4, or shortly for its trimerization domain
ALV	Avian Leukosis Virus	gDNA	genomic DNA
AP	Alkaline phosphatase	GFP	Green Fluorescent Protein
ART	anti-retroviral therapy	gp41	glycoprotein of 41 kDa = HIV transmembrane protein
Amp	ampicillin	gp41ctm	engineered protein comprising CHR, TM and truncated CT of gp41
APC	Allophycocyanin	gp120	glycoprotein of 120 kDa = HIV surface protein
ATCC	American Type Culture Collection	gp145	glycoprotein of 145 kDa = HIV envelope precursor protein with truncated CT
β-Gal	β-Galactosidase	gp160	glycoprotein of 160 kDa = HIV envelope precursor protein
BGH	bovine growth hormone	H3	Hemagglutinin type 3. here: trimerization domain from HA2 protein of H3 strain
BNMAb	broadly neutralizing monoclonal antibody	HA	Hemagglutinin, or shortly for HA-tag
bp	base pairs	HEK293	human embryonal kidney cell line 293
BSA	bovine serum albumin	HeLa	a human cervix carcinoma cell line
CA or p24	capsid protein	HIV	Human Immunodeficiency Virus
CCR5	chemokine receptor type 5	HRP	horseradish peroxidase
CD4	cluster of differentiation 4	ID	immunodominant
CHR	C-terminal heptad repeat	IVS	Intervening sequence
CIP	calf intestine phosphatase	IRES	Internal Ribosomal Entry Site
(h)CMV	(human) cytomegalovirus	kb	kilobases
CT	Cytoplasmic tail	LANL	Los Alamos National Library
CTB	<i>Cholera</i> toxin B subunit	LB	Lysogeny Broth medium
CTM	shortly for gp41ctm	LLP	Lentivirus lytic peptide
CXCR4	chemokine receptor type 4	LTR	long terminal repeat
DC	Dendritic cell	MAB	monoclonal antibody
DMEM	Dulbecco's modified Eagle's medium	MACS	Magnetic Cell Separation
DMR	aa D474, M475, R476 of HIV-1 Env	MCS	multiple cloning site
DMSO	Dimethyl sulfoxide	MFI	mean fluorescence intensity
DOPE	Discrete Optimized Protein Energy	MLV	Murine leukemia virus
DOX	doxycycline	MOI	Multiplicity of infection
ds	double strand	MOPS	3-(N-morpholino)propanesulfonic acid
DTT	Dithiothreitol	MPER	membrane-proximal external region
EDTA	Ethylenediaminetetraacetic acid	mRNA	messenger RNA
ELISA	Enzyme-Linked Immunosorbent Assay	NAb	neutralizing antibody
Env	envelope protein	Nef	Negative factor
EU	endotoxin units	NHR	N-terminal heptad repeat
Fab	Fragment antigen binding	PAGE	polyacrylamide gel electrophoresis
FACS	Fluorescence-Activated Cell Sorting		
Fc	Fragment, crystallizable = constant antibody region		
FCS	fetal calf serum		
FD	Foldon domain of phage T4 fibrin		
FP	Fusion peptide		
FPPR	Fusion peptide-proximal region		

6 Appendix

PBS	Phosphate buffered saline	TO	Tetracycline-inducible
PE	Phycoerythrin	TPA	Tissue Plasminogen Activator, or shortly for signal peptide thereof
PEI	poly-ethylenimine	Tris	tris(hydroxymethyl)aminomethane
Pol	Polymerase, or polymerase precursor protein	TTBS	Tris plus Tween-20
poly(A)	polyadenylation site	TZM-bl	HeLa-cell derivatives expressing CD4, CXCR4, CCR5 and Tat-inducible RLuc and β -Gal
RLU	relative light units	U	Unit
RLuc	<i>Renilla</i> luciferase	VLP	Virus-like particle
rpm	revolutions per minute	vpr	viral protein R
scFv	single-chain variable fragment	vpu	viral protein U
SDS	Sodium dodecyl sulfate	VSV-G	Viral Stomatitis Virus Glycoprotein
sec.	section	WPRE	Woodchuck Hepatitis Virus Posttranscriptional Regulatory Element
SIV(mac)	Simian Immunodeficiency Virus (of macaque)	wt	wild type
Tat	Trans-Activator of Transcription	x	times
TB	Terrific Broth medium		
TM	transmembrane region		

Bibliographic references and abbreviations therein are given following recommendations of the National Library of Medicine, MD, USA (300).

6.5 References

1. Barre-Sinoussi F, Chermann J, Rey F, Nugeyre M, Chamaret S, Gruest J, Dautet C, Axler-Blin C, Vezinet-Brun F, Rouzioux C, Rozenbaum W, Montagnier L. Isolation of a T-lymphotropic retrovirus from a patient at risk for acquired immune deficiency syndrome (AIDS). *Science* 1983;220(4599):868-871.
2. Popovic M, Sarngadharan M, Read E, Gallo R. Detection, isolation, and continuous production of cytopathic retroviruses (HTLV-III) from patients with AIDS and pre-AIDS. *Science* 1984;224(4648):497-500.
3. Cohen J, Enserink M. NOBEL PRIZE IN PHYSIOLOGY OR MEDICINE: HIV, HPV Researchers Honored, But One Scientist Is Left Out. *Science* 2008;322(5899):174-175.
4. UNAIDS. UNAIDS Report on the global AIDS epidemic 2010. Geneva: Joint United Nations Programme on HIV/AIDS (UNAIDS); 2010.
5. Moir S, Chun T, Fauci AS. Pathogenic Mechanisms of HIV Disease. *Annu Rev Pathol* 2011;6:223-48.
6. Holt N, Wang J, Kim K, Friedman G, Wang X, Taupin V, Crooks GM, Kohn DB, Gregory PD, Holmes MC, Cannon PM. Human hematopoietic stem/progenitor cells modified by zinc-finger nucleases targeted to CCR5 control HIV-1 in vivo. *Nat Biotechnol* 2010;28(8):839-847.
7. Sarkar I, Hauber I, Hauber J, Buchholz F. HIV-1 Proviral DNA Excision Using an Evolved Recombinase. *Science* 2007;316(5833):1912-1915.
8. Abdool Karim Q, Abdool Karim SS, Frohlich JA, Grobler AC, Baxter C, Mansoor LE, Kharsany ABM, Sibeko S, Mlisana KP, Omar Z, Gengiah TN, Maarschalk S, Arulappan N, Mlotshwa M, Morris L, Taylor D, on behalf of the CAPRISA 004 Trial Group. Effectiveness and Safety of Tenofovir Gel, an Antiretroviral Microbicide, for the Prevention of HIV Infection in Women. *Science* 2010;329(5996):1168-1174.
9. Grant RM, Lama JR, Anderson PL, McMahan V, Liu AY, Vargas L, Goicochea P, Casapía M, Guanira-Carranza JV, Ramirez-Cardich ME, Montoya-Herrera O, Fernández T, Veloso VG, Buchbinder SP, Chariyalertsak S, Schechter M, Bekker L, Mayer KH, Kallás EG, Amico KR, Mulligan K, Bushman LR, Hance RJ, Ganoza C, Defechereux P, Postle B, Wang F, McConnell JJ, Zheng J, Lee J, Rooney JF, Jaffe HS, Martinez AI, Burns DN, Glidden DV. Preexposure chemoprophylaxis for HIV prevention in men who have sex with men. *N. Engl. J. Med* 2010 Dec;363(27):2587-2599.
10. Hoxie JA. Toward an antibody-based HIV-1 vaccine. *Annu. Rev. Med* 2010;61:135-152.
11. Keele BF, Giorgi EE, Salazar-Gonzalez JF, Decker JM, Pham KT, Salazar MG, Sun C, Grayson T, Wang S, Li H, Wei X, Jiang C, Kirchherr JL, Gao F, Anderson JA, Ping L, Swanstrom R, Tomaras GD, Blattner WA, Goepfert PA, Kilby JM, Saag MS, Delwart EL, Busch MP, Cohen MS, Montefiori DC, Haynes BF, Gaschen B, Athreya GS, Lee HY, Wood N, Seoighe C, Perelson AS, Bhattacharya T, Korber BT, Hahn BH, Shaw GM. Identification and characterization of transmitted and early founder virus envelopes in primary HIV-1 infection. *Proceedings of the National Academy of Sciences* 2008;105(21):7552-7557.
12. Goonetilleke N, Liu MK, Salazar-Gonzalez JF, Ferrari G, Giorgi E, Gantsov VV, Keele BF, Learn GH, Turnbull EL, Salazar MG, Weinhold KJ, Moore S, CHAVI Clinical Core B, Letvin N, Haynes BF, Cohen MS, Hraber P, Bhattacharya T, Borrow P, Perelson AS, Hahn BH, Shaw GM, Korber BT, McMichael AJ. The first T cell response to transmitted/founder virus contributes to the control of acute viremia in HIV-1 infection. *Journal of Experimental Medicine* 2009;206(6):1253-1272.
13. Kuiken C, Foley B, Leitner T, Apetrei C, Hahn B, Mizrahi I, Mullins J, Rambaut A, Wolinsky S, Korber B. HIV Sequence Compendium 2010. Los Alamos, New Mexico: Theoretical Biology and Biophysics Group, Theoretical Biology and Biophysics Group; 2010.
14. Lu S, Wang S, Grimes Serrano JM. Polyvalent AIDS Vaccines. *Curr HIV Res* 2010 Dec;8(8):622-9.
15. McBurney SP, Ross TM. Developing broadly reactive HIV-1/AIDS vaccines: a review of polyvalent and centralized HIV-1 vaccines. *Curr. Pharm. Des* 2007;13(19):1957-1964.

16. Santra S, Korber BT, Muldoon M, Barouch DH, Nabel GJ, Gao F, Hahn BH, Haynes BF, Letvin NL. A centralized gene-based HIV-1 vaccine elicits broad cross-clade cellular immune responses in rhesus monkeys. *Proc. Natl. Acad. Sci. U.S.A* 2008 Jul;105(30):10489-10494.
17. Sodora DL, Allan JS, Apetrei C, Brechley JM, Douek DC, Else JG, Estes JD, Hahn BH, Hirsch VM, Kaur A, Kirchhoff F, Muller-Trutwin M, Pandrea I, Schmitz JE, Silvestri G. Toward an AIDS vaccine: lessons from natural simian immunodeficiency virus infections of African nonhuman primate hosts. *Nat Med* 2009;15(8):861-865.
18. Mascola JR, Montefiori DC. The Role of Antibodies in HIV Vaccines. *Annu. Rev. Immunol.* 2010;28(1):413-444.
19. Ross AL, Br ave A, Scarlatti G, Manrique A, Buonaguro L. Progress towards development of an HIV vaccine: report of the AIDS Vaccine 2009 Conference. *The Lancet Infectious Diseases* 2010;10(5):305-316.
20. Pitisuttithum P, Gilbert P, Gurwith M, Heyward W, Martin M, van Griensven F, Hu D, Tappero J, Choopanya K, Bangkok Vaccine Evaluation Group. Randomized, Double - Blind, Placebo - Controlled Efficacy Trial of a Bivalent Recombinant Glycoprotein 120 HIV - 1 Vaccine among Injection Drug Users in Bangkok, Thailand. *J INFECT DIS* 2006;194(12):1661-1671.
21. Flynn NM, Forthal DN, Harro CD, Judson FN, Mayer KH, Para MF. Placebo-controlled phase 3 trial of a recombinant glycoprotein 120 vaccine to prevent HIV-1 infection. *J. Infect. Dis* 2005 Mar;191(5):654-665.
22. Buchbinder S, Mehrotra D, Duerr A, Fitzgerald D, Mogg R, Li D, Gilbert P, Lama J, Marmor M, Delrio C. Efficacy assessment of a cell-mediated immunity HIV-1 vaccine (the Step Study): a double-blind, randomised, placebo-controlled, test-of-concept trial. *The Lancet* 2008;372(9653):1881-1893.
23. Gray G, Buchbinder S, Duerr A. Overview of STEP and Phambili trial results: two phase IIb test-of-concept studies investigating the efficacy of MRK adenovirus type 5 gag/pol/nef subtype B HIV vaccine. *Current Opinion in HIV and AIDS* 2010;5(5):357-361.
24. Rerks-Ngarm S, Pitisuttithum P, Nitayaphan S, Kaewkungwal J, Chiu J, Paris R, Premisri N, Namwat C, de Souza M, Adams E, Benenson M, Gurunathan S, Tartaglia J, McNeil JG, Francis DP, Stablein D, Birx DL, Chunsuttiwat S, Khamboonruang C, Thongcharoen P, Robb ML, Michael NL, Kunasol P, Kim JH. Vaccination with ALVAC and AIDSVAX to prevent HIV-1 infection in Thailand. *N. Engl. J. Med* 2009 Dec;361(23):2209-2220.
25. Kim JH, Rerks-Ngarm S, Excler J, Michael NL. HIV vaccines: lessons learned and the way forward. *Curr Opin HIV AIDS* 2010 Sep;5(5):428-434.
26. Turner BG, Summers MF. Structural biology of HIV. *J. Mol. Biol* 1999 Jan;285(1):1-32.
27. McElrath MJ, Haynes BF. Induction of immunity to human immunodeficiency virus type-1 by vaccination. *Immunity* 2010 Oct;33(4):542-554.
28. Haase AT. Targeting early infection to prevent HIV-1 mucosal transmission. *Nature* 2010;464(7286):217-223.
29. McMichael AJ, Borrow P, Tomaras GD, Goonetilleke N, Haynes BF. The immune response during acute HIV-1 infection: clues for vaccine development. *Nat Rev Immunol* 2009;10(1):11-23.
30. Hessel AJ, Poignard P, Hunter M, Hangartner L, Tehrani DM, Bleeker WK, Parren PWHI, Marx PA, Burton DR. Effective, low-titer antibody protection against low-dose repeated mucosal SHIV challenge in macaques. *Nat Med* 2009;15(8):951-954.
31. Hessel AJ, Hangartner L, Hunter M, Havenith CEG, Beurskens FJ, Bakker JM, Lanigan CMS, Landucci G, Forthal DN, Parren PWHI, Marx PA, Burton DR. Fc receptor but not complement binding is important in antibody protection against HIV. *Nature* 2007;449(7158):101-104.
32. Montefiori DC, Mascola JR. Neutralizing antibodies against HIV-1: can we elicit them with vaccines and how much do we need? *Current Opinion in HIV and AIDS* 2009;4(5):347-351.
33. Haynes BF, Liao H, Tomaras GD. Is developing an HIV-1 vaccine possible? *Curr Opin HIV AIDS* 2010 Sep;5(5):362-367.

34. Hessel AJ, Rakasz EG, Tehrani DM, Huber M, Weisgrau KL, Landucci G, Forthal DN, Koff WC, Poignard P, Watkins DI, Burton DR. Broadly Neutralizing Monoclonal Antibodies 2F5 and 4E10 Directed against the Human Immunodeficiency Virus Type 1 gp41 Membrane-Proximal External Region Protect against Mucosal Challenge by Simian-Human Immunodeficiency Virus SHIVBa-L. *Journal of Virology* 2009;84(3):1302-1313.
35. Stamatatos L, Morris L, Burton DR, Mascola JR. Neutralizing antibodies generated during natural HIV-1 infection: good news for an HIV-1 vaccine? *Nat Med* 2009;15(8):866-70.
36. Parren PW, Moore JP, Burton DR, Sattentau QJ. The neutralizing antibody response to HIV-1: viral evasion and escape from humoral immunity. *AIDS* 1999;13 Suppl A:S137-162.
37. Binley JM, Ban YEA, Crooks ET, Eggink D, Osawa K, Schief WR, Sanders RW. Role of Complex Carbohydrates in Human Immunodeficiency Virus Type 1 Infection and Resistance to Antibody Neutralization. *Journal of Virology* 2010;84(11):5637-5655.
38. Wei X, Decker JM, Wang S, Hui H, Kappes JC, Wu X, Salazar-Gonzalez JF, Salazar MG, Kilby JM, Saag MS, Komarova NL, Nowak MA, Hahn BH, Kwong PD, Shaw GM. Antibody neutralization and escape by HIV-1. *Nature* 2003;422(6929):307-312.
39. Frey G, Peng H, Rits-Volloch S, Morelli M, Cheng Y, Chen B. A fusion-intermediate state of HIV-1 gp41 targeted by broadly neutralizing antibodies. *Proceedings of the National Academy of Sciences* 2008;105(10):3739-3744.
40. Schief WR, Ban YA, Stamatatos L. Challenges for structure-based HIV vaccine design. *Curr Opin HIV AIDS* 2009 Sep;4(5):431-440.
41. Kwong PD, Doyle ML, Casper DJ, Cicala C, Leavitt SA, Majeed S, Steenbeke TD, Venturi M, Chaiken I, Fung M, Katinger H, Parren PWIH, Robinson J, Van Ryk D, Wang L, Burton DR, Freire E, Wyatt R, Sodroski J, Hendrickson WA, Arthos J. HIV-1 evades antibody-mediated neutralization through conformational masking of receptor-binding sites. *Nature* 2002;420(6916):678-682.
42. Astronomo RD, Lee H, Scanlan CN, Pantophlet R, Huang C, Wilson IA, Blixt O, Dwek RA, Wong C, Burton DR. A Glycoconjugate Antigen Based on the Recognition Motif of a Broadly Neutralizing Human Immunodeficiency Virus Antibody, 2G12, Is Immunogenic but Elicits Antibodies Unable To Bind to the Self Glycans of gp120. *Journal of Virology* 2008;82(13):6359-6368.
43. Haynes BF. Cardiophilin Polyspecific Autoreactivity in Two Broadly Neutralizing HIV-1 Antibodies. *Science* 2005;308(5730):1906-1908.
44. Verkoczy L, Diaz M, Holl TM, Ouyang Y, Bouton-Verville H, Alam SM, Liao H, Kelsoe G, Haynes BF. Autoreactivity in an HIV-1 broadly reactive neutralizing antibody variable region heavy chain induces immunologic tolerance. *Proceedings of the National Academy of Sciences* 2009;107(1):181-186.
45. Davis KL, Gray ES, Moore PL, Decker JM, Salomon A, Montefiori DC, Graham BS, Keefer MC, Pinter A, Morris L. High titer HIV-1 V3-specific antibodies with broad reactivity but low neutralizing potency in acute infection and following vaccination. *Virology* 2009;387(2):414-426.
46. Moore PL, Gray ES, Morris L. Specificity of the autologous neutralizing antibody response. *Curr Opin HIV AIDS* 2009 Sep;4(5):358-363.
47. Richman DD. Rapid evolution of the neutralizing antibody response to HIV type 1 infection. *Proceedings of the National Academy of Sciences* 2003;100(7):4144-4149.
48. Simek MD, Rida W, Priddy FH, Pung P, Carrow E, Laufer DS, Lehrman JK, Boaz M, Tarragona-Fiol T, Miirio G, Birungi J, Pozniak A, McPhee DA, Manigart O, Karita E, Inwoley A, Jaoko W, DeHovitz J, Bekker L, Pitisuttithum P, Paris R, Walker LM, Poignard P, Wrin T, Fast PE, Burton DR, Koff WC. Human Immunodeficiency Virus Type 1 Elite Neutralizers: Individuals with Broad and Potent Neutralizing Activity Identified by Using a High-Throughput Neutralization Assay together with an Analytical Selection Algorithm. *Journal of Virology* 2009;83(14):7337-7348.

49. Euler Z, van Gils M, Bunnik E, Phung P, Schweighardt B, Wrin T, Schuitemaker H. Cross - Reactive Neutralizing Humoral Immunity Does Not Protect from HIV Type 1 Disease Progression. *J INFECT DIS* 2010;201(7):1045-1053.
50. Sather DN, Armann J, Ching LK, Mavrantoni A, Sellhorn G, Caldwell Z, Yu X, Wood B, Self S, Kalams S, Stamatatos L. Factors associated with the development of cross-reactive neutralizing antibodies during human immunodeficiency virus type 1 infection. *J. Virol* 2009 Jan;83(2):757-769.
51. Wyatt R. The HIV-1 Envelope Glycoproteins: Fusogens, Antigens, and Immunogens. *Science* 1998;280(5371):1884-1888.
52. Ganser-Pornillos BK, Yeager M, Sundquist WI. The structural biology of HIV assembly. *Curr. Opin. Struct. Biol* 2008 Apr;18(2):203-217.
53. Dalgleish AG, Beverley PC, Clapham PR, Crawford DH, Greaves MF, Weiss RA. The CD4 (T4) antigen is an essential component of the receptor for the AIDS retrovirus. *Nature* 1984 Jan;312(5996):763-767.
54. Zhu P, Liu J, Bess J, Chertova E, Lifson JD, Grisé H, Ofek GA, Taylor KA, Roux KH. Distribution and three-dimensional structure of AIDS virus envelope spikes. *Nature* 2006 Jun;441(7095):847-852.
55. Zanetti G, Briggs JAG, Grünewald K, Sattentau QJ, Fuller SD. Cryo-electron tomographic structure of an immunodeficiency virus envelope complex in situ. *PLoS Pathog* 2006 Aug;2(8):e83.
56. Liu J, Bartesaghi A, Borgnia MJ, Sapiro G, Subramaniam S. Molecular architecture of native HIV-1 gp120 trimers. *Nature* 2008 Sep;455(7209):109-113.
57. Zhu P, Winkler H, Chertova E, Taylor KA, Roux KH. Cryoelectron Tomography of HIV-1 Envelope Spikes: Further Evidence for Tripod-Like Legs. *PLoS Pathog* 2008;4(11):e1000203.
58. Kwong PD, Wyatt R, Robinson J, Sweet RW, Sodroski J, Hendrickson WA. Structure of an HIV gp120 envelope glycoprotein in complex with the CD4 receptor and a neutralizing human antibody. *Nature* 1998 Jun;393(6686):648-659.
59. Zhou T, Xu L, Dey B, Hessel AJ, Van Ryk D, Xiang S, Yang X, Zhang M, Zwick MB, Arthos J, Burton DR, Dimitrov DS, Sodroski J, Wyatt R, Nabel GJ, Kwong PD. Structural definition of a conserved neutralization epitope on HIV-1 gp120. *Nature* 2007 Feb;445(7129):732-737.
60. Liu J, Deng Y, Dey AK, Moore JP, Lu M. Structure of the HIV-1 gp41 membrane-proximal ectodomain region in a putative prefusion conformation. *Biochemistry* 2009 Apr;48(13):2915-2923.
61. Wu S, Loving R, Lindqvist B, Hebert H, Koeck PJB, Sjöberg M, Garoff H. Single-particle cryoelectron microscopy analysis reveals the HIV-1 spike as a tripod structure. *Proceedings of the National Academy of Sciences* 2010;107(44):18844-18849.
62. White TA, Bartesaghi A, Borgnia MJ, Meyerson JR, de la Cruz MJV, Bess JW, Nandwani R, Hoxie JA, Lifson JD, Milne JLS, Subramaniam S. Molecular architectures of trimeric SIV and HIV-1 envelope glycoproteins on intact viruses: strain-dependent variation in quaternary structure. *PLoS Pathog* 2010;6(12):e1001249.
63. Scheid JF, Mouquet H, Feldhahn N, Seaman MS, Velinzon K, Pietzsch J, Ott RG, Anthony RM, Zebroski H, Hurley A, Phogat A, Chakrabarti B, Li Y, Connors M, Pereyra F, Walker BD, Wardemann H, Ho D, Wyatt RT, Mascola JR, Ravetch JV, Nussenzweig MC. Broad diversity of neutralizing antibodies isolated from memory B cells in HIV-infected individuals. *Nature* 2009;458(7238):636-640.
64. Walker LM, Simek MD, Priddy F, Gach JS, Wagner D, Zwick MB, Phogat SK, Poignard P, Burton DR. A limited number of antibody specificities mediate broad and potent serum neutralization in selected HIV-1 infected individuals. *PLoS Pathog* 2010 Aug;6(8):e1001028.
65. Wu X, Yang Z, Li Y, Hogerkorp C, Schief WR, Seaman MS, Zhou T, Schmidt SD, Wu L, Xu L, Longo NS, McKee K, O'Dell S, Louder MK, Wycuff DL, Feng Y, Nason M, Doria-Rose N, Connors M, Kwong PD, Roederer M, Wyatt RT, Nabel GJ, Mascola JR. Rational Design of Envelope Identifies Broadly Neutralizing Human Monoclonal Antibodies to HIV-1. *Science* 2010;329(5993):856-861.

-
66. Corti D, Langedijk JPM, Hinz A, Seaman MS, Vanzetta F, Fernandez-Rodriguez BM, Silacci C, Pinna D, Jarrossay D, Balla-Jhagjhoorsingh S, Willems B, Zekveld MJ, Dreja H, O'Sullivan E, Pade C, Orkin C, Jeffs SA, Montefiori DC, Davis D, Weissenhorn W, McKnight A, Heeney JL, Sallusto F, Sattentau QJ, Weiss RA, Lanzavecchia A. Analysis of memory B cell responses and isolation of novel monoclonal antibodies with neutralizing breadth from HIV-1-infected individuals. *PLoS ONE* 2010;5(1):e8805.
 67. Hicar MD, Chen X, Briney B, Hammonds J, Wang J, Kalams S, Spearman PW, Crowe JE. Pseudovirion Particles Bearing Native HIV Envelope Trimers Facilitate a Novel Method for Generating Human Neutralizing Monoclonal Antibodies Against HIV. *JAIDS Journal of Acquired Immune Deficiency Syndromes* 2010;54(3):223-235.
 68. Liao H, Levesque MC, Nagel A, Dixon A, Zhang R, Walter E, Parks R, Whitesides J, Marshall DJ, Hwang K. High-throughput isolation of immunoglobulin genes from single human B cells and expression as monoclonal antibodies. *Journal of Virological Methods* 2009;158(1-2):171-179.
 69. Labrijn AF, Poignard P, Raja A, Zwick MB, Delgado K, Franti M, Binley J, Vivona V, Grundner C, Huang C, Venturi M, Petropoulos CJ, Wrin T, Dimitrov DS, Robinson J, Kwong PD, Wyatt RT, Sodroski J, Burton DR. Access of antibody molecules to the conserved coreceptor binding site on glycoprotein gp120 is sterically restricted on primary human immunodeficiency virus type 1. *J. Virol* 2003 Oct;77(19):10557-10565.
 70. Pietzsch J, Scheid JF, Mouquet H, Klein F, Seaman MS, Jankovic M, Corti D, Lanzavecchia A, Nussenzweig MC. Human anti-HIV-neutralizing antibodies frequently target a conserved epitope essential for viral fitness. *Journal of Experimental Medicine* 2010;207(9):1995-2002.
 71. Zhou T, Georgiev I, Wu X, Yang Z, Dai K, Finzi A, Do Kwon Y, Scheid JF, Shi W, Xu L, Yang Y, Zhu J, Nussenzweig MC, Sodroski J, Shapiro L, Nabel GJ, Mascola JR, Kwong PD. Structural Basis for Broad and Potent Neutralization of HIV-1 by Antibody VRC01. *Science* 2010;329(5993):811-817.
 72. Zolla-Pazner S, Cardozo T. Structure–function relationships of HIV-1 envelope sequence-variable regions refocus vaccine design. *Nat Rev Immunol* 2010;10(7):527-535.
 73. Pancera M, McLellan JS, Wu X, Zhu J, Changela A, Schmidt SD, Yang Y, Zhou T, Phogat S, Mascola JR, Kwong PD. Crystal Structure of PG16 and Chimeric Dissection with Somatically Related PG9: Structure-Function Analysis of Two Quaternary-Specific Antibodies That Effectively Neutralize HIV-1. *Journal of Virology* 2010;84(16):8098-8110.
 74. Walker LM, Phogat SK, Chan-Hui P, Wagner D, Phung P, Goss JL, Wrin T, Simek MD, Fling S, Mitcham JL, Lehrman JK, Priddy FH, Olsen OA, Frey SM, Hammond PW, Protocol G Principal Investigators, Kaminsky S, Zamb T, Moyle M, Koff WC, Poignard P, Burton DR. Broad and Potent Neutralizing Antibodies from an African Donor Reveal a New HIV-1 Vaccine Target. *Science* 2009;326(5950):285-289.
 75. Burton DR, Weiss RA. AIDS/HIV. A boost for HIV vaccine design. *Science* 2010 Aug;329(5993):770-773.
 76. Walker LM, Burton DR. Rational antibody-based HIV-1 vaccine design: current approaches and future directions. *Curr. Opin. Immunol* 2010 Jun;22(3):358-366.
 77. Calarese DA. Antibody Domain Exchange Is an Immunological Solution to Carbohydrate Cluster Recognition. *Science* 2003;300(5628):2065-2071.
 78. Doores KJ, Bonomelli C, Harvey DJ, Vasiljevic S, Dwek RA, Burton DR, Crispin M, Scanlan CN. Envelope glycans of immunodeficiency virions are almost entirely oligomannose antigens. *Proceedings of the National Academy of Sciences* 2010;107(31):13800-13805.
 79. Cardoso R, Zwick M, Stanfield R, Kunert R, Binley J, Katinger H, Burton D, Wilson I. Broadly Neutralizing Anti-HIV Antibody 4E10 Recognizes a Helical Conformation of a Highly Conserved Fusion-Associated Motif in gp41. *Immunity* 2005;22(2):163-173.
 80. Ofek G, Tang M, Sambor A, Katinger H, Mascola JR, Wyatt R, Kwong PD. Structure and mechanistic analysis of the anti-human immunodeficiency virus type 1 antibody 2F5 in complex with its gp41 epitope. *J. Virol* 2004 Oct;78(19):10724-10737.

81. Nelson JD, Brunel FM, Jensen R, Crooks ET, Cardoso RMF, Wang M, Hessel A, Wilson IA, Binley JM, Dawson PE, Burton DR, Zwick MB. An affinity-enhanced neutralizing antibody against the membrane-proximal external region of human immunodeficiency virus type 1 gp41 recognizes an epitope between those of 2F5 and 4E10. *J. Virol* 2007 Apr;81(8):4033-4043.
82. Rappuoli R. Reverse vaccinology. *Curr. Opin. Microbiol* 2000 Oct;3(5):445-450.
83. Korber B, Foley B, Kuiken C, Pillai S, Sodroski J. Numbering Positions in HIV Relative to HXB2CG. Los Alamos: Los Alamos National Library; 1998.
84. Welch BD, VanDemark AP, Heroux A, Hill CP, Kay MS. Potent D-peptide inhibitors of HIV-1 entry. *Proceedings of the National Academy of Sciences* 2007;104(43):16828-16833.
85. Lu M, Stoller MO, Wang S, Liu J, Fagan MB, Nunberg JH. Structural and Functional Analysis of Interhelical Interactions in the Human Immunodeficiency Virus Type 1 gp41 Envelope Glycoprotein by Alanine-Scanning Mutagenesis. *Journal of Virology* 2001;75(22):11146-11156.
86. Grasnack D, Sternberg U, Strandberg E, Wadhwani P, Ulrich AS. Irregular structure of the HIV fusion peptide in membranes demonstrated by solid-state NMR and MD simulations [Internet]. *Eur Biophys J* 2011 Jan; Available from: <http://www.ncbi.nlm.nih.gov/pubmed/21274707>
87. Chan DC, Fass D, Berger JM, Kim PS. Core structure of gp41 from the HIV envelope glycoprotein. *Cell* 1997 Apr;89(2):263-273.
88. Tan K, Liu J, Wang J, Shen S, Lu M. Atomic structure of a thermostable subdomain of HIV-1 gp41. *Proc. Natl. Acad. Sci. U.S.A* 1997 Nov;94(23):12303-12308.
89. Weissenhorn W, Dessen A, Harrison SC, Skehel JJ, Wiley DC. Atomic structure of the ectodomain from HIV-1 gp41. *Nature* 1997;387(6631):426-430.
90. Harrison SC. Viral membrane fusion. *Nat. Struct. Mol. Biol* 2008 Jul;15(7):690-698.
91. Melikyan GB, Markosyan RM, Hemmati H, Delmedico MK, Lambert DM, Cohen FS. Evidence That the Transition of HIV-1 Gp41 into a Six-Helix Bundle, Not the Bundle Configuration, Induces Membrane Fusion. *The Journal of Cell Biology* 2000;151(2):413-424.
92. Weiss CD. HIV-1 gp41: mediator of fusion and target for inhibition. *AIDS Rev* 2003 Dec;5(4):214-221.
93. Shi W, Bohon J, Han DP, Habte H, Qin Y, Cho MW, Chance MR. Structural characterization of HIV gp41 with the membrane-proximal external region. *J. Biol. Chem* 2010 Jul;285(31):24290-24298.
94. Buzon V, Natrajan G, Schibli D, Campelo F, Kozlov MM, Weissenhorn W. Crystal structure of HIV-1 gp41 including both fusion peptide and membrane proximal external regions. *PLoS Pathog* 2010 May;6(5):e1000880.
95. Frey G, Chen J, Rits-Volloch S, Freeman MM, Zolla-Pazner S, Chen B. Distinct conformational states of HIV-1 gp41 are recognized by neutralizing and non-neutralizing antibodies. *Nat Struct Mol Biol* 2010;17:1486-1491.
96. Gallaher WR, Ball JM, Garry RF, Griffin MC, Montelaro RC. A general model for the transmembrane proteins of HIV and other retroviruses. *AIDS Res. Hum. Retroviruses* 1989 Aug;5(4):431-440.
97. Haffar OK, Dowbenko DJ, Berman PW. The cytoplasmic tail of HIV-1 gp160 contains regions that associate with cellular membranes. *Virology* 1991 Jan;180(1):439-441.
98. Cleveland SM, McLain L, Cheung L, Jones TD, Hollier M, Dimmock NJ. A region of the C-terminal tail of the gp41 envelope glycoprotein of human immunodeficiency virus type 1 contains a neutralizing epitope: evidence for its exposure on the surface of the virion. *J. Gen. Virol* 2003 Mar;84(Pt 3):591-602.
99. Hollier MJ, Dimmock NJ. The C-terminal tail of the gp41 transmembrane envelope glycoprotein of HIV-1 clades A, B, C, and D may exist in two conformations: an analysis of sequence, structure, and function. *Virology* 2005 Jul;337(2):284-296.
100. Steckbeck JD, Sun C, Sturgeon TJ, Montelaro RC. Topology of the C-Terminal Tail of HIV-1 gp41: Differential Exposure of the Kennedy Epitope on Cell and Viral Membranes. *PLoS ONE* 2010;5(12):e15261.

101. Zwick MB, Jensen R, Church S, Wang M, Stiegler G, Kunert R, Katinger H, Burton DR. Anti-human immunodeficiency virus type 1 (HIV-1) antibodies 2F5 and 4E10 require surprisingly few crucial residues in the membrane-proximal external region of glycoprotein gp41 to neutralize HIV-1. *J. Virol* 2005 Jan;79(2):1252-1261.
102. Zwick MB, Labrijn AF, Wang M, Spenlehauer C, Saphire EO, Binley JM, Moore JP, Stiegler G, Katinger H, Burton DR, Parren PWHI. Broadly Neutralizing Antibodies Targeted to the Membrane-Proximal External Region of Human Immunodeficiency Virus Type 1 Glycoprotein gp41. *Journal of Virology* 2001;75(22):10892-10905.
103. Salzwedel K, West JT, Hunter E. A conserved tryptophan-rich motif in the membrane-proximal region of the human immunodeficiency virus type 1 gp41 ectodomain is important for Env-mediated fusion and virus infectivity. *J. Virol* 1999 Mar;73(3):2469-2480.
104. Sun ZJ, Oh KJ, Kim M, Yu J, Brusica V, Song L, Qiao Z, Wang J, Wagner G, Reinherz EL. HIV-1 broadly neutralizing antibody extracts its epitope from a kinked gp41 ectodomain region on the viral membrane. *Immunity* 2008 Jan;28(1):52-63.
105. Coutant J, Yu H, Clément M, Alfsen A, Toma F, Curmi PA, Bomsel M. Both lipid environment and pH are critical for determining physiological solution structure of 3-D-conserved epitopes of the HIV-1 gp41-MPER peptide P1. *FASEB J* 2008 Dec;22(12):4338-4351.
106. Pejchal R, Gach JS, Brunel FM, Cardoso RM, Stanfield RL, Dawson PE, Burton DR, Zwick MB, Wilson IA. A Conformational Switch in Human Immunodeficiency Virus gp41 Revealed by the Structures of Overlapping Epitopes Recognized by Neutralizing Antibodies. *Journal of Virology* 2009;83(17):8451-8462.
107. Schibli DJ, Montelaro RC, Vogel HJ. The Membrane-Proximal Tryptophan-Rich Region of the HIV Glycoprotein, gp41, Forms a Well-Defined Helix in Dodecylphosphocholine Micelles. *Biochemistry* 2001;40(32):9570-9578.
108. Song L, Sun ZJ, Coleman KE, Zwick MB, Gach JS, Wang J, Reinherz EL, Wagner G, Kim M. Broadly neutralizing anti-HIV-1 antibodies disrupt a hinge-related function of gp41 at the membrane interface. *Proceedings of the National Academy of Sciences* 2009;106(22):9057-9062.
109. Montero M, van Houten NE, Wang X, Scott JK. The membrane-proximal external region of the human immunodeficiency virus type 1 envelope: dominant site of antibody neutralization and target for vaccine design. *Microbiol. Mol. Biol. Rev* 2008 Mar;72(1):54-84, table of contents.
110. Horal P, Svennerholm B, Jeansson S, Rymo L, Hall WW, Vahne A. Continuous epitopes of the human immunodeficiency virus type 1 (HIV-1) transmembrane glycoprotein and reactivity of human sera to synthetic peptides representing various HIV-1 isolates. *J. Virol* 1991 May;65(5):2718-2723.
111. Xu JY, Gorny MK, Palker T, Karwowska S, Zolla-Pazner S. Epitope mapping of two immunodominant domains of gp41, the transmembrane protein of human immunodeficiency virus type 1, using ten human monoclonal antibodies. *J. Virol* 1991 Sep;65(9):4832-4838.
112. Nicely NI, Dennison SM, Spicer L, Searce RM, Kelsoe G, Ueda Y, Chen H, Liao H, Alam SM, Haynes BF. Crystal structure of a non-neutralizing antibody to the HIV-1 gp41 membrane-proximal external region. *Nat Struct Mol Biol* 2010;17(12):1492-1494.
113. Kennedy RC, Henkel RD, Pauletti D, Allan JS, Lee TH, Essex M, Dreesman GR. Antiserum to a synthetic peptide recognizes the HTLV-III envelope glycoprotein. *Science* 1986 Mar;231(4745):1556-1559.
114. Mühlbacher M, Spruth M, Siegel F, Zangerle R, Dierich MP. Longitudinal study of antibody reactivity against HIV-1 envelope and a peptide representing a conserved site on Gp41 in HIV-1-infected patients. *Immunobiology* 1999 Jun;200(2):295-305.
115. Srisurapanon S, Louisiriratchanakul S, Sumransurp K, Ratanasrithong M, Chuenchitra T, Jintakatkorn S, Wasi C. Binding antibody to neutralizing epitope gp41 in HIV-1 subtype CRF 01_AE infection related to stage of disease. *Southeast Asian J. Trop. Med. Public Health* 2005 Jan;36(1):221-227.

116. Opalka D, Pessi A, Bianchi E, Ciliberto G, Schleif W, McElhaugh M, Danzeisen R, Geleziunas R, Miller M, Eckert DM, Bramhill D, Joyce J, Cook J, Magilton W, Shiver J, Emini E, Esser MT. Analysis of the HIV-1 gp41 specific immune response using a multiplexed antibody detection assay. *J. Immunol. Methods* 2004 Apr;287(1-2):49-65.
117. Dhillon AK, Donners H, Pantophlet R, Johnson WE, Decker JM, Shaw GM, Lee F, Richman DD, Doms RW, Vanham G, Burton DR. Dissecting the Neutralizing Antibody Specificities of Broadly Neutralizing Sera from Human Immunodeficiency Virus Type 1-Infected Donors. *Journal of Virology* 2007;81(12):6548-6562.
118. Braibant M, Brunet S, Costagliola D, Rouzioux C, Agut H, Katinger H, Autran B, Barin F. Antibodies to conserved epitopes of the HIV-1 envelope in sera from long-term non-progressors: prevalence and association with neutralizing activity. *AIDS* 2006 Oct;20(15):1923-1930.
119. Buchacher A, Predl R, Strutzenberger K, Steinfellner W, Trkola A, Purtscher M, Gruber G, Tauer C, Steindl F, Jungbauer A. Generation of human monoclonal antibodies against HIV-1 proteins; electrofusion and Epstein-Barr virus transformation for peripheral blood lymphocyte immortalization. *AIDS Res. Hum. Retroviruses* 1994 Apr;10(4):359-369.
120. Stiegler G, Kunert R, Purtscher M, Wolbank S, Voglauer R, Steindl F, Katinger H. A potent cross-clade neutralizing human monoclonal antibody against a novel epitope on gp41 of human immunodeficiency virus type 1. *AIDS Res. Hum. Retroviruses* 2001 Dec;17(18):1757-1765.
121. Binley JM, Wrin T, Korber B, Zwick MB, Wang M, Chappey C, Stiegler G, Kunert R, Zolla-Pazner S, Katinger H, Petropoulos CJ, Burton DR. Comprehensive cross-clade neutralization analysis of a panel of anti-human immunodeficiency virus type 1 monoclonal antibodies. *J. Virol* 2004 Dec;78(23):13232-13252.
122. Muster T, Steindl F, Purtscher M, Trkola A, Klima A, Himmler G, Rüker F, Katinger H. A conserved neutralizing epitope on gp41 of human immunodeficiency virus type 1. *J. Virol* 1993 Nov;67(11):6642-6647.
123. Conley AJ, Gorny MK, Kessler JA, Boots LJ, Ossorio-Castro M, Koenig S, Lineberger DW, Emini EA, Williams C, Zolla-Pazner S. Neutralization of primary human immunodeficiency virus type 1 isolates by the broadly reactive anti-V3 monoclonal antibody, 447-52D. *J. Virol* 1994 Nov;68(11):6994-7000.
124. Hager-Braun C, Katinger H, Tomer KB. The HIV-neutralizing monoclonal antibody 4E10 recognizes N-terminal sequences on the native antigen. *J. Immunol* 2006 Jun;176(12):7471-7481.
125. Brunel FM, Zwick MB, Cardoso RMF, Nelson JD, Wilson IA, Burton DR, Dawson PE. Structure-function analysis of the epitope for 4E10, a broadly neutralizing human immunodeficiency virus type 1 antibody. *J. Virol* 2006 Feb;80(4):1680-1687.
126. Alam SM, McAdams M, Boren D, Rak M, Searce RM, Gao F, Camacho ZT, Gewirth D, Kelsoe G, Chen P, Haynes BF. The role of antibody polyspecificity and lipid reactivity in binding of broadly neutralizing anti-HIV-1 envelope human monoclonal antibodies 2F5 and 4E10 to glycoprotein 41 membrane proximal envelope epitopes. *J. Immunol* 2007 Apr;178(7):4424-4435.
127. Dennison SM, Stewart SM, Stempel KC, Liao H, Haynes BF, Alam SM. Stable docking of neutralizing human immunodeficiency virus type 1 gp41 membrane-proximal external region monoclonal antibodies 2F5 and 4E10 is dependent on the membrane immersion depth of their epitope regions. *J. Virol* 2009 Oct;83(19):10211-10223.
128. Joos B, Trkola A, Kuster H, Aceto L, Fischer M, Stiegler G, Armbruster C, Vcelar B, Katinger H, Gunthard HF. Long-Term Multiple-Dose Pharmacokinetics of Human Monoclonal Antibodies (MAbs) against Human Immunodeficiency Virus Type 1 Envelope gp120 (MAb 2G12) and gp41 (MAbs 4E10 and 2F5). *Antimicrobial Agents and Chemotherapy* 2006;50(5):1773-1779.
129. Vcelar B, Stiegler G, Wolf HM, Muntean W, Leschnik B, Mehendru S, Markowitz M, Armbruster C, Kunert R, Eibl MM, Katinger H. Reassessment of autoreactivity of the broadly neutralizing HIV antibodies 4E10 and 2F5 and retrospective analysis of clinical safety data. *AIDS* 2007 Oct;21(16):2161-2170.

130. Scherer EM, Zwick MB, Teyton L, Burton DR. Difficulties in eliciting broadly neutralizing anti-HIV antibodies are not explained by cardiolipin autoreactivity. *AIDS* 2007;21(16):2131-2139.
131. Scherer EM, Leaman DP, Zwick MB, McMichael AJ, Burton DR. Aromatic residues at the edge of the antibody combining site facilitate viral glycoprotein recognition through membrane interactions. *Proc. Natl. Acad. Sci. U.S.A* 2010 Jan;107(4):1529-1534.
132. Grundner C, Mirzabekov T, Sodroski J, Wyatt R. Solid-Phase Proteoliposomes Containing Human Immunodeficiency Virus Envelope Glycoproteins. *Journal of Virology* 2002;76(7):3511-3521.
133. Veiga AS, Pattenden LK, Fletcher JM, Castanho MARB, Aguilar MI. Interactions of HIV-1 antibodies 2F5 and 4E10 with a gp41 epitope prebound to host and viral membrane model systems. *Chembiochem* 2009 Apr;10(6):1032-1044.
134. Sánchez-Martínez S, Lorizate M, Katinger H, Kunert R, Nieva JL. Membrane Association and Epitope Recognition by HIV-1 Neutralizing Anti-gp41 2F5 and 4E10 Antibodies. *AIDS Research and Human Retroviruses* 2006;22(10):998-1006.
135. Huarte N, Lorizate M, Maeso R, Kunert R, Arranz R, Valpuesta JM, Nieva JL. The Broadly Neutralizing Anti-Human Immunodeficiency Virus Type 1 4E10 Monoclonal Antibody Is Better Adapted to Membrane-Bound Epitope Recognition and Blocking than 2F5. *Journal of Virology* 2008;82(18):8986-8996.
136. Dimitrov AS, Jacobs A, Finnegan CM, Stiegler G, Katinger H, Blumenthal R. Exposure of the membrane-proximal external region of HIV-1 gp41 in the course of HIV-1 envelope glycoprotein-mediated fusion. *Biochemistry* 2007 Feb;46(5):1398-1401.
137. Crooks ET, Moore PL, Richman D, Robinson J, Crooks JA, Franti M, Schülke N, Binley JM. Characterizing anti-HIV monoclonal antibodies and immune sera by defining the mechanism of neutralization. *Hum Antibodies* 2005;14(3-4):101-113.
138. de Rosny E, Vassell R, Jiang S, Kunert R, Weiss CD. Binding of the 2F5 Monoclonal Antibody to Native and Fusion-Intermediate Forms of Human Immunodeficiency Virus Type 1 gp41: Implications for Fusion-Inducing Conformational Changes. *Journal of Virology* 2004;78(5):2627-2631.
139. Carter D, Reed SG. Role of adjuvants in modeling the immune response. *Curr Opin HIV AIDS* 2010 Sep;5(5):409-413.
140. Krashias G, Simon A, Wegmann F, Kok W, Ho L, Stevens D, Skehel J, Heeney JL, Moghaddam AE, Sattentau QJ. Potent adaptive immune responses induced against HIV-1 gp140 and influenza virus HA by a polyanionic carbomer. *Vaccine* 2010 Mar;28(13):2482-2489.
141. McBurney SP, Young KR, Ross TM. Membrane embedded HIV-1 envelope on the surface of a virus-like particle elicits broader immune responses than soluble envelopes. *Virology* 2007 Feb;358(2):334-346.
142. Speth C, Bredl S, Hagleitner M, Wild J, Dierich M, Wolf H, Schroeder J, Wagner R, Deml L. Human immunodeficiency virus type-1 (HIV-1) Pr55gag virus-like particles are potent activators of human monocytes. *Virology* 2008 Dec;382(1):46-58.
143. Sailaja G, Skountzou I, Quan F, Compans RW, Kang S. Human immunodeficiency virus-like particles activate multiple types of immune cells. *Virology* 2007 Jun;362(2):331-341.
144. Sergeeva A, Kolonin MG, Molldrem JJ, Pasqualini R, Arap W. Display technologies: application for the discovery of drug and gene delivery agents. *Adv. Drug Deliv. Rev* 2006 Dec;58(15):1622-1654.
145. Rothe A, Hosse RJ, Power BE. Ribosome display for improved biotherapeutic molecules. *Expert Opin Biol Ther* 2006 Feb;6(2):177-187.
146. Yan X, Xu Z. Ribosome-display technology: applications for directed evolution of functional proteins. *Drug Discov. Today* 2006 Oct;11(19-20):911-916.
147. Takahashi TT, Roberts RW. In vitro selection of protein and peptide libraries using mRNA display. *Methods Mol. Biol* 2009;535:293-314.

148. Lipovsek D, Plückthun A. In-vitro protein evolution by ribosome display and mRNA display. *J. Immunol. Methods* 2004 Jul;290(1-2):51-67.
149. Liu DR. Translating DNA into synthetic molecules. *PLoS Biol* 2004 Jul;2(7):E223.
150. Wrenn SJ, Weisinger RM, Halpin DR, Harbury PB. Synthetic ligands discovered by in vitro selection. *J. Am. Chem. Soc* 2007 Oct;129(43):13137-13143.
151. Bratkovic T. Progress in phage display: evolution of the technique and its application. *Cell. Mol. Life Sci* 2010 Mar;67(5):749-767.
152. Kotlan B, Glassy MC. Antibody phage display: overview of a powerful technology that has quickly translated to the clinic. *Methods Mol. Biol* 2009;562:1-15.
153. Mäkelä AR, Ernst W, Grabherr R, Oker-Blom C. Baculovirus-based display and gene delivery systems. *Cold Spring Harb Protoc* 2010 Mar;2010(3):pdb.top72.
154. Grabherr R, Ernst W. Baculovirus for eukaryotic protein display. *Curr Gene Ther* 2010 Jun;10(3):195-200.
155. Buchholz CJ, Duerner LJ, Funke S, Schneider IC. Retroviral display and high throughput screening. *Comb. Chem. High Throughput Screen* 2008 Feb;11(2):99-110.
156. Urban JH, Merten CA. Retroviral Display in Gene Therapy, Protein Engineering, and Vaccine Development. *ACS Chem Biol* 2011 Jan;6(1):61-74.
157. Müller OJ, Kaul F, Weitzman MD, Pasqualini R, Arap W, Kleinschmidt JA, Trepel M. Random peptide libraries displayed on adeno-associated virus to select for targeted gene therapy vectors. *Nat. Biotechnol* 2003 Sep;21(9):1040-1046.
158. Daugherty PS. Protein engineering with bacterial display. *Curr. Opin. Struct. Biol* 2007 Aug;17(4):474-480.
159. Desvaux M, Dumas E, Chafsey I, Hébraud M. Protein cell surface display in Gram-positive bacteria: from single protein to macromolecular protein structure. *FEMS Microbiol. Lett* 2006 Mar;256(1):1-15.
160. Pepper LR, Cho YK, Boder ET, Shusta EV. A decade of yeast surface display technology: where are we now? *Comb. Chem. High Throughput Screen* 2008 Feb;11(2):127-134.
161. Shibasaki S, Maeda H, Ueda M. Molecular display technology using yeast-arming technology. *Anal Sci* 2009 Jan;25(1):41-49.
162. Ho M, Nagata S, Pastan I. Isolation of anti-CD22 Fv with high affinity by Fv display on human cells. *Proc. Natl. Acad. Sci. U.S.A* 2006 Jun;103(25):9637-9642.
163. Taube R, Zhu Q, Xu C, Diaz-Griffero F, Sui J, Kamau E, Dwyer M, Aird D, Marasco WA. Lentivirus display: stable expression of human antibodies on the surface of human cells and virus particles. *PLoS ONE* 2008;3(9):e3181.
164. Wolkowicz R, Jager GC, Nolan GP. A random peptide library fused to CCR5 for selection of mimetopes expressed on the mammalian cell surface via retroviral vectors. *J. Biol. Chem* 2005 Apr;280(15):15195-15201.
165. Lin W, Kurosawa K, Murayama A, Kagaya E, Ohta K. B-cell display-based one-step method to generate chimeric human IgG monoclonal antibodies. *Nucleic Acids Res* 2011;39(3):e14.
166. Beerli RR, Bauer M, Buser RB, Gwerder M, Muntwiler S, Maurer P, Saudan P, Bachmann MF. Isolation of human monoclonal antibodies by mammalian cell display. *Proc. Natl. Acad. Sci. U.S.A* 2008 Sep;105(38):14336-14341.
167. Alonso-Camino V, Sánchez-Martín D, Compte M, Sanz L, Alvarez-Vallina L. Lymphocyte display: a novel antibody selection platform based on T cell activation. *PLoS ONE* 2009;4(9):e7174.
168. Levin A, Hayouka Z, Brack-Werner R, Volsky DJ, Friedler A, Loyter A. Novel regulation of HIV-1 replication and pathogenicity: Rev inhibition of integration. *Protein Engineering Design and Selection* 2009;22(12):753-763.
169. Hu WS, Temin HM. Retroviral recombination and reverse transcription. *Science* 1990 Nov;250(4985):1227-1233.
170. Bieniasz PD. The cell biology of HIV-1 virion genesis. *Cell Host Microbe* 2009 Jun;5(6):550-558.

171. Gheysen D, Jacobs E, de Foresta F, Thiriart C, Francotte M, Thines D, De Wilde M. Assembly and release of HIV-1 precursor Pr55gag virus-like particles from recombinant baculovirus-infected insect cells. *Cell* 1989 Oct;59(1):103-112.
172. Sakalian M, Hunter E. Molecular events in the assembly of retrovirus particles. *Adv. Exp. Med. Biol* 1998;440:329-339.
173. Khare PD, Rosales AG, Bailey KR, Russell SJ, Federspiel MJ. Epitope selection from an uncensored peptide library displayed on avian leukosis virus. *Virology* 2003 Oct;315(2):313-321.
174. Granieri L, Baret J, Griffiths AD, Merten CA. High-throughput screening of enzymes by retroviral display using droplet-based microfluidics. *Chem. Biol* 2010 Mar;17(3):229-235.
175. Rodi DJ, Soares AS, Makowski L. Quantitative assessment of peptide sequence diversity in M13 combinatorial peptide phage display libraries. *J. Mol. Biol* 2002 Oct;322(5):1039-1052.
176. Urban JH, Schneider RM, Compte M, Finger C, Cichutek K, Alvarez-Vallina L, Buchholz CJ. Selection of functional human antibodies from retroviral display libraries. *Nucleic Acids Res* 2005;33(4):e35.
177. Sambrook J, Russel DW. *Molecular Cloning: A Laboratory Manual*, 3 Vol. 3. ed. Cold Spring Harbor (N.Y.): Cold Spring Harbor Laboratory Press; 2001.
178. Mullis KB, Faloona FA. Specific synthesis of DNA in vitro via a polymerase-catalyzed chain reaction. *Meth. Enzymol* 1987;155:335-350.
179. Hanahan D. Studies on transformation of *Escherichia coli* with plasmids. *J. Mol. Biol* 1983 Jun;166(4):557-580.
180. Grant SG, Jessee J, Bloom FR, Hanahan D. Differential plasmid rescue from transgenic mouse DNAs into *Escherichia coli* methylation-restriction mutants. *Proc. Natl. Acad. Sci. U.S.A* 1990 Jun;87(12):4645-4649.
181. Bertani G. Studies on lysogenesis. I. The mode of phage liberation by lysogenic *Escherichia coli*. *J. Bacteriol* 1951 Sep;62(3):293-300.
182. Birnboim HC, Doly J. A rapid alkaline extraction procedure for screening recombinant plasmid DNA. *Nucleic Acids Res* 1979 Nov;7(6):1513-1523.
183. Lenz O, Dittmar MT, Wagner A, Ferko B, Vorauer-Uhl K, Stiegler G, Weissenhorn W. Trimeric membrane-anchored gp41 inhibits HIV membrane fusion. *J. Biol. Chem* 2005 Feb;280(6):4095-4101.
184. Benson DA, Karsch-Mizrachi I, Lipman DJ, Ostell J, Sayers EW. GenBank. *Nucleic Acids Res* 2010 Jan;38(Database issue):D46-51.
185. Raab D, Graf M, Notka F, Schödl T, Wagner R. The GeneOptimizer Algorithm: using a sliding window approach to cope with the vast sequence space in multiparameter DNA sequence optimization. *Syst Synth Biol* 2010;4(3):215-225.
186. Sonnhammer EL, von Heijne G, Krogh A. A hidden Markov model for predicting transmembrane helices in protein sequences. *Proc Int Conf Intell Syst Mol Biol* 1998;6:175-182.
187. Li Z, Howard A, Kelley C, Delogu G, Collins F, Morris S. Immunogenicity of DNA vaccines expressing tuberculosis proteins fused to tissue plasminogen activator signal sequences. *Infect. Immun* 1999 Sep;67(9):4780-4786.
188. Wanninger V. Strategien zur Modulation der Immunogenität des HIV-1 Hüllproteins als Vakzinekomponente [Dissertation]. University of Regensburg; 2008.
189. Bendtsen JD, Nielsen H, von Heijne G, Brunak S. Improved prediction of signal peptides: SignalP 3.0. *J. Mol. Biol* 2004 Jul;340(4):783-795.
190. Kozak M. Compilation and analysis of sequences upstream from the translational start site in eukaryotic mRNAs. *Nucleic Acids Res* 1984 Jan;12(2):857-872.
191. Wilson IA, Niman HL, Houghten RA, Cherenson AR, Connolly ML, Lerner RA. The structure of an antigenic determinant in a protein. *Cell* 1984 Jul;37(3):767-778.

192. Grote A, Hiller K, Scheer M, Münch R, Nörtemann B, Hempel DC, Jahn D. JCat: a novel tool to adapt codon usage of a target gene to its potential expression host. *Nucleic Acids Res* 2005 Jul;33(Web Server issue):W526-531.
193. Käll L, Krogh A, Sonnhammer ELL. A combined transmembrane topology and signal peptide prediction method. *J. Mol. Biol* 2004 May;338(5):1027-1036.
194. Hinz A, Schoehn G, Quendler H, Hulsik DL, Stiegler G, Katinger H, Seaman MS, Montefiori D, Weissenhorn W. Characterization of a trimeric MPER containing HIV-1 gp41 antigen. *Virology* 2009 Aug;390(2):221-227.
195. Weissenhorn W, Calder LJ, Dessen A, Laue T, Skehel JJ, Wiley DC. Assembly of a rod-shaped chimera of a trimeric GCN4 zipper and the HIV-1 gp41 ectodomain expressed in *Escherichia coli*. *Proc. Natl. Acad. Sci. U.S.A* 1997 Jun;94(12):6065-6069.
196. Eswar N, Webb B, Marti-Renom MA, Madhusudhan MS, Eramian D, Shen M, Pieper U, Sali A. Comparative protein structure modeling using MODELLER. *Curr Protoc Protein Sci* 2007 Nov;Chapter 2:Unit 2.9.
197. Shen M, Sali A. Statistical potential for assessment and prediction of protein structures. *Protein Sci* 2006 Nov;15(11):2507-2524.
198. DeLano, Warren, L. The PyMOL Molecular Graphics System [Internet]. San Carlos, CA, USA: DeLano Scientific; 2002. Available from: <http://www.pymol.org/>
199. Graf M, Ludwig C, Kehlenbeck S, Jungert K, Wagner R. A quasi-lentiviral green fluorescent protein reporter exhibits nuclear export features of late human immunodeficiency virus type 1 transcripts. *Virology* 2006 Sep;352(2):295-305.
200. Graf M, Bojak A, Deml L, Bieler K, Wolf H, Wagner R. Concerted action of multiple cis-acting sequences is required for Rev dependence of late human immunodeficiency virus type 1 gene expression. *J. Virol* 2000 Nov;74(22):10822-10826.
201. Boshart M, Weber F, Jahn G, Dorsch-Häsler K, Fleckenstein B, Schaffner W. A very strong enhancer is located upstream of an immediate early gene of human cytomegalovirus. *Cell* 1985 Jun;41(2):521-530.
202. Goodwin EC, Rottman FM. The 3'-flanking sequence of the bovine growth hormone gene contains novel elements required for efficient and accurate polyadenylation. *J. Biol. Chem* 1992 Aug;267(23):16330-16334.
203. Dittmar MT, Eichler S, Reinberger S, Henning L, Kräusslich HG. A recombinant virus assay using full-length envelope sequences to detect changes in HIV-1 co-receptor usage. *Virus Genes* 2001 Dec;23(3):281-290.
204. Adachi A, Gendelman HE, Koenig S, Folks T, Willey R, Rabson A, Martin MA. Production of acquired immunodeficiency syndrome-associated retrovirus in human and nonhuman cells transfected with an infectious molecular clone. *J. Virol* 1986 Aug;59(2):284-291.
205. Karkhanis YD, Cormier MJ. Isolation and properties of Renilla reniformis luciferase, a low molecular weight energy conversion enzyme. *Biochemistry* 1971 Jan;10(2):317-326.
206. Ali A, Jamieson BD, Yang OO. Half-genome human immunodeficiency virus type 1 constructs for rapid production of reporter viruses. *J. Virol. Methods* 2003 Jun;110(2):137-142.
207. Ternette N, Stefanou D, Kuate S, Uberla K, Grunwald T. Expression of RNA virus proteins by RNA polymerase II dependent expression plasmids is hindered at multiple steps. *Virol. J* 2007;4:51.
208. Schilling K, Wagner R, Kliche A. P05-01. Generation of a HI-viral packaging cell line as scaffolding for a lentiviral display system. *Retrovirology* 2009;6(Suppl 3):P77.
209. Schilling K. Etablierung eines lentiviralen Display-Systems mithilfe eines auf einer HI-viralen Verpackungszelllinie basierenden Vektor-Systems - Proof of concept anhand des HIV-1 envelope [Dissertation]. University of Hamburg; 2010.
210. Donello JE, Loeb JE, Hope TJ. Woodchuck hepatitis virus contains a tripartite posttranscriptional regulatory element. *J. Virol* 1998 Jun;72(6):5085-5092.
211. Bruun T, Kliche A, Wagner R. P12-02. Cell-surface display and panning of HIV-1 derived envelope proteins. *Retrovirology* 2009;6(Suppl 3):P168.

212. Bernard P, Couturier M. Cell killing by the F plasmid CcdB protein involves poisoning of DNA-topoisomerase II complexes*1. *Journal of Molecular Biology* 1992;226(3):735-745.
213. Kim DW, Uetsuki T, Kaziro Y, Yamaguchi N, Sugano S. Use of the human elongation factor 1 alpha promoter as a versatile and efficient expression system. *Gene* 1990 Jul;91(2):217-223.
214. Huang MT, Gorman CM. Intervening sequences increase efficiency of RNA 3' processing and accumulation of cytoplasmic RNA. *Nucleic Acids Res* 1990 Feb;18(4):937-947.
215. Jang SK, Kräusslich HG, Nicklin MJ, Duke GM, Palmenberg AC, Wimmer E. A segment of the 5' nontranslated region of encephalomyocarditis virus RNA directs internal entry of ribosomes during in vitro translation. *J. Virol* 1988 Aug;62(8):2636-2643.
216. Laemmli UK. Cleavage of structural proteins during the assembly of the head of bacteriophage T4. *Nature* 1970 Aug;227(5259):680-685.
217. Wolf H, Modorow S, Soutschek E, Motz M, Grunow R, Döbl H, Von Baehr R. Production, mapping and biological characterisation of monoclonal antibodies to the core protein (p24) of the human immunodeficiency virus type 1. *AIFO* 1990;5(1):24-29.
218. Ludwig C, Leiherer A, Wagner R. Importance of protease cleavage sites within and flanking human immunodeficiency virus type 1 transframe protein p6* for spatiotemporal regulation of protease activation. *J. Virol* 2008 May;82(9):4573-4584.
219. Deml L, Bojak A, Steck S, Graf M, Wild J, Schirmbeck R, Wolf H, Wagner R. Multiple effects of codon usage optimization on expression and immunogenicity of DNA candidate vaccines encoding the human immunodeficiency virus type 1 Gag protein. *J. Virol* 2001 Nov;75(22):10991-11001.
220. DuBridge RB, Tang P, Hsia HC, Leong PM, Miller JH, Calos MP. Analysis of mutation in human cells by using an Epstein-Barr virus shuttle system. *Mol. Cell. Biol* 1987 Jan;7(1):379-387.
221. Wei X, Decker JM, Liu H, Zhang Z, Arani RB, Kilby JM, Saag MS, Wu X, Shaw GM, Kappes JC. Emergence of Resistant Human Immunodeficiency Virus Type 1 in Patients Receiving Fusion Inhibitor (T-20) Monotherapy. *Antimicrobial Agents and Chemotherapy* 2002;46(6):1896-1905.
222. Graham FL, Smiley J, Russell WC, Nairn R. Characteristics of a Human Cell Line Transformed by DNA from Human Adenovirus Type 5. *Journal of General Virology* 1977;36(1):59-72.
223. Boussif O, Lezoualc'h F, Zanta MA, Mergny MD, Scherman D, Demeneix B, Behr JP. A versatile vector for gene and oligonucleotide transfer into cells in culture and in vivo: polyethylenimine. *Proc. Natl. Acad. Sci. U.S.A* 1995 Aug;92(16):7297-7301.
224. Paulus C, Ludwig C, Wagner R. Contribution of the Gag-Pol transframe domain p6* and its coding sequence to morphogenesis and replication of human immunodeficiency virus type 1. *Virology* 2004;330(1):271-283.
225. Montefiori DC. Evaluating neutralizing antibodies against HIV, SIV, and SHIV in luciferase reporter gene assays. *Curr Protoc Immunol* 2005 Jan;Chapter 12:Unit 12.11.
226. Chapman BS, Thayer RM, Vincent KA, Haigwood NL. Effect of intron A from human cytomegalovirus (Towne) immediate-early gene on heterologous expression in mammalian cells. *Nucleic Acids Res* 1991 Jul;19(14):3979-3986.
227. Dimmock NJ. The complex antigenicity of a small external region of the C-terminal tail of the HIV-1 gp41 envelope protein: a lesson in epitope analysis. *Rev. Med. Virol* 2005 Dec;15(6):365-381.
228. Kapzan R. Directing the immune response to well-defined envelope epitopes provokes neutralization using the mucosal adjuvant Cholera toxin B as carrier. Regensburg: University of Regensburg; 2010.
229. Wagner R, Deml L, Schirmbeck R, Niedrig M, Reimann J, Wolf H. Construction, expression, and immunogenicity of chimeric HIV-1 virus-like particles. *Virology* 1996 Jun;220(1):128-140.
230. Costin JM. Cytopathic Mechanisms of HIV-1. *Virol J* 2007;4(1):100.

231. Zelenin AV, Poletaev AI, Stepanova NG, Barsky VE, Kolesnikov VA, Nikitin SM, Zhuze AL, Gnutchnev NV. 7-amino-actinomycin D as a specific fluorophore for DNA content analysis by laser flow cytometry. *Cytometry* 1984;5(4):348-354.
232. Homburg CH, de Haas M, von dem Borne AE, Verhoeven AJ, Reutelingsperger CP, Roos D. Human neutrophils lose their surface Fc gamma RIII and acquire Annexin V binding sites during apoptosis in vitro. *Blood* 1995 Jan;85(2):532-540.
233. Leung L, Srivastava IK, Kan E, Legg H, Sun Y, Greer C, Montefiori DC, zur Megede J, Barnett SW. Immunogenicity of HIV-1 Env and Gag in baboons using a DNA prime/protein boost regimen. *AIDS* 2004 Apr;18(7):991-1001.
234. Wang S, Arthos J, Lawrence JM, Van Ryk D, Mboudjeka I, Shen S, Chou TW, Montefiori DC, Lu S. Enhanced Immunogenicity of gp120 Protein When Combined with Recombinant DNA Priming To Generate Antibodies That Neutralize the JR-FL Primary Isolate of Human Immunodeficiency Virus Type 1. *Journal of Virology* 2005;79(12):7933-7937.
235. Johnson PR, Montefiori DC, Goldstein S, Hamm TE, Zhou J, Kitov S, Haigwood NL, Misher L, London WT, Gerin JL. Inactivated whole-virus vaccine derived from a proviral DNA clone of simian immunodeficiency virus induces high levels of neutralizing antibodies and confers protection against heterologous challenge. *Proc. Natl. Acad. Sci. U.S.A* 1992 Mar;89(6):2175-2179.
236. Stott EJ. Anti-cell antibody in macaques. *Nature* 1991 Oct;353(6343):393.
237. Montefiori DC, Hirsch VM, Johnson PR. AIDS response. *Nature* 1991;354(6353):439-440.
238. Osterhaus A, de Vries P, Heeney J. AIDS vaccine developments. *Nature* 1992 Feb;355(6362):684-685.
239. Cranage MP, Ashworth LA, Greenaway PJ, Murphey-Corb M, Desrosiers RC. AIDS vaccine developments. *Nature* 1992 Feb;355(6362):685-686.
240. Cranage MP, Fraser CA, Stevens Z, Huting J, Chang M, Jeffs SA, Seaman MS, Cope A, Cole T, Shattock RJ. Repeated vaginal administration of trimeric HIV-1 clade C gp140 induces serum and mucosal antibody responses. *Mucosal Immunol* 2010 Jan;3(1):57-68.
241. Alam SM, Morelli M, Dennison SM, Liao H, Zhang R, Xia S, Rits-Volloch S, Sun L, Harrison SC, Haynes BF, Chen B. Role of HIV membrane in neutralization by two broadly neutralizing antibodies. *Proc. Natl. Acad. Sci. U.S.A* 2009 Dec;106(48):20234-20239.
242. Arai T, Takada M, Ui M, Iba H. Dose-dependent transduction of vesicular stomatitis virus G protein-pseudotyped retrovirus vector into human solid tumor cell lines and murine fibroblasts. *Virology* 1999 Jul;260(1):109-115.
243. Yuste E, Reeves JD, Doms RW, Desrosiers RC. Modulation of Env content in virions of simian immunodeficiency virus: correlation with cell surface expression and virion infectivity. *J. Virol* 2004 Jul;78(13):6775-6785.
244. Firth AE, Patrick WM. Statistics of protein library construction. *Bioinformatics* 2005 Aug;21(15):3314-3315.
245. Muster T, Guinea R, Trkola A, Purtscher M, Klima A, Steindl F, Palese P, Katinger H. Cross-neutralizing activity against divergent human immunodeficiency virus type 1 isolates induced by the gp41 sequence ELDKWAS. *J. Virol* 1994 Jun;68(6):4031-4034.
246. Joyce JG, Hurni WM, Bogusky MJ, Garsky VM, Liang X, Citron MP, Danzeisen RC, Miller MD, Shiver JW, Keller PM. Enhancement of alpha-helicity in the HIV-1 inhibitory peptide DP178 leads to an increased affinity for human monoclonal antibody 2F5 but does not elicit neutralizing responses in vitro. Implications for vaccine design. *J. Biol. Chem* 2002 Nov;277(48):45811-45820.
247. Coëffier E, Clément J, Cussac V, Khodaei-Boorane N, Jehanno M, Rojas M, Dridi A, Latour M, El Habib R, Barré-Sinoussi F. Antigenicity and immunogenicity of the HIV-1 gp41 epitope ELDKWA inserted into permissive sites of the MalE protein. *Vaccine* 2000;19(7-8):684-693.

-
248. Kim M, Qiao Z, Yu J, Montefiori D, Reinherz EL. Immunogenicity of recombinant human immunodeficiency virus type 1-like particles expressing gp41 derivatives in a pre-fusion state. *Vaccine* 2007 Jun;25(27):5102-5114.
249. Law M, Cardoso RMF, Wilson IA, Burton DR. Antigenic and immunogenic study of membrane-proximal external region-grafted gp120 antigens by a DNA prime-protein boost immunization strategy. *J. Virol* 2007 Apr;81(8):4272-4285.
250. Garrity RR, Rimmelzwaan G, Minassian A, Tsai WP, Lin G, de Jong JJ, Goudsmit J, Nara PL. Refocusing neutralizing antibody response by targeted dampening of an immunodominant epitope. *J. Immunol* 1997 Jul;159(1):279-289.
251. Pantophlet R, Ollmann Saphire E, Poignard P, Parren PWHI, Wilson IA, Burton DR. Fine mapping of the interaction of neutralizing and nonneutralizing monoclonal antibodies with the CD4 binding site of human immunodeficiency virus type 1 gp120. *J. Virol* 2003 Jan;77(1):642-658.
252. Beddows S, Franti M, Dey AK, Kirschner M, Iyer SPN, Fisch DC, Ketas T, Yuste E, Desrosiers RC, Klasse PJ, Maddon PJ, Olson WC, Moore JP. A comparative immunogenicity study in rabbits of disulfide-stabilized, proteolytically cleaved, soluble trimeric human immunodeficiency virus type 1 gp140, trimeric cleavage-defective gp140 and monomeric gp120. *Virology* 2007 Apr;360(2):329-340.
253. Kim M, Qiao Z, Montefiori DC, Haynes BF, Reinherz EL, Liao H. Comparison of HIV Type 1 ADA gp120 monomers versus gp140 trimers as immunogens for the induction of neutralizing antibodies. *AIDS Res. Hum. Retroviruses* 2005 Jan;21(1):58-67.
254. Liu S, Kondo N, Long Y, Xiao D, Iwamoto A, Matsuda Z. Membrane topology analysis of HIV-1 envelope glycoprotein gp41. *Retrovirology* 2010;7(1):100.
255. Iwatani Y, Song SK, Wang L, Planas J, Sakai H, Ishimoto A, Cloyd MW. Human immunodeficiency virus type 1 Vpu modifies viral cytopathic effect through augmented virus release. *J. Gen. Virol* 1997 Apr;78 (Pt 4):841-846.
256. Apellániz B, García-Sáez A, Nir S, Nieva JL. Destabilization exerted by peptides derived from the membrane-proximal external region of HIV-1 gp41 in lipid vesicles supporting fluid phase coexistence [Internet]. *Biochim Biophys Acta* 2011 Feb; Available from: <http://www.ncbi.nlm.nih.gov/pubmed/21316335>
257. Brito LA, Singh M. Acceptable levels of endotoxin in vaccine formulations during preclinical research. *J. Pharm. Sci.* 2011;100(1):34-37.
258. Grundner C, Pancera M, Kang J, Koch M, Sodroski J, Wyatt R. Factors limiting the immunogenicity of HIV-1 gp120 envelope glycoproteins. *Virology* 2004 Dec;330(1):233-248.
259. Alam SM, Searce RM, Parks RJ, Plonk K, Plonk SG, Sutherland LL, Gorny MK, Zolla-Pazner S, VanLeeuwen S, Moody MA, Xia S, Montefiori DC, Tomaras GD, Weinhold KJ, Karim SA, Hicks CB, Liao H, Robinson J, Shaw GM, Haynes BF. Human Immunodeficiency Virus Type 1 gp41 Antibodies That Mask Membrane Proximal Region Epitopes: Antibody Binding Kinetics, Induction, and Potential for Regulation in Acute Infection. *Journal of Virology* 2007;82(1):115-125.
260. Devito C, Zuber B, Schröder U, Benthin R, Okuda K, Broliden K, Wahren B, Hinkula J. Intranasal HIV-1-gp160-DNA/gp41 peptide prime-boost immunization regimen in mice results in long-term HIV-1 neutralizing humoral mucosal and systemic immunity. *J. Immunol* 2004 Dec;173(11):7078-7089.
261. Eckhart L, Raffelsberger W, Ferko B, Klima A, Purtscher M, Katinger H, Ruker F. Immunogenic Presentation of a Conserved gp41 Epitope of Human Immunodeficiency Virus Type 1 on Recombinant Surface Antigen of Hepatitis B Virus. *Journal of General Virology* 1996;77(9):2001-2008.
262. Marusic C, Rizza P, Lattanzi L, Mancini C, Spada M, Belardelli F, Benvenuto E, Capone I. Chimeric Plant Virus Particles as Immunogens for Inducing Murine and Human Immune Responses against Human Immunodeficiency Virus Type 1. *Journal of Virology* 2001;75(18):8434-8439.

-
263. Zhang H, Huang Y, Fayad R, Spear GT, Qiao L. Induction of Mucosal and Systemic Neutralizing Antibodies against Human Immunodeficiency Virus Type 1 (HIV-1) by Oral Immunization with Bovine Papillomavirus-HIV-1 gp41 Chimeric Virus-Like Particles. *Journal of Virology* 2004;78(15):8342-8348.
264. Kusov YY, Zamjatina NA, Poleschuk VF, Michailov MI, Morace G, Eberle J, Gauss-Müller V. Immunogenicity of a chimeric hepatitis A virus (HAV) carrying the HIV gp41 epitope 2F5. *Antiviral Res* 2007 Feb;73(2):101-111.
265. Liang X, Munshi S, Shendure J, Mark G, Davies ME, Freed DC, Montefiori DC, Shiver JW. Epitope insertion into variable loops of HIV-1 gp120 as a potential means to improve immunogenicity of viral envelope protein. *Vaccine* 1999 Jul;17(22):2862-2872.
266. Ofek G, Guenaga FJ, Schief WR, Skinner J, Baker D, Wyatt R, Kwong PD. Elicitation of structure-specific antibodies by epitope scaffolds. *Proc. Natl. Acad. Sci. U.S.A* 2010 Oct;107(42):17880-17887.
267. Ho J, Uger RA, Zwick MB, Luscher MA, Barber BH, MacDonald KS. Conformational constraints imposed on a pan-neutralizing HIV-1 antibody epitope result in increased antigenicity but not neutralizing response. *Vaccine* 2005 Feb;23(13):1559-1573.
268. Decroix N, Hocini H, Quan CP, Bellon B, Kazatchkine MD, Bouvet JP. Induction in mucosa of IgG and IgA antibodies against parenterally administered soluble immunogens. *Scand. J. Immunol* 2001 Apr;53(4):401-409.
269. Decroix N, Pamonsinlapatham P, Quan CP, Bouvet J. Impairment by mucosal adjuvants and cross-reactivity with variant peptides of the mucosal immunity induced by injection of the fusion peptide PADRE-ELDKWA. *Clin. Diagn. Lab. Immunol* 2003 Nov;10(6):1103-1108.
270. Lorizate M, Gómara MJ, de la Torre BG, Andreu D, Nieva JL. Membrane-transferring sequences of the HIV-1 Gp41 ectodomain assemble into an immunogenic complex. *J. Mol. Biol* 2006 Jun;360(1):45-55.
271. Tumanova OI, Kuvshinov VN, Orlovskaja IA, Proniaeva TR, Pokrovskii AG, Il'ichev AA, Sandakhchiev LS. [Immunogenetic properties of peptides mimicking a human immunodeficiency virus gp41 (HIV-1) epitope recognized by virus-neutralizing antibody 2F5]. *Mol. Biol. (Mosk.)* 2003 Jun;37(3):556-560.
272. Qi Z, Pan C, Lu H, Shui Y, Li L, Li X, Xu X, Liu S, Jiang S. A recombinant mimetics of the HIV-1 gp41 prehairpin fusion intermediate fused with human IgG Fc fragment elicits neutralizing antibody response in the vaccinated mice. *Biochem. Biophys. Res. Commun* 2010 Jul;398(3):506-512.
273. Bianchi E, Joyce JG, Miller MD, Finnefrock AC, Liang X, Finotto M, Ingallinella P, McKenna P, Citron M, Ottinger E, Hepler RW, Hrin R, Nahas D, Wu C, Montefiori D, Shiver JW, Pessi A, Kim PS. Vaccination with peptide mimetics of the gp41 prehairpin fusion intermediate yields neutralizing antisera against HIV-1 isolates. *Proc. Natl. Acad. Sci. U.S.A* 2010 Jun;107(23):10655-10660.
274. Luo M, Yuan F, Liu Y, Jiang S, Song X, Jiang P, Yin X, Ding M, Deng H. Induction of neutralizing antibody against human immunodeficiency virus type 1 (HIV-1) by immunization with gp41 membrane-proximal external region (MPER) fused with porcine endogenous retrovirus (PERV) p15E fragment. *Vaccine* 2006 Jan;24(4):435-442.
275. Ye L, Sun Y, Lin J, Bu Z, Wu Q, Jiang S, Steinhauer DA, Compans RW, Yang C. Antigenic properties of a transport-competent influenza HA/HIV Env chimeric protein. *Virology* 2006 Aug;352(1):74-85.
276. Matyas GR, Wiczorek L, Beck Z, Ochsenbauer-Jambor C, Kappes JC, Michael NL, Polonis VR, Alving CR. Neutralizing antibodies induced by liposomal HIV-1 glycoprotein 41 peptide simultaneously bind to both the 2F5 or 4E10 epitope and lipid epitopes. *AIDS* 2009;23(16):2069-2077.
277. Sadler K, Zhang Y, Xu J, Yu Q, Tam JP. Quaternary protein mimetics of gp41 elicit neutralizing antibodies against HIV fusion-active intermediate state. *Biopolymers* 2008;90(3):320-329.
278. Crooks ET, Moore PL, Franti M, Cayan CS, Zhu P, Jiang P, de Vries RP, Wiley C, Zharkikh I, Schülke N, Roux KH, Montefiori DC, Burton DR, Binley JM. A comparative immunogenicity study of HIV-1 virus-like particles bearing various forms of envelope proteins, particles bearing no envelope and soluble monomeric gp120. *Virology* 2007 Sep;366(2):245-262.

279. Killian JA, Nyholm TKM. Peptides in lipid bilayers: the power of simple models. *Curr. Opin. Struct. Biol* 2006 Aug;16(4):473-479.
280. Matoba N, Geyer BC, Kilbourne J, Alfsen A, Bomsel M, Mor TS. Humoral immune responses by prime-boost heterologous route immunizations with CTB-MPR(649-684), a mucosal subunit HIV/AIDS vaccine candidate. *Vaccine* 2006 Jun;24(23):5047-5055.
281. Moore MJ, Dorfman T, Li W, Wong SK, Li Y, Kuhn JH, Coderre J, Vasilieva N, Han Z, Greenough TC, Farzan M, Choe H. Retroviruses pseudotyped with the severe acute respiratory syndrome coronavirus spike protein efficiently infect cells expressing angiotensin-converting enzyme 2. *J. Virol* 2004 Oct;78(19):10628-10635.
282. Deml L, Kratochwil G, Osterrieder N, Knüchel R, Wolf H, Wagner R. Increased incorporation of chimeric human immunodeficiency virus type 1 gp120 proteins into Pr55gag virus-like particles by an Epstein-Barr virus gp220/350-derived transmembrane domain. *Virology* 1997 Aug;235(1):10-25.
283. Grothaus M. Selection of an immunogenic peptide mimic of the capsular polysaccharide of *Neisseria meningitidis* serogroup A using a peptide display library. *Vaccine* 2000;18(13):1253-1263.
284. Cristillo A, Weiss D, Hudacik L, Restrepo S, Galmin L, Suschak J, Draghiaakli R, Markham P, Pal R. Persistent antibody and T cell responses induced by HIV-1 DNA vaccine delivered by electroporation. *Biochemical and Biophysical Research Communications* 2008;366(1):29-35.
285. Vasan S, Hurley A, Schlesinger S, Hannaman D, Gardiner D, Dugin D, Boente-Carrera M, Vittorino R, Caskey M, Andersen J, Huang Y, Cox J, Tarragona T, Gill D, Cheeseman H, Clark L, Dally L, Smith C, Schmidt C, Park H, Sayeed E, Gilmour J, Fast P, Bernard R, Ho D. OA05-01. In vivo electroporation enhances the immunogenicity of ADVAX, a DNA-based HIV-1 vaccine candidate, in healthy volunteers. *Retrovirology* 2009;6(Suppl 3):O31.
286. Pulendran B. Learning immunology from the yellow fever vaccine: innate immunity to systems vaccinology. *Nat. Rev. Immunol* 2009 Oct;9(10):741-747.
287. Bomsel M, Tudor D, Drillet A, Alfsen A, Ganor Y, Roger M, Mouz N, Amacker M, Chalifour A, Diomede L, Devillier G, Cong Z, Wei Q, Gao H, Qin C, Yang G, Zurbruggen R, Lopalco L, Fleury S. Immunization with HIV-1 gp41 Subunit Virosomes Induces Mucosal Antibodies Protecting Nonhuman Primates against Vaginal SHIV Challenges. *Immunity* 2011 Feb;34(2):269-280.
288. McKeating JA, McKnight A, Moore JP. Differential loss of envelope glycoprotein gp120 from virions of human immunodeficiency virus type 1 isolates: effects on infectivity and neutralization. *J. Virol* 1991 Feb;65(2):852-860.
289. Leiherer A, Ludwig C, Wagner R. Influence of extended mutations of the HIV-1 transframe protein p6* on Nef-dependent viral replication and infectivity in vitro. *Virology* 2009;387(1):200-210.
290. Aiken C. Pseudotyping human immunodeficiency virus type 1 (HIV-1) by the glycoprotein of vesicular stomatitis virus targets HIV-1 entry to an endocytic pathway and suppresses both the requirement for Nef and the sensitivity to cyclosporin A. *J. Virol* 1997 Aug;71(8):5871-5877.
291. Menendez A, Chow KC, Pan OC, Scott JK. Human Immunodeficiency Virus Type 1-neutralizing Monoclonal Antibody 2F5 is Multispecific for Sequences Flanking the DKW Core Epitope. *Journal of Molecular Biology* 2004;338(2):311-327.
292. Bryson S, Julien J, Hynes RC, Pai EF. Crystallographic definition of the epitope promiscuity of the broadly neutralizing anti-human immunodeficiency virus type 1 antibody 2F5: vaccine design implications. *J. Virol* 2009 Nov;83(22):11862-11875.
293. Perelson AS, Neumann AU, Markowitz M, Leonard JM, Ho DD. HIV-1 dynamics in vivo: virion clearance rate, infected cell life-span, and viral generation time. *Science* 1996 Mar;271(5255):1582-1586.
294. Rodrigo AG, Shpaer EG, Delwart EL, Iversen AK, Gallo MV, Brojtsch J, Hirsch MS, Walker BD, Mullins JL. Coalescent estimates of HIV-1 generation time in vivo. *Proc. Natl. Acad. Sci. U.S.A* 1999 Mar;96(5):2187-2191.

295. Grewe B, Uberla K. The human immunodeficiency virus type 1 Rev protein: menage a trois during the early phase of the lentiviral replication cycle. *Journal of General Virology* 2010;91(8):1893-1897.
296. Hermes JD, Parekh SM, Blacklow SC, Köster H, Knowles JR. A reliable method for random mutagenesis: the generation of mutant libraries using spiked oligodeoxyribonucleotide primers. *Gene* 1989 Dec;84(1):143-151.
297. The Chicago manual of style. 16. ed. Chicago: The University of Chicago Press; 2010.
298. McNaught A, International Union of Pure and Applied Chemistry. Compendium of chemical terminology: IUPAC recommendations. 2. ed. Oxford, England; Malden, MA, USA: Blackwell Science; 1997.
299. Journal of Biological Chemistry: Abbreviations [Internet]. 2011;[cited 2011 Jan 26] Available from: <http://www.jbc.org/site/misc/abbrev.xhtml>
300. Patrias K. NLM recommended formats for bibliographic citation. Bethesda, MD: National Library of Medicine; 1991.

6.6 Acknowledgements

I am cordially thankful to Prof. Dr. R. Wagner for his supervision at the University of Regensburg, for the development of many ideas presented in this work, for fundraising, for his support of congress participations and for his backup during all phases of this work.

I deeply thank Prof. Dr. T. Dobner for his supervision and support at the University of Hamburg.

I owe thanks to Prof. Dr. J. Hauber, Prof. Dr. G. Adam and Prof. Dr. A. Haas at the University of Hamburg for supervising the disputation.

I thank Prof. Dr. H. Wolf and Prof. Dr. Dr. A. Gessner for conveyance of lab space and consumables at the University of Regensburg.

I enjoyed working within the team of the VDC project, namely my lab supervisor Dr. A. Kliche, and my colleagues T.-H. Bruun, K. Schilling and R. Kapzan. Thank you for the cooperative work, for sharing reagents and for helpful discussions.

I thank Dr. J. Wild for his incessant support in animal experiments and cytometric analyses.

Thanks to Dr. A. Kliche, B. Asbach, J. Wild and T.-H. Bruun for suggestions regarding the manuscript.

I thank S. Feiner for her tireless help in administrative issues.

A big “thank you” goes to all members of the Wagner lab in Regensburg for the friendly and cooperative atmosphere and many beautiful moments during work and leisure time of the past years.

I am very thankful for all advice and experimental support that I have received from any collaboration partner. Without external expertise and support, such a comprehensive project would not have been possible.

Advice for molecular modeling was kindly given by Dr. M. Bocola, Institute of Biophysics and Physical Biochemistry, University of Regensburg, Germany.

Electron microscopy was carried out by Dr. J. Schröder, H.I. Sigmund and B. Voll at the Institute of Pathology, University of Regensburg.

Design of hemagglutinin zipper H3 and provision with recombinant GCN4-gp41-FD protein were done as part of a collaboration project with Prof. Dr. W. Weissenhorn, Dr. A. Hinz and Dr. D. Hulsik from the Unit of Virus Host Cell Interactions (UVHCI), Grenoble, France.

Immunization of rabbits was carried out in collaboration with Prof. Dr. J. Heeney and performed by P. Tonks at the Department of Veterinary Medicine, University of Cambridge, UK.

Neutralization tests were done by Prof. D. Montefiori and his group including K.M. Greene, Dr. H. Gao, P. Gao and Dr. C.C. Labranche at Duke Human Vaccine Institute, Duke University School of Medicine, Durham, NC, USA.

Plasmid pTN7-Stop was provided as courtesy by Dr. M.T. Dittmar, Blizard Institute of Cell and Molecular Science, London School of Medicine and Dentistry, UK.

Advice for library setup and subcloning was kindly given by Dr. M. Liss at Geneart AG, Regensburg.

FACS sorting was supervised by Dr. P. Hoffmann and kindly assisted by J. Igl, R. Eder and J. Stahl from the Institute of Internal Medicine, University of Regensburg.

Thanks to Prof. R. Weiss at University College London for the supportive meetings.

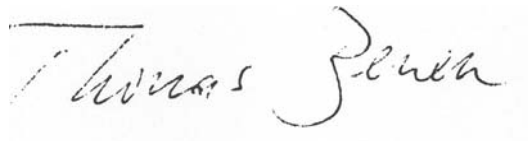
This research project was sponsored by a research grant of the Bill & Melinda Gates Foundation (Collaboration for AIDS Vaccine Discovery (CAVD)) and an EU grant (Cutaneous and Mucosal HIV Vaccination, CUT'HIVAC) to R. Wagner.

I declare that I have no competing interests that might be perceived to influence the results and/or discussion reported in this study.

Eidesstattliche Versicherung

Ich versichere gemäß §7(d) der Promotionsordnung des Fachbereichs Biologie der Universität Hamburg, dass ich die Dissertation „Novel Immunogens based on the gp41 protein of Human Immunodeficiency Virus type 1 and Display Systems for their Affinity Maturation“ selbständig angefertigt habe, die wörtlich oder inhaltlich aus anderen Quellen übernommen Stellen als solche kenntlich gemacht habe und die Inanspruchnahme fremder Hilfen namentlich aufgeführt habe.

2011-06-17, Thomas D. Benen

A handwritten signature in black ink, reading "Thomas Benen". The signature is written in a cursive style with a horizontal line above the first name.

Confirmation

I hereby confirm as a native English speaker and Australian citizen, that the dissertation “Novel Immunogens based on the gp41 protein of Human Immunodeficiency Virus type 1 and Display Systems for their Affinity Maturation” submitted by Thomas D. Benen is written in correct English language.

2011-06-17, Hisham Hassan

A handwritten signature in black ink, appearing to read 'Hisham Hassan', is written on a light blue grid background.

Hisham Hassan, MSc
Malergasse 12
93047 Regensburg